RELATIVE SEA LEVEL, SEDIMENT SUPPLY AND BARRIER DYNAMICS AS DRIVING MECHANISMS OF HOLOCENE COASTAL CHANGE

CHRISTINE ANNE HAMILTON

A thesis submitted in partial fulfilment of the requirements of Liverpool John Moores University for the degree of Doctor of Philosophy

March 2019

Abstract

The combined effects of climate change and population pressure lead to regional and local coastal responses that pose major challenges for the future resilience of coastal landscapes, increasing the vulnerability of communities, infrastructure and nature conservation interests. Improving understanding of coastline evolution in the past, using the Holocene record of geomorphological change preserved within coastal stratigraphy, is one way to improving understanding of coastal evolution and coastal response to climate and geomorphic change. This thesis aims to improve understanding of long-term coastal system behaviour by investigating the role of relative sea level, sediment supply and barrier dynamics as driving mechanisms of Holocene coastal change.

The Suffolk coast, an understudied and vulnerable section of coastline in southeast England, is used as a case study to improve understanding of the mechanisms driving Holocene coastal change. Stratigraphic investigation demonstrated significant spatial and temporal differences in sedimentation. A multiproxy approach, comprising lithostratigraphic, sedimentological, bio- and chronostratigraphic methods, identified and constrained the timing of major phases of coastal change. New sea-level index points (11 intercalated peat and 6 basal peat samples) constrain the position of relative sea level during the Holocene and support the gradual rise reconstructed by the existing data for southeast England.

Changes in sea-level tendency during the mid-Holocene are consistent on the Suffolk coast and wider East Anglia region, with predominantly positive (increase in marine influence) changes recorded, indicating that coastal sedimentation was controlled predominantly by relative sea level. In contrast, changes in sea-level tendency during the late Holocene varied substantially, indicating that local factors, notably sediment supply and barrier dynamics, were the main influences on coastal sedimentation, with relative sea level acting only as a background control. The importance of sedimentological and morphological factors in shaping Holocene coastal changes requires consideration when using the southern North Sea basin database of evidence as an analogue for future change under accelerated sea-level rise.

Contents

List of tables

List of figures

(1988; 1993). Permission to reproduce this figure has been granted by Springer Nature.

Chapter 5   **Page**

Chapter 6 **Page**

Chapter 7   **Page**

the late Holocene. The associated site is denoted by the colour with labels added for sites were multiple cores were sampled.

area. Permission to reproduce aerial images has been granted by Mike Page.

Declaration of copyright

I confirm that no part of the material presented in this thesis has previously been submitted by me or any other person for a degree in this or any other university. In all cases, where it is relevant, material from the work of others has been acknowledged.

The copyright of this thesis rests with the author. No quotation from it should be published without prior written consent and information derived from it should be acknowledged.

Acknowledgements

Chapter 1: Introduction

1.1 Project rationale

Coastal environments are currently experiencing the fastest rate of relative sea-level (RSL) rise in at least the past 2800 years, with anthropogenic climate change responsible for over half of the observed 14 cm rise during the 20th century (Kopp et al., 2016). The rate of RSL rise increased at the end of the 20th century, with satellite altimetry determining a global mean sea level rise rate of 3.1 ± 0.3 mm yr^{-1} for the last 25 years (Cazenave et al., 2018). Future climate change scenarios (AR5-RCPs) predict this will continue, with global mean sea level estimated to rise 0.62 ± 0.36 m above present by 2081-2100 for a RCP 8.5 scenario (Church et al., 2013). In addition to this, coastal populations are predicted to increase, reaching 1.8-5.2 billion by 2080, placing the coast under increasing human-induced pressure (Nicholls et al., 2007). The future vulnerability and resilience of coastal landscapes, and their associated communities, infrastructure and nature conservation interests, is therefore of increasing concern due to the combined effects of climate change-induced sea-level rise and population pressure.

Coastal management strategies aim to develop resilient coastlines, as they have the capacity to respond and evolve to forcing by natural and anthropogenic processes (Nicholls and Branson, 1998; Long et al., 2006a). Coastal resilience is best informed by an understanding of the local coastal response to global forcing mechanisms and how this fits within the regional setting. Historical records of coastal response to forcing provide context over the last 1000 years. However, geological archives are required in order to understand response over longer timescales. A record of changes in RSL, storm frequency and magnitude, climate change and sediment supply during the Holocene (11.7 ka to present day) is preserved in coastal stratigraphy (e.g. Bao et al., 1999; Plater et al., 1999; Shennan et al., 2005; Long et al., 2006a; Clarke et al., 2014). Records of Holocene coastal change extend understanding beyond the instrumental era and help evidence based management decision-making by improving understanding of the long-term behaviour of coastal systems and their response to climate and geomorphic change.

Coastal barriers protect sensitive back-barrier wetlands and adjacent coastal environments from the direct impacts of storms and erosion on ~ 15 % of the world's coastline (Cooper et al., 2018). RSL change, sediment supply, and storm frequency and magnitude are factors critical to the growth, stability and destruction of coastal barriers, which play a key role in shaping the pattern of coastal and estuary evolution (Orford et al., 1991; Long et al., 2006a). Reconstructing barrier evolution improves understanding of the long-term controls on coastal system behaviour, thereby informing future management

strategies. Long-term reconstructions of coastal barrier systems have highlighted the inherent dynamism of coastlines, a factor which must be considered when developing management schemes (Long et al., 2006a). It is only through this that capacity can be allowed for internal readjustment to future changes in the driving mechanisms of coastal change. Extending understanding of the driving mechanisms of coastal change beyond the instrumental era is therefore crucial, as it enables the relative importance of these mechanisms, and how they have varied spatially and temporally, to be considered.

1.1.1 Site context- Suffolk coast, southeast England

This thesis focuses on the Suffolk coast, an understudied area of the UK coastline in southeast England, to reconstruct Holocene coastal change and improve understanding of the mechanisms driving evolution using the record of coastal geomorphological change preserved in back-barrier wetlands. The existing information on Holocene stratigraphy for the Suffolk coast is spatially and temporally limited, restricting an understanding of the system's long-term behaviour (Carr and Baker, 1968; Carr, 1971; Brew et al., 1992; Lloyd et al., 2008). However, the existing data illustrates the potential of the archives available for Holocene coastal research. Additionally, contrasting Holocene stratigraphic records have been identified from existing research focussing on the Norfolk and Essex coast, to the north and south of Suffolk respectively (Carr and Baker, 1968; Carr, 1971; Funnell, 1979; Coles and Funnell, 1981; Alderton, 1983; Brew et al., 1992; Boomer and Godwin, 1993).

Long-term subsidence, RSL rise and a lack of sediment supply significantly compromise the present-day stability of the Suffolk coast (Shennan and Horton, 2002; Pye and Blott, 2006; Haskoning, 2009). The coastline has experienced erosion rates of up to 4.5 m yr^{-1} during the 20th century (Cambers, 1975; Carr, 1981; Brooks and Spencer, 2010; 2012). Historical records indicate that the configuration of the Suffolk coast has changed dramatically in the last 1000 years (Pye and Blott, 2006; Sear et al., 2011), with storms having a catastrophic impact on coastal development (Pye and Blott, 2006). The most notable example of this is Dunwich, a medieval port settlement that is now 90 % submerged beneath the sea due to coastal recession since the 11th century (Sear et al., 2011). In addition, the sediment supply to the gravel beaches is no longer adequate to retain system resilience to storms (Haskoning, 2009).

The Suffolk coast alternates between cliffs formed from soft unconsolidated Quaternary sediments and low-lying wetlands, separated from the sea by a narrow beach-barrier system. The region has high conservation value with significant proportions situated within protections such as the Suffolk Coast and Heaths Area of Outstanding National Beauty (AONB), the Suffolk Coast National Nature Reserve and the Minsmere-Walberswick

Heaths and Marshes Site of Special Scientific Interest (SSSI). In addition to the conservation value, significant infrastructure is also located on this coastline, namely Sizewell B nuclear power station and the planned Sizewell C nuclear new build. The geology underlying the region is a sandstone containing shells (Coralline Crag, Norwich Crag, and Red Crag) dating from the Pliocene and Pleistocene (Hamblin et al., 1997). The tidal regime on the coast is semi-diurnal with a minimum mean spring tidal range of 1.9 m at Lowestoft, increasing with distance south to 2.4 m at Aldeburgh (Pye and Blott, 2006). The wave regime is bimodal, with waves approaching predominantly from the north and northeast or south and southwest, and moderate, with most waves not exceeding 2 m (Pye and Blott, 2006; 2009; Brooks and Spencer, 2010).

1.2 Research aims and objectives

This research aims to reconstruct Holocene coastal evolution in Suffolk, southeast England, in order to improve understanding of the long-term behaviour of coastal systems. It represents an important, understudied region in which to investigate the driving mechanisms controlling Holocene coastal change.

A stratigraphic framework was developed and a combination of sedimentological, bio- and chrono-stratigraphic methods used to meet the following objectives:

(1) Reconstruct changes in RSL on the Suffolk coastline.

(2) Identify variations in sediment supply and determine the influence of barrier dynamics.

(3) Determine the behaviour of barrier and back-barrier environments in response to (1) and (2).

1.3 Thesis outline

Literature relating to the driving mechanisms of Holocene coastal change in the southern North Sea Basin is reviewed in **Chapter 2**. The existing Holocene stratigraphic record for the East Anglia region is outlined, focusing on the pattern of sedimentation and the responsible driving mechanisms. Following a discussion of the reconstruction of RSL change, with respect to the creation of sea-level index points and associated errors, the pattern of RSL change in the UK and East Anglia region is summarised. Attention is given to the factors controlling barrier evolution and historical and stratigraphic evidence of these features on the Suffolk coast. The sediment dynamics of the Suffolk coast, with respect to erosion, sediment transport and interactions with offshore banks, are also discussed. The final section of the chapter discusses the influence of human land use change on coastal environments and the notable signatures this can create in back-barrier sediment records.

The field and laboratory methodology undertaken to reconstruct palaeoenvironmental changes at each site is outlined in **Chapter 3**. The process of site selection is outlined in the field methodology section of this chapter, in addition to the methodology for stratigraphic survey, sediment sampling and surveying. The laboratory methodology is subdivided into sedimentological, biostratigraphical and chronological methods.

The site description, results, and associated palaeoenvironmental interpretation, are presented in **Chapters 4, 5 and 6** on a site-by-site basis. **Chapter 4** focusses on Westwood Marsh, Oldtown Marsh and Great Dingle Hill, which are all situated within the Walberswick National Nature Reserve between Southwold and Dunwich. **Chapter 5 and 6** focusses on Minsmere and Sizewell respectively, neighbouring sites situated ~ 6 km south of the Walberswick National Nature Reserve.

The pattern and chronology of sedimentation for each of the investigated sites is collated, compared and contrasted in **Chapter 7**. The sea-level index points and freshwater limiting data resulting from the palaeoenvironmental reconstructions are presented. Comparisons are made with the existing sea-level index points and the most recent glacial isostatic adjustment (GIA) model prediction of RSL for the wider East Anglia region. RSL, in addition to sediment supply and barrier dynamics, are evaluated as driving mechanisms for the changes identified for the Suffolk coast. Finally, conclusions are presented in **Chapter 8**.

Chapter 2: Literature Review

This chapter provides an overview of the dominant driving mechanisms controlling back-barrier sedimentation for the southern North Sea basin during the early (c. 11.7- 8.2 ka), mid- (c. 8.2-4.2 ka) and late (c. 4.2 ka- present day) Holocene (Walker et al., 2018). The Suffolk coast, southeast England, is used as a case study in this thesis to improve understanding of the driving mechanisms of Holocene coastal evolution. The pattern of Holocene sedimentation in the East Anglia region of southeast England is therefore discussed. Consideration is also given to RSL change, variation in sediment supply and barrier dynamics and human land use change on the Suffolk coast.

2.1. Holocene evolution of the southern North Sea basin

The southern North Sea basin (Figure 2.1) has undergone dramatic changes in palaeogeography since the Last Glacial Maximum (LGM) (Shennan et al., 2000a). Back-barrier stratigraphy contains a detailed and complex record of the driving mechanisms of coastal change, which vary through space and time, modulated by local factors. Extensive research has been undertaken on the coastal plains of the Netherlands, Belgium and southern England to elucidate the pattern of Holocene coastal evolution (e.g. van de Plassche, 1982a; Beets et al., 1992; Long and Innes, 1993; 1995; Denys and Baeteman, 1995; Long et al., 1996; 2002; Spencer et al., 1998; Beets and van der Spek, 2000; Baeteman and Declercq, 2002). Research investigating the Holocene evolution of these coastal plains has shown that the driving mechanisms of coastal change vary spatially and temporally. The rate of RSL rise greatly influenced the southern North Sea depositional record. Local factors, such as variation in sediment supply, morphology of the pre-flooded surface, barrier presence and status, and the influence of river catchments, modulate how the sedimentological signal is recorded (Beets et al., 1992; Beets and van der Spek, 2000; Baeteman and Declercq, 2002; Pierik et al., 2017).
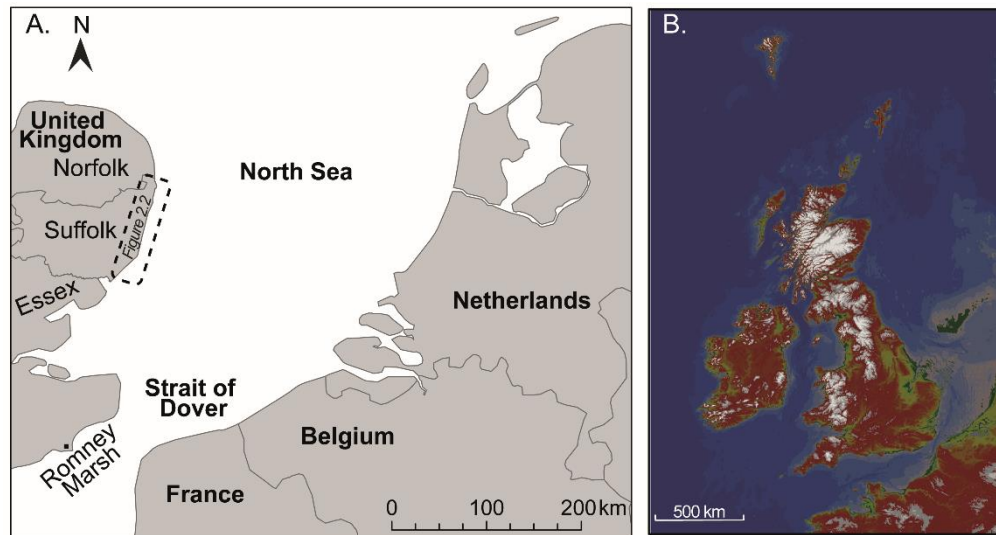
Figure 2.1: A. Map of southern North Sea basin with the dashed box denoting the Suffolk coastline, which is shown in greater detail in Figure 2.3. B. Palaeogeographical model of the UK and southern North Sea basin at 8 ka BP illustrating the Strait of Dover connecting the Southern Bight and northern North Sea, with Dogger Bank remaining a large island. Adapted from Sturt et al. (2013).

2.1.1 Overview of drivers of Holocene coastal change in the southern North Sea basin

Minerogenic sedimentation representative of tidal environments dominates the early Holocene depositional history of the southern North Sea basin, as high rates of RSL rise resulted in landward advancement of the coast. By 8 ka BP, the Southern Bight and northern North Sea were connected, with Dogger Bank (Figure 2.1B) remaining a large island (Beets and van der Spek, 2000). Palaeotidal modelling indicates that the opening of the Strait of Dover at c. 8.2 ka BP rapidly increased the tidal range in the English Channel (Austin, 1991). A high RSL rise rate is recorded throughout the southern North Sea Basin prior to c. 7500 cal BP, exceeding 7 mm yr^{-1} on the Belgian and Dutch coast (e.g. van de Plassche, 1982a; Denys and Baeteman, 1995; Beets and Van Der Spek, 2000; Baeteman and Declercq, 2002) whilst on Romney Marsh RSL rose by 20 m between c. 9000 and 6000 cal BP (Long and Innes, 1993). The coastal response, and resulting depositional history, to this relatively rapid rate of early Holocene RSL rise was modulated by local factors. In Belgium for example, thin peat and vegetation layers occur intercalated within early Holocene estuarine deposits, indicating short-lived periods when organic sedimentation outpaced minerogenic deposition (Beets and van der Spek, 2000; Baeteman and Declercq, 2002). One explanation for these thin organic layers is fluctuating dominance between the RSL rise rate and sedimentation rate, with periods when the RSL rise rate is exceeded by the sediment supply rate resulting in the initiation of freshwater vegetation (Waller and Kirby, 2002). In contrast, sediment supply in the Netherlands was

unable to keep pace with the creation of accommodation space prior to 7 ka BP, resulting in subtidal sedimentation dominating (Beets and van der Spek, 2000). After 7 ka BP RSL rise rate decreased throughout the southern North Sea basin (Figure 2.2), to less than 3 mm yr^{-1} on the Belgian and Dutch coast (van de Plassche, 1982; Denys and Baeteman, 1995; Baeteman and Declercq, 2002), balancing the rate of sediment supply with the creation of accommodation space, resulting in local barrier stabilisation, progradation and silting of tidal basins and their inlets (Beets and van der Spek, 2000).
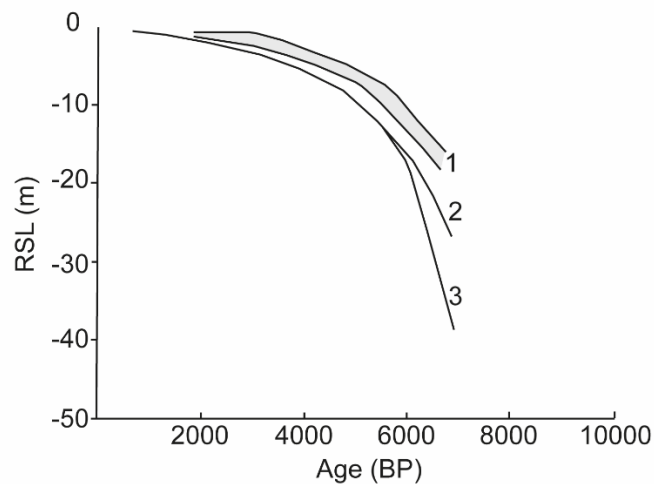
Figure 2.2: Schematic of Holocene RSL change for (1) the Belgian coastal plain, (2) the Dutch coastal plain and (3) the northern North Sea (Jelgersma, 1961; Ludwig et al., 1981; van de Plassche, 1982; Denys and Baeteman, 1995). Adapted from Beets and van der Spek (2000). Permission to reproduce this figure has been granted by Cambridge University Press.

The transition from the early to mid-Holocene in the southern North Sea basin is marked by a shift in the relative importance of the driving mechanisms controlling sedimentation, with RSL rise rate decreasing in importance and sediment supply increasing, highlighting that the relative dominance of a driving mechanism varies spatially and temporally. The RSL rise rate declined after 7 ka throughout the southern North Sea basin to less than 3 mm yr^{-1} (van de Plassche, 1982; Denys and Baeteman, 1995; Baeteman and Declercq, 2002; Long et al., 2006a). This enabled sediment supply to equal, and eventually surpass, the creation of accommodation space, halting the landwards migration of tidal sedimentary environments and stabilising the shoreface, resulting in shoreline progradation (Beets and van der Spek, 2000; Baeteman and Declercq, 2002). Freshwater marsh and peat sedimentation was dominant throughout the majority of the Belgian coastal plain between 5.5 and 4.5 ka (Beets and van der Spek, 2000; Baeteman and Declercq, 2002) whilst the central section of the Dutch coast had prograded nearly 10 km by 2 ka (Beets and van der Spek, 2000). The widespread accumulation of peat by 4 ka in the Rye area of Romney Marsh corresponds with a fall in the rate of RSL rise and indicates barrier formation and

stabilisation, enabling the accumulation of thick peat sequences (Long and Innes, 1995; Long et al., 1996; Spencer et al., 1998). This interpretation is supported by a shift from wet alder-dominated vegetation to acidic pollen, as the later communities require isolation from eutrophic terrestrial and coastal waters therefore indicating that the coastal barrier was stable (Waller, 1993; Long and Innes, 1995; Long et al., 1996).

The late Holocene is characterised by a return to minerogenic, tidal sedimentation and the culmination of a 2000-3000 year period of peat accumulation (Beets et al., 1992; Long and Innes, 1993; 1995; Long et al., 1996; Spencer et al., 1998; Baeteman and Declercq, 2002). Between 4 ka and 2.5 ka mud intercalations occur within the peat in seawards areas on the Belgian coast (Baeteman and Declercq, 2002). These mud intercalations are interpreted as the culmination of the coastal plain progradation and the re-entrance of the tidal system to the Belgian coastal plain. In the Romney Marsh area, widespread marine conditions returned after 3-2 ka, coincident with the landwards migration of the barrier, indicating a reduced sediment supply and increased barrier instability (Long et al., 1996; Spencer et al., 1998). Aquatic and salt marsh pollen from Romney Marsh record an increase in water table height and salinity, indicating penetration of saline water and progressive barrier breakdown, likely through the creation, widening and landward penetration of tidal inlets (Long and Innes, 1993; 1995; Long et al., 1996). The mechanisms responsible for the cessation of peat sedimentation throughout the southern North Sea basin are not fully understood, with the following local factors suggested as potential explanations (Long et al., 2006b). Long et al. (2000) proposed that conditions may have been unfavourable for the preservation of organic sedimentation during the late Holocene. The low RSL rise rate during the late Holocene was argued to be unfavourable for the preservation of organic deposits as a rising water table is necessary to create and maintain the anaerobic conditions required for preservation (Long et al., 2000). The digging and excavation of peat for industrial purposes during the Iron Age and Roman Period is suggested to have enhanced the natural process of late Holocene inundation of peat in Zeeland, southern Netherlands (Vos and van Heeringen, 1997). Reclamation and drainage of late Holocene wetlands, by tidal creek extension or lowering of the water table, is proposed to have further compacted the peat, creating accommodation space and increasing vulnerability to tidal flooding (Baeteman et al., 2002; Mrani-Alaoui and Anthony, 2011). Natural preconditions, such as sediment delivery and coastal plain extent, are also argued to have been influential for the cessation of late Holocene peat sedimentation in the southern North Sea basin (Pierik et al., 2017).

2.1.2 Overview of Holocene stratigraphic record for East Anglia

This section will provide a general overview of the stratigraphic investigation undertaken across East Anglia (Figure 2.3; Norfolk, Suffolk and Essex), highlighting the similarities and differences in the frequency, altitude and chronology of peat horizons in Holocene records. Lithostratigraphic similarities exist between the Holocene sequences of intercalated peat horizons in northern Suffolk (Bure-Yare-Waveney estuary and Blyth estuary) and east Norfolk (Funnell, 1979; Coles and Funnell, 1981; Alderton, 1983; Brew et al., 1992; Boomer and Godwin, 1993). These alternations between organic and minerogenic sediment units indicates periods of marine influence and absence and therefore changes in sea-level tendency (changes in marine influence). Sedimentation changes, and therefore changes in sea-level tendency, preserved in sediment records do not necessarily equate to changes in RSL, and assuming so fails to consider the influence of sedimentological factors (Duffy et al., 1989; Jennings et al., 1995). For example, barrier dynamics was identified as an influential driving mechanism of Holocene sedimentation in east Norfolk (Coles and Funnell, 1981; Alderton, 1983; Boomer and Godwin, 1993). The Holocene sequence from southern Suffolk contrasts with northern Suffolk and Norfolk, as minerogenic estuarine sedimentation dominates and peat is limited or absent (Carr & Baker 1968; Carr 1971; Brew et al. 1992).

Peat formation on the pre-Holocene basement of the north Norfolk coast began between 11000 and 10000 cal BP, continuing until at least 7000 cal BP in western sections of the coast. However, minerogenic sedimentation generally dominates the Holocene sediment sequence (Figure 2.4A) from the north Norfolk coastline (Andrews et al., 2000; Boomer and Horton, 2006). A transition to marine mudflats and saltmarsh environments occurred in eastern sections of the north Norfolk coast between 7000 and 6000 cal BP, and from 6000 cal BP onwards on western sections (Andrews et al., 2000; Boomer and Horton, 2006). A between-site comparison of the saltmarsh units of the north Norfolk coast identified small scale changes in sea-level tendency, which occur at variable altitudes and cannot be correlated beyond several hundred metres (Andrews et al., 2000). In addition, localised late Holocene peat deposits were identified at several locations. Andrews et al. (2000) highlights the autocyclic nature of Holocene saltmarsh and mudflat development on the north Norfolk coast, concluding that the general pattern of sedimentation reflects the influence of barrier and tidal creek evolution superimposed upon regional RSL change.
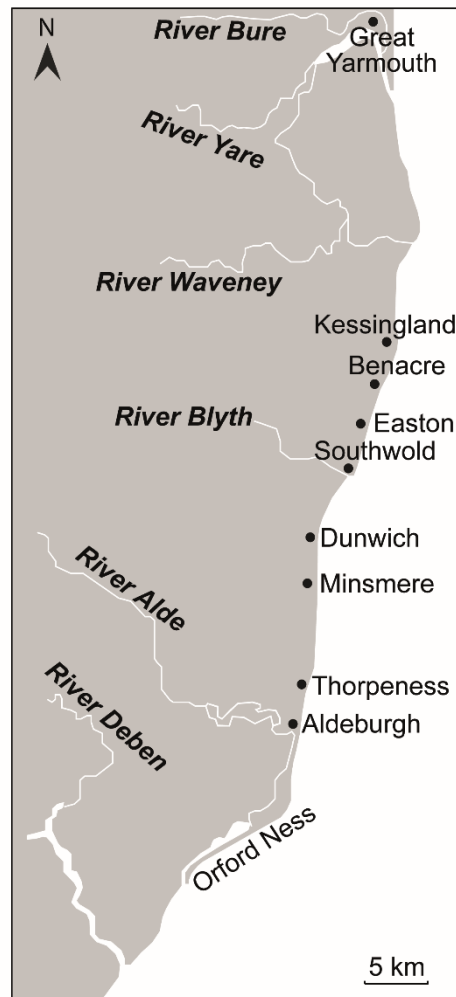
Figure 2.3: Map of Suffolk coast with locations mentioned in text. The location of the Suffolk coast relate to the southern North Sea basin is illustrated on Figure 2.1.

Extensive stratigraphic investigation of the valleys of the Bure-Yare-Waveney estuary system identified a Holocene sediment sequence generally comprised of a lower, middle and upper freshwater peat separated by estuarine clay units (Funnell, 1979; Coles and Funnell, 1981; Alderton, 1983; Boomer and Godwin, 1993). Pollen evidence (e.g. Jennings, 1955), in addition to radiocarbon dating, have provided chronological constraint for the sedimentation changes in this region (Figure 2.4C). The role of tidal influence on the valleys of the Bure-Yare-Waveney estuary system has long been acknowledged (Innes, 1912). Coles and Funnell (1981) associate the Holocene sediment sequences from this estuary system with changes in RSL as well as the development and destruction of barrier systems. The onset of upper clay sedimentation at the coast, for example, is associated with sandy sediment containing open estuarine and estuarine channel foraminifera interpreted as the destruction of a barrier and strong incursion of marine water (Coles and Funnell, 1981).
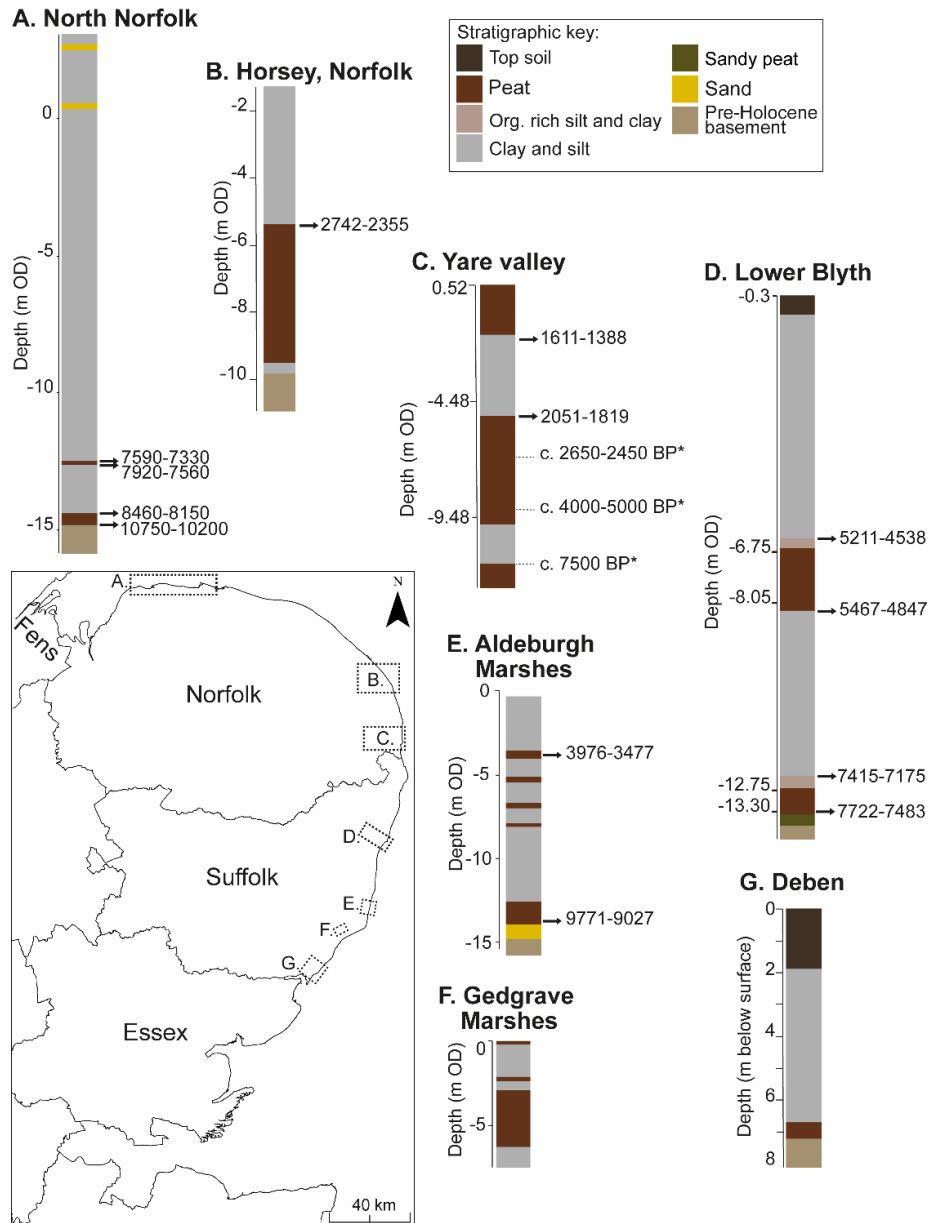
Figure 2.4: Spatial variability of Holocene sedimentation in Norfolk, Suffolk and Essex. The Holocene sediment sequences illustrated present the general stratigraphic changes at each site, synthesising the research undertaken on the East Anglian coast to improve understanding of Holocene coastal evolution, RSL and environmental change. Greater detail, in particular the within site variability resulting from local factors, is provided in the literature associated with this figure. The location of each site is shown on the map inset. A. North Norfolk (Andrews et al., 2000; Boomer and Horton, 2006), B. Horsey, Norfolk (Horton et al., 2004), C. Yare valley (Funnell, 1979; Coles and Funnell, 1981; Alderton, 1983), D. lower Blyth (Brew et al., 1992), E. and F. Aldeburgh and Gedgrave marshes respectively (Carr and Baker, 1968), G. Deben (Brew et al., 1992) and H. Blackwater estuary (Wilkinson and Murphy, 1995). * denotes a chronology based on pollen assemblage.

The Holocene sequence from the lower Blyth estuary in north Suffolk (Figure 2.4D) is comprised of a basal freshwater peat, overlain by a lower clay, middle peat and upper clay (Brew et al., 1992). The transition from basal peat to lower clay sedimentation is denoted by a shelly horizon, in addition to intertidal environments replacing freshwater environments. The rapidity of the litho- and bio-stratigraphic changes indicates that this contact is eroded. Brew et al. (1992) hypothesise that the influx of sandy marine water indicates the breach of a barrier or spit feature.

The Holocene sediment sequence from the lower Blyth is stratigraphically similar to those in the Bure-Yare-Waveney estuary system with two notable differences (Funnell, 1979; Coles and Funnell, 1981; Alderton, 1983; Brew et al., 1992; Boomer and Godwin, 1993).

(1) Middle peat growth in the Blyth estuary culminates at c. 4850 cal BP, much earlier than in the Bure-Yare-Waveney estuary system, where growth continues until c. 2000 cal BP. This later cessation of peat growth in the Bure-Yare-Waveney system may have resulted from continued terrestrial freshwater input restricting marine conditions from re-establishing (Coles and Funnell, 1981). The onset of peat growth at c. 4.5 ka BP in the Blyth (Brew et al., 1992) corresponds with the onset of peat sedimentation in the Fens (Godwin, 1978; Shennan, 1986) and north Norfolk (Funnell, 1979; Funnell and Pearson, 1989).

(2) An upper peat unit only occurred in peripheral locations across the lower Blyth (Brew et al., 1992). The cessation of upper clay sedimentation and return to peat growth after 2 ka BP in the Bure-Yare-Waveney estuary is attributed to the development of the Great Yarmouth spit and resulting reduction in tidal influence (Jennings, 1955; Coles and Funnell, 1981; Brew et al., 1992).

The stratigraphy of the south Suffolk estuary systems, the Alde-Ore and Deben-Stour-Orwell (Figure 2.4E-G), contrasts with that of the Bure-Yare-Waveney estuary system and the Blyth. South of Aldeburgh, and on the marshes associated with Orford Ness, peat deposits are limited and discontinuous within the Holocene records (Carr and Baker, 1968; Carr, 1971). There is no evidence of significant or consistent Holocene changes in sea-level tendency in the south Suffolk estuaries (Brew et al., 1992). The Holocene sequences of the marshes neighbouring the River Ore are dominated by silt and clay and presumed to be of estuarine origin (Carr and Baker, 1968; Carr, 1971), whilst Holocene sequences comprised of alluvial silt and clay, nearly absent of peat, occur in the Deben-Stour-Orwell system (Brew et al., 1992). Further south, the Holocene sequence from Essex (Figure 2.4H), is primarily composed of calcareous clayey silts and sands believed to be sub-tidal and intertidal in origin (Greensmith and Tucker, 1971; Wilkinson et al., 1988). Biogenic deposits (e.g. freshwater fen or *Phragmites* peat) are present at variable altitudes on the

Essex coast. In the Blackwater estuary, for example, continuous sedimentation, reflecting a transition from brackish swamp to intertidal mudflats, dominates with freshwater sedimentation absent (Wilkinson and Murphy, 1995). Elsewhere, such as Dovercourt Bay in northern Essex, variations in diatom assemblage composition and biota preservation indicate fluctuations between terrestrial high marsh conditions, low salt marsh and mudflats (Wilkinson and Murphy, 1995).

As demonstrated above, the Holocene sediment sequences from East Anglia show some evidence of regional similarities in sea-level tendency, particularly for east Norfolk and northern Suffolk (Figure 2.4). Although the overall pattern of changes in sea-level tendency between east Norfolk and northern Suffolk is comparable, the sedimentary response shows substantial inter- and intra-site variability. For example, a transition from middle peat to upper clay occurs in the Blyth estuary and the Bure-Yare-Waveney estuary system, however, the timing of this transition varies by c. 2 ka between sites. Despite this, existing research indicates that similar driving mechanisms (barrier dynamics, sediment supply, RSL change) have been influential for the pattern of sedimentation on the East Anglian coast (Coles and Funnell, 1981; Brew et al., 1992; Boomer and Godwin, 1993).

2.2 RSL change

2.2.1 Reconstructing changes in RSL

The nature of RSL data

A robust methodology for producing sea-level index points developed during the International Geological Correlation Programme (IGCP) Projects 61 and 200 (Preuss, 1979; Shennan, 1982; 1986; Tooley, 1982; van de Plassche, 1982; 1986; Shennan et al., 1983). RSL change (ΔRSL), relative to present, is defined as follows for a geographical location (σ) and time (t) (Shennan et al., 2012; Shennan, 2015):

$$\Delta RSL\ (\sigma, t) = \Delta RSL\ (\sigma, t) + \Delta EUS\ (t) + \Delta ISO\ (\sigma, t) + \Delta TECT\ (\sigma, t) + \Delta LOCAL\ (\sigma, t) + \Delta UNSP\ (\sigma, t)$$

Where:

- ΔEUS (t) is the time-dependent eustatic function

- ΔISO (σ, t) is the combined isostatic effect of glacial rebound processes resulting from ice load (glacio-isostatic), water load (hydro-isostatic) and the redistribution of ocean mass due to rotational contributions

- ΔTECT (σ, t) is the tectonic effect (e.g. plate movements, uplift, mountain building)

- ΔLOCAL (σ, t) is the total effect of local processes in the coastal system, including the total effects of tidal regime change and sediment compaction

- ΔUNSP (σ, t) is the effect of factors that have not been thought of or quantified.

In situ sediments and fossil organisms, as well as morphological and archaeological features, can be utilised to estimate changes in sea level relative to present when shown that palaeo sea level controlled their origin (Shennan, 2015). Estimates of vertical movements in RSL can be determined from these indicators by producing sea-level index points (Shennan, 1982; Tooley, 1982; van de Plassche, 1986), which are defined by their location, age, elevation and tendency (Shennan, 2015).

Reconstructions of post-LGM RSL change have extensively used radiocarbon dating to determine the age attribute of sea-level index points (see Shennan et al. (2018) and references within database), whilst the location is simply defined by geographical co-ordinates. Tendency relates to the direction of marine influence recorded by an index point, with a positive or negative tendency equating to an increase or decrease in marine influence respectively (Shennan, 1982; 2015; van de Plassche, 1986). Comparisons of the tendency of sea-level index points provides a means for evaluating RSL data to determine if the changes recorded by a sea-level indicator are of local or regional significance (Shennan, 1986; Long, 1992; Shennan et al., 2018).

The elevation attribute, termed the indicative meaning, denotes the vertical relationship between the local environment a sea-level indicator formed at and a contemporaneous reference tide level (van de Plassche, 1986; Shennan, 2015). The indicative meaning (Figure 2.5) is defined by the present day vertical tidal range over which a sea-level indicator occurs (indicative range), measured relative to an assigned tide level (reference water level) (van de Plassche, 1986; Horton et al., 2013; Shennan, 2015). The indicative meaning developed from the theory that sediments within intercalated sediment sequences, which occur vertically adjacent to each other with no evidence of a hiatus, formed in environments horizontally adjacent to each other (Shennan, 1980; Horton, 1997).

Estimates of the indicative meaning of sea-level indicators from temperate coastlines were determined by Shennan (1980; 1982; 1986), based on inferences made from Godwin (1940; 1978), Kidson and Heyworth (1978), van de Plassche (1986) and Tooley (1979). Brooks and Edwards (2006) and Shennan et al. (2018) later modified these indicative meaning estimates. Estimates of the indicative meaning, determined by the aforementioned references, have been used for the various iterations of the geological RSL database created for the UK and Ireland to establish a relationship between the

elevation of a sea-level indicator and a reference tide level (Shennan and Horton, 2002; Brooks and Edwards, 2006; Shennan et al., 2018).

Indicative meanings are determined for each individual sea-level index point based on the stratigraphic transition under consideration. Table 2.1 outlines the reference water level, listed as a mathematical expression of tidal parameters, and the associated indicative range, for various sample types based on the existing literature (Shennan, 1980; 1986; Brooks and Edwards, 2006; Shennan et al., 2018). The indicative range for each sample is minimised by dating close to the position at which a change in microfossil and/or stratigraphic evidence occurs. Freshwater limiting sea-level index points are produced from samples that do not show a direct relationship with a contemporaneous tide level, they may have formed at or above mean high water spring tide (MHWST) therefore constraining RSL at, or below, the level at which they are found.
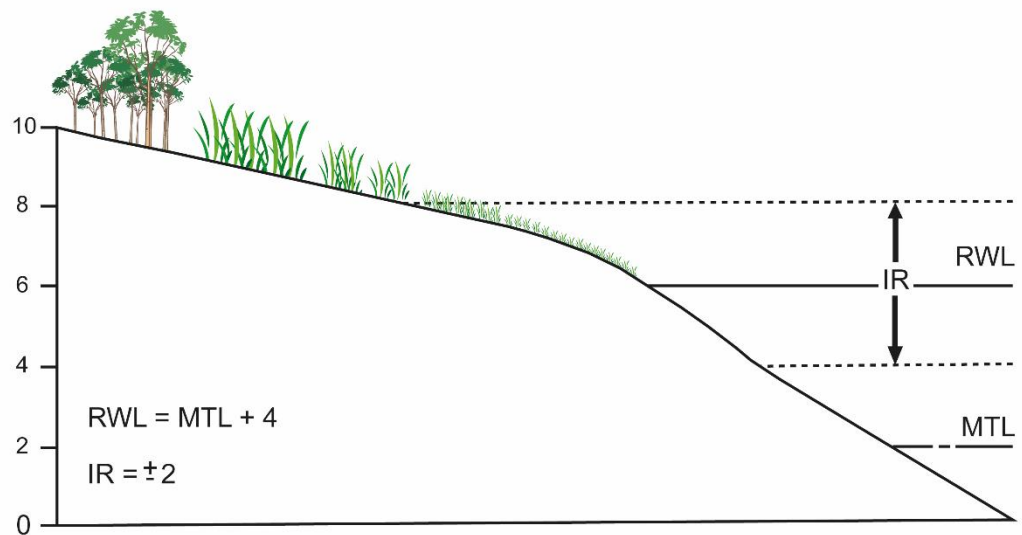
Figure 2.5: Schematic representation of the indicative meaning determined from the reference water level (RWL) and indicative range (IR) and calculated using mean tide level (MTL). Adapted from Horton et al. (2004). Permission to reproduce this figure has been granted by Elsevier.

Table 2.1: Indicative meanings used to determine the position of RSL for different types of samples, given as the present day vertical tidal range over which a sea-level indicator occurs (indicative range), measured relative to an assigned tide level (reference water level). Mean high water spring tides (MHWST), highest astronomical tide (HAT), mean tide level (MTL) and M^1 ((MHWST+HAT)/2).

Sample type	Evidence	Reference water level (m)	Indicative range (m)	Reference
High marsh environment	Herbaceous or *Phragmites* peat directly below tidal marsh deposit.	MHWST – 0.2	0.2	Shennan (1986), Brooks and Edwards (2006), Shennan et al. (2018)
Basal peat	Freshwater peat or wood that shows a direct relationship to a contemporaneous tide.	MHWST + 0.2	0.8	Brooks and Edwards (2006)
Freshwater to high marsh transition	Fen wood peat directly above *Phragmites* peat or tidal marsh deposits.	(MHWST + HAT)/2	0.2	Shennan et al. (2018)
Mid-marsh environment	Reedswamp above marine minerogenics.	MHWST + 0.6	0.4	Brooks and Edwards (2006)
High marsh environment.	Herbaceous or *Phragmites* peat directly above tidal marsh deposit.	M^1 - 0.2	0.2	Shennan (1986), Shennan et al. (2018)
Freshwater/terrestrial limiting	Freshwater peat or wood that does not show a direct relationship to a contemporaneous tide.	(MTL+HAT)/2	MTL to HAT	Shennan et al. (2018)

Errors associated with RSL reconstruction

Potential sources of error, resulting from the collection and interpretation of RSL data, are associated with the age and elevation estimates of a sea-level index point. Major sources of uncertainty include; spatial scale of the study, for example crustal movements and the coastal setting; temporal scale, such as changes in tidal range since sample deposition; indicative meaning of a sample; and compaction (Shennan, 2007; Baeteman et al., 2011). The total error (E_t) is the 'sum of all quantified errors', such as field levelling, changes in tidal range and sediment compaction, determined as follows:

$E_t = \sqrt{(e_1^2 + e_2^2 + e_3^2 + \ldots + e_n^2)}$

where $e_1 \ldots e_n$ are individual sources of error (Preuss, 1979; Shennan, 2015).

Compaction relates to the suite of syn- and post-depositional processes that affect sediment volume and distort stratigraphy, resulting in considerable altitudinal uncertainty for highly compressible peats and fine-grained minerogenic sediments (Allen, 2000; Baeteman et al., 2011). The total effect of compaction equates to post-depositional lowering of the original elevation of the sediment, this introduces uncertainties into estimates of the rate and magnitude of RSL change (Kaye and Baghoorn, 1964; Allen, 2000; Brain, 2006; 2015). Allen (2000, pp 1187) defines compaction as "*the set of processes whereby the sediment within a growing stratigraphic column diminishes in volume by the rearrangement of the mineral skeleton, and a range of post-depositional effects, on account of its self-weight and age.*" The magnitude of compaction is dependent on lithology, thickness and morphology of the stratigraphic column, mechanical and chemical sediment properties, loading history, water content variation and time (Brain, 2006; 2015). Mechanical processes of compaction (consolidation and creep) compress sediments due to the vertical stress and pressure exerted by overburdening material, resulting in sediment particles becoming tightly packed due to the expulsion of pore water, in addition to causing sediment particles to move and rearrange (Brain, 2015). Compaction can also result from the interaction between biological and chemical processes, causing organic matter humification (Brain, 2015). Highly organic material can decrease in volume by 90 % due to its highly porous structure whilst the compaction of sand is subordinate (Kaye and Baghoorn, 1964; Haslett et al., 1998; Shennan and Horton, 2002). As a result, compaction can be considerable within cores comprised of peat intercalated between thick Holocene minerogenic sediments (Jelgersma, 1961; Kaye and Baghoorn, 1964; Horton et al., 2013). For example, Zong and Tooley (1996) interpreted that peat units had reduced by over 50 % due to thick (> 15 m) minerogenic sediments overlying them. Overburdening loads can result in the compaction of peat to at least one-eighth of its original thickness (Kaye and Baghoorn, 1964; van de Plassche, 1980). Altitudinal variability of peat beds across a site has been attributed to compaction. Variability of peat bed altitude at Romney Marsh has been suggested to indicate lowering locally of 4.2 m, if a large planar peat surface previously existed (Long et al., 2006b) whilst differential compaction exceeding 6 m has been identified in the Rhine-Meuse Delta in The Netherlands (de Groot and de Gans, 1996). Sea-level index points from estuaries in the south and east of England plot consistently below GIA model predictions (e.g. Shennan et al., 2018) due to compaction, with average Holocene rates of 0.4 ± 0.3 mm yr^{-1} estimated for the east coast of England (Horton and Shennan, 2009).

Correction for compaction varies in complexity. Sediments from the base of the basal unit cannot be lowered by compaction because they overly an incompressible substrate, providing an opportunity to avoid the effect of compaction when reconstructing RSL (Brain, 2015). However, any basal sediments not in direct contact with the basement surface will have experienced a degree of compaction due to the underlying compressible sediments. An initial assessment of the influence of compaction can be made by comparing the altitude of basal, base of basal and intercalated sea-level index points (e.g. Boomer and Horton, 2006; Horton and Shennan, 2009; Shennan et al., 2018). Geotechnical modelling can be used to decompact sediment sequences and correct the elevation of sea-level index points to their original depositional altitude. Model accuracy is dependent on an empirically informed and validated model that is suitable for low-energy intertidal sediments and stress conditions (e.g. Paul and Barras, 1998; Massey et al., 2006; Brain et al., 2012). Geotechnical models require testing (e.g. the oedometer test) on undisturbed sediments to produce sediment compressibility information (Brain, 2015). Samples from depth are difficult to obtain and therefore empirical relationships between physical properties and/or environmental conditions are always used instead. Despite the development of decompaction models, compaction remains an error which is difficult to quantify as information, such as the initial composition, moisture content and pore-water space of the sediment, is often unobtainable (e.g. Baeteman et al., 2011).

Changes in tidal range are a major temporal uncertainty associated with sea-level index points (Brooks and Edwards, 2006; Baeteman et al., 2011; Griffiths and Hill, 2015), with numerical models indicating significant global changes in tides since the LGM (Gehrels et al., 1995; Shennan et al., 2000b; Neill et al., 2010; Griffiths and Hill, 2015; Ward et al., 2016). Changes in tidal dynamics influence the location of tidal mixing fronts, the dissipation of tidal energy, shelf sea biogeochemistry, estimates of land and RSL movement, sediment transportation and deposition as well as tidal range (Shennan et al., 2003; Griffiths and Hill, 2015; Ward et al., 2016). Changes in water depth and shelf width, resulting from RSL change, cause tidal range change (Griffiths and Hill, 2015). In addition, changes in tidal range will affect reconstructions of the position of RSL change, as the tides used to calculate the indicative meaning of a sea-level index point (e.g. MHWST) will vary through time with tidal amplitude (Gehrels et al., 1995; Shennan et al., 2000a; Uehara et al., 2006; Neill et al., 2010; Ward et al., 2016). Consideration of a palaeotidal correction is therefore necessary when determining the indicative meaning of a sea-level index point to ensure the RSL curve is "true" (Griffiths and Hill, 2015; Ward et al., 2016). Tidal evolution modelling for the northwest European shelf seas indicates that the tidal amplitude for the east coast of Britain has remained close to its present day location since 8 ka BP (Uehara et al., 2006; Ward et al., 2016). Changes in tidal range for the east coast of England were

minimal at the open coast, but much more substantial in large estuaries, such as the Humber and the Fenlands, where modelled tidal ranges were 20 - 40 % smaller between 6 and 3 ka BP (Shennan et al., 2003; Horton and Shennan, 2009). In addition, changes in tidal parameters require consideration as changes in coastal configuration, local morphology and relatively small changes in RSL can result in non-trivial changes in tidal parameters (Griffiths and Hill, 2015; Shennan et al., 2018).

2.2.2 RSL change in UK

RSL change has been extensively studied throughout the UK and Ireland, beginning with the screening and compiling of RSL data during IGCP Project 61 (1974-1982) (Shennan, 1989; Shennan and Horton, 2002; Brooks and Edwards, 2006; Shennan et al., 2006; 2018). A wealth of sediment archives and landforms (e.g. raised beaches, isolation basins, salt marsh sediments) are available to assist production of quantitative constraints on the age and altitude of RSL position since the LGM. During the LGM, the British and Irish Ice Sheet covered much of northern Britain and Ireland and coalesced with ice from Fennoscandia to form the European Ice Sheet Complex (Patton et al., 2015). At maximum extent, reached by 27000 BP, the volume of the British and Irish Ice Sheet was equivalent, when melted, to ~ 2.5 m rise in global sea level when melted and comparable to one third of the volume of the West Antarctic Ice Sheet (Clark et al., 2012). Although the British and Irish Ice Sheet is small in global terms, the interaction between regional GIA, deformation of the ocean geoid and changes in the global ocean volume created a spatially diverse and complex post-LGM RSL history (Figure 2.6) for the UK and Ireland (Flemming, 1982; Shennan, 1989). The reconstructions and model predictions for locations situated under the thicker areas of ice cover record a fall-rise-fall RSL history (e.g. Arisaig – see Figure 2.6), whilst locations at or beyond the margins record a rising RSL during the Holocene (e.g. Norfolk). As the UK and Ireland are located on the boundary of the Fennoscandian ice-sheet, they experienced the collapse of the proglacial forebulge, which provides excellent constraint for the earth model parameters of GIA models (e.g. Bradley et al., 2011; Kuchar et al., 2012). The rapidity of deglaciation, aided by ice streams (e.g. Bradwell and Stoker, 2015), increases the potential for long records, extending beyond 15,000 years ago, due to areas becoming free of ice sooner.

Records of past RSL change are vital for constraining and validating GIA, ice sheet and RSL models, in order to improve understanding and predictions of future changes. GIA models contain Late Pleistocene ice sheet models, an earth model replicating the rheology of the solid earth and a RSL change model to determine the redistribution of ocean mass (Farrell and Clark, 1976; Lambeck, 1993a; 1993b; Peltier, 1998). Model parameters have evolved through time, for example, lithospheric thickness has been altered due to the

sensitivities of RSL predictions to variations in shallow earth model parameters (Shennan et al., 2000a; 2002). Glacial isostatic rebound is particularly sensitive to lithospheric thickness in Scotland (Peltier, 2002), illustrated in Edinburgh where lithospheric thicknesses, ranging from 50 to 150 km, resulted in early Holocene RSL predictions that varied by ~50 m (Lambeck, 1993a). The 'optimum' lithospheric thickness varies for GIA models, with values for the UK and Ireland varying between 65 km and 120 km (Lambeck, 1995; Peltier, 2002; Peltier et al., 2002; Shennan et al., 2002; Bradley et al., 2011).
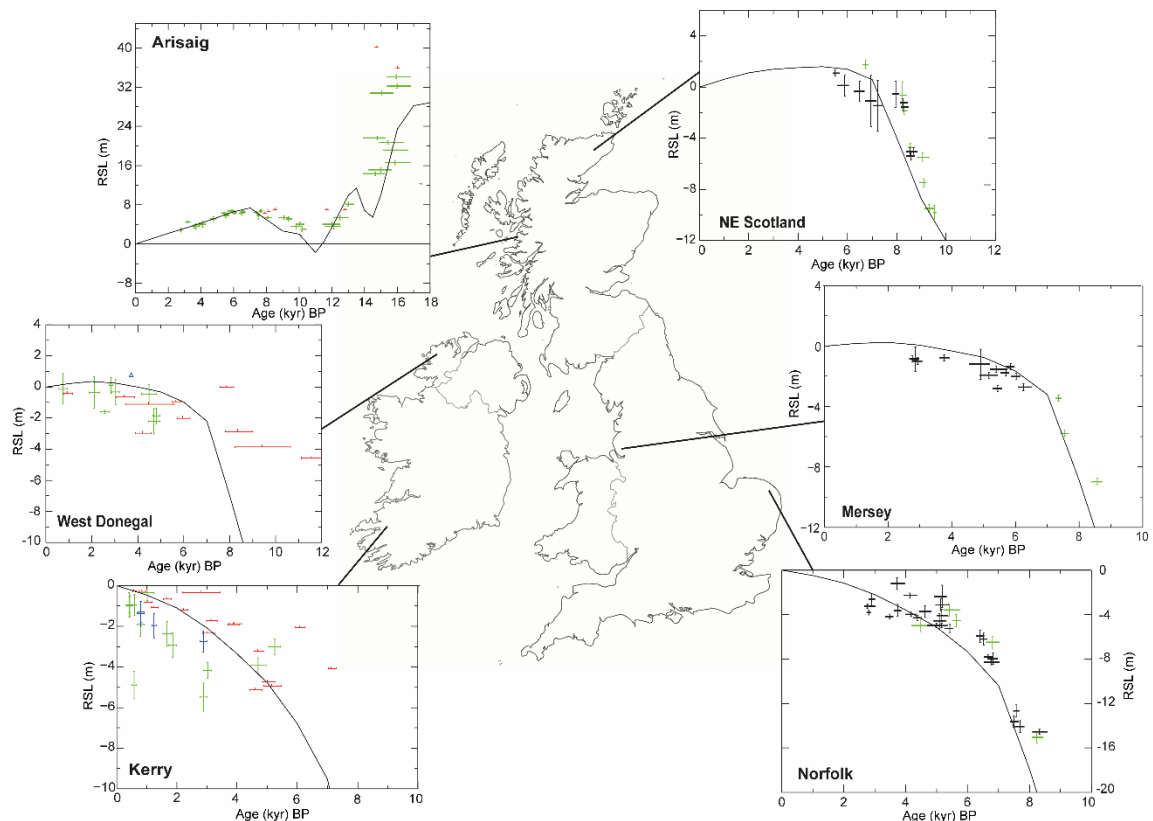
Figure 2.6: Spatial variability of RSL history in the UK and Ireland. The proximity of sites to the centre of uplift, close to Forth Valley, Scotland, influences the occurrence and height of the mid-Holocene highstand. Data point colour indicates data type, with green equating to basal sea-level index points and black to intercalated sea-level index points. Limiting data is subdivided into primary (red) and secondary (blue) points, with the source environment defined for the former but unclear or contested for the later. Adapted from Bradley et al. (2011). Permission to reproduce this figure has been granted by Sarah Bradley.

RSL data helps to constrain and refine GIA models, such as Bradley et al. (2011) and Kuchar et al. (2012) for the UK and Ireland, leading to an improved understanding of ice sheet configuration, earth rheology, lithospheric thickness and mantle viscosity. Comparison of the existing RSL database for the UK and Ireland (Shennan et al., 2018) with RSL predictions from GIA models for the Holocene identified good fit for southern England, including East Anglia, using the Bradley et al. (2011) model, with a poorer fit

being obtained using the Kuchar et al. (2012) model. In addition, the Kuchar et al. (2012) model tends to overestimate isostatic rebound around the centre of the British and Irish Ice Sheet, whilst the Bradley et al. (2011) model underestimates. The disparity between the RSL predictions produced by these GIA models relates to the reinterpretation of trimline data. Kuchar et al. (2012) uses a three-dimensional thermomechanical ice sheet model (Hubbard et al., 2009) to test the interpretation of trimline data as englacial thermal boundaries, rather than vertical ice limits (Ballantyne and Hall, 2008; Ballantyne, 2010; Fabel et al., 2012). The resulting ice sheet is thicker than that modelled by Bradley et al. (2011) but less extensive laterally as it is not constrained by geomorphological evidence. The next generation of GIA models will benefit from the updated RSL database (Shennan et al., 2018) and new iterations of British and Irish Ice Sheet models resulting from the BRITICE project (e.g. Clark et al., 2018).

A revision of the Bradley et al., (2011) model provides the most up-to-date GIA predictions for the East Anglia region (Bradley, personal communication 2019). This revised model utilises the same ice sheet reconstruction and earth model as the Bradley et al. (2011) model but the regional ice model is run at twice the resolution (~ 35 km grid resolution). The Bradley et al. (2011) model for the UK and Ireland uses a lithospheric thickness of 71 km, an upper mantle viscosity ranging from 4 to 6 x 10^{20} Pa s and a lower mantle viscosity ≥ 3 x 10^{22} Pa s. Bradley et al. (2011) utilises an ice model, which combines the Brooks et al. (2008) model for the British and Irish Ice Sheet with a revised global ice model. The global ice model was revised due to misfits between reconstructions and predictions for the Holocene, attributed to the rapid termination of global ice melting during the mid-Holocene (Shennan et al., 2006; Brooks et al., 2008; Bradley et al., 2011). Bradley et al. (2011) altered the Bassett et al. (2005) global ice model for the Holocene period to fit a suite of far-field data from China and Malay-Thailand for the Holocene (Bradley et al., 2008), resulting in ice melt ceasing by 1 ka. The GIA model prediction for the East Anglia region (Bradley, personal communication 2019) documents an upward Holocene RSL trend and the decrease in the rate of RSL rise that occurs during this period (Figure 2.7). Comparison between the RSL data and the GIA model prediction for the East Anglian region is made in section 2.2.3.

2.2.3 RSL change in East Anglia and Suffolk

The most recent RSL database for the UK and Ireland collates data from east Norfolk and Suffolk together as East Anglia (Shennan et al., 2018), based on their similar distance from former ice loads and GIA effects. Norfolk and Essex are considered as separate areas in the most recent RSL database (Shennan et al., 2018). The RSL data (Coles and Funnell, 1981; Devoy, 1982; Alderton, 1983; Brew et al., 1992; Horton et al., 2004) documents an

upward Holocene RSL trend with a declining rate recorded throughout the mid- and late Holocene (Figure 2.7). This is typical of an area in southeast England that is at, or beyond, the margins of the British and Irish Ice Sheet (Flemming, 1982; Shennan, 1989). Geologic, geodetic and tide gauge data have illustrated that southeast England is subsiding due to its location on the periphery of the last British and Irish Ice Sheet (e.g. Flemming, 1982; Shennan, 1989; Shennan and Horton, 2002; Shennan et al., 2012), with recent late Holocene estimates 0.61 mm yr^{-1} determined for East Anglia (Shennan and Horton, 2002). The RSL data for East Anglia (Figure 2.7) plot consistently below GIA predictions (Bradley, personal communication 2019) and this is attributed by Shennan et al. (2018) to compaction.
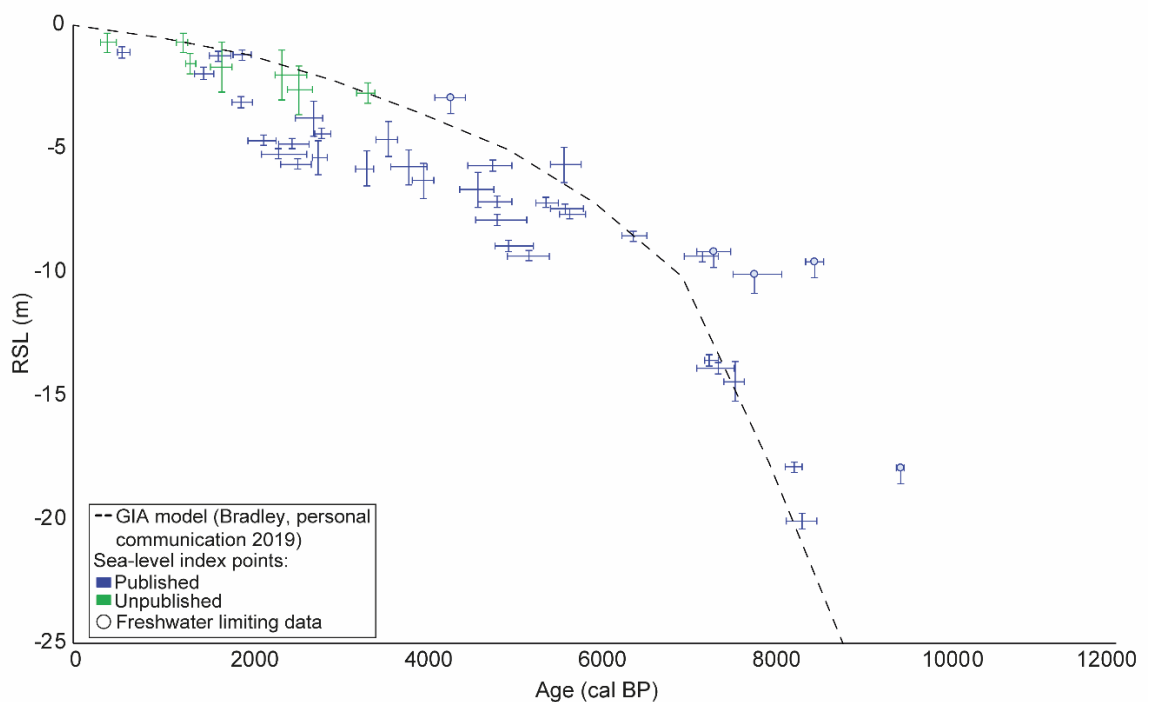
Figure 2.7: Existing sea-level index points (crosses) and freshwater limiting data (circles), published (blue) and unpublished (green), for East Anglia (Coles and Funnell, 1981; Devoy, 1982; Alderton, 1983; Brew et al., 1992; Horton et al., 2004; Lloyd et al., 2008). The dashed line denotes the most recent GIA model predictions of RSL for the region (Bradley, personal communication 2019).

Many of the index points from the mid-Holocene to present day are intercalated i.e. obtained from compacted or consolidated deposits, producing a sea-level indicator that has undergone lowering with time. Other explanations proposed for the scatter of data include an underestimation of the age and/or elevation error or differential GIA, resulting from plotting data from too large a region (Shennan et al., 2018). Shennan (1989) highlighted the susceptibility of the thick sediment sequences from southeast England to compaction, with Shennan et al. (2018) suggesting a compaction correction in the order of 0.4 ± 0.3 mm yr^{-1} is required (Horton and Shennan, 2009).

Published sea-level index points from Suffolk are confined to the southwest section of the River Waveney (Alderton, 1983), the Blyth estuary (Brew et al., 1992) and the marshes neighbouring the River Alde (Devoy, 1982). Additional, unpublished, research was commissioned by the Centre for Environment, Fisheries and Aquaculture Science at Minsmere and Sizewell to improve understanding of changes in RSL and marine incursion during the late Holocene, resulting in new sea-level points for Suffolk (Lloyd et al., 2008). A summary of the sediment sequences sampled by Lloyd et al. (2008), and the associated palaeoenvironmental interpretation, is presented in Appendix 1. Index points from East Anglia cover the last 10 ka, with a cluster around the mid- Holocene and limited data for last 2 ka to constrain GIA model predictions (Figure 2.7). These sea-level index points and freshwater limiting data document a RSL rise from -20 m OD to present.

2.3 Sediment supply and barrier dynamics

Controls of barrier and back-barrier evolution

Barrier coasts form ~ 15 % of the world's coastline, providing protection for sensitive back-barrier wetlands and adjacent coastal environments from the direct impacts of storms and erosion (Cooper et al., 2018). Coastal barriers play a key geomorphological role in shaping the long-term pattern of coastal and estuary evolution (Long et al., 2006a). Barrier and back-barrier evolution are controlled by RSL change, sediment supply, barrier grain-size, substrate gradient, geological inheritance and wave and tidal energy (Roy, 1984; Roy et al., 1994; Cooper et al., 2018). Back-barrier sediments can be used to determine variation in barrier coherence and identify the mechanisms controlling barrier evolution (e.g. Spencer et al., 1998; Lario et al., 2002; Clarke et al., 2014). Given the interconnected nature of these processes, investigation in unison is required, as they can result in a range of responses, dependent on the specific geomorphological character of the coast (Carter and Woodroffe, 1994). For example, the control RSL rise has on barrier and back-barrier evolution is directly influenced by sediment supply (e.g. barrier rollover, overstepping or erosion) (Carter, 1988; Carter et al., 1989; Forbes et al., 1995; Jennings et al., 1998; Rosati, 2005; Fitzgerald et al., 2008; Plater and Kirby, 2011). Barrier stabilisation or growth occurs when the rate of RSL rise is low or stable (Roy et al., 1994) whilst a reduced sediment supply can result in sediment reworking and thinning which weakens barrier architecture (Orford et al., 1991).

Tidal inlets are dynamic features of barrier coastlines that allow the landwards penetration of tidal waters every tidal cycle, providing a connection between the ocean and back-barrier environments (Fitzgerald et al., 2002; 2008). The complex interactions of waves, tides and currents continually alters the morphology and sedimentary structure of tidal inlets (Fitzgerald et al., 2002; 2008; Long et al., 2006a; Mellett et al., 2012). Their location,

relative to a barrier coastline, influences sediment input to the coastal system and therefore the pattern of sediment processing (Long et al., 2006a).

Spit development and barrier dynamics on the Suffolk coast

Barriers are, and historically have been, a feature of the Suffolk coastline (Pye and Blott, 2006). The present day coastline alternates between cliffs formed from soft unconsolidated Quaternary sediments and low-lying wetlands that are separated from the sea by a narrow beach-barrier system (Figure 2.8), with substantial spits, such as Orford Ness and Landguard point, also present (Pye and Blott, 2006; 2009; Burningham and French, 2017). The narrow barrier ridge is comprised of coarse sand and gravel and is susceptible to overtopping and breaching during storm surges (Steers, 1953; Pye and Blott, 2009).

Figure 2.8: A. and B. Soft, unconsolidated cliffs, fronted by a narrow beach, extend along the coastline from Dunwich to Minsmere.

Historical maps and documents indicate that the growth of major spits and barriers has occurred along the Suffolk coast since at least the 12th century (Boer and Carr, 1969; Carr, 1970; Pye and Blott, 2006). Small, open coast, estuaries, previously existed at Kessingland, Benacre, Easton, Dunwich, Minsmere and Thorpeness, prior to the 6th century and have since been blocked by shingle and sand barriers (Pye and Blott, 2006). Dunwich is a well-documented example of this, as the Old Dunwich River previously flowed east, meeting the southwards flowing Blyth River to form an estuary (Figure 2.9) from Roman times (Gardner, 1754; Steers, 1927; Chant, 1974; Parker, 1978; Comfort, 1994; Pye and Blott, 2006). The Blyth was diverted south by Kingsholme spit, estimated to have developed between c. 1500 and 700 AD (Parker, 1978). The configuration of the coast between Southwold and Dunwich from Roman times played an influential role in Dunwich becoming one of the most important cities in Suffolk by Saxon times (e.g. Chant, 1974; Comfort, 1994). However, storms during the 13th and 14th century (1287, 1328) are documented to have blocked the harbour, resulting in the southwards progradation of Kingsholme spit and subsequently Dunwich's decline (Sear et al., 2011). Steers (1926) states that smaller rivers, such as the Minsmere Old River, became blocked because they

were unable to sustain themselves against the southward movement of sediment, leading to the development of spits and bars and eventual blocking.

Palaeogeographical reconstructions of the Holocene evolution of Dungeness, a coastal lowland on the Kent coast, have highlighted the inherent instability of coastal barrier systems once a geomorphic threshold, such as sediment availability or RSL change, is reached or boundary conditions altered (e.g. Plater et al., 1999; 2009; Long et al., 2006a). The development of spit and barrier features therefore places increased demands on the sediment supply required to maintain landform integrity. An insufficient sediment supply, for example, would result in the recycling of sediment within the spit, creating points of weakness and increasing the risk of breaching. Existing stratigraphic research on the Suffolk coast indicates that these geomorphological features influence back-barrier sediment records. Spit development and barrier dynamics were identified as primary controls of the Holocene coastal evolution in the Blyth estuary, particularly for the late Holocene (Brew et al., 1992). Further south, litho- and bio-stratigraphic research on Dingle Marshes, neighbouring Dunwich, sought to reconstruct changes in the palaeoenvironment associated with the former Dunwich estuary (Figure 2.9) and harbour (Sear et al., 2015). An environmental shift in a freshwater retting pit to marine saltmarsh and estuarine mud was identified at c. 1100 AD and attributed to storms breaching a gravel barrier or spit (Sear et al., 2015). Cartographic evidence from the 17th-19th century for Orford Ness, a cuspate foreland shingle spit extending from Aldeburgh to North Weir Point, documents the variable growth rate and fluctuating distal point location (Boer and Carr, 1969), demonstrating the development of major spits or barriers on this coast in the past. Peat deposits occuring regularly within the sediment records of the marshes neighbouring Orford Ness (Carr and Baker, 1968; Carr, 1970), indicates the existence of a protective barrier during the late Holocene (3976-3477 cal BP) to allow for peat development (Carr and Baker, 1968; Carr, 1970).
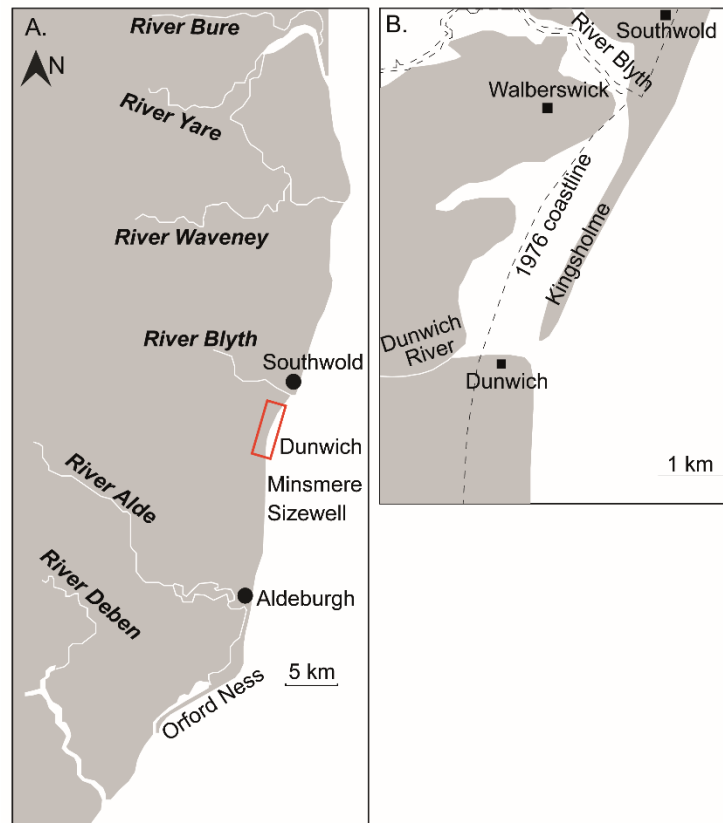
Figure 2.9: A. Map of the Suffolk coast with the location of the estuary that previously existed between Southwold and Dunwich highlighted in red B. Reconstruction of palaeogeography between Southwold and Dunwich for 1250 AD illustrating that the River Blyth was previously diverted south by Kingsholme spit to form an estuary with the eastwards flowing Dunwich river. Adapted from Pye and Blott (2006). Permission to reproduce this figure has been granted by Coastal Education and Research Foundation, Inc.

Existing stratigraphic evidence has identified episodes of higher energy deposition linked with storms breaching or overwashing the coastal barrier. Distinct silt and sand layers were identified in Dingle Marshes both prior to the onset of marine conditions at c. 1100 AD and after the return to freshwater conditions at c. 1600 AD (Sear et al., 2015). Further south, stratigraphic investigation completed in the back-barrier wetlands at Minsmere identified minerogenic sedimentation in the upper units of sequences nearest the coast, providing clear evidence of storm over wash in the last few hundred years (Lloyd et al., 2008).

Sediment supply on the Suffolk coast

As mentioned above, sediment availability influences the development of barrier and spit features. Sediment supply since the 19th century has been limited, greatly influencing the evolution of the Suffolk coast. At present, the sediment supply to Suffolk's gravel beaches is insufficient to ensure coastline resilience to storms, with the barrier moving shoreward in places during periods of RSL rise and increased storminess (Haskoning, 2009). Aerial

photographs document extensive overwash fans at the northern end of RSPB Minsmere following the 1938 event (Steers, 1951) and at Orford Ness following the 1938, 1949 and 1953 storm events (Arnott, 1973; Simper, 1994).

Suffolk's cliffs, a major input into East Anglia's sediment budget, have exhibited high rates of spatially and temporally variable historical change, over decadal timescales, with a well-defined trend of declining cliff retreat rates from north to south documented since the late 19th century (Cambers, 1973; 1975; Robinson, 1980; Carr, 1981; McCave, 1987; Brooks and Spencer, 2010; Burningham and French, 2017). Brooks and Spencer (2010) identified a median retreat rate for Covehithe of 3.5 m yr^{-1} in contrast to 1 m yr^{-1} on the Dunwich-Minsmere cliffs for the period 1882-2008. In addition, the average retreat rate increased from ~ 3 m yr^{-1} pre-1980 to ~ 5 m yr^{-1} after this at Covehithe whilst the Dunwich-Minsmere cliff retreat rate diminished by a third, from >1.5 m yr^{-1} to <0.5 m yr^{-1}, after 1925 (Brooks and Spencer, 2010). Cluster analysis of the relative position of the shoreline of the Suffolk coast (1881-2015), combined with metrics of shoreline change, identified multiple modes of change, highlighting the importance of sediment budget variations as a driver of multi-decadal coastal behaviour (Burningham and French, 2017). Predictions of the future sediment release behaviour of the Suffolk cliff system identified a dynamic and spatially variable sediment budget, that is switching states, between sediment release, no release, and no change (Brooks and Spencer, 2012).

Sediment transportation on the Suffolk coast remains debated (Vincent, 1979; Onyett and Simmonds, 1983; McCave, 1987), with the orientation of the coastline indicating a primarily southwards transport of sediment (McCave, 1987; Pye and Blott, 2006; Burningham and French, 2014) whilst tracer experiments highlight multidirectional transport of sediment, under most conditions (Kidson et al., 1958; Kidson and Carr, 1959; McCave, 1987). Brooks and Spencer (2010) identifies the transportation of sediment northwards, to the Lowestoft Bank system, during periods of high cliff retreat (e.g. 1992-2001) when sufficient sediment is released (Robinson, 1966; McCave, 1978).

Offshore bank systems on the Suffolk coast
Regional sediment transport is complicated by dynamic offshore bank systems, which have the potential to act as a sediment sink and provide morphological influence on wave climate and tidal currents (Lees, 1983; Brooks and Spencer, 2010). Research into the evolution of the Sizewell-Dunwich Bank system, situated offshore of the Dunwich-Minsmere cliffs (Figure 2.10), has mapped the extent of the Sizewell Bank, its coalescence with the Dunwich Bank in the 1920's, and their migration landwards (Carr, 1979).
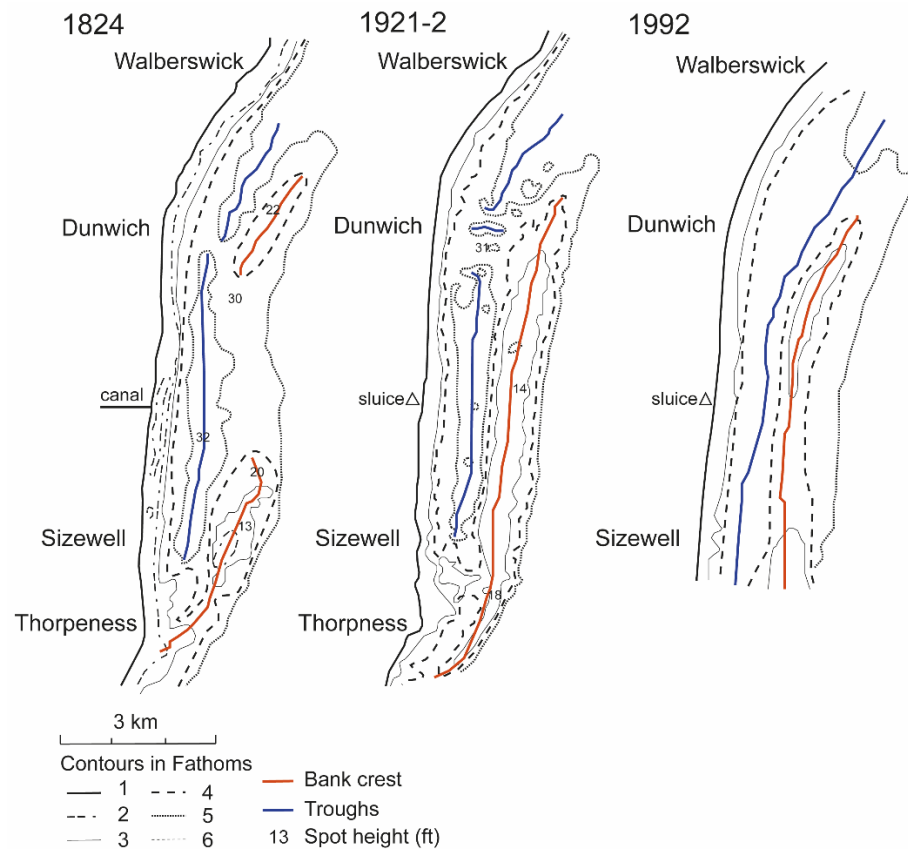
Figure 2.10: Synoptic bathymetric analysis offshore of the Dunwich-Minsmere cliffs. The northwards progradation of Sizewell Bank and coalescence with Dunwich bank is illustrated by the red line representative of bank crest. Adapted from Sear et al. (2013). Permission to reproduce this figure has been granted by David Sear.

The transport of sediment within the nearshore system and its interaction with the offshore banks is greatly debated (Carr, 1981). Similarities have been drawn between the volume of sediment eroded from the Suffolk coast and that gained on the offshore banks between 1824 and 1965 (Carr, 1979; 1981; Brooks and Spencer, 2010). The continued growth of the Sizewell-Dunwich banks between 1868 and 1992, despite the slowdown in cliff retreat between Dunwich and Minsmere since 1925, is argued to indicate sediment input from the rapidly eroding Covehithe, Easton Wood and Benacre cliffs further north of the banks (Pye and Blott, 2006; Brooks and Spencer, 2010). Others, however, have been more tentative in suggesting a direct exchange, acknowledging a potential link between sediment transport and the offshore banks, but arguing that the offshore zone is not influential within the sediment budget (McCave, 1987). Tracer experiments by the Institute of Oceanographic Sciences (IOS) found limited evidence of shoreward movement (Reid, 1958; Lees, 1981), whilst other research found that sediment was exchanged between Lowestoft Bank, further north, and the adjacent shoreline (Joliffe, 1963). This hypothesised connection between the offshore zone and coastal erosion has been attributed to the

28

influence of residual currents, with favourable offshore conditions minimising the impact of shoreline erosion by wave action and providing protection for the beach (Robinson, 1966; 1980). Wave rider buoys on either side of Sizewell Bank found that large waves (>2.2 m in height) broke on the bank, providing a degree of protection, although potentially under only specific wave height and direction conditions (Carr, 1981). Despite the complex relationship between the offshore banks and their adjacent shoreline it is highly likely that these dynamic geomorphologic features influence coastal sediment transport. For example, cliff erosion on the present-day coast of Dunwich is minimal and in parts stable despite the narrow, sediment limited beach fronting the cliffs. This has led to the suggestion of a possible sheltering effect from the Sizewell Bank in this section of the coast (Robinson, 1980; Brooks and Spencer, 2010), however the degree of protection may be variable and only under restricted conditions (Carr, 1981).

2.4 Human influence and land use change

The coastal plains of northwest Europe have long provided humans with important coastal resources (Allen, 2000; Pierik et al., 2017). Human use of coastal wetlands has evolved from the exploitation of natural resources, to the modification, by enclosure, for agriculture, to the transformation of these environments by reclamation (Allen, 2000; Rippon, 2009). The utilisation and management of coastal wetlands by humans has left distinctive signatures on the landscape and within the sediment records, with evidence of human activity visible on the surface or buried at depth (e.g. Wilkinson and Murphy, 1995; Vos and van Heeringen, 1997; Allen, 2000). For example, much of the upper peat unit within the Holocene sequence from east Norfolk has been lost due to a combination of embankment, drainage and agricultural practices (Coles and Funnell, 1981) whilst at Romney Marsh, intensive reclamation was influential for the closure or contraction of tidal inlets (Rippon, 2002; Long et al., 2006a). This section highlights the ways in which populations have utilised and altered coastal landscapes in East Anglia, and adjacent areas, and how this has intensified with time.

The early Holocene pollen spectra for east Norfolk and Suffolk is dominated by A*lnus* (alder) (Godwin, 1940; Brew et al., 1996; Wells and Wheeler, 1999; Horton et al., 2004), indicating a fen carr community, regarded as the 'natural' vegetation of areas such as the Broadlands in Norfolk (Wells and Wheeler, 1999). Neolithic (c. 4000-2500 BC), Bronze Age (c. 2500-800 BC) and Iron Age (c. 800 BC – 43 AD) evidence indicates that Suffolk's settlers primarily inhabited the lighter soils of southeast Suffolk, grass and health mosaic in the northwest and the major river valleys (Dymond and Martin, 1999). Archaeological evidence of human land use identified early Iron Age material used for seawater salt extraction in Suffolk, on the marshes of the Blyth, Alde and Orwell estuaries, with dense

concentrations of evidence also recovered from Essex and north Kent (Nenquin, 1961; Fawn et al., 1990; Rippon, 2000). Evidence for the use of resources from the marshes in Norfolk and Suffolk is limited during the Roman period (43-410 AD), potentially due to cliff erosion (Rippon, 2000) or the existence of open embayments, indicated by stratigraphic evidence north of Suffolk in the Yare valley (Coles, 1977; Coles and Funnell, 1981). However, salt-production is documented to have remained abundant in Essex and Kent during the Roman period (Andrews and Brooks, 1989; Medlycott, 1994). Pollen evidence from east Norfolk corresponds with archaeological evidence, indicating that significant human populations were not present during the Bronze and Iron Age (Jennings, 1955). Human interference and control of fen vegetation occurred relatively recently on the East Anglian coastline, beginning in east Norfolk during the last 400 cal BP (Jennings, 1955; Wells and Wheeler, 1999).

The anthropogenic influences on the environment of the East Anglian coast are evident after 400 cal BP from pollen records. A typical late historic environment (c. 1000 AD) indicating mixed arable and pasture, with some retained woodland, has been identified for east Norfolk and Suffolk (Jennings, 1955; Sear et al., 2015). An abundance of herbaceous pollen, alongside cereal pollen indicates upland clearance and cultivation whilst non-native species, such as pine and spruce, indicate planation. A rise in pine pollen from c. 1650-1700 AD has been found in a number of sites (e.g. Long et al., 1999), associated with the planting of exotic conifers for forestry.

During the early medieval period Suffolk became an extremely influential political power in England (Williamson, 2005), with an increased population placing an enhanced strain on salt production, fishing and embankment for agriculture (Rippon, 2000). The vegetation history for the 11th and 12th century indicates openness, with marginal woodland, tree growth and open agricultural habitats indicating an agrarian landscape (Sear et al., 2015). Rippon (2000) regards the mid-medieval period as a transition from landscape exploitation, through modification, to transformation, including the expansion of enclosure and drainage further inland in the Fens from the 11th century. Embankment was also extensive on the marshes of East Kent, in addition to early instances of extensive reclamation occurring in certain locations, such as Orford (Allen et al., 2002). Improvements such as river canalisation also become prevalent during the medieval period to improve drainage and navigation.

Dunwich, Suffolk, was a thriving settlement by the end of the 11th century, with one of the largest ports on the east coast (Darby, 1935). Pollen evidence from Dunwich identified a hemp cultivation and processing site after c. 1050 AD, indicating that retting was being used to obtain fibres and make rope, likely for maritime use given the international

importance of Dunwich port (Sear et al., 2015). Dunwich's importance during this period was influenced by local coastal configuration, as spit development led to the creation of a sheltered estuary by Roman times (Gardner, 1754; Steers, 1927; Chant, 1974; Parker, 1978; Comfort, 1994; Pye and Blott, 2006). Storms in the 13th and 14th century halted spit development and blocked the mouth of the estuary (Steers, 1927), with the populations of Dunwich, Walberswick and Blythburgh attempting to maintain access to the sea by creating artificial breaches in the spit (Comfort, 1994).

The post-medieval landscape of Suffolk was influenced by the enclosure of open fields and planting of new woodland by substantial landowners, a process that accelerated during 19th century (Williamson, 2005). Woodland was not extensive in Suffolk during the medieval period due to prehistoric deforestation to make way for farmland or heath. From the 17th century, tree plantations were created and new fodder crops, such as turnip and clover, were introduced to regularly rotate with cereals (Dymond and Martin, 1999).

Reclamation of coastal wetlands occurred at an accelerated rate from the 16th century. Early reclamation is characterised by irregular, sinuous channels whilst areas drained in the 18th or 19th century tend to have a highly rectangular pattern (Williamson, 2005). Differentiating between these types can be complicated due to their simultaneous occurrence in places. For example, marshes extending between Southwold and Dunwich, such as Dingle, Oldtown and Westwood Marshes, contain a mixture of sinuous and straight drains indicating that drainage likely began in the 16th century and has been maintained and extended with time (Good and Plouviez, 2007; Sear et al., 2008; Alison Farmer Associates, 2012).

The local and general Parliamentary Acts, known as the Enclosure Acts, were enforced in the 18th and 19th centuries. This resulted in open fields, commons and marshlands, considered 'wastes', being enclosed to form fenced off plots of land (Dymond and Martin, 1999). A notable example of this is Minsmere, Suffolk, where frequent freshwater flooding throughout the late 18th and 19th century led to the creation of the Minsmere Level Drainage Trust and a sophisticated new drainage system (Williamson, 2005; Pye and Blott, 2006; Good and Plouviez, 2007). Post-medieval drainage schemes were also associated with the building of windmills, for example on Westwood and Walberswick Marshes in 1743 (Warner, 2000).

The agricultural recession in the late 19th century and early 20th century, as well as the onset of WW2, resulted in neglection of drainage, initially as a defensive measure, and latterly as reclaimed wetland reverting to reed bed. A noteworthy example is Westwood Marshes which, following abandonment throughout the 20th century, became one of the largest and most environmentally important areas of reed bed in east England.

Human activities have left notable signatures within back-barrier sediment records of southeast England. For example, in east Norfolk peats were excavated for fuel after 1 ka (Coles and Funnell, 1981) and this has led to ~90 % of the fen surface in east Norfolk being damaged for peat extraction (Wells and Wheeler, 1999). Not all of the changes preserved in Holocene sediment records may be the result of natural processes and therefore care must be taken to consider the impact of human activities.

Chapter 3: Methodology

The field and laboratory methods used to reconstruct palaeoenvironmental change at the sites investigated are reviewed and outlined. The field methods relating to site selection, coring, sampling and surveying are initially outlined. Following which, details are provided for the sedimentological, biostratigraphic and chronostratigraphic laboratory methods used.

3.1. Field methods

3.1.1 Site selection

Historical maps and documents, aerial photography and conceptual models, in addition to geological and topographical maps, were utilised to identify sites which may yield records of Holocene coastal geomorphological change. Historical maps (Agas, 1587; Kirby, 1737; Gardner, 1754) provide illustrations of the palaeogeography of the coastline during the last 1000 years and have been utilised to create conceptual models (Figure 2.9) documenting the potential evolution of the Suffolk coast during this time period (Chant, 1974; Parker, 1978; Comfort, 1994; Pye and Blott, 2006). These resources identify the existence of numerous havens along the coast, at Kessingland, Benacre, Dunwich and Minsmere, prior to the Middle Ages, which have since been blocked by shingle and sand barriers (Comfort, 1994; Pye and Blott, 2006). Existing stratigraphic evidence, whilst limited for the Suffolk coast, has identified the existence of thick Holocene sediment sequences containing a series of alternating estuarine-marine and freshwater deposits in low-lying coastal wetlands, such as the marshes of the Blyth valley (Brew et al., 1992), near Southwold, and the Alde/Ore valley further south (e.g. Carr and Baker, 1968; Carr, 1971). Sites at altitudes critical for testing the Holocene RSL history of the Suffolk coast (elevation < 5 m OD) and known to have been tidally influenced in the past from historical maps, were selected for stratigraphic investigation. Three sections of the Suffolk coast, Walberswick National Nature Reserve, Minsmere and the Sizewell Marshes, were identified as suitable areas for histories of coastal and RSL evolution histories to be determined. Full descriptions of the five sites investigated are provided in Chapters 4 (Walberswick National Nature Reserve), 5 (Minsmere) and 6 (Sizewell Marshes).

3.1.2 Stratigraphic survey

Inter-regional comparisons are needed to determine the extent to which local or regional processes are responsible for the patterns of sedimentation identified from the records preserved in Suffolk's coastal wetlands, an extensive stratigraphic dataset is required to achieve this. This framework was established on a site-by-site basis between 2015 and

2017; November 2015 (Westwood Marsh), April 2016 (Oldtown Marsh and Great Dingle Hill), November 2016 (Minsmere) and December 2017 (Sizewell).

A gouge corer was used to determine spatial and temporal stratigraphic variability along transects at each site. Sediment cores were retrieved every ~ 25-50 m and characteristics were logged using the Troels-Smith (1955) classification scheme (Appendix 2). The spacing interval chosen for core retrieval from each site was selected in order to sufficiently map the lateral sediment variability. Where possible, sampling extended from the ground surface to the underlying geology, termed Crag, typically either Coralline Crag, Norwich Crag or Red Crag (Hamblin et al., 1997). The Crag underlying the region is composed mainly of sand with thinner sandy gravel units and occasional silty-clay laminae. All cores bottomed-out in saturated, irrecoverable sand or Crag, identified by grinding noise of the gouge corer, the angular gravel clasts and the compacted nature of the sediment at the base of the gouge core. Areas where disturbance of the stratigraphic record was likely were avoided. For example, areas proximal to steep sided relief were avoided due to potential colluvium deposits at valley edges that would complicate the stratigraphic record. Anthropogenic drainage channels are extensive throughout the coastal wetlands of the Suffolk coast and proximity to these features was kept to a minimum where practical.

3.1.3 Sediment sampling

Sediment sequences suitable for laboratory analysis were identified based on complete, representative stratigraphy with, ideally, no visible evidence of erosion or depositional hiatus. The depth was also considered as it provides an indication of the longest record of environmental change. A Russian-type corer was used to collect sediment samples for analysis. It is best suited to peats and well consolidated limnic sediments, with contamination reduced by the sample being contained within the barrel of the Russian corer (Glew et al., 2001). Sampling was completed using two parallel cores with an overlap of 5 cm between to ensure complete recovery of the sediment record. Each section of the sampled sediment sequence was photographed, stored in plastic guttering and wrapped in plastic film for storage in the dark, under refrigeration at 4°C, at Liverpool John Moores University.

3.1.4 Surveying

The location and altitude of all cores were surveyed using a Topcon dGPS (Topcon HiPer Pro) and post-processed to Ordnance Datum (m OD), to give a vertical precision of 10 cm.

3.2 Sedimentology

3.2.1 Particle Size Analysis

Particle size analysis is a long established sedimentary diagnostic tool utilised for palaeoenvironmental reconstruction to improve understanding of sedimentary processes and depositional conditions (Lowe and Walker, 1997; Switzer and Pile, 2015). Particle size is indicative of relative energy, a primary environmental factor controlling erosion, transportation and deposition (Briggs and Smithson, 1987; Switzer and Pile, 2015). The relationship between particle size and velocity is shown by the Hjulström curve, which illustrates the velocity required for the movement, transportation and deposition of a particle. The particle size distribution of a sample, and its morphological characteristics, are therefore indicative of the depositional environment and resulting landform development (Lario et al., 2002; Switzer and Pile, 2015). Stokes' Law underpinned early techniques used to determine particle size analysis and expresses the settling velocities of spherical particles within a fluid medium, with respect to the forces acting on a particle as it sinks in a liquid column.

Particle size analysis is an important component of palaeogeographical reconstruction, and has been used alongside other methods to reconstruct barrier development (Clarke et al., 2014), coastal evolution (Long et al., 1996; 2006b; Brew et al., 2000; Lario et al., 2002), high magnitude events (Switzer and Jones, 2008; Plater et al., 2009) and RSL change (Zong and Horton, 1998; Woodroffe and Long, 2010).

Laser diffraction, is now the primary method used to determine particle size of fine sediment <2 mm in diameter (e.g. Spencer et al., 1998; Brew et al., 2000; Lario et al., 2002; Plater et al., 2009; Watson et al., 2013; Clarke et al., 2014). Laser diffraction produces a rapid and automated measurement of particle size, enabling large numbers of samples to be run to obtain a statistically significant data spread (Lowe and Walker, 1997; Pye and Blott, 2004; Switzer and Pile, 2015). In the instrument, sediment is suspended in a liquid and a laser travelling through a detection cell determines particle size based on the angle at which the laser is diffracted off the particles, a modified Stokes' Law principal (Switzer, 2013). The angle of diffraction is directly proportional to the angle of particle size therefore the light intensity scattered by the laser hitting the suspended sediment is measured and the volume distribution calculated.

A Beckman Coulter LS13320 was used to determine the dimensions of particles ranging from 0.04 μm to 2 mm using the laser diffraction method. Prior to analysis, the aggregating effects of organics were removed using hydrogen peroxide digestion (Kunze and Dixon, 1987) and Calgon added to aid dispersal of flocculated clay particles. Organic matter acts

as a cementing agent, binding particles together, therefore its removal is required prior to particle size analysis. Dilute (< 10 %) hydrogen peroxide is the chemical reagent extensively used to achieve this despite some literature indicating it should be used cautiously for this purpose due the implications for clay minerology (e.g. Allen and Thornley, 2004). Hydrochemistry influences the ability for clay particles to form clusters (termed flocs), which will have a larger diameter than the individual particles, affecting the particle size distribution of a sample. Flocculation influences the hydrodynamic relationship between particle size and settling velocity because the suspended flocs may settle quicker than the individual particle based on Stokes' Law (1851). The addition of Calgon as a dispersing agent introduces an assumption that clay particles were not transported as flocs (Switzer and Pile, 2015).

A range of analytical techniques, of varying complexity, have been developed to analyse particle size data and interpret information relating to sediment sources and depositional environments. Descriptive statistics, i.e. mean, standard deviation, skew and kurtosis, developed in the early and mid-20th century remain commonly used to characterise particle size distribution and remain a preferred method of displaying particle size data (Krumbein, 1934; Inman, 1952; Folk and Ward, 1957; Switzer and Pile, 2015). Particle size can be described arithmetically, geometrically or logarithmically using the method of moments or Folk and Ward method. The method of moments can place too much emphasis on low frequency, long tails within the distribution, whilst the Folk and Ward method can be insensitive to samples with a large particle size range (Inman, 1952; Blott and Pye, 2001). Method comparison undertaken by Blott and Pye (2001) identified that the Folk and Ward measures, determined in metric units, produced the strongest foundation for routinely comparing compositionally variable sediments. Particle size distribution statistics for each site were determined using Gradistat, software developed by Blott and Pye (2001), to enable rapid calculation of particle size statistics.

Bivariate plots of statistical particle size parameters (Figure 3.1) have led to the identification of environment specific graphic envelopes (e.g. Friedman and Sanders, 1978; Tanner, 1991a, 1991b; Lario *et al.*, 2002). Early attempts focusing on the sample size spectrum were largely unsuccessful at determining depositional environments from particle size data (e.g. Friedman and Sanders, 1978). Environment determination is based on statistical parameters reliably indicating different transportation and deposition processes and therefore environment (Sutherland and Lee, 1994). Gale and Hoare (1991) state that the complexity and overlap of the processes investigated and the lithological, mineralogical and source material controls produce results that tend to be inadequate. Developments made by Tanner (1991a; 1991b), plotting mean particle size against

standard deviation, enabled "large new supply", associated with rivers and closed basins, to be distinguished from winnowing environments, associated with beaches and dunes, and therefore wave and wind driven processes. Mean particle size and standard deviation are regarded as hydraulically controlled and are therefore positively correlated with the energy of the environment and degree of sediment processing (Tanner, 1991a; 1991b; Long et al., 1996; Lario et al., 2002; Priju and Narayana, 2007).
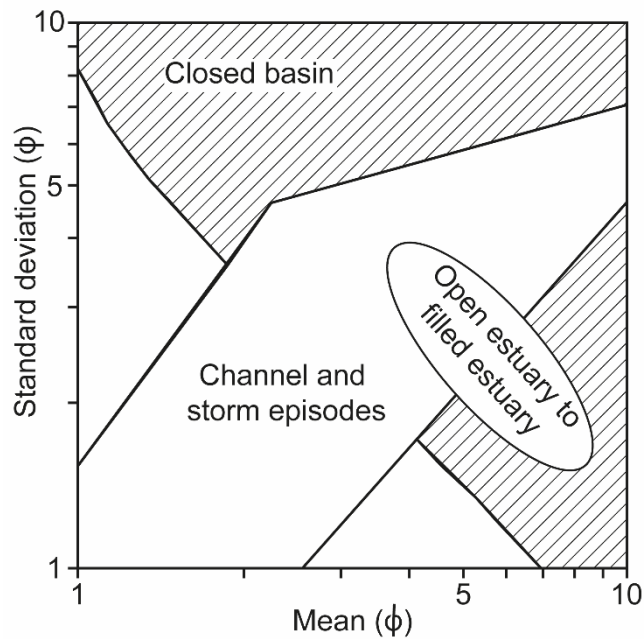
Figure 3.1: Depositional environment domains identified by Tanner (1991a; 1991b) and modified by Lario et al. (2002) *based on hydraulic conditions and identified by plotting mean particle size against standard deviation (phi). Permission to reproduce this figure has been granted by Elsevier.*

Tanner's (1991a; 1991b) bivariate plot is subdivided into zones representing differing depositional energy conditions- fluvial and storm episodes, partially open to restricted estuary and closed basin. This provides information on the influence of sediment supply, RSL trends, barrier integrity and terrestrial inwash on back-barrier sedimentation whilst the addition of a new transitional domain by Lario et al. (2002) enabled differentiation between abrupt and gradual coastal change. Bivariate plots require sufficient context to determine the depositional environment associated with a sediment sample (Clarke et al., 2014). Producing bivariate plots for each site, and considering the results alongside the biological indicators used, can help determine if periods of marine influence are associated with open- or closed-basin conditions and help to determine the influence of barrier evolution on back-barrier sedimentation (Lario et al., 2002).

Descriptive moments struggle to interpret multimodal distributions (e.g. Folk and Ward, 1957; Blott and Pye, 2001). This is problematic for particle size analysis because sediment

mixing, and resulting multimodal distributions, are ever-present in nature (Folk and Ward, 1957; Flemming, 2007). This is due to the multiple subpopulations, which result from different sediment sources and processes, being contained in particle size distributions (Weltje and Prins, 2007; Dietze et al., 2014). In addition, sediment processes are influenced by factors such as sediment sources and their availability, surface roughness and transport energies therefore resulting in sediments containing complex sediment signatures (Dietze et al., 2014). As a result, statistical models have been developed to quantitatively unmix multimodal distributions into their composite sub-populations, termed end-members, to reveal greater information on sediment dynamics (e.g. Imbrie, 1963; Sun et al., 2002; Dietze et al., 2012). Numerically unmixing particle size data into associated end-members can provide useful information on sediment provenance and depositional processes (Weltje and Prins, 2007; Dietze et al., 2012; Paterson and Heslop, 2015). End-member modelling is underlain by the assumption that a particle size distribution at a particular spatial-temporal coordinate is comprised of multiple sediment populations, each corresponding to a different sediment source or transport mechanism (Weltje and Prins, 2007).

Supplementary information, such as the number of end-members, their composition and variability, is required to unmix a particle size data set. Assumptions therefore have to be made and these are dependent on the decomposition approach chosen (i.e. parametric vs non-parametric). A parametric approach assumes that the dynamic populations within a particle size distribution are unimodal. An example is standard curve-fitting techniques which decompose a single observed particle size distribution into proportional components, each belonging to a predefined class (e.g. Sun et al., 2002). A non-parametric approach considers particle size distributions as a combination of an initial population modified by sediment processes. End-member analysis algorithms are utilised in this approach to determine the relative importance of an optimal number of end-members, the distribution of which is not restricted (Weltje, 1997; Dietze et al., 2012). Parametric approaches, such as curve fitting, fail to produce physically meaningful interpretations of particle size data and are not suitable for identifying underlying mixing processes. A parametric approach therefore does not provide the complete picture of the mechanisms controlling the distribution of natural sediments (Weltje and Prins, 2007; Paterson and Heslop, 2015). Despite these shortfalls, parametric approaches remain widely used because they can represent particle subpopulations with unimodal distributions corresponding to a single sediment source, whereas non-parametric end-member analysis struggles to achieve this. These issues have resulted in the development of a new algorithm for non-parametric end-member analysis which facilitates the unmixing of particle size data into unimodal parametric end-members (Paterson and Heslop, 2015).

This algorithm firstly completes non-parametric end-member analysis, to determine the maxima of the non-parametric end-members, in order to estimate the parametric end-members therefore considering uni- and multi-modal distributions present in a data set (Paterson and Heslop, 2015). This approach, whilst novel, provides greater detail on subpopulations potentially representing different sources or source processes therefore overcoming an issue with previous non-parametric end-member analysis.

Paterson and Heslop's (2015) non-parametric end-member analysis was used to identify subpopulations within the particle size data as multimodal distributions are common within the datasets for each site. The AnalySize software developed by Paterson and Heslop (2015) was used to achieve this. End-member analysis could only be completed for sites with a particle size dataset exceeding 10 samples, a prerequisite of the AnalySize software. This is due to the geological context of samples being required (Weltje and Prins, 2007; Paterson and Heslop, 2015). Identifying the sub-populations present in the dataset will aid interpretations of the dominant depositional processes and enable end-member comparison between sites. Further information on the process of selecting the optimal number of end-members is provided in Appendix 3. The physical plausibility and geological context was considered when performing this analysis and interpreting results. Clarke et al. (2014) acknowledges the statistical robustness of end-member analysis but also highlights that more qualitative statistical approaches can also enable insightful interpretations of the depositional environment preserved in the sediment record, highlighting the efficiency of visual inspection.

3.2.2 Loss on Ignition

Organic matter is an important sediment component originating from past biota, the quantity and type of which provides information relating to the environmental conditions during deposition (Meyers and Teranes, 2001). The occurrence of terrestrialisation, accumulation rates, compaction, water level changes and temporary or subtle environmental changes, can be deciphered from trends in organic matter content (Plater et al., 2015).

Organic matter content has been utilised when reconstructing changes in RSL to identify and verify lithostratigraphic changes, determine the tidal frame position of a depositional environment and improve vertical accuracy in determining the altitude of sea-level indicators (e.g. Shennan et al., 1995; 1996; Horton et al., 1999; 2006; Zong and Horton, 1999). In addition, organic matter content has been used to estimate the post-depositional lowering resulting from the compaction of unconsolidated organic-rich Holocene sediments (Brain et al., 2011; 2012; van Asselen, 2011). The organic matter content has

been extensively determined using the standard loss on ignition (LOI) methodology. LOI is the inorganic material which remains following the ignition of dried sediment and is calculated as the percentage of organic matter in the dry weight (Aaby, 1986). It can rapidly and effectively determine the organic matter content of soils (Ball, 1964; Plater et al., 2015).

Boyle (2001) states that the accuracy of the LOI methodology is determined by the nature of the sediment, its organic matter concentration and the ignition temperature selected. Many minerals lose mass when heated due to processes such as dewatering, pyrolisation and dihydroxylation. The ignition temperature selected for the LOI methodology influences the loss of volatile salts, structural water from clay and inorganic carbon (Ball, 1964; Dean, 1974; Heiri et al., 2001). Mineral and organic matter breakdown occurs over a large and overlapping temperature range whilst carbonate minerals generally breakdown at temperatures exceeding 650 °C (Neuman, 1977). Keeling (1962) and Ball (1964) illustrated that the dewatering of clay minerals can be minimised by restricting the ignition temperature to 375 °C. However, the combustion of organic matter at this temperature underestimates the total organic matter content, selectively excluding the more humified portion and reducing the accuracy of this methodology for determining organic matter content (Boyle, 2004).

Differential thermogravimetric analysis found that an ignition temperature of 550 °C burnt the organic matter present, with the dewatering of minerals also occurring (Plater et al., 2015). Care must be taken to not over interpret minor fluctuations in LOI results for clay-rich sediment units. The structural waters of clay minerals can represent one tenth of the mineral weight, therefore an LOI value of 10 % does not necessarily reflect the presence of organic matter (Boyle, 2001). Investigations undertaken by De Leenheer et al. (1957) concluded that variable clay content can create an inaccuracy of approximately 4-6 % LOI when comparing a soil containing 5 % clay with one containing 50 %.

The chosen LOI method follows that developed by Heiri et al. (2001) whereby samples are ignited at 550 °C for an exposure time of 4 hours. This methodology has been previously used to obtain changes in organic matter content for investigations of RSL changes (e.g. Woodroffe and Long, 2010; Barlow et al., 2014; Long et al., 2014). A consistent sample size of c. 5 g was used throughout, dried overnight at 105 °C and weighed accurately prior

to and after ignition. Following ignition, organic content was calculated as the percentage weight of the original sample.

3.3 Biostratigraphy

3.3.1 Diatoms

Background context of diatoms

Biological indicators have been extensively used in coastal settings to differentiate between freshwater and marine palaeoenvironments, as lithostratigraphy alone is unable to reliably do this. A combined litho- and bio-stratigraphic approach enables the shift from marine to terrestrial environments, and vice-versa, to be determined and changes in the coastal environment identified. This approach enables the indicative meaning, a pre-requisite for sea-level index points, to be precisely defined. Biological indicators improve constraint on the position of RSL for a small geographical area, enabling a larger number of sea-level index points, at different altitudes, in close geographical proximity, to be produced.

Diatoms are siliceous, unicellular algae, ranging from 5 to 200 μm, and are considered a valuable tool in Quaternary research (Denys, 1984; Palmer and Abbott, 1986; Lowe and Walker, 1997). Diatom distribution is controlled by ecological preference to environmental conditions such as salinity, temperature and nutrient level (Lowe and Walker, 1997). Most diatom taxa have well documented, niche ecological preferences, allowing a diatom assemblage to reflect a type of environment. The ubiquitous distribution of diatoms, good preservation in fine-grained sediments, resistance to post-burial chemical alterations and insensitivity to oxidation make them an attractive tool for palaeoenvironmental reconstructions (Denys, 1984; Palmer and Abbott, 1986; Denys and De Wolf, 1999; Zong and Sawai, 2015).

Diatom sensitivity to changes in salinity (Figure 3.2) has resulted in their extensive use within Quaternary research to reconstruct marine, brackish and freshwater palaeoenvironments and the boundary between these (Palmer and Abbott, 1986; Vos and De Wolf, 1993; Denys and De Wolf, 1999). This led to the development of the halobian classification scheme (Table 3.1) based on diatom sensitivity to salinity (Kolbe, 1927;

Hustedt, 1953; Simonsen, 1969; Palmer and Abbott, 1986). Kolbe (1927) first proposed this scheme and Hustedt (1953) and Hemphill-Haley (1993) later modified it (Table 3.1).
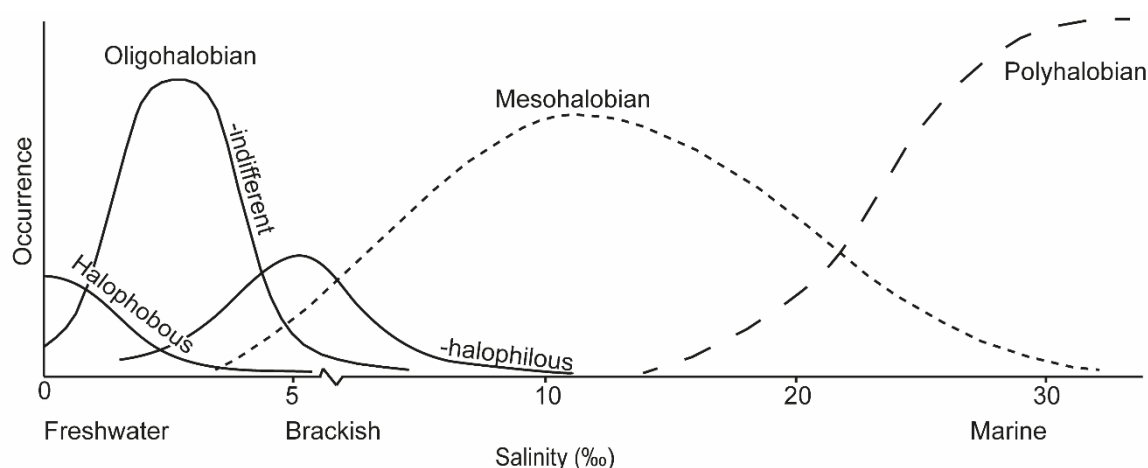
Figure 1.2: Schematic representation of diatom occurrence relative to salinity ranges, based on the halobian classification scheme (see Table 3.1). Adapted from Robinson (1982)*. Permission to reproduce this figure has been granted by Wiley.*

Table 3.1: The halobian classification scheme for diatoms (Hustedt, 1953)*.*

Classification	Salinity range (‰)	Description
Polyhalobian	>30	Marine
Mesohalobian	0.2-30	Brackish
Oligohalobian-halophilous	<0.2	Freshwater- stimulated at low salinity
Oligohalobian-indifferent	<0.2	Freshwater-tolerates low salinity
Halophobous	0	Salt-intolerant

The relationship between diatom distribution and salinity was first used to reconstruct variations in sea level associated with land uplift, shoreline displacement and lake isolation, in Scandinavia in the 1920s (Cleve-Euler, 1923; 1944). Diatom analysis is an established methodology for identifying changes in sea-level tendency in coastal sediments. Their utility for reconstructing post-LGM RSL change, particularly in northern Europe, has been substantial during the 20th century (e.g. Shennan et al., 1994; Zong and Horton, 1999; Horton et al., 2006; Woodroffe and Long, 2010; Watcham et al., 2013). In addition, diatoms have been previously used in conjunction with other methods to aid reconstructions of ice-sheet morphology and deglaciation (e.g. Barlow et al., 2016; Brader et al., 2017), coseismic uplift or subsidence (e.g. Shennan et al., 1999; Shennan and Hamilton, 2006; Dura et al., 2016) and groundwater salinisation (e.g. Best, 2016).

Variables such as water temperature, pH, nutrient content and geographic location also influence diatom distribution (Denys, 1984; Vos and De Wolf, 1993). Research by Roelofs

(1984), investigating the distribution patterns and valve size variations of *Paralia sulcata*, noted that distribution is controlled by interrelated variables which are difficult to isolate. Fine grained sediments and sandy substrates have been associated with an abundance of epipelic (mobile and can migrate through sediment) and episammic (immobile, firmly attached to sand grains) diatoms respectively, highlighting the importance of substrate type (Nelson and Kashima, 1993; Zong, 1997; Zong and Horton, 1998; 1999). Zong and Horton (1999) highlighted the influence of pH level on diatom distribution in western Scotland, where *Eunotia valida*, an acidophilous taxa, was abundant within a raised bog where acidic run-off was prevalent (Zong and Horton, 1999). It is therefore important to utilise a multi-proxy approach, combining lithostratigraphical methods with diatom analysis to obtain palaeoenvironmental data extending beyond the relationship between diatom distribution and salinity.

Diatom life form can be classified with respect to tidal exposure and dessication gradient to enable palaeosedimentary environments (subtidal, intertidal, supratidal and non-tidal) to be reconstructed (Vos and De Wolf, 1988; 1993). The ecological classification of diatoms is not based on tidal range. However, an indirect relationship exists between the ecological groups and sedimentary environments because life form distribution is primarily dependent on tidal energy and flooding frequency (Vos and De Wolf, 1988). For example, brackish epiphytic taxa live on macroalgae and waterplants and are associated with low-energy environments permanently under water therefore indicative of lagoonal conditions. The classification of diatom life form has been previously used to identify marine floods during storm conditions (Zong and Horton, 1999) and reconstruct barrier dynamics and back-barrier evolution (Bao et al., 1999; Freitas et al., 2002; Sáez et al., 2018).

Diatom life form (Figure 3.3) was classified predominantly using the ecological codes outlined in Vos and De Wolf (1988; 1993), which is largely based on De Wolf (1982). Additional resources were used to provide greater detail for species exceeding 5 % of the total count at each site (Zong and Horton, 1998; Albay and Aykulu, 2002; Lange and Tiffany, 2002; García-Rodríguez et al., 2004; Bao et al., 2007; Lysakova et al., 2007; Mann and Poulickova, 2010; Beltrones and Hernández, 2014). Benthic diatoms are subdivided into epipelic (mobile and can migrate through sediment), epipsammic (immobile, firmly attached to sand grains), aerophilous (adapted to irregular flooding and periods of subaerial exposure) and epiphytic (live attached to macrophytes) taxa (Vos and De Wolf, 1988; 1993). Planktonic and tychoplanktonic taxa both occur within the water column

however the latter can also be associated with another habitat therefore they are subdivided.

Salinity

		Marine		Brackish			Freshwater
	Salinity range (‰)	30 20 10	5	1	0.5	0.2	0.1
Plankton	Plankton s.s.	Marine plankton	Brackish plankton	Brackish/freshwater plankton			Freshwater plankton
	Tychoplankton	Marine tycho-plankton	—	Brackish/freshwater tychoplankton			
Epiphytes		Marine epiphyte	Marine/ brackish epiphytes	Brackish/freshwater epiphytes			Freshwater epiphytes
Benthos	Epipelon	Marine epipelon	Marine/brackish epipelon				Freshwater epipelon
	Episammon	Marine/brackish epipsammon	—				
	Aerophilous	Marine/brackish aerophilous	Brackish/freshwater aerophilous				

(Life form)

Figure 3.3: Ecological classification of diatom groups, based on salinity tolerance and life form of taxa. Adapted from Vos and De Wolf (1988; 1993)*. Permission to reproduce this figure has been granted by Springer Nature.*

Diatoms taphonomy

Palaeoenvironmental interpretations based on the fossil diatom record can be biased or misrepresented in all environments by local taphonomic processes, allochthonous taxa, spatial and temporal mixing, frustule breakage and chemical dissolution of frustule silica (Flower, 1993; Barker et al., 1994; Ryves et al., 2001). These factors are not independent of each other, for example, partial dissolution increases the likelihood of diatom frustule breakage (Flower, 1993; Barker et al., 1994). Palaeoecological interpretations, and resulting palaeoenvironmental reconstructions, are restricted by the quality of the primary diatom data (Ryves et al., 2001; 2009) however little information tends to be provided on this. The loss of information, as contemporary biological indicators are preserved in the fossil record, restricts the accuracy of palaeoenvironmental reconstructions and interpretations (Ryves et al., 2009). An over-reliance on biological indicators, such as diatoms, in previous research has had implications for the palaeoecological interpretations made for coastal environments due to limited preservation, highlighting the importance of a multi-proxy approach (Long and Innes, 1995; Spencer et al., 1998; Plater et al., 2009; Lloyd et al., 2013).

Autochthonous diatoms are species which have remained *in situ* at the deposition location, reflecting the local environment, whilst allochthonous diatoms are species which have been transported and are representative of the wider environment (Vos and De Wolf, 1993). Diatoms can be easily transported due to their size and shape resulting in

allochthonous valves being present in diatom assemblages (Beyens and Denys, 1982; Lowe and Walker, 1997). The allochthonous component tends to be negligible in low energy conditions however is problematic in coastal environments (Brockmann, 1940; Simonsen, 1969; Vos and De Wolf, 1988; Denys and De Wolf, 1999; Zong and Sawai, 2015). Denys and De Wolf (1999) note that a range of different habitats can occur proximal to each other within coastal environments, potentially resulting in parautochthonous (intermediate in character between autochthonous and allochthonous) assemblages. For example, freshwater valves, such as *Synedra ulna*, can be transported seawards in water courses and run-off (Hendey, 1974; Beyens and Denys, 1982) whilst marine and brackish taxa can be transported into inner estuaries by tidal currents (Brockmann, 1940; Simonsen, 1969) or ships (Hendey, 1974). Du Saar (1967) also identified the transportation of allochthonous diatoms by the wind, within the sea spray or being blown up from the beach sand. The large range of allochthonous sources can result in their population exceeding that of the autochthonous component, leading to erroneous interpretations of the local environment (Beyens and Denys, 1982).

Strategies have been proposed to identify the allochthonous component of a diatom assemblage however it can be complex (Beyens and Denys, 1982). Simonsen (1969) suggested characterising the assemblage into benthic and planktonic taxa and considering only the former due to the latter being more frequently transported. Simonsen (1969) applied this method to diatom analysis completed for the Amazon by Gessner (1959) and illustrated a reversal of the results. The subdivision of diatoms into benthic and planktonic removed the erroneous identification of samples as brackish-marine origin where salinities were known to be zero (Simonsen, 1969). Omitting fragmented diatoms, based on the assumption of long distance transportation, has also been proposed however fragmentation can occur due to proximity to the coast (Berglund, 1971), very shallow environments (Denys, 1993), exposure to the air or storm surges (Brockmann, 1940), sediment compaction or sample pre-treatment. Only diatom fragments exceeding at least half of the original valve, including the central part, were counted in samples analysed for this thesis.

Beyens and Denys (1982) consider the ecology of diatom taxa alongside additional evidence such as lithostratigraphy and palaeontology to identify allochthonous valves. Denys and De Wolf (1999) state that factors such as life form, abundance and frequency, valve preservation, palaeogeographic setting and ecological comparability within the assemblage should be considered when differentiating between the autochthonous and allochthonous components of diatom assemblages. Although planktonic taxa have been identified as allochthonous, due to their transportation within tidal environments

(Simonsen, 1969; Vos and De Wolf, 1993), their increased input, or dominance, strongly indicates tidally influenced hydrodynamic conditions, providing useful information for palaeoenvironmental interpretations.

Diatom dissolution can be problematic for interpretations of all aquatic environments but is particularly significant in marine or saline environments (Johnson, 1974; Flower, 1993; Barker et al., 1994; Ryves et al., 2001). Dissolution experiments completed by Ryves et al. (2001) identified that resistance to dissolution varies morphologically (i.e. larger, more silicified taxa are more resilient) and exhibits inter- (e.g. within *Cocconeis* genus) and intra-specific (e.g. raphid vs. araphid) variation. It is well documented that selective dissolution results in heavily silicified valves being preferentially preserved over weakly silicified valves (Jorgensen, 1955; Lewin, 1961; Round, 1964; Johnson, 1974; Denys, 1984). The occurrence of weakly silicified diatom valves such as *Fragilaria striatula* or *Pleurosigma aestuarii* is an indication that dissolution is limited (Denys, 1984). Species-specific solubility rates occur due to variation in the surface/volume ratio and thickening of diatom cell walls (Lewin, 1961). The dominance of heavily silicified marine species such as *Paralia sulcata* has been well documented (Vos and De Wolf, 1988; Denys and De Wolf, 1999; McQuoid and Nordberg, 2003). Jorgensen (1955) completed experiments assessing how diatom solubility varies between species with changes in pH. Differences in solubility rate between diatom species were noted for the same pH, indicating that hydrolysis of silicon compounds within diatom cells can occur at different rates (Jorgensen, 1955). *Thalassiosira nana* was shown to completely dissolve in pH 10 whilst only ~ 17 % of the silicon in *Nitzschia linearis* had dissolved over the same time period at the same pH (Jorgensen, 1955). Factors such as low sedimentation or low productivity rate have also been shown to adversely affect the preservation of siliceous microfossils (Johnson, 1974).

Diatom preparation methodology

Diatom preparation followed the standard method summarised by Palmer and Abbott (1986) and Battarbee (1986) using hydrogen peroxide digestion and slide mounting with Naphrax (Appendix 4). Sample resolution was led by the stratigraphic record. Transitions of initial interest were investigated at a high resolution of 2 cm to 4 cm whilst low resolution samples, taken every approximately 16 to 32 cm, filled in the gaps in diatom analysis where the lithology was more consistent. A minimum of 250 diatoms were counted systematically per slide in a vertical transverse to obtain a statistically robust assemblage following Zong and Tooley (1999); Hamilton and Shennan,(2005); Woodroffe and Long (2010); Barlow et al. (2014) and avoid multiple counts of the same valves.

Diatoms were identified using the visual guides and taxonomic principles of van der Werff and Huls (1957-1974), Krammer and Lange-Bertalot (1991) and Hartley et al. (1996).

Diatom taxa were classified based on their salinity preferences using the halobian classification scheme (Hustedt, 1953). Scientific names have been updated only for diatom species exceeding 5 % of the total count for each site using AlgaeBase (Guiry and Guiry, 2019) and the World Register of Marine Species (WoRMS Editorial Board, 2019). Changes in the counted diatom assemblage, and their salinity preferences, were illustrated using C2 (Juggins, 2003). Zonations within the data set for each site were determined using the constrained incremental sums of squares (CONISS) program in *Tilia*, informed by palaeoecological evidence and reasoning (Grimm, 1987). Data was transformed using the square root transformation within CONISS due to interest in the dominant trends within the overall dataset rather than individual indicative species which may be subordinate (Grimm, 1987).

3.3.4 Foraminifera

Foraminifera were picked and counted were diatom preservation was problematic to determine the onset or culmination of marine influence. Foraminifera are single-celled animals advantageous for reconstructing past ocean conditions due to their ubiquity, preservation potential and sensitivity to environmental variables, in particular temperature and salinity (Edwards and Wright, 2015). Intertidal foraminifera inhabit distinct vertical zones which can be correlated with tidal elevation. For example, *Jadammina macrescens* occurs within a very narrow zone near the HAT tide and therefore has the potential to constrain RSL with a precision of ± 0.05 m (Scott and Medioli, 1980). As a result, intertidal foraminifera have been used within RSL research since the 1970s (Scott and Medioli, 1978; 1980; Gehrels, 1999; Massey et al., 2006; Kemp et al., 2009).

Foraminifera samples were analysed at a 5 cm resolution and sample preparation followed the standard method of wet picking the 500 μm and 63 μm sieved fraction outlined in Appendix 5 (Scott and Medioli, 1980). Where possible, a minimum of 100 foraminifera were counted per sample. Identification follows the resources produced by Murray (1979) and Gehrels (2002), with the former used to determine taxonomy.

3.4 Chronology
3.4.1 Radiocarbon Dating

AMS radiocarbon dating has been extensively used to determine the age of post-LGM changes in sea-level tendency (e.g. Shennan et al., 2018) and was used to constrain the chronology of major coastal behavioural changes identified in this thesis using microfossil and stratigraphic analyses. Material to constrain the timing of these changes was sampled within organic units adjacent to the lithological transitions. Basal peat samples from a

range of altitudes were also submitted for AMS radiocarbon dating to constrain the onset of peat deposition and rising regional ground water level (Törnqvist et al., 1998; 2004).

Plant macrofossils and seeds were preferentially selected for radiocarbon analysis, where possible. Ages based on bulk sediment are less reliable as the potential for non-representative sample ages, due to the influence of younger or older carbon, is greater. Geyh et al. (1974) illustrated that microbial growth can introduce contamination from modern carbon into sediments whilst the downward reworking of humic acids and rootlets can also yield younger radiocarbon ages (Balesdent, 1987). Radiocarbon dating of bulk peat samples and *in situ* plant macrofossils extracted from the same peat sample by Shennan et al. (2008) identified significant differences in the ages obtained. Quantitative analysis by Hu (2010) suggests a "bulk error" of ± 100 ^{14}C be applied to radiocarbon dates based on bulk peat (Hijma et al., 2015). Reservoir effects, resulting from the ^{14}C content of the marine and freshwater reservoirs being offset from the atmospheric reservoir, need to also be considered when selecting samples for radiocarbon dating (Olsson, 1991; Ascough et al., 2011; Törnqvist et al., 2015). Care was therefore taken to select material comprised of terrestrially sourced carbon, such as emergent plants, for radiocarbon dating (Olsson, 1991; Ascough et al., 2011; C. Hunt, personal communication). Appendix 6 outlines the methodology for picking material for radiocarbon analysis and details of sample pre-treatment.

17 samples were submitted for radiocarbon analysis at the Natural Environment Research Council (NERC) Radiocarbon dating facility in three sets of analysis (Set 1: 5 samples (Allocation no: 2037.1016), set 2: 7 samples (Allocation no: 2075.1017), set 3: 5 samples (Allocation no: 2112.0418)). An additional two samples were analysed at BETA Analytic. Plant macrofossils and/or seeds were picked and submitted for analysis for 17 samples whilst one sample is based on bulk material, due to the absence of plant macrofossils and seed, and another on wood. Details of the material submitted for AMS radiocarbon analysis is outlined in the associated results chapters. The AMS radiocarbon dating results are outlined for each date in Appendix 7. Dates were calibrated using CALIB 7.1 (Stuiver et al., 2018) and the IntCal13 calibration curve to determine the 2 sigma age range and are presented as the full age range within the text. Dates were rounded to the nearest 10 years for samples with a standard deviation for the radiocarbon age exceeding 50 years (Stuiver et al., 2018).

Chapter 4: Results and interpretation-Walberswick National Nature Reserve

This chapter presents the results for the three sites investigated in the Walberswick National Nature Reserve (NNR), Westwood Marsh, Oldtown Marsh and Great Dingle Hill. A background to this section of the coast, relating to changes in coastal configuration and human land use change, is initially provided. Following which, each site is split into five sections; site description and survey, lithostratigraphy and sedimentology, biostratigraphy, chronology and finally a palaeoenvironmental interpretation. The results and palaeoenvironmental interpretation presented for Oldtown Marsh and Great Dingle Hill in this chapter have been published in Quaternary International (Hamilton et al., 2019; Appendix 8).

4.1 Study area background

Westwood Marsh, Oldtown Marsh and Great Dingle Hill are situated between Southwold and Dunwich, in the Walberswick NNR (Figure 4.1). The Walberswick NNR contains a range of habitats, including reedbeds, grazing marsh, woodland, intertidal mudflats and the Blyth tidal estuary. The area is of national and international importance for nature conservation, falling within protections including the Suffolk Coast and Heaths AONB, Minsmere-Walberswick Heaths and Marshes SSSI, Walberswick Heaths and Marshes Special Area of Conservation (SAC), Minsmere-Walberswick Special Area of Protection (SPA) as well as the Minsmere-Walberswick Ramsar site (Natural England, 2013).

Conceptual reconstructions, based on historical maps and documents, indicate that the configuration of the coastline of the Walberswick NNR has changed dramatically over the last 1500 years. Between c. 1500 and 700 AD the Blyth River was diverted south by the development of Kingsholme spit (Figure 2.9) to form a common estuary with the eastwards flowing Old Dunwich River (Gardner, 1754; Steers, 1927; Chant, 1974; Parker, 1978; Comfort, 1994; Pye and Blott, 2006). This configuration of the coast was influential in Dunwich becoming one of the largest ports on the east coast, with a thriving fishing industry, by the time of the Domesday Survey in 1089 AD (Darby, 1935). Storms during the 13th and 14th century are documented to have blocked the entry to the estuary, connecting the distal point of Kingsholme spit with the Dunwich cliffs (Steers, 1927). Aside from this historical information, the understanding of the Holocene evolution of the area associated with the Walberswick NNR on the Suffolk coast is limited.

Human intervention is important for landscape change from the 16th century, with evidence of extensive drainage and reclamation well documented. Westwood Marsh was reclaimed from fens and saltings at the end of the 16th century despite being of limited value (Warner, 2000; Good and Plouviez, 2007). In addition, a drainage windmill, associated with post-medieval drainage schemes, was built at the coastal tip of Westwood Marsh (Figure 4.2) during the mid-18th century to drain the marshes (Warner, 2000).
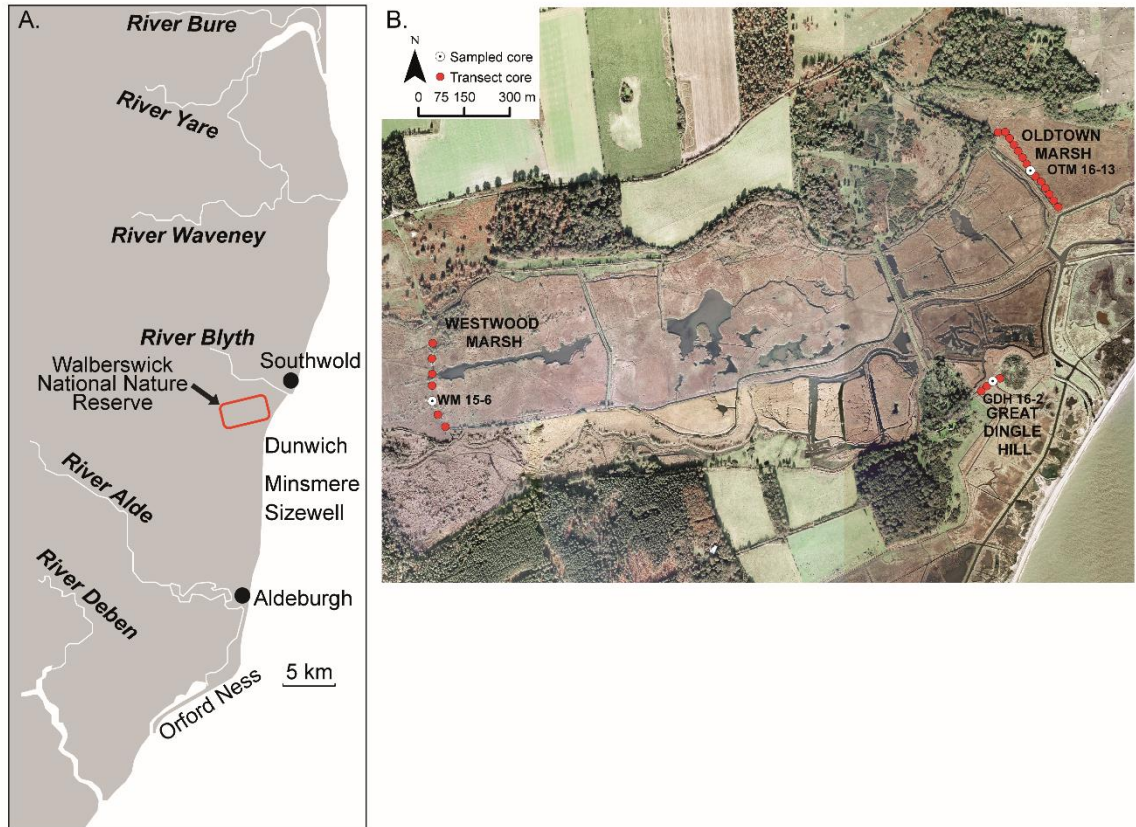
Figure 4.1: A. Suffolk coast with the Walberswick NNR highlighted in red. B. Stratigraphic transects completed at Westwood Marsh, Oldtown Marsh and Great Dingle. The red filled circles represent gouge cores and the white filled circles denote the sediment sequences sampled for analysis. Aerial imagery: © Getmapping Plc.

The timing of enclosure can be inferred from the sinuosity of the drainage channels. The complex pattern of curvilinear and straight dykes throughout the Walberswick NNR are characteristic of 18th and 19th century drainage improvements whilst the highly serpentine pattern of dykes in Oldtown Marsh suggests that this area was enclosed earlier (Good and Plouviez, 2007). Maintenance of the drainage schemes was neglected throughout the 19th century, due to the decline in agriculture, and throughout WW2, as a defensive measure, resulting in the extensive return of reed bed throughout the area during the 20th century (Williamson, 2005). The management of the Walberswick NNR since the 16th century has

left a distinctive signature on this landscape in the form of extensive drainage subdividing the marshes.

Figure 4.2: Disused drainage windmill situated at coastal tip of Westwood Marsh. Dingle Little Hill and Dingle Great Hill are visible in the distance, on the left and right side of the windmill respectively. The dome of Sizewell B nuclear power station is also visible further down the coast.

4.2 Westwood Marsh

4.2.1 Site description and survey

Westwood Marsh is one of Britain's largest reedbeds, extending 2.5 km southwest of the coastline between Southwold and Dunwich (Figure 4.1). The site infills a valley, with higher relief surrounding and woodland and heath dominant on the southern and southwestern boundary. The catchment area is small and characterised by a blind-ended basin with no significant freshwater drainage entering the system. Large man made areas of open water, many of which were created in the mid-20th century for wildlife interests, extend through the central section of the marsh. Drainage channels are extensive across the longitudinal and latitudinal axis, running parallel to tracks.

Access to Westwood Marsh, and coring on it, was restricted by the open water, extensive reeds and drainage channels. Stratigraphy was therefore investigated near to a raised track extending north-south at the western end of the marsh. The stratigraphy along this most westerly north-south track was investigated using a gouge corer at a maximum

interval of 50 m. A core for analysis was sampled using a Russian corer and selected based on its position in the middle of the marsh, preservation of transitional contacts and representative stratigraphy. Drainage channels prevented a complete transect across the longitudinal axis of the site however the evidence suggests that the deepest sediments were reached because the basement was beginning to shallow again in the final core investigated.

4.2.2 Lithostratigraphy and sedimentology

The transect completed along the north-south axis of Westwood Marsh revealed woody, basal peat, underlain by a sandy basement, which transitions upwards into minerogenic deposits overlain by *Phragmites* peat (Figure 4.3). The sampled core (WM-15-6) is 370 cm deep and consists of three main units (Table 4.1). The peat unit (370 cm to 140 cm) contains frequent rootlets, occasional wood fragments and sand in the bottom 50 cm. Rootlets are present throughout the overlying silty clay unit (140 cm to 24 cm), with patches of concentrated herbaceous material occurring irregularly (e.g. 140 cm to 110 cm). This is replaced by a well rooted *Phragmites* peat deposit (24 cm to 0 cm).

The clay, silt and sand fractions were analysed from 12 samples, in the silty clay deposit, between 142 cm and 20 cm (Figure 4.4). Samples were analysed at a 2 cm resolution close to transitions with the under- and over-lying organic units, with resolution increasing in the homogenous silty clay unit. The silt and clay fraction fluctuate between 142 and 134 cm, with a small sand peak occurring at 134 cm (3 %). The silt fraction dominates the samples, exceeding 50 % from 132 cm to 20 cm. Using the graphic sedimentary domains defined by Tanner (1991a; 1991b) and modified by Lario et al. (2002), the bivariate plot of mean particle size against standard deviation shows that the majority of the sediments were deposited in an open to filled estuary environment (Figure 4.5). End-member mixing analysis, using the Paterson and Heslop (2015) model, identified one particle size end-member that accounts for 97.9 % of the variance in the Westwood Marsh data. This end-member is composed primarily of silt (60 %), with clay (40 %) and a subordinate sand component (< 1 %). A second end-member is not included due to linear correlation indicating that the end-members are not linearly independent, with a R^2 exceeding 0.8 indicating overfitting.
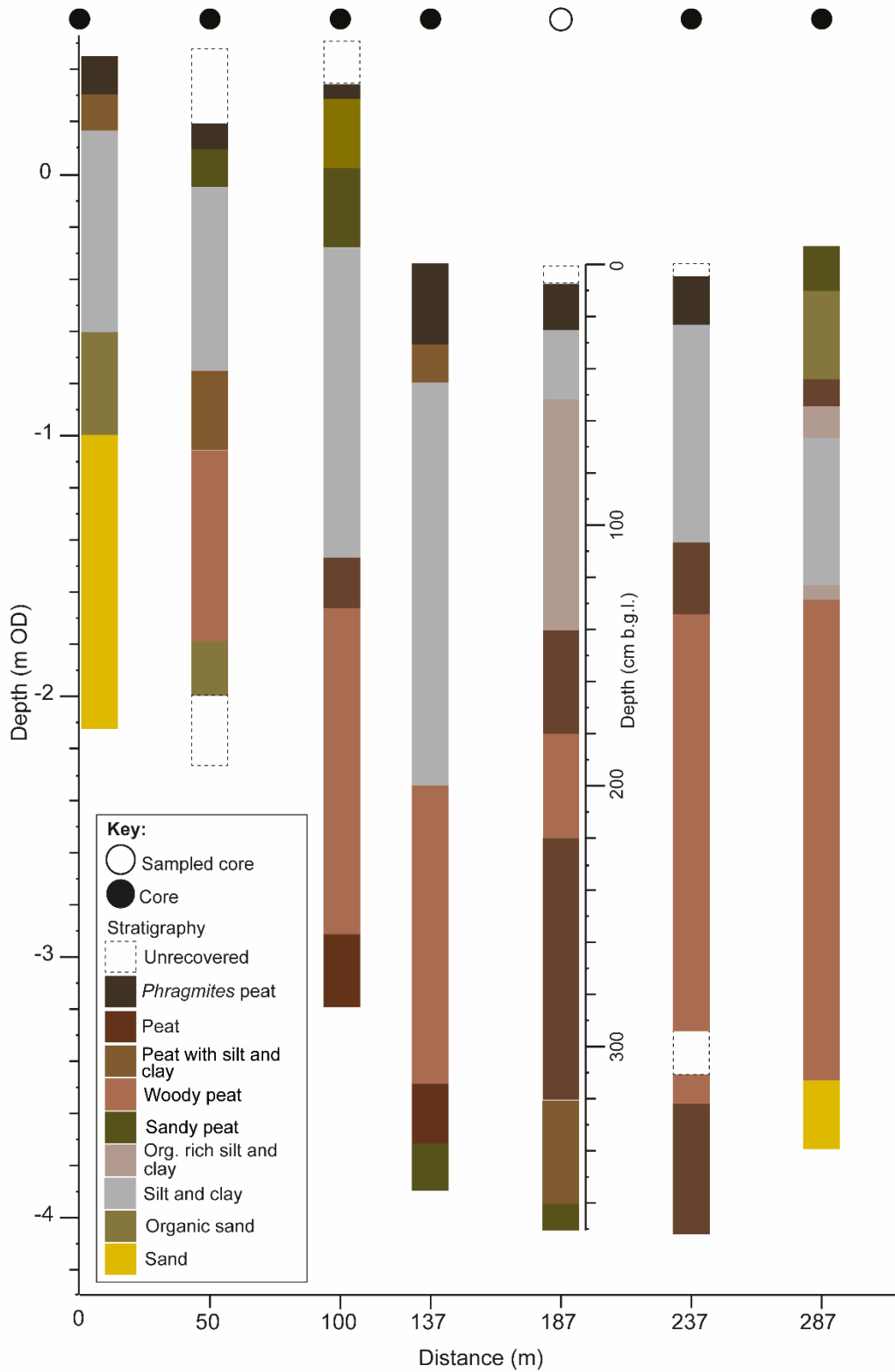
Figure 4.3: Stratigraphic transect completed at Westwood Marsh. See Figure 4.1B for the location of Westwood Marsh, and the stratigraphic transect, in relation to other sections of the coastline. The depth (cm) below ground level is provided for the sampled sediment sequence, WM-15-6.

Table 4.1: Description of main sediment units identified in WM-15-6 and associated Troels-Smith *(1955) classification.*

Unit depth (cm)	Description	Troels-Smith log
0-6	Unrecovered	
6-24	Well rooted *Phragmites* peat	Sh2 Th[1] Th^{phrag}+ nig 3+ strf 0 elas 1 sicc 2 lim sup 0
24-45	Silty clay with modern *Phragmites* penetrating	As3 Ag1 Th^{phrag}+ nig 2+ strf 0 elas 0 sicc 3 lm sup 0
45-140	Silty clay with rootlets, patches of herbaceous material and *Phragmites* rhizomes.	As3 Ag1 Th^2+ Sh+ Th^{phrag}+ nig 3 strf 0 elas 0 sicc 3 lm sup 0
140-180	Crumbly, humified peat with modern P*hragmites* rhizones penetrating and rootlets throughout	Sh3 Th^{2}1 Th^{phrag}+ nig 4 strf 0 elas 1 sicc 2 lm sup 3
180-220	Well humified peat with frequent rootlets, occasional wood fragments, *Phragmites* and herbaceous remains	Sh2 Th^{3}2 Dl+ nig 4 strf 0 elas 0 sicc 3 lm sup 0
220-320	Well humified peat penetrated by modern P*hragmites,* with reeds and herbaceous remains throughout	Sh2 Th^{3}2++ Th^{phrag}+ nig 4 strf 0 elas 0 sicc 3 lm sup 0
320-360	Herbaceous silty peat with wood	Sh2 Th^{3}1 Ag1 Dl+ nig 3++ strf 0 elas 0 sicc 3 lm sup 0
360-370	Herbaceous silty peat with sand	Sh2 Th^{3}1 Ag1 Ga+ nig 3++ strf 0 elas 0 sicc 3 lm sup 0

54
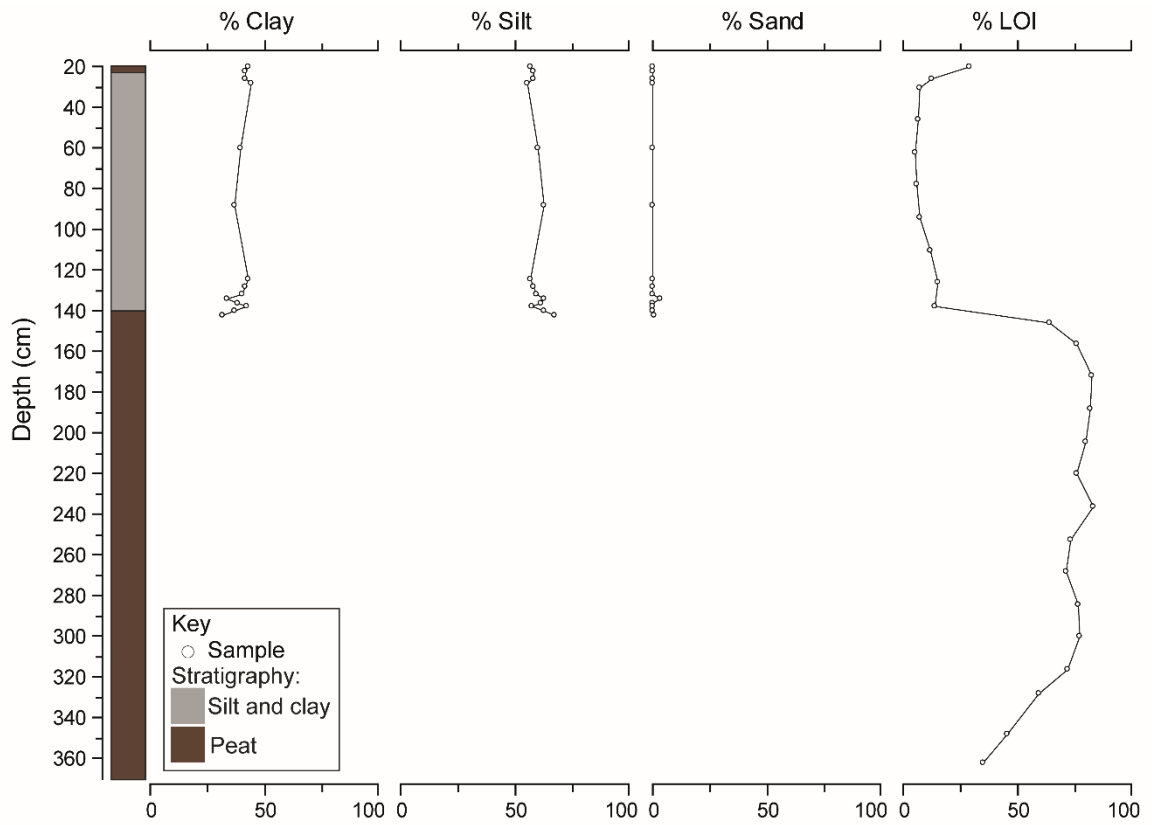
Figure 4.4: Stratigraphy, particle size and LOI for WM-15-6. The boundaries for the clay, silt and sand fraction are defined by Wentworth (1922)*.*
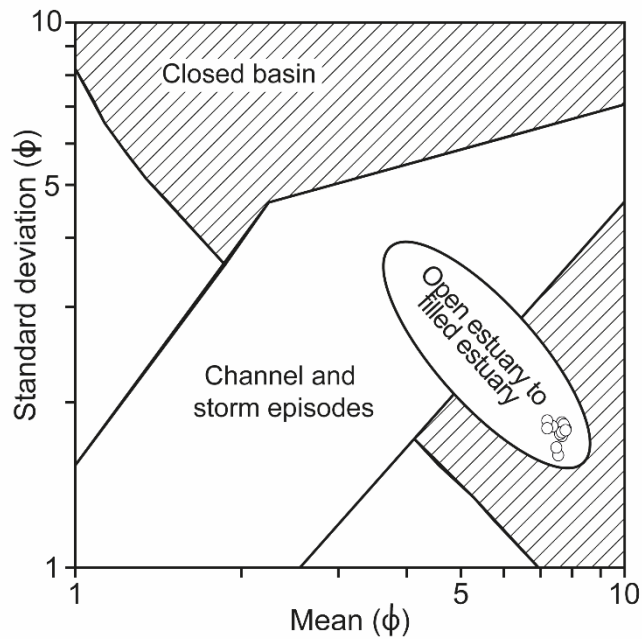
Figure 4.5: Bivariate plot of mean against standard deviation (phi) for WM-15-6. The graphic sedimentary domains determined by Tanner (1991a; 1991b)*, and later modified by* Lario et al. (2002) *are overlain onto this plot. Permission to reproduce this figure has been granted by Elsevier.*

The percentage LOI was analysed in 25 samples at a resolution ranging from 16 cm to 4 cm in the core (Figure 4.4). The organic content gradually increases, from 35 % to 72 %, in the bottom 50 cm, as the sand content decreases upwards from the basement. The organic content remains stable for the upper section of the peat unit, exceeding 70 %. The gradual decline from 170 cm is followed by a sharp decrease from 64 % to 14 % associated with the shift from peat to silty clay sedimentation at 140 cm. The low organic content is sustained until 30 cm following which it increases prior to the deposition of the well rooted *Phragmites* peat unit.

4.2.3 Biostratigraphy

Diatom preservation was problematic in WM-15-6. Diatoms were preserved at the lower boundary of the silty clay unit (140 cm to 24 cm) however were scarce throughout the rest of the sampled core.

Diatom analysis identified 130 species from nine samples (all raw counts are presented in Appendix 9). Four zones were identified, based on diatom flora and lithostratigraphy however Zone 1 and 4 are only characterised by one diatom sample and are used with due caution (Figure 4.6 and 4.7). The diatom assemblage is divided into an isolated brackish dominance (Zone 1: 370 cm to 141 cm), a brackish-marine zone with a subordinate freshwater component (Zone 2: 141 cm to 135 cm), a brackish-marine zone with a decreasing freshwater component (Zone 3: 135 cm to 123 cm) and a brackish dominated zone (Zone 4: 123 cm to 20 cm).

Brackish epipelic taxa, such as *Caloneis westii* and *Diploenis didyma*, dominate the single sample in Zone 1. Marine taxa, particularly *Paralia sulcata* species, are abundant in this sample and a subordinate freshwater component (4 % of the total count) is present. Samples for foraminifera were picked at 320 cm and 205 cm however no tests were found.

Brackish epipelic and marine planktonic taxa dominate Zone 2, each reaching 51 % of the total count in this zone. *Diploneis ovalis*, a freshwater aerophilous taxa, is also present in this zone, peaking at 8 % of the total count.

Brackish epipelic taxa, such as *Scolioneis tumida* and *Diploneis didyma*, dominant Zone 3, increasing from 50 % to 76 % of the total count between the lower and upper boundary of this zone. Marine taxa, particularly planktonic species, decrease in this zone. The freshwater component of this assemblage decreases to less than 1 % at the upper boundary of Zone 3.

Zone 4 is characterised by a single diatom sample. Brackish epipelic taxa, particularly *Diploneis didyma*, dominate this sample (81 % of the total count). *Paralia sulcata*, a marine planktonic taxa, is also present and represents 8 % of the total count.
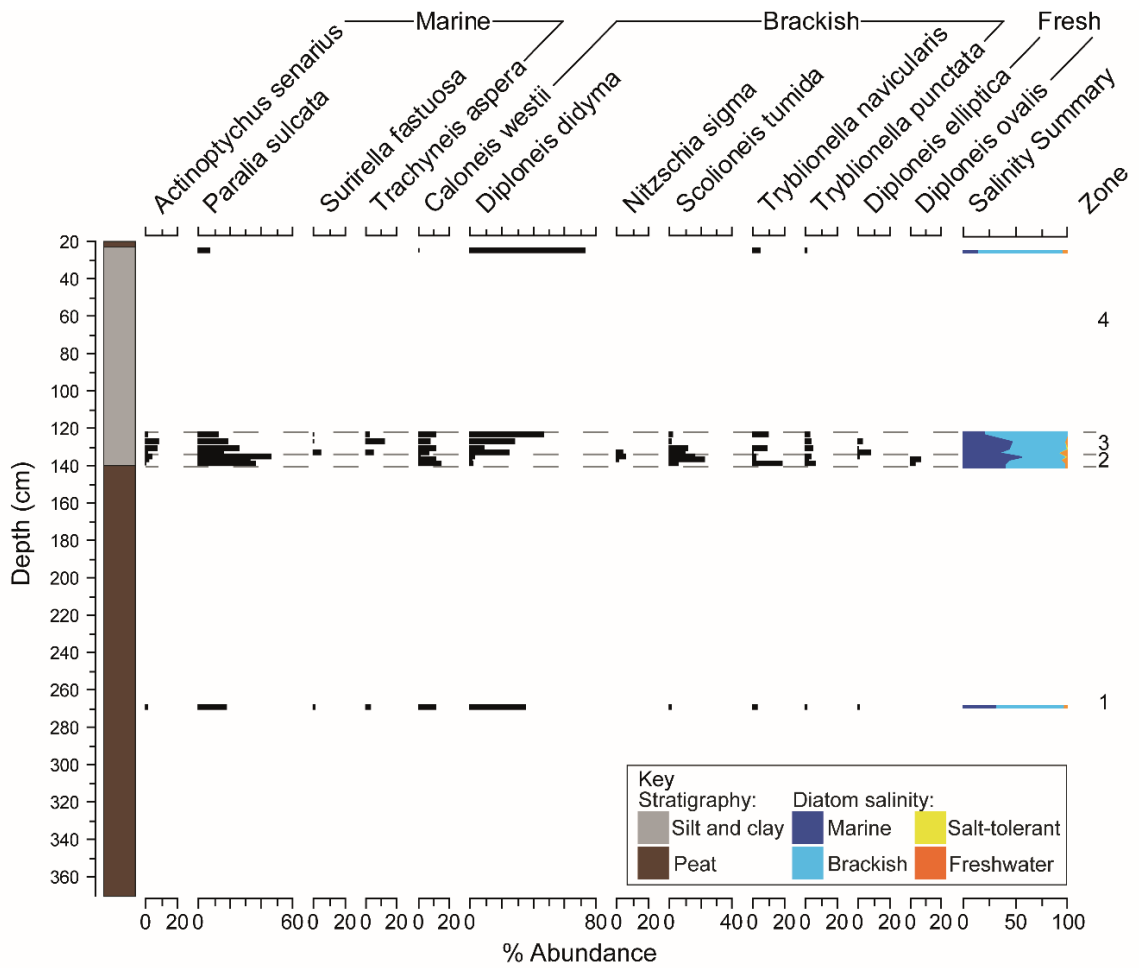
Figure 4.6: Diatom assemblage for WM-15-6; species shown exceed 5 % of the total count. Diatoms are grouped based on their salinity tolerance using the halobian classification (Hustedt, 1953)*.*
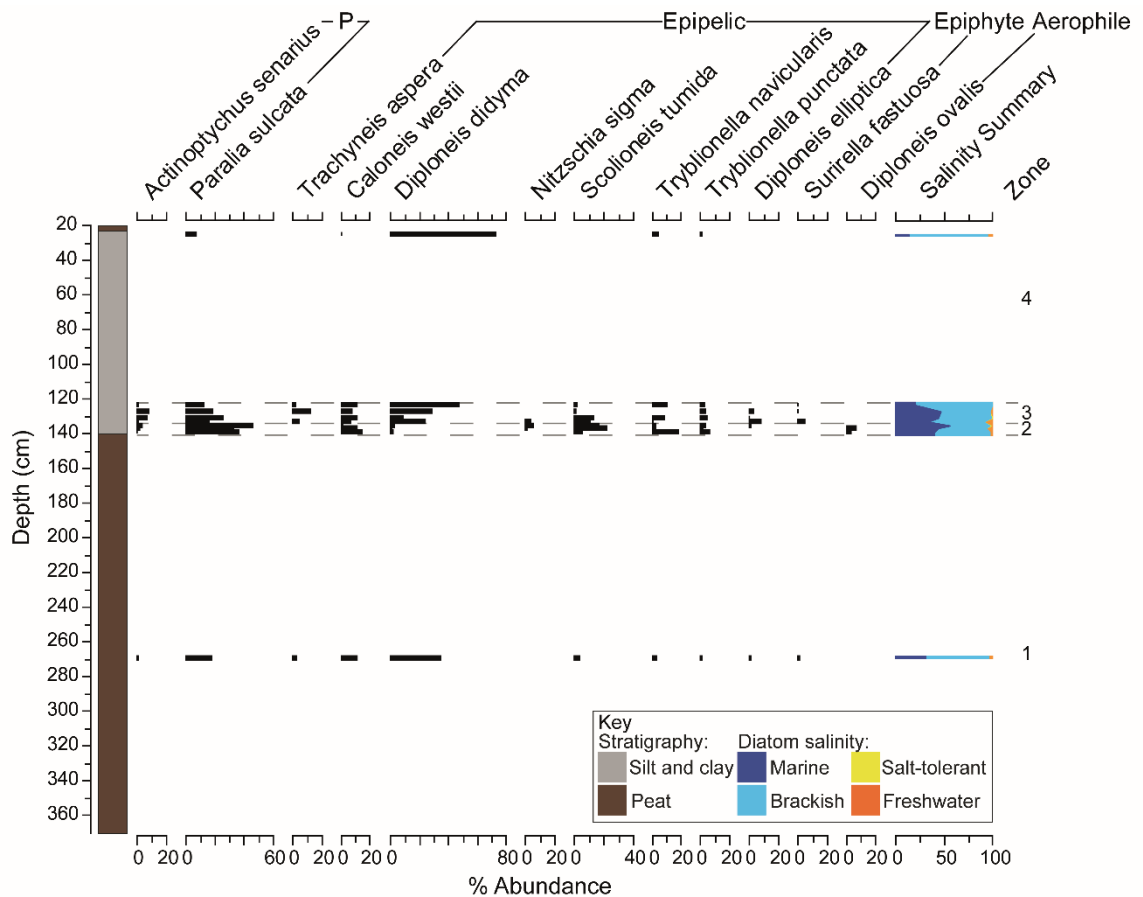
Figure 4.7: Diatom assemblage for WM-15-6; species shown exceed 5 % of the total count. Diatoms are grouped based on their life form using Vos and De Wolf (1988; 1993)*.*

4.2.4 Chronology

The base of the Westwood Marsh core was sampled to constrain the timing of the onset of peat deposition and the rising regional ground water level using AMS radiocarbon dating. A sample from 365.5 cm (-4.01 m OD), comprised of *Poaceae* remains and *Carex* seeds, was radiocarbon dated at Beta Analytic, Miami. Plant macrofossils were limited at the base of WM-15-6 resulting in a small sample (0.51 mg) being submitted for radiocarbon dating Diatoms were not preserved at the base of the core, which along with the stratigraphic context suggests the radiocarbon date is freshwater limiting. The onset of peat deposition was dated to 10501-10258 cal BP (Laboratory code: BETA-512111) (Table 4.2).

A shift in sedimentation, from minerogenic peat to silty clay, occurs at 140 cm (-1.76 m OD). Brackish-marine species dominate the diatom assemblage of the silty clay unit. A sample for AMS radiocarbon dating to constrain the timing of this transition was collected at 141 cm (-1.77 m OD). Plant macrofossils, such as *Rumex* and *Poaceae* seeds, were

sent to the NERC Radiocarbon Facility, East Kilbride. The shift in sedimentation was dated to 894-683 cal BP (Laboratory code: SUERC-72906).

Table 4.2: AMS radiocarbon dates produced for Westwood Marsh.

Site	Sample ID	Laboratory code	NERC Allocation number	^{14}C ± 1σ BP	Cal age (cal BP)- 2σ range	
					Max	Min.
Westwood Marsh	WM-15-6 - 1.77 m OD	SUERC-72906	2037.1016	836 ± 35	894	683
	WM-15-6 - 4.01 m OD	BETA-512111	NA	9220 ± 40	10501	10258

4.2.5 Palaeoenvironmental interpretation

Peat sedimentation initially dominates the transect completed at Westwood Marsh, with biostratigraphic analysis of WM-15-6 indicating that the onset of minerogenic sedimentation is associated with an intertidal environment. Poor diatom preservation restricts the palaeoenvironmental interpretations that can be made from WM-15-6 (Figure 4.8). The dominance of brackish epipelic taxa from the single sample in the peat unit (370 to 140 cm), as well as the silty clay unit (140 to 24 cm), indicates that Westwood Marsh has been tidally influenced throughout the Holocene.

The diatom sample analysed in the peat unit (370 to 140 cm) is indicative of an intertidal mudflat environment however the organic content remains high, exceeding 50 %, throughout this unit. The dominance of wood peat prior to 140 cm indicates a local depositional system of fen carr, with occasional influx of brackish tidal waters. Foraminifera were not found in the samples analysed (320 cm and 205 cm) therefore not identifying a marine influence elsewhere in this unit. The localised migration of tidal channels, or occasional inwashing of tidal waters close to HAT is therefore a likely explanation for the isolated occurrence of brackish-marine conditions at 270 cm.

The onset of silty clay sedimentation at 894-683 cal BP (140 cm) is associated with a dominance of brackish epipelic diatoms and occurrence of marine planktonic diatoms. The assemblage of this unit therefore strongly indicates tidally influenced hydrodynamic conditions. The brackish epipelic taxa (e.g. *Caloneis westii*, *Tryblionella navicularis* and *Diploneis didyma*) dominating the lower and upper contact of the silty clay unit are indicative of intertidal to lower supratidal mudflats and creeks, as well as subtidal marine basins and lagoons (Vos and De Wolf, 1988; 1993). Marine planktonic taxa, which comprise over a third of the assemblage at the lower contact of the silty clay unit, are

associated with sub-tidal areas or large tidal channels (Vos and De Wolf, 1988; 1993). The presence of marine planktonic diatoms has been associated with open-inlet conditions (Bao et al., 1999; Freitas et al., 2002) as well as barrier breaching (Sáez et al., 2018). Marine planktonic taxa decrease in abundance following the shift to silty clay sedimentation and this decline continues between 124 cm and 26 cm despite the absence of diatoms between these samples. This decrease, in addition to the reoccurrence of freshwater taxa by 26 cm and the change in stratigraphy to organic sedimentation, suggests the annealing of a barrier breach or tidal inlet.

There is no clear stratigraphic signature of reclamation at Westwood marsh. The transition from minerogenic to organic sedimentation is denoted by a slightly truncated boundary in several cores in the transect. This provides evidence for disturbance, potentially relating to peat cutting. In addition, differences in relief are visible in the north-northeast section of Westwood Marsh, with reeds at different heights.
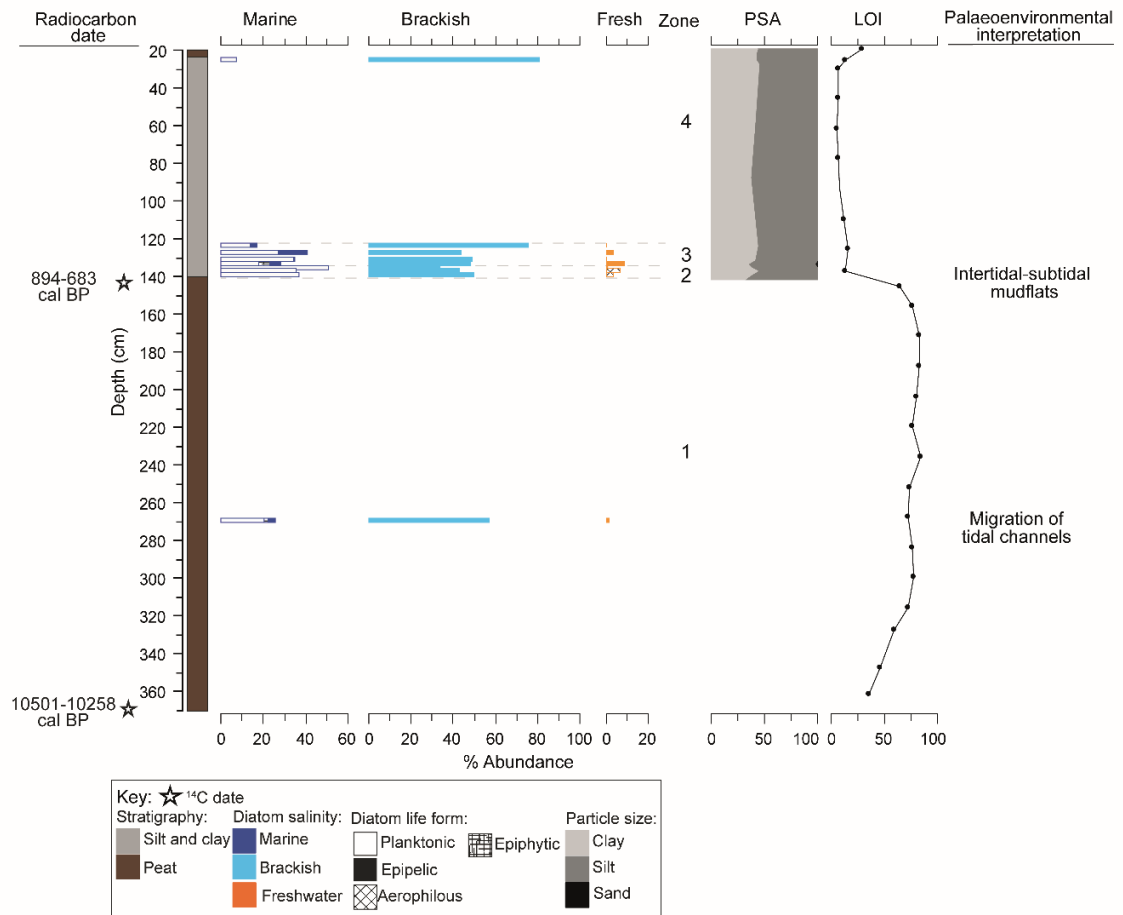
Figure 4.8: Summary diagram of results produced for WM-15-6 with palaeoenvironmental interpretation. Stratigraphy, particle size, organic content and the diatom summary, illustrating changes in salinity and life form, are presented.

4.3 Oldtown Marsh

4.3.1 Site description and survey

Oldtown Marsh is situated at the coastal end of Westwood Marsh (Figure 4.1). The site is surrounded by forested land of increasing relief and separated from the sea by the Dunwich River and Corporation Marshes. The medieval port of Walberswick is believed to have been situated in the area of Oldtown Marsh (Suffolk Coastal District Council, 2013).

Reeds are abundant at Oldtown Marsh however fieldwork in April 2016 coincided with the annual cutting period which occurs prior to bird breeding season (Figure 4.9). This provided access to the central parts of the marsh away from paths bordering its edge. Changes in stratigraphy were documented along a transect extending from the back of Oldtown Marsh, towards the sea (Figure 4.10). The location and direction of the seawards transect was largely predetermined by the section of the marsh where the reeds had been cut. The stratigraphy was investigated every c. 25 m, using a gouge core, revealing a series of alternating organic and minerogenic units. A sample for analysis was taken using a Russian corer from the central section of the seawards transect, near the south western boundary of the marsh, where the stratigraphy captured the main units representative of the site.

Figure 4.9: Photograph of Oldtown Marsh transect, illustrating the section of the site were reeds were cut. The disused drainage windmill situated at coastal tip of Westwood Marsh (Figure 4.2) is visible.

4.3.2 Lithostratigraphy and sedimentology

The stratigraphy at Oldtown Marsh contains a series of alternating organic and minerogenic units (Figure 4.10). The sampled sediment sequence from Oldtown Marsh (OTM-16-13) is comprised of five main sediment units (Table 4.3). A lower, variably humified, peat unit with occasional wood fragments (589 to 332.5 cm) is overlain by an organic clayey silt unit (332.5 cm to 254 cm), a middle fibrous woody peat unit (254 cm to 214.5 cm), a silty clay unit (214.5 cm to 45 cm) and an upper fibrous peat unit (45 cm to 0 cm).
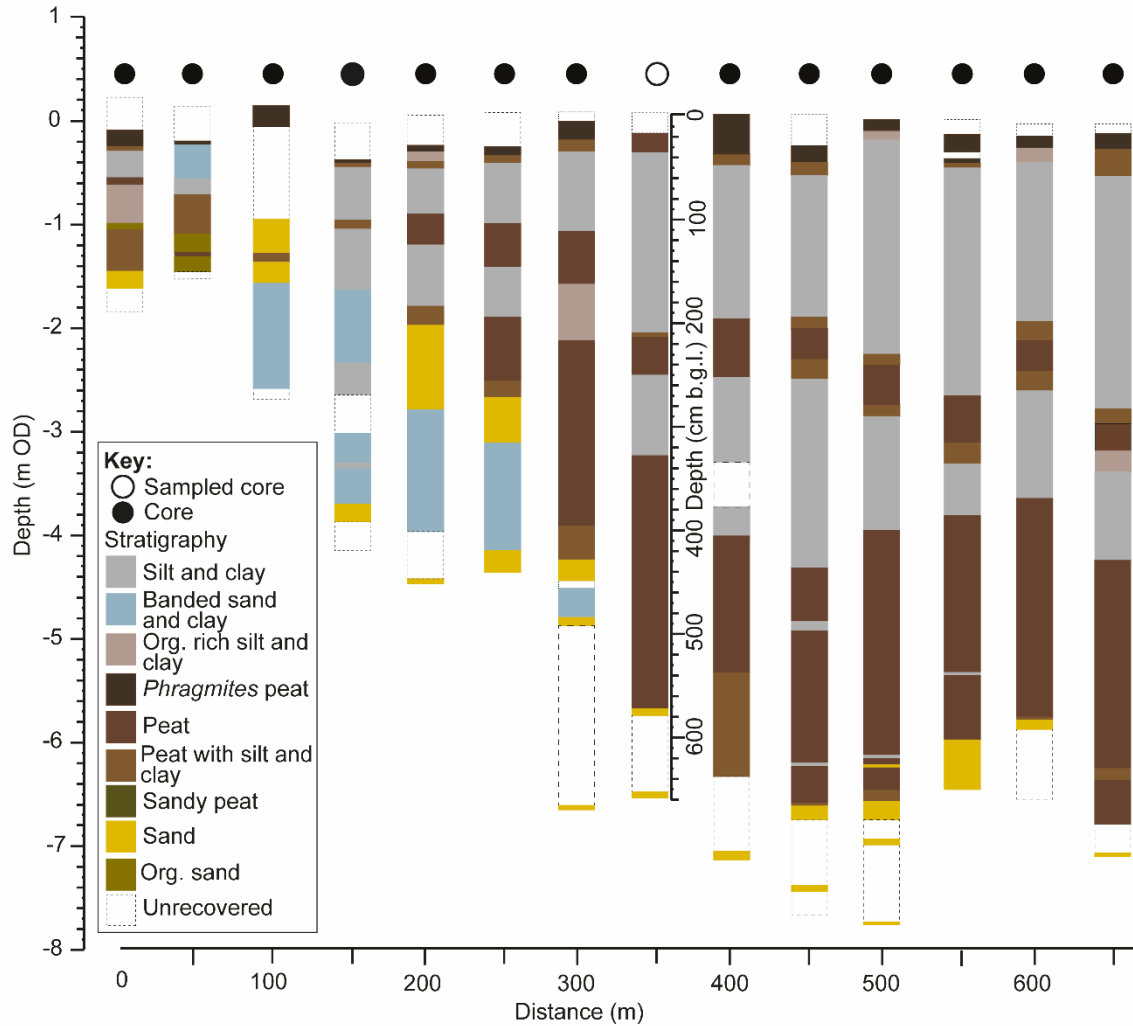
Figure 4.10: Stratigraphic transect completed at Oldtown Marsh. See Figure 4.1B for the location of Oldtown Marsh, and the stratigraphic transect, in relation to other sections of the coastline. The depth (cm) below ground level is provided for the sampled sediment sequence, OTM-16-13.

The particle size data set for Oldtown Marsh extends from 332 cm to 41 cm and contains 46 samples, at a resolution ranging from 1 cm to 32 cm depending on the stratigraphic variability (Figure 4.11). A fining upwards trend occurs between 332 cm and 256 cm, with the clay fraction peaking at 76 %, followed by a sharp increase in silt. A minor peak in the

sand (5 %) occurs at 240 cm, with this fraction remaining subordinate (< 1 %) until ~ 211 cm. The particle size is highly variable between 224 cm and 168 cm, with dominance fluctuating between the clay and silt fraction. The particle size stabilises from 168 cm, with the silt fraction remaining at c. 62 %.

Table 4.3: Description of main sediment units identified in OTM-16-13 and associated Troels-Smith (1955) *classification.*

Unit depth (cm)	Description	Troels-Smith log
0-45	Fibrous peat with abundant *Phragmites*	Sh2 Th^{0}2 Ag+ nig 3 strat 0 elas 1 sicc 1+
45-210	Clayey silt with increasing traces of organics with depth	Ag2+ As2 Th^0+ Th^1+ Sh+ nig 2+ strat 0 elas 0 sicc 2+ lm.sup 2
210-216	Silty peat	Sh3 Ag1+ Th^0+ Th^1+ As+ nig strat 0 elas 0 sicc 2+ lm.sup 1
216-254	Fibrous woody peat	Sh2 Th^{1}2 Th^0+ Dl++ As+ Ag+ nig 3+ strat 0 elas 1 sicc 1+ lm.sup 0
254-332.5	Clayey silt with abundant rootlets and patches of organics	Ag2+ As2 Th^1+ Th^2+ Sh+ nig 2+ strat 0 elas 0 sicc 2+ lm.sup 0
332.5-572	Peat with rootlets, traces of silt and clay and sections of wood throughout	Sh2 Th^{1}1 Th^{2}1 As+ Ag+ Dl+ nig 4 strat 0 elas 0+ sicc 1+ lm.sup 4
572-580	Organic sand	Ga4 Sh++ Gmaj+ As+ Ag+ Dl+ nig 2 strat 0 elas 0 sicc 2+ lm.sup 0

The bivariate plot of mean particle size against standard deviation (Tanner, 1991a; 1991b; Lario et al., 2002) shows that the majority of the sediments were deposited in an open to filled estuary environment (Figure 4.12). Of the 45 samples analysed, 10 were deposited during closed-basin conditions. These samples are poorly sorted with a mean particle size predominantly in the clay fraction. Several sediments in the closed basin envelope were deposited prior to shifts in sedimentation at 256 cm and 248 cm, close to transition from organic clayey silt to woody peat at 254 cm. In contrast, a cluster of the sediments (~ 204 -172 cm) in the closed-basin envelope originate from the upper silty clay unit (214.5 cm to 45 cm) in the Oldtown Marsh core.

End-member mixing analysis, using the Paterson and Heslop (2015) model, identified three particle size end-members that account for 98.5 % of the variance in the OTM-16-13 data. The proportional down-core distribution of each end-member is illustrated in Figure 4.13. End-member 1 (EM1) is comprised predominantly of clay (79 %) with a proportion of

silt (21 %), whilst EM2 is the opposite (24 % clay, 76 % silt). EM2 and EM3 are comparable however the later also contains a subordinate sand component (1 %). EM3 increases sharply at 332 cm, dominating until c. 280 cm, when EM2, followed by EM1, increase in abundance, peaking at c. 250 cm. Between 230 cm and 170 cm, EM1 and 2 dominate with the relative abundance of each fluctuating in a given sediment sample. EM2 dominates from 170 cm, with EM3 gradually increasing up core.

The organic content was determined for 44 samples, at a minimum resolution of 16 cm (Figure 4.11). The organic content increases from less than 10 % at the base of the core to c. 88 % by 558 cm. This is sustained until 334 cm when the organic content decreases sharply to 8 % in 8 cm. The organic content gradually increases from 326 cm, peaking at 80 % at 250 cm, with a faster rate occurring from c. 278 cm. The organic content then gradually declines, with a sharp decrease from 213 cm, to 6 % by 200 cm and this is sustained.
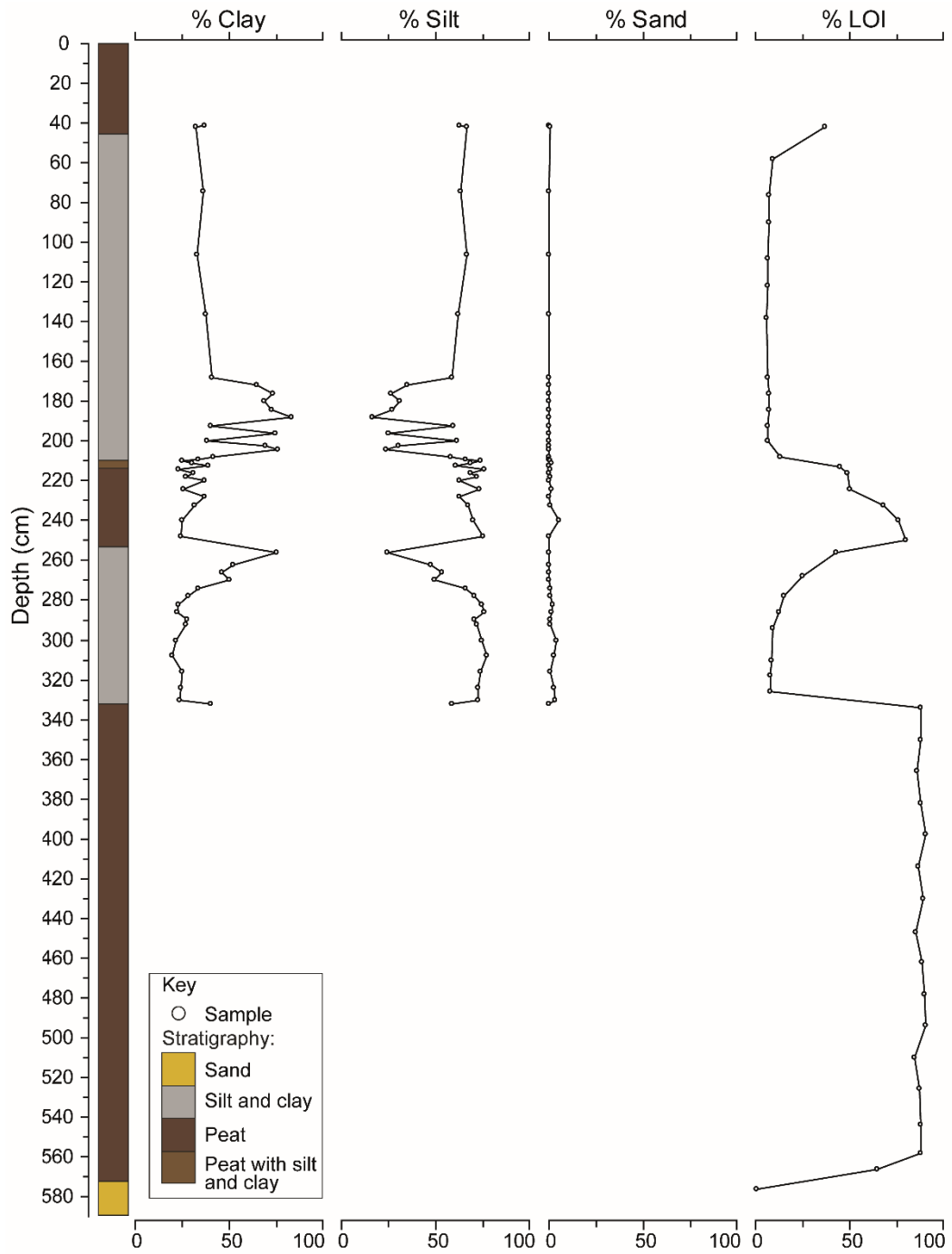
Figure 4.11: Stratigraphy, particle size and LOI for sampled sequence from OTM-16-13. The boundaries for the clay, silt and sand fraction are defined by Wentworth (1922).
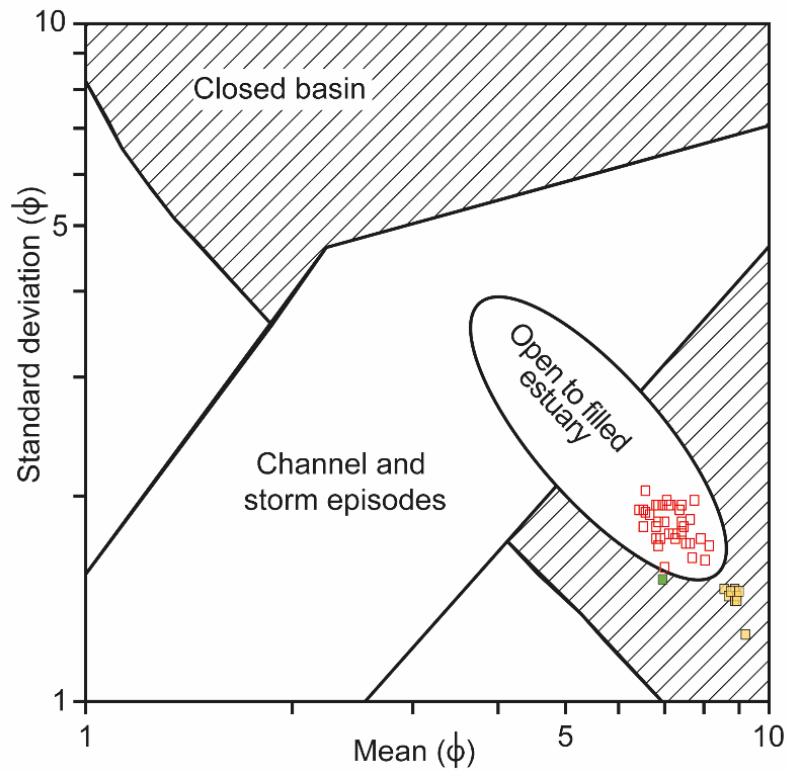
Figure 4.12: Bivariate plot of mean against standard deviation (phi) for OTM-16-13. The graphic sedimentary domains determined by Tanner (1991a; 1991b), and later modified by Lario et al. (2002) are overlain onto this plot. Permission to reproduce this figure has been granted by Elsevier.
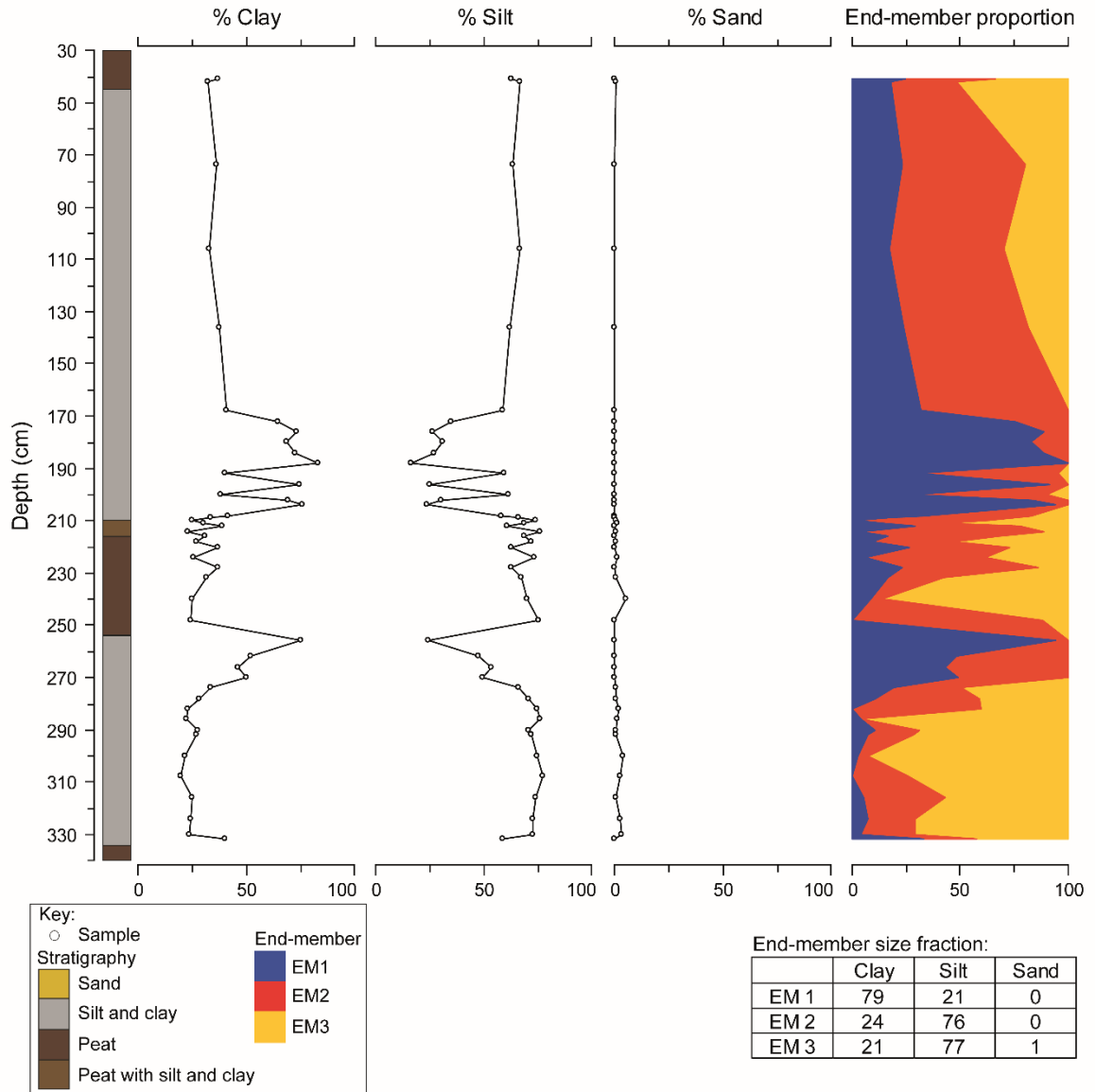
Figure 4.13: The proportional down-core distribution of end-members determined from OTM-16-13 particle size data using the end-member analysis algorithm developed by Paterson and Heslop (2015)*. The stratigraphy and clay, silt and sand fractions (defined by* Wentworth (1922)*) are plotted alongside this for comparison.*

4.3.3 Biostratigraphy

Diatom preservation was problematic in OTM-16-13. Diatoms were preserved in the upper portion of the clayey silt unit (332.5 cm to 254 cm) and at the transition from the middle fibrous woody peat to overlying silty clay at 214.5 cm. Foraminifera were therefore counted at the transgressive and regressive contact at 332.5 cm and 254 cm respectively (raw counts are presented in Appendix 10).

Diatom analysis of 22 samples identified 159 species (all raw counts are presented in Appendix 11). Five zones, based on diatom flora and lithostratigraphy, were identified

between 300 and 170 cm (Figures 4.14 and 4.15). The diatom assemblage is dominated by brackish-marine taxa between 300 cm and 274 cm (Zone 1; 300 cm to 288 cm), with a subordinate freshwater component occurring between 288 cm and 274 cm (Zone 2). Diatoms are not preserved in Zone 3 (274 cm to 232 cm). A freshwater dominated zone, with brackish species also present (Zone 4; 232 cm to 209 cm), is succeeded by a brackish-marine zone (Zone 5; 209 cm to 170 cm).

Zone 1 is dominated by brackish epipelic taxa, particularly *Tryblionella punctata* which exceeds 50 % of the total count for this zone. Marine planktonic (e.g. *Paralia sulcata*) and tychoplanktonic (e.g. *Pseudopodosira westii*) taxa are also present in this zone, exceeding 20 % throughout. Zone 2, like Zone 1, is also comprised of a brackish-marine assemblage however a subordinate freshwater component (< 5 %) is also present. Foraminifera analysis identified the occurrence of *Jadammina macrescens*, *Miliammina fusca* and *Trochammina inflata* prior to Zone 1 (324 cm to 330 cm) at 330 cm, 328 cm and 324 cm.

Diatoms are not preserved in Zone 3 however *Jadammina macrescens* is abundant at 258 cm (156 tests counted). Freshwater species dominate Zone 4, averaging 63 % of the total count. Freshwater epipelic taxa, such as *Staurosirella lapponica*, and tychoplanktonic taxa, such as *Staurosira construens* and *Pseudostaurosira elliptica*, are particularly abundant. *Pinnularia noblis*, a salt-intolerant species, is also present in Zone 4. Brackish taxa account for less than 33 % of the total count of this zone whilst marine taxa are minimal (< 12 % of total count).

The transition from Zone 4 to 5 is denoted by a sharp increase in brackish and marine taxa as well as the disappearance of freshwater taxa. *Paralia sulcata* (marine planktonic taxa) and *Scolioneis tumida* (brackish epipelic taxa) dominate this zone, reaching 50 % and 51 % of the total count respectively. Marine taxa peak in abundance at 202 cm, following which brackish taxa increase and dominate.
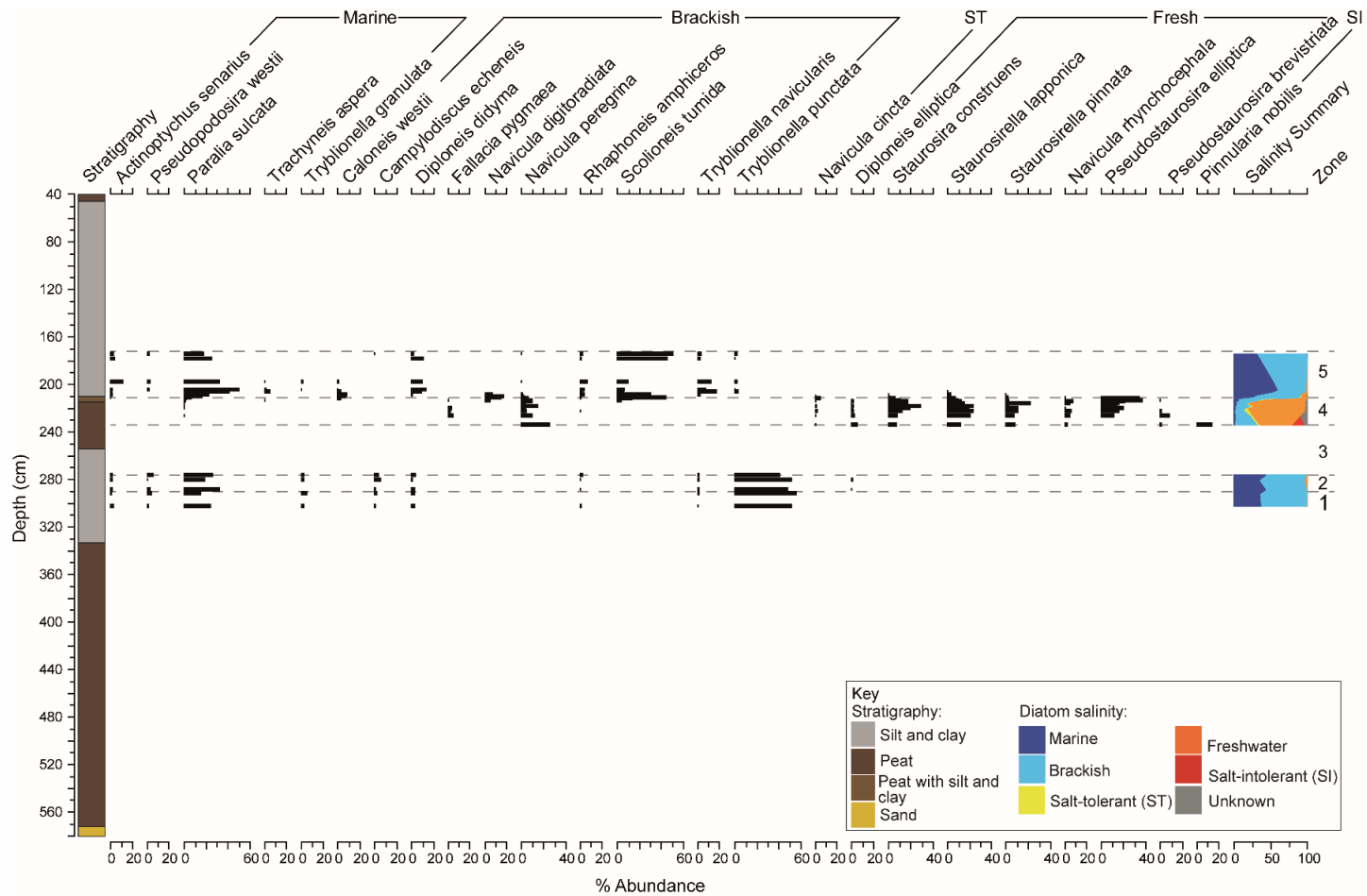
Figure 4.14: Diatom assemblage for OTM-16-13; species shown exceed 5 % of the total count. Diatoms are grouped based on their salinity tolerance using the halobian classification (Hustedt, 1953).

Figure 4.15: Diatom assemblage for OTM-16-13; species shown exceed 5 % of the total count. Diatoms are grouped based on their life form using Vos and De Wolf (1988; 1993).

4.3.4 Chronology

The timing of the onset of peat deposition and rising regional ground water level at Oldtown Marsh was determined by submitting a basal sample for AMS radiocarbon dating (Table 4.4). A sample comprised of wood, including external bark, was taken from 573 cm (-5.64 m OD). The sample was dated at the NERC Radiocarbon Facility, East Kilbride (Allocation number: 2037.1016). Diatoms were not preserved at the base of the Oldtown Marsh core, which along with the stratigraphic context, suggests the radiocarbon date is from a freshwater context, situated above direct tidal influence. The onset of peat deposition at Oldtown Marsh was dated to 6170-5906 cal BP (Laboratory code: SUERC-72911).

Analysis across the transition from organic clayey silt to woody peat at 254 cm (-2.45 m OD) identified a shift from a marine-brackish to freshwater-brackish diatom assemblage and disappearance of foraminifera. Plant macrofossils (e.g. *Poaceae* remains) were sampled at 253.5 cm (-2.45 m OD) for AMS radiocarbon dating and submitted to Beta Analytic, Miami. The sedimentation shift was dated to 933-796 cal BP (Laboratory code: BETA-498399).

The transition from silty peat to clayey silt at 210 cm (-2.01 m OD) is associated with an increase in brackish-marine conditions, determined from diatom analysis. Plant macrofossils and seeds, such as *Poaceae* nodes and stem fragments, *Brassicaceae* seed and *Carex* nutlets, were sampled at 212 cm (-2.03 m OD) and submitted to the NERC Radiocarbon Facility, East Kilbride for AMS radiocarbon dating (Allocation number: 2037.1016). The increasing dominance of marine and brackish conditions was dated to 952-789 cal BP (Laboratory code: SUERC-72907).

Table 4.4: AMS radiocarbon dates produced for Oldtown Marsh.

Site	Sample ID	Laboratory code	NERC Allocation number	^{14}C ± 1σ BP	Cal age (cal BP)- 2σ range	
					Max	Min.
Oldtown Marsh	OTM-16/13 -2.03 m OD	SUERC-72907	2037.1016	965 ± 39	952	789
	OTM-16.13 -2.45 m OD	BETA-498399	NA	970 ± 30	933	796
	OTM-16/13 -5.64 m OD	SUERC-72911	2037.1016	5209 ± 35	6170	5906

4.3.5 Palaeoenvironmental interpretation

The stratigraphic transect identified a series of alternating organic and minerogenic units, which biostratigraphic analysis of OTM-16-13 indicates are associated with periods of

decreased and increased tidal influence respectively. A summary of the results for the sampled core (OTM-16-13) from the Oldtown Marsh core are presented in Figure 4.16. The sharp decline in organic content associated with the onset of minerogenic deposition (332.5 cm) indicates that the contact is eroded. The assemblage of the lower minerogenic unit (332.5 cm to 254 cm) is dominated by brackish epipelic taxa, with marine planktonic taxa also present, indicating an intertidal mud flat environment. The upwards fining and increasing organic content, predominantly from c. 278 cm, indicates a decrease in the depositional energy and gradual increase in position of the site in the tidal frame suggesting a transition, from intertidal mud flat to salt marsh environment, in the organic clayey silt unit.

Organic content initially remains high, following the sedimentation shift from organic clayey silt to fibrous peat (254 cm), indicating a gradual transition from a high-marsh environment. The gradually decreasing organic content and upwards fining following the onset of peat sedimentation (254 cm) may indicate tidal influence is increasing. The sediments (256 cm and 248 cm) associated with the transition to peat sedimentation at 254 cm plot in the closed basin envelope of the bivariate plot. However, the remaining samples in this unit (254 cm to 214.5 cm) plot in the open to filled estuary envelope, suggesting tidal influence in this unit. In addition, a small sand component (< 5 %) is present in the peat unit from 240 cm to 211 cm. Freshwater tychoplanktonic taxa (e.g. *Staurosira construens* and *Pseudostaurosira elliptica*), indicative of freshwater environments such as rivers, lakes and ditches, dominate the assemblage of the peat (Vos and De Wolf, 1993). Assemblages dominated by freshwater conditions with a small brackish component can indicate a shallow lagoon environment with slightly brackish water, low-energy hydrodynamic conditions and aquatic vegetation growth (Bao et al., 1999). It cannot be determined if tidal influence is increasing in the middle fibrous peat because diatoms are not preserved at the lower boundary of this unit.

Barrier dynamics may have strongly influenced the onset of peat accumulation (254 cm) and reduced marine influence from 933-796 cal BP. A sufficient sediment supply is a prerequisite for a stable barrier position, as an abundant sediment supply will improve the capabilities for internal reorganisation and growth of a barrier. Back-barrier tidal basins will accrete sediment rapidly when sediment supply exceeds the creation of accommodation space by RSL rise, decreasing the frequency of tidal inundation (Baeteman et al., 2011). Salt marsh environments develop with time, replacing mud flats, and peat accumulation begins due to the asymptotic relationship between sediment accretion rates and time when sediment supply is adequate (Jennings et al., 1995).
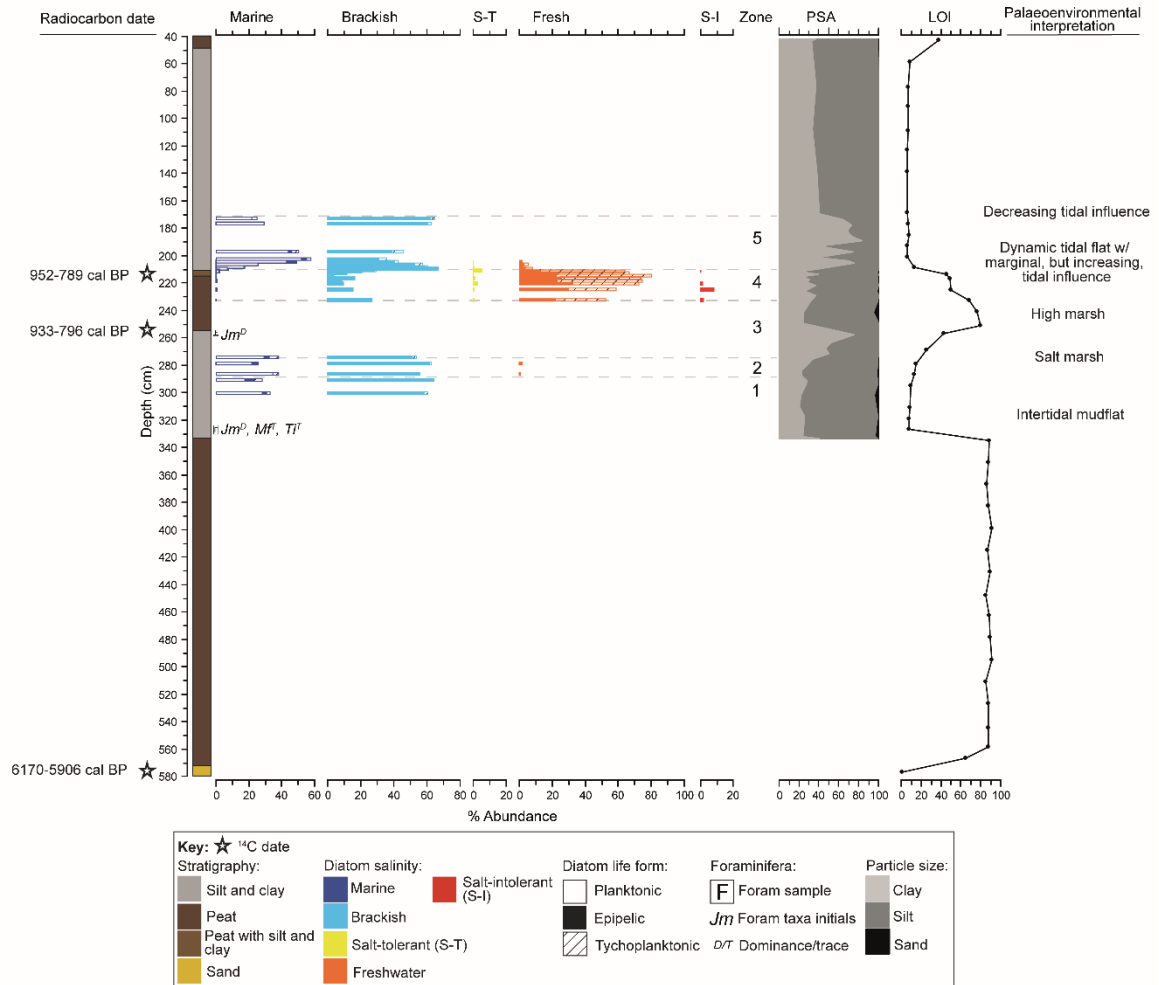
Figure 4.16: Summary diagram of results produced for OTM-16-13 with palaeoenvironmental interpretation. Stratigraphy, particle size, organic content, foraminifera (Jm- Jadammina macrescens, Mf- Miliammina fusca, Ti- Trochammina inflata) and the diatom summary, illustrating changes in salinity and life form, are presented. The abundance (D- dominance, T- trace) of foraminifera species is noted for each sample.

Particle size data, following the onset of clayey silt sedimentation (214.5 cm), indicates that the site was highly dynamic, with variable tidal influence. The bivariate plot supports this interpretation, as the sediment analysed at this transition (214 cm) occurs on the boundary between open to filled estuary and closed basin conditions. In addition, the fluctuating dominance between the clay dominated EM1 and silt dominated EM2 from ~ 212 cm indicates a dynamic tidal environment. The diatom assemblage is dominated by marine planktonic and brackish epipelic taxa, indicating tidal influence. The increased abundance of marine planktonic taxa indicates that the position of the site is lowering in the tidal frame. The diatom and particle size analysis indicate a mud flat environment, experiencing increasing tidal influence. Freshwater taxa are present until 206 cm and fully marine conditions absent, indicating that the tidal influence was marginal at this site.

The shift in dominance from marine planktonic to brackish epipelic taxa, from 202 cm, indicates decreasing tidal influence. This coincides with a coarsening and eventual stabilisation of the particle size, indicating an increase in depositional energy followed by a stabilisation of the environment. Sediments, between 204 cm and 172 cm, are deposited under predominantly closed basin conditions, based on the bivariate plot of mean particle size and standard deviation. The decreasing tidal influence and change in depositional environment from 202 cm may indicate the annealing of a tidal inlet or previous barrier breach. Interpretations in the clayey silt unit are restricted because diatoms are not preserved in the top 1.5 m of OTM-16-13 however the bivariate plot indicates that there is a return to open estuary conditions. The upper stratigraphy of cores (top 50 cm) furthest from the coast in the Oldtown Marsh transect contained peat with traces of silt, clay and sand. The traces of sand may indicate human influence as historical records indicate sand spreading was undertaken during the 18th century to improve land drainage.

4.4 Great Dingle Hill

4.4.1 Site description and survey

Dingle Marshes extend between Dingle Great Hill and Dunwich and are separated from the sea by Reedland Marshes and a shingle barrier (Figure 4.1). The large harbour which existed on this section of the coast during the Middle Ages is believed to have been located in Dingle Marshes (Parker, 1978; Comfort, 1994; Pye and Blott, 2006; 2009). Dingle and Reedland Marshes were embanked from the river by the end of the 16th century (Sear et al., 2008; Alison Farmer Associates, 2012). Drains are both sinuous and straight in nature, indicating drainage works over a prolonged period (Alison Farmer Associates, 2012), whilst bodies of open water are common. Barrier breaching and inundation of Dingle Marshes, due to storm surge events, has been common in the recent past. For example, the combined high-water levels and large onshore waves in October/November 2006 resulted in 2 km of the barrier being flattened and Dingle Marshes and neighbouring areas being flooded to a depth of 2 m (Pye and Blott, 2009).

A transect, extending between Dingle Great Hill and Dingle Little Hill, at the northern boundary of Dingle Marshes was investigated. The transect ran northeast to southwest, alongside the footpath and drainage ditch separating Dingle Great and Little Hill, which are mounds of higher relief exceeding 10 m and 5 m respectively in the open landscape of the Walberswick NNR (Figure 4.3). Changes in stratigraphy were determined every 12.5 m with a gouge core and revealed a shallow (< 3 m OD), gently inclined basement providing an opportunity to obtain late Holocene, compaction free, basal peat samples (Figure 4.17). Deposits underlain by pre-Holocene basement present an opportunity to obtain basal sea-

level index points (Törnqvist et al., 1998; 2004). These are advantageous for reconstructing RSL history due to the minimal impact of compaction (Gehrels, 1999) in contrast to intercalated index points. Proximity to the Great and Little Dingle Hill, as well as the neighbouring drainage channels were considered when identifying a suitable sample for analysis.

4.4.2 Lithostratigraphy and sedimentology

Representative stratigraphy at Great Dingle Hill contains five main sediment units outlined in Table 4.5 for the sampled core (GDH-16-2). A well humified sandy peat unit (200-196 cm) is overlain by a well humified peat unit (196-179 cm) subdivided by a silty clay peat unit (190-185 cm), a mottled silty clay unit (179 cm to 36 cm) and an upper unit comprised of organic-rich sand (36 cm to 0 cm) (Figure 4.17).
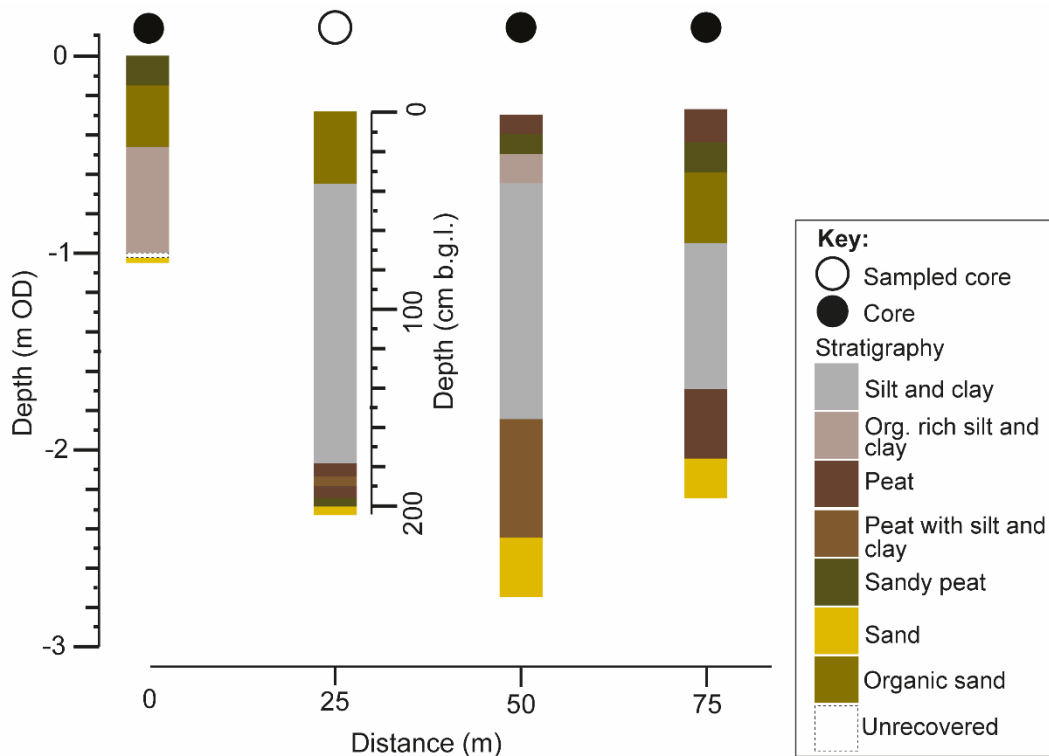
Figure 4.17: Stratigraphic transect completed at Great Dingle Hill. See Figure 4.1B for the location of Great Dingle Hill, and the stratigraphic transect, in relation to other sections of the coastline. The depth (cm) below ground level is provided for the sampled sediment sequence, GDH-16-2.

Particle size analysis was completed for 23 samples, at a minimum resolution of 4 cm (Figure 4.18). The silt fraction dominates the sampled sequence, with a slight upwards coarsening trend occurring throughout. Sand is present in the bottom 6 cm of the core and increases with depth.

The sediments from the Great Dingle Hill core plot in the graphic sedimentary domain indicative of open to filled estuarine environments when standard deviation is plotted against mean particle size (Figure 4.19). These sediments are poorly sorted with a mean particle size predominantly in the fine silt fraction.

Table 4.5: Description of main sediment units identified in GDH-16-2 and associated Troels-Smith (1955) *classification.*

Unit depth (cm)	Description	Troels-Smith log
0-36	Organic-rich sand	Ga2 Sh1 As1 Th1+ Th0+ nig 3+ strat 0 elas 0 sicc 2+
36-179	Silty clay with black mottling and occassional rootlets which increase with depth	As3 Ag1 Sh+ Th^1+ nig 2+ strat 0 elas 0 sicc 2+ lm.sup 1
179-185	Well humified, crumbly peat with irregular rootlets and trace of clay	Sh4 Th^1+ Th^0+ As+ nig 4 strat 0 elas 0+ sicc 1+ lm.sup 3
185-190	Silty clay peat with irregular rootlets and black mottling	As1+ Ag1 Sh2 Th^1+ Th^0+ nig 2+ strat 0 elas 0 sicc 2 lm.sup 2
190-196	Well humified, crumbly peat with irregular rootlets and trace of clay	Sh4 Th^1+ Th^0+ As++ nig 4 strat 0 elas 0+ sicc 1+ lm.sup 1
196-200	Well humified sandy peat	Sh2 Ga2 Th^0+ Th^1+ As+ nig 3++ strat 0 elas 0+ sicc 1+ lm.sup 0

End-member mixing analysis identified three particle size end-members, which account for 98.5 % of the variance in the GDH-16-2 particle size data. The proportional down-core distribution of each end-member is illustrated in Figure 4.20. EM1 and EM2 are poorly sorted, with the former comprised of nearly equal proportions of clay and silt and the later comprised predominantly of silt (72 %), with clay (28 %) also present. EM3 has the best standard deviation and contains a sand component (16 %) in addition to silt (69 %) and clay (16 %). EM3 dominates until 195 cm, when EM1 becomes most abundant. The relative dominance of the particle size end-members present in each sediment sample fluctuates between EM1 and EM2 between 170 cm and 120 cm with minor peaks in EM3 occurring (e.g. 158 cm).

Comparison of the composition of each end-member with the Great Dingle Hill particle size data highlights contrasting proportions of sand. EM3 is comprised of 16 % sand and the down-core distribution of this end-member indicates that sand is present throughout most of the core. Sand dominated the particle size data at the base of the Great Dingle core

however did not exceed 3 % between 124 cm and 190 cm. Goodness-of-fit statistics (i.e. linear correlation and angular deviation) determined that three particle size end-members produced the best compromise of the number of end-members compared to the coefficient of determination. This contrast highlights the importance of comparing the results of analytical techniques used to analyse particle size data.

The organic content was determined for 10 samples, at an 8 cm resolution (Figure 4.18). The organic content increases from the base of the core to a peak at 181 cm (55 %), following which it declines to 13 % by 168 cm and remains low for the remainder of the sampled sequence.
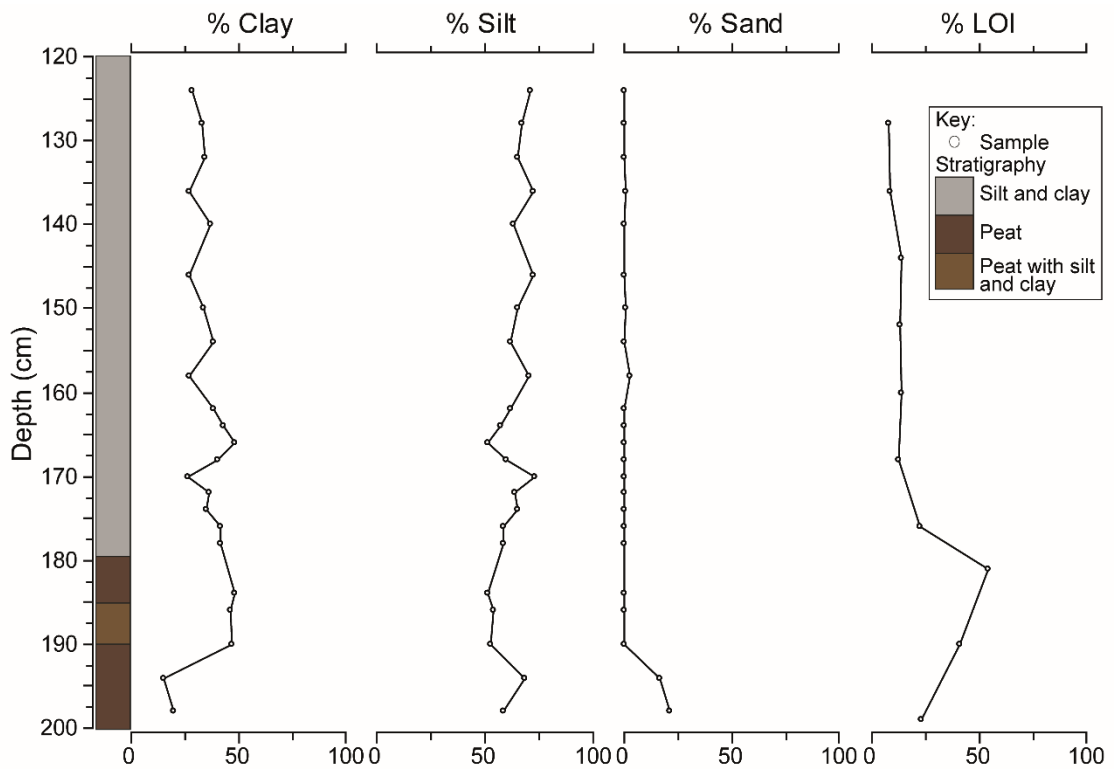
Figure 4.18: Stratigraphy, particle size and LOI for GDH-16-2. The boundaries for the clay, silt and sand fraction are defined by Wentworth (1922).
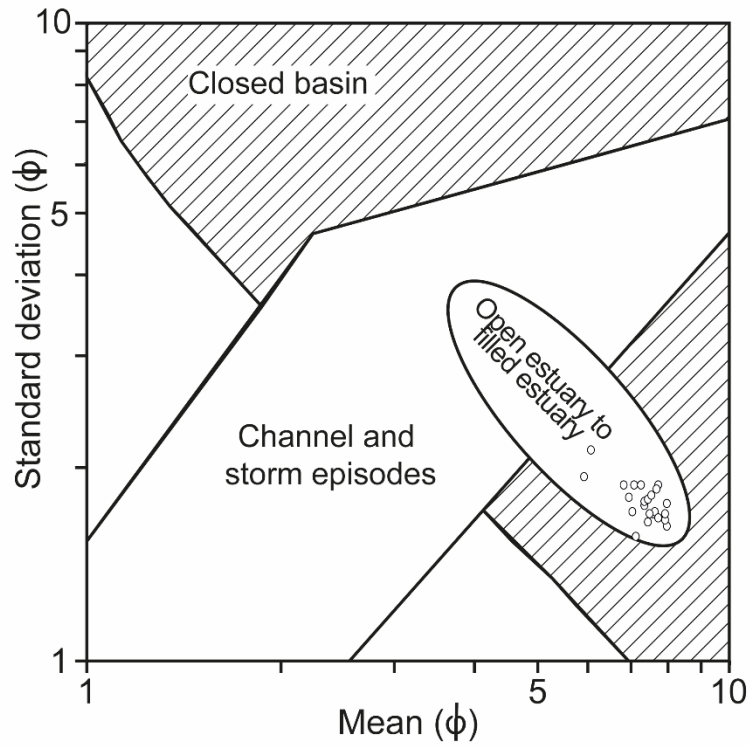
Figure 4.19: Bivariate plot of mean against standard deviation (phi) for GDH-16-2. The graphic sedimentary domains determined by Tanner (1991a; 1991b)*, and later modified by Lario et al. (2002) are overlain onto this plot. Permission to reproduce this figure has been granted by Elsevier.*

Figure 4.20: The proportional down-core distribution of end-members determined from GDH-16-2 particle size data using the end-member analysis algorithm developed by Paterson and Heslop (2015)*. The stratigraphy and clay, silt and sand fractions (defined by* Wentworth (1922)*) are plotted alongside this for comparison.*

4.4.3 Biostratigraphy

Diatom analysis was completed for 14 samples (raw diatom counts are presented in Appendix 12), resulting in the identification of 142 diatom species (Figures 4.21 and 4.22). The diatom assemblage is divided into 5 zones: a brackish zone (Zone 1; 200 cm to 183 cm), an intermediate brackish zone with decreased freshwater species (Zone 2; 183 cm to 177 cm), a brackish-marine zone with variable marine influence (Zone 3; 177 cm to 165 cm), followed by a zone of increased marine influence (Zone 4; 165 cm to 156.5 cm) which is sustained (Zone 5; 156.5 cm to 122 cm).

Brackish epipelic taxa dominate Zone 1 of the diatom assemblage, with *Caloneis westii* and *Navicula peregrina* comprising over 50 % of the total count in this zone. Freshwater taxa, such as the aerophilous *Diploneis ovalis*, decrease in abundance, from 26 % to 10 %, in Zone 1.

Figure 4.21: Diatom assemblage for GDH-16-2; species shown exceed 5 % of the total count. Diatoms are grouped based on their salinity tolerance using the halobian classification (Hustedt, 1953).
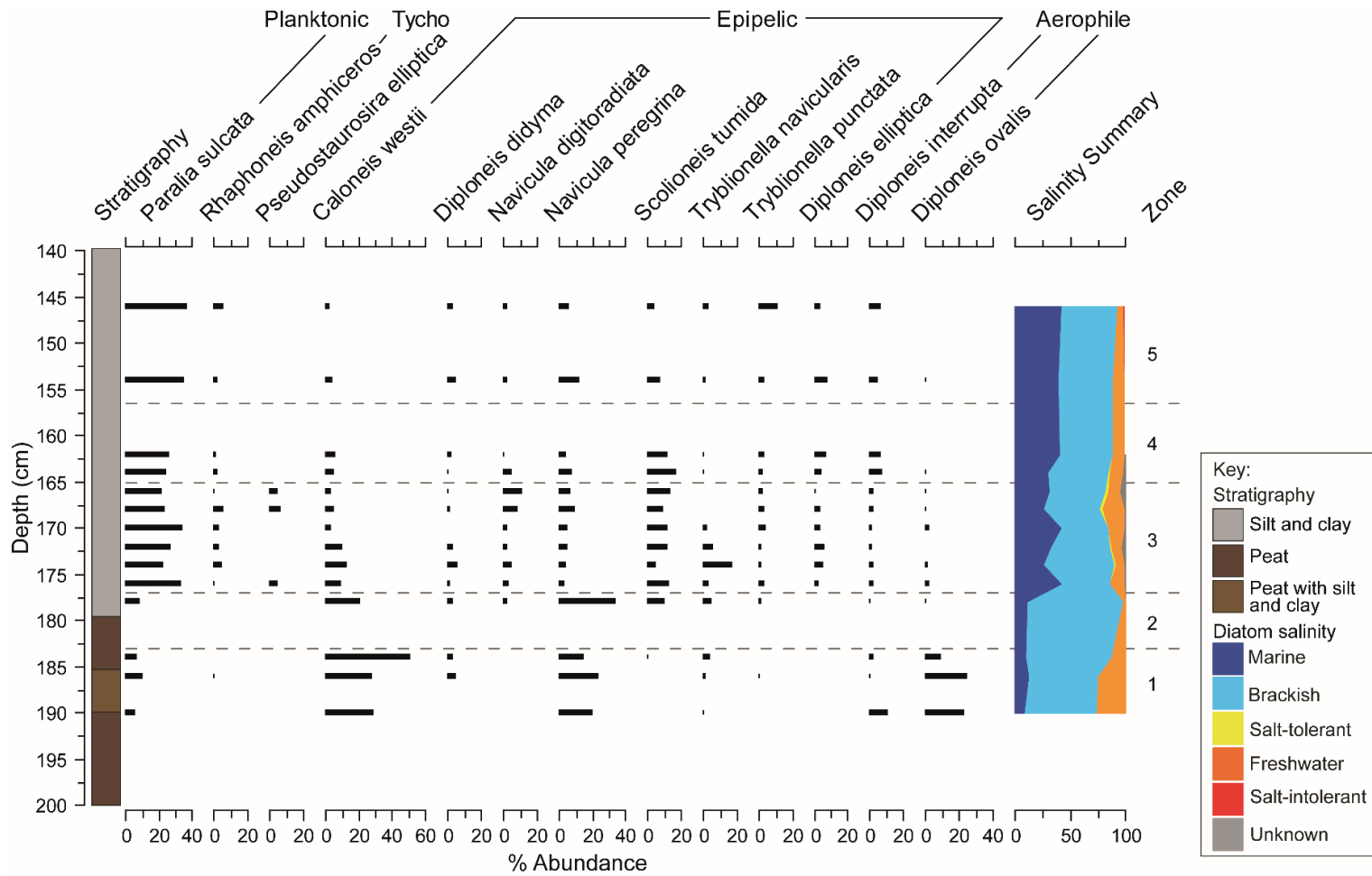
Figure 4.22: Diatom assemblage for GDH-16-2; species shown exceed 5 % of the total count. Diatoms are grouped based on their life form using Vos and De Wolf (1988; 1993).

Zone 2 is characterised by only one sample due to poor diatom preservation. Freshwater taxa decrease gradually, from 13 % to 2 %, from Zone 1 to 2 whilst brackish species continue to dominate. Zone 2 is also defined by the occurrence of the marine planktonic species *Paralia sulcata*.

The transition from Zone 2 to 3 is denoted by an increase in the abundance of marine species, which reach 41 % of the total count in this zone. Diatom dominance fluctuates between marine and brackish species throughout Zone 3, with the former ranging from 25 % to 41 % of the total count. The freshwater species remain consistently low, averaging 13 % of the total count.

Zone 4 and 5 are characterised by a gradual increase in marine species, predominantly *Paralia sulcata*, and decrease in freshwater species, such as *Diploneis elliptica*, whilst the brackish component of the assemblage remains largely constant. A subordinate salt-intolerant component (< 2 %) is also present in the upper section of Zone 5, at 146 cm.

4.4.4 Chronology

All radiocarbon dated samples from GDH-16-2 (Table 4.6) were analysed at the NERC Radiocarbon Facility, East Kilbride (Allocation number: 2037.1016). A sample for AMS radiocarbon dating was taken from the base of GDH-16-2 to constrain the onset of peat deposition and rising regional ground water level. Brackish diatoms dominate at 190 cm therefore the resulting date is not freshwater limiting. Plant macrofossils, such as *Poaceae* remains, as well as seeds were sampled at 200 cm (-2.29 m OD). The onset of peat deposition at GDH-16-2 was dated to 2956-2783 cal BP (Laboratory code: SUERC-76469).

A sample was submitted for radiocarbon dating to constrain the timing of the increase in marine conditions, associated with the sedimentation shift from peat to organic rich silty clay, at 179 cm. Plant macrofossils and seeds (e.g. *Brassicaceae* and *Chenopodiaceae* seeds and *Poaceae* remains) were sampled from 180 cm (-2.09 m OD). The increased marine conditions from 178 cm (-2.07 m OD) is dated to 2701-2357 cal BP (Laboratory code: SUERC-72912).

Table 4.6: AMS radiocarbon dates produced for Great Dingle Hill. All samples from GDH-16-2 were
radiocarbon dated at NERC Radiocarbon Facility, East Kilbride (Allocation number: 2037.1016).

Site	Sample ID	Laboratory code	^{14}C ± 1σ BP	Cal age (cal BP)- 2σ range	
				Max	Min.
Great Dingle Hill	GDH-16-2 -2.11 m OD	SUERC-72912	2440 ± 35	2701	2357
	GDH-16-2 -2.29 m OD	SUERC-76469	2775 ± 37	2956	2783

4.4.5 Palaeoenvironmental interpretation

Minerogenic sedimentation dominates the stratigraphic transect completed at Great Dingle
Hill. The marine conditions sustained after 2701-2357 cal BP indicates a continuous tidal
influence throughout the late Holocene (Figure 4.23). The bivariate plot of mean particle
size against standard deviation suggests that the sediments were deposited under
estuarine conditions. The continued dominance of marine and brackish conditions after
2701-2357 cal BP is more likely due to barrier breaching than over washing over the barrier
crest. Barrier breaching could have been created by a high magnitude event whilst a
restricted sediment supply could have resulted in sediment reworking and increased
barrier instability and permeability. The particle size coarsens slightly across the transition
at 179 cm indicating an increase in depositional energy however there is no sand present
to provide evidence of a high magnitude event.

The dominance of brackish epipelic taxa (e.g. *Caloneis westii*, *Diploneis didyma* and
Navicula peregrina) in the diatom assemblage of the peat unit (200 cm to 179 cm) is
indicative of intertidal to lower supratidal mudflats and creeks, as well as subtidal marine
basins and lagoons (Vos and De Wolf, 1988; 1993). Marine and brackish planktonic taxa
(e.g. *Paralia sulcata* and *Rhaphoneis amphiceros*), associated with sub-tidal areas or large
tidal channels (Vos and De Wolf, 1988; 1993; Zong and Tooley, 1999), increase in
abundance from 176 cm. The slight upwards coarsening and decreased organic content
associated with the shift to minerogenic sedimentation, indicates an increase in
depositional energy and lowering of the position of this site in the tidal frame. Aerophilous
diatoms (e.g. *Diploneis ovalis* and *Diploneis interrupta*), indicative of a salt marsh
environment, decrease in abundance across the transition and are subordinate in the silty
clay unit (179 cm to 36 cm). The changes in diatom ecology (i.e. salinity and life form),
associated with the shift from peat to silty clay sedimentation (179 cm), indicates an
increase in tidal influence. The increased input of planktonic species strongly indicates
tidally influenced hydrodynamic conditions (Simonsen, 1969; Vos and De Wolf, 1993), with

increases in allochthonous marine planktonic taxa associated with episodes of barrier breaching (Sáez et al., 2018) and the opening of tidal inlets (Bao et al., 1999; Freitas et al., 2002). A range of habitats can occur in close proximity to each other in some coastal situations therefore care must be taken to focus on the dominant trends when interpreting changes in sedimentary environments (e.g. Simonsen, 1969).
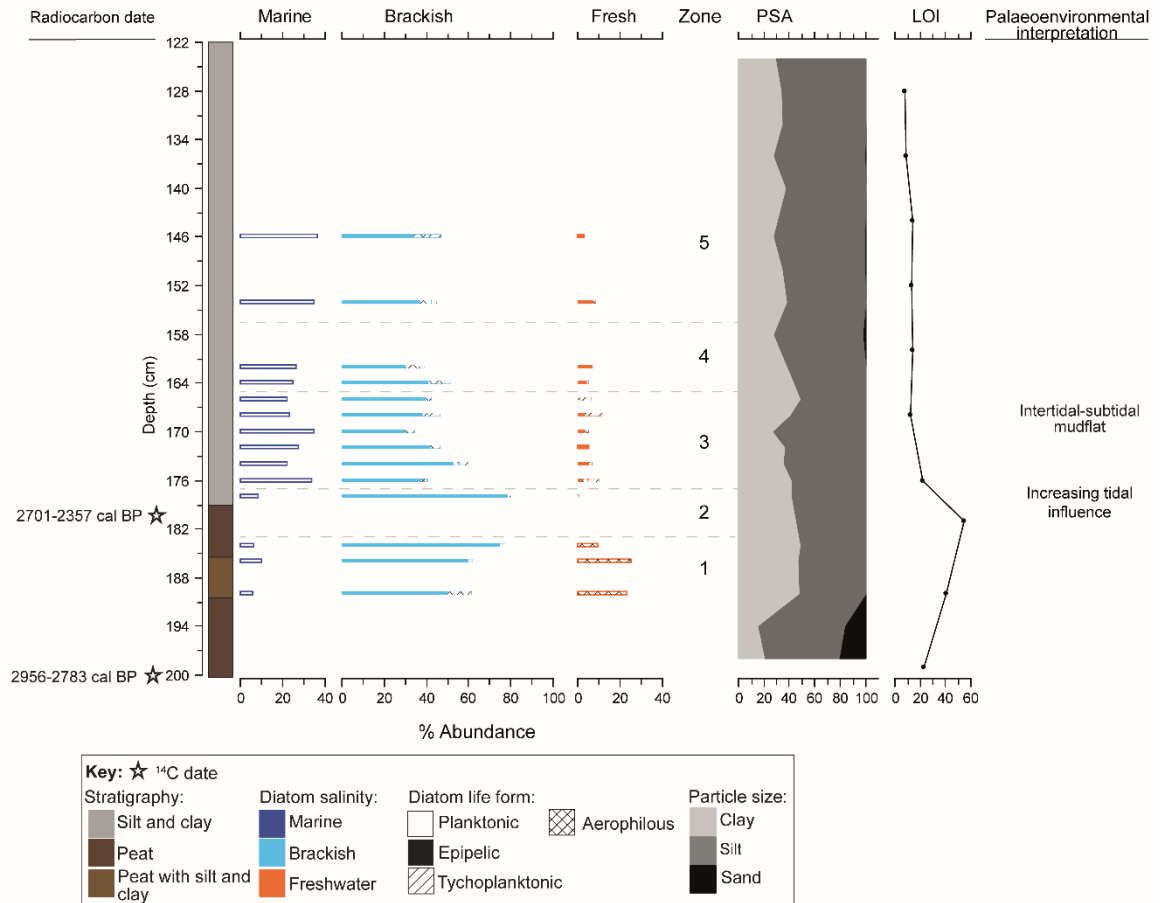
Figure 4.23: Summary diagram of results produced for GDH-16-2 with palaeoenvironmental interpretation. Stratigraphy, particle size, organic content and the diatom summary, illustrating changes in salinity and life form, are presented.

Chapter 5: Results and interpretation- Minsmere

This chapter presents the results for Minsmere. An overview of this section of the coast, relating to changes in coastal configuration, human land use and coastal management, is initially presented followed by a description of the site and stratigraphic survey. The chapter is then subdivided into the lithostratigraphy and sedimentology, biostratigraphy, chronology and resulting palaeoenvironmental interpretation. Multiple cores were sampled for analysis from the stratigraphic transect. The results are presented on a core-by-core basis in each section with sampled cores situated nearest the coast presented first and subsequent cores being discussed with distance inland.

5.1 Study area background

Minsmere is one of the largest wetland areas on the Suffolk coast, situated midway between Southwold and Aldeburgh (Figure 5.1), stretching from the Minsmere cliffs, south of Dunwich, to the Sizewell Power Station and extending over 5 km inland (Williamson, 2005; Good and Plouviez, 2007). The habitats present include lowland heath, woodland, grazing marshes and extensive freshwater wetland and reedbeds. A significant proportion of this area is owned and managed by the Royal Society for the Protection of Birds (RSPB) as a nature reserve whilst the wider area is protected as an AONB, SSSI, SAC, SPA and Ramsar site.

Existing stratigraphic data identified that intercalated sequences dominated by minerogenic sediments occur in the seawards areas of Minsmere whilst organic sedimentation dominates inland, extending at least 3 km into the freshwater system (Lloyd et al., 2008). The study by Lloyd et al. (2008) provided late-Holocene RSL information from fragmented and spatially disconnected sites at Minsmere, highlighting the complexity of the system and the potential for more detailed and extensive stratigraphic data to resolve the spatial and temporal environmental changes at the site during the Holocene (see Appendix 1 for summary of stratigraphy and palaeoenvironmental interpretation).

Historical maps, such as Saxton's 1575 and Kirby's 1737 map, illustrate the existence of a small open coast estuary (Figure 5.2) at Minsmere (Axel and Hosking, 1977; Parker, 1978; Pye and Blott, 2006). Records from Leiston Abbey (Figure 5.1B) note that Minsmere River was a landing place for unloading cargo in the grounds of the Abbey and sheltering from bad weather in 1293 (Rea Price and Robb, 2015). 'The Butlery Cartulary', a document dated to 1237, states that small streams such as Minsmere were operating as havens at

this time (Steers, 1927). Leiston Abbey, founded in 1182, was located near the Minsmere estuary shore and remained here until the end of the 14th century when severe storms (1247 and 1363) led to its relocation further inland to higher ground (Axel and Hosking, 1977; Pye and Blott, 2006). Hodskinson's 1783 map (Figure 5.2) illustrates that a barrier had developed, blocking the mouth of the estuary by this time (Axel and Hosking, 1977; Pye and Blott, 2006; Rea Price and Robb, 2015). Following this, a large mere feature existed behind the barrier, disappearing by the latter half of the 19th century due to drainage works.
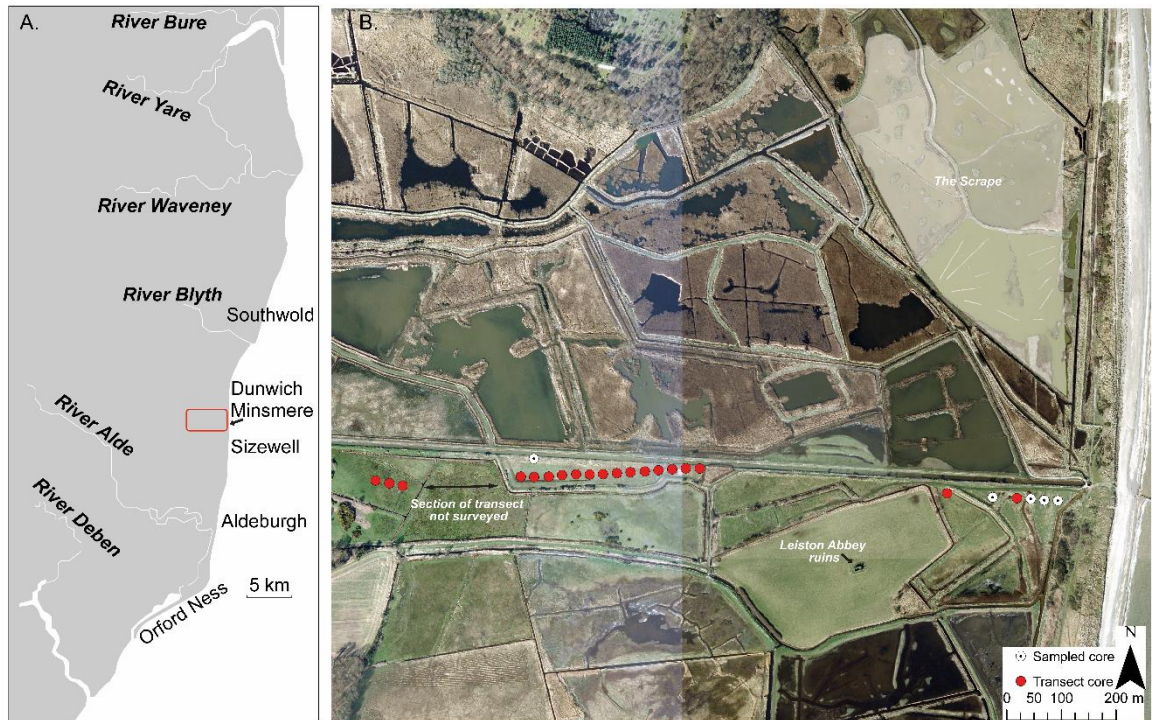
Figure 5.1: A. Suffolk coast with location of Minsmere highlighted in red. B. Stratigraphic transect completed at Minsmere. The red filled circles represent gouge cores and the white filled circles denote the sediment sequences sampled for analysis. The location of The Scrape (dashed area) and the ruins of Leiston Abbey are highlighted. Aerial imagery: © Getmapping Plc.
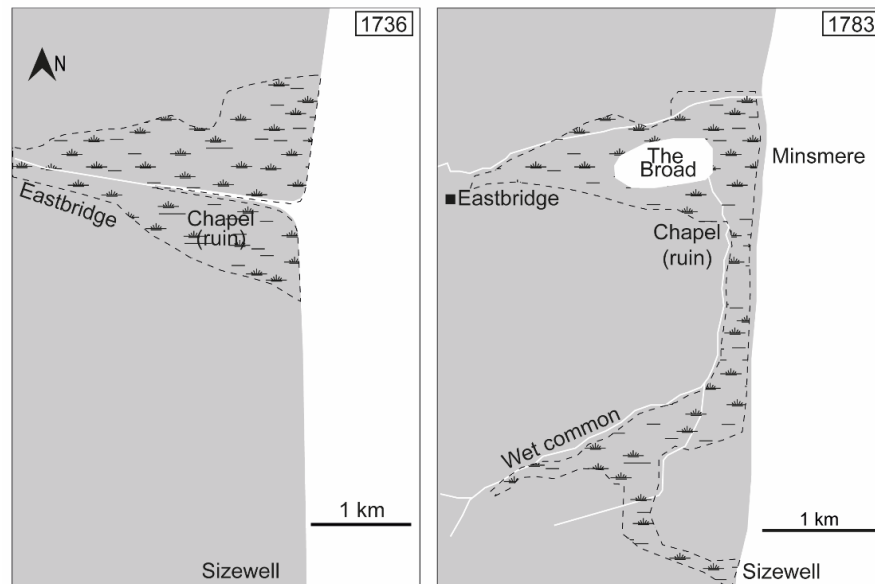
Figure 5.2: Conceptual model of Suffolk coastline between Minsmere and Sizewell at c. 1736 and 1783 AD. Adapted from Pye and Blott (2006)) and based on historical maps (e.g. Kirby's 1737 and Hodskinson's 1783 map), documents and aerial photography. Permission to reproduce this figure has been granted by Coastal Education and Research Foundation, Inc.

Freshwater flooding of the poorly drained fen and grazing marsh habitats at Minsmere was frequent throughout the late 18th and early 19th century until the creation of an Act of Parliament in 1810 to drain the Minsmere Levels (Pye and Blott, 2006; Good and Plouviez, 2007). This 1810 Act led to the establishment of the Minsmere Level Drainage Trust, associated with the creation of enclosure acts for neighbouring locations (Williamson, 2005). A new main drain was created (the New Cut), extending 5 km through the middle of Minsmere Levels to a substantial and sophisticated sluice by 1815, allowing freshwater to discharge and seawater to ingress. The complex mixture of serpentine and straight dykes at Minsmere indicates reclamation associated with Leiston Abbey prior to its relocation at c. 1363 (Good and Plouviez, 2007). Land claim efforts likely pre-date the 1810 Enclosure Act as monks are believed to have created clay embankment structures following the founding of Leiston Abbey (Pye and Blott, 2006).

Minsmere was intentionally flooded as a defensive measure, following the outbreak of WW2, with the freshwater outlets of the sluice remaining closed until 1945. Following decommissioning, the RSPB purchased a large portion of Minsmere and this became the Minsmere Nature Reserve, a 2500 acre site that attracts over 90000 visitors annually. The site is managed with the aim to safeguard the ecosystems of the reserve. Coastal lagoon features are maintained by regulating water levels and salinity using a series of sluices.

Vegetation is removed from the open water features annually whilst livestock graze reed beds to ensure the boundary with open water features is maintained.

The Shoreline Management Plan for this section of coast extends from the Minsmere cliffs to the Sizewell cliffs (Figure 5.1) and is comprised of a range of policies (Suffolk Coastal District Council, 2010). No active intervention will be undertaken on the Minsmere and Sizewell cliffs for the remainder of the century, whilst a policy of 'Managed Realignment' is adopted for the low-lying wetlands separating these cliff systems during this period. Managed realignment at Minsmere includes management of the sluice, in a manner that does not impact sediment movement, and minor works on the coast to address potential weak spots which may develop. A policy of 'Hold the Line' is adopted for the section of the coast on which the Sizewell Nuclear Power Station is situated. Coastal defences at Coney Hill, the northern section of low-lying wetlands at Minsmere, offered limited protection for back-barrier environments, with future erosion likely to result in breach (Environment Agency, 2009). A programme of works was undertaken on behalf of the Environment Agency to allow Coney Hill to evolve with natural processes, with a new coastal defence embankment protecting the remaining section of Minsmere.

5.2 Site description and survey

The Minsmere New Cut, completed in 1815, extends down the centre of the Minsmere Levels, segmenting the valley of the Old Minsmere River. Higher relief, comprised of farmland and woodland, surround the northern and southern boundary of Minsmere. Shingle beach, backed by vegetated dunes, extends along the Minsmere frontage, containing anti-tank cubes that were deployed as a defensive measure during WW2. Contrasting landscapes occur north and south of the New Cut. North of the New Cut, reedbeds dominate with open water features present throughout, particularly nearest the coast where there is a large area known as The Scrape (Figure 5.1B), an artificial wetland created by the RSPB to attract birds. The southern side of the New Cut is bounded by grazing marsh with wet grassland occurring further south. The original site of Leiston Abbey is situated on a low hill on the south side of the New Cut. A small chapel (Figure 5.1B) is all that remains of the original Abbey and a pill box was built within these ruins to camouflage it from aerial view.

A transect extending east to west was completed in the grazing marshes situated adjacent to the southern bank of the New Cut (Figure 5.1B). This area was selected due to the absence of extensive reedbeds and open water features, which enabled easy access and coring. The stratigraphy was investigated every 25 m, where possible, using a gouge core. The land surrounding the former site of Leiston Abbey has been designated a Scheduled

Monument by Historic England therefore restricting coring in this section of the grazing marshes. Samples for laboratory analysis, collected using a Russian corer, were taken nearest the coast and further inland to capture the stratigraphic contrast documented from the gouge core transect. Sediment sequences sampled near the coast (MN-16-2, MN-16-3, MN-16-5) captured the relatively high peat overlying an incompressible substrate and younger sediments at a location more responsive coastal change, whilst further inland (MN-16-19) yielded thicker sequences of Holocene coastal change. The complete sediment sequence was not collected for all the sampled locations. Sampling with the Russian corer at MN-16-1, MN-16-2, MN-16-3 and MN-16-19 focussed on retrieving basal peats, with the main stratigraphic transitions also targeted at MN-16-2, MN-16-3 and MN-16-19.

The base of the cores was identified as reached by the grinding noise of the corer, the angular gravel clasts at the base of the core and the compacted nature of the sediment in the gouge corer. However, coring less than 400 m east of the coastline identified shallow sediment sequences, less than 0.5 m deep, comprised of sand dominated soil with sub-angular or sub-rounded gravels, underlain by a gravel platform, hypothesised to be a relict beach feature (Hamilton, 2017). Consideration must therefore be given to whether the base of the sediment sequences sampled nearest the coast represents a continuation of this gravel platform rather than the underlying geology.

The fieldwork (18-27th November 2016) coincided with Storm Angus (20th November), which resulted in extensive freshwater flooding at Minsmere. As a result, 7 points of the gouge core transect were submerged beneath water for the remainder of the week (Figure 5.3). These could not be safely accessed for surveying due to deep water and the location of drainage channels not being visible. Their altitude has therefore been estimated based on adjacent cores. The most inland location selected for sampling, MN-16-19, was also submerged by the freshwater flooding. A location close to this point with comparable stratigraphy was therefore sampled for analysis instead.
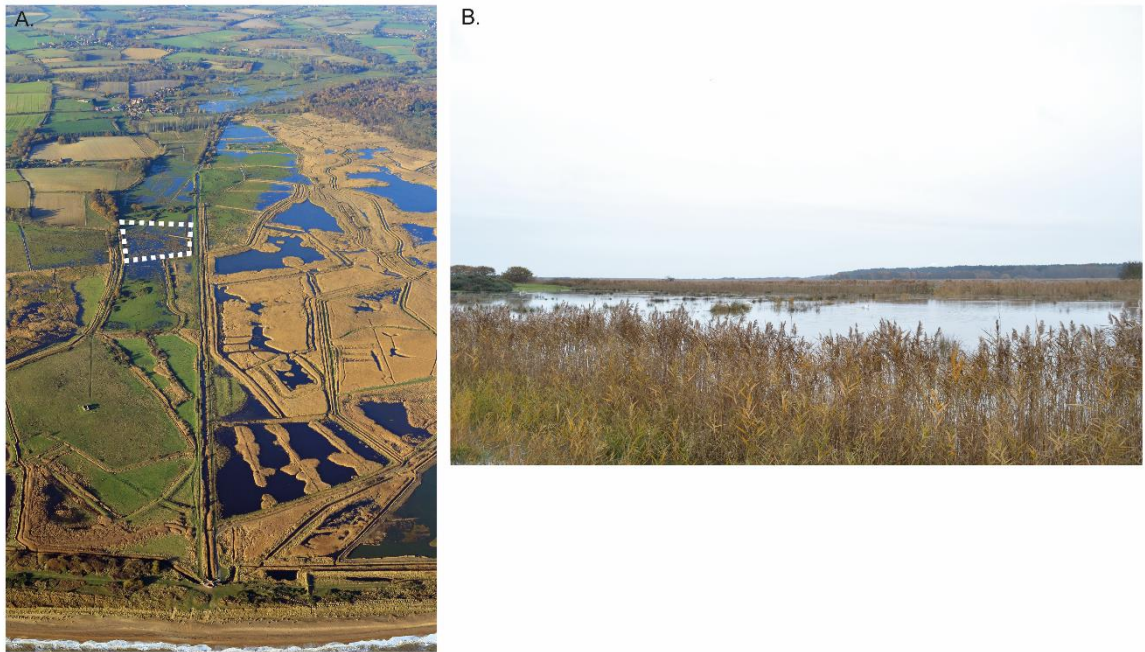
Figure 5.3: A. Aerial photograph of Minsmere illustrating the extent of freshwater flooding inland Permission to reproduce aerial image has been granted by Mike Page. The white dashed area is the section of the transect that could not be surveyed (see Figure 5.1B). B. Freshwater flooding in the field that could not be surveyed at Minsmere due to the water depth.

5.3 Lithostratigraphy and sedimentology

The stratigraphic transect completed at Minsmere (Figure 5.4) identified contrasting sedimentation patterns with distance from the coast. Minerogenic sedimentation dominates the Holocene sequence nearest the coast, with this dominance decreasing with distance further inland (~ 1 km) to reveal a peat infilled basin which following inundation was later drained.
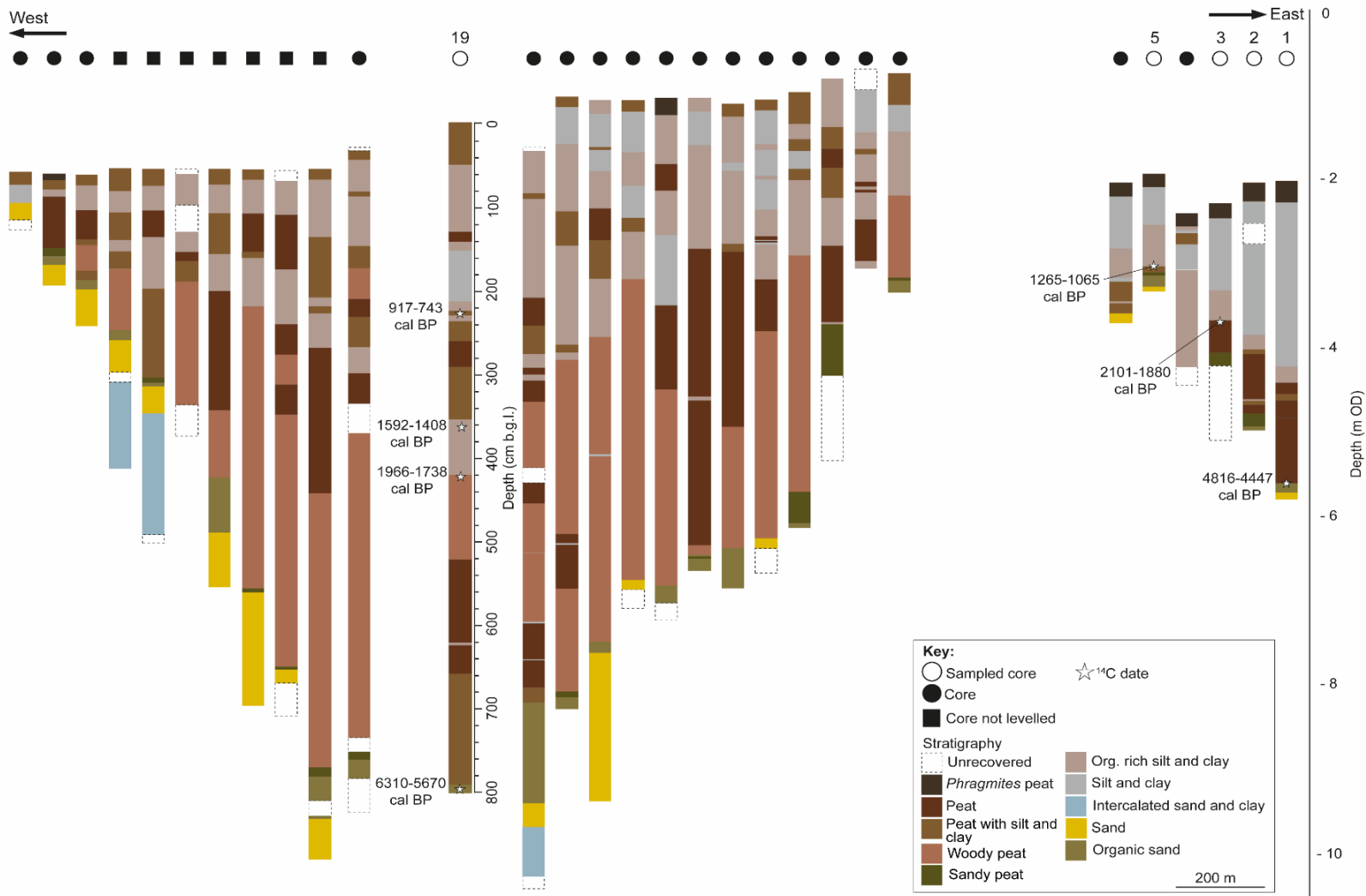
Figure 5.4: Stratigraphic transect completed at Minsmere, with associated radiocarbon dates for sampled sediment sequences, MN-16-1, MN-16-2, MN-16-3, MN-16-5 and MN-16-19. The depth (cm) below ground level is provided for the primary sampled sediment sequence, MN-16-19.

5.3.1 MN-16-2

The main sediment units in MN-16-2 are outlined in Table 5.1. Organic sedimentation dominates from the base of the sequence until the transition to silty peat at 205 cm. A gradual transition from silty peat to organic clayey silt occurs at 198 cm, with minerogenic sedimentation dominating from 181 cm until near the surface. The sediment sequence was sampled between 294 cm and 180 cm, obtaining the basal peat and transition from silty peat to organic clayey silt at 198 cm.

Table 5.1: Description of main sediment units identified in MN-16-2 and associated Troels-Smith (1955) *classification.*

Unit depth (cm)	Description	Troels-Smith log
0-22	Disturbed top soil	
22-47	Clay with silt	As4 Ag+ nig 1 strat 2 elas 1 sicc 3 lm.sup 1
47-70	Unrecovered	
70-180	Clay with silt	As4 Ag+ nig 1 strat 2 elas 1 sicc 3 lm.sup 1
180-198	Organic clayey silt	Ag3 As1 Sh+ Ptm+ nig 2 strf 0 sicc 2+ elas 0 lm N/A
198-205	Peat with clay and silt	Sh1 Th^{2}1 Ag2 As+ Ptm+ Gmin+ nig 2++ strf 0+ sicc 2+ elas 0 lm 0
205-259	Peat	Sh3 Th^{2}1+ nig 3+ strf 0 sicc 3 elas 0 lm1
259-260	Organic silt with clay	Ag3 As1 Sh+ nig 2+ strf 0 elas 0 sicc 2+ lm 4
260-263	Peat with clay and silt	Sh2+ Ag1+ As+ Th^{2}1 nig 3+ strf 0 sicc 3 elas 0 lm 3
263-274	Well rooted peat	Sh3 Th^{1}1 Anth+ nig 4 strf 0 elas 0 sicc 3 lm 0
274-290	Sandy peat	Sh3 Th^{1}1 Gmin+ Gmaj+ nig 4 strf 0 elas 0 sicc 3 lm 0
290-294	Organic rich sand	Gmin3 Sh1 Th^1+ nig 3 strf 0 sicc 3 elas 0 lm 0

The particle size data set for MN-16-2 extends from 262 cm to 184 cm and contains six samples (Figure 5.5). Silt dominates the samples analysed at 262 cm and 260 cm, exceeding 70 %, with an upwards coarsening trend occurring between 196 cm and 184 cm. End-member mixing analysis could not be completed for the sampled sequences for the cores sampled near the coast (MN-16-2, MN-16-3 and MN-16-5) as over 10 samples are required by the AnalySize software to ensure geological context (Weltje and Prins, 2007; Paterson and Heslop, 2015).

The bivariate plot of mean particle size against standard deviation, coupled with the graphic sedimentary domains developed by Tanner (1991a; 1991b) and modified by Lario et al. (2002), illustrates that the majority of the sediments analysed from MN-16-2 were deposited in an open to filled estuarine environment (Figure 5.6). One of the six samples analysed was deposited during closed-basin conditions, whilst an additional sample plots on the transition between the closed-basin and open to filled estuary domains. Both of these samples were collected from a narrow organic rich band of silt with clay (260 cm to 259 cm) separating organic sedimentation. The sediments analysed are poorly sorted with a mean particle size in the fine silt fraction.

Changes in the organic content were determined for MN-16-2 from six samples at a 16 cm resolution (Figure 5.5). The organic content increases from 24 % at the base of the sequence to 73 % at 270 cm, remaining stable until 254 cm, following which it decreases to 6 % at 190 cm.
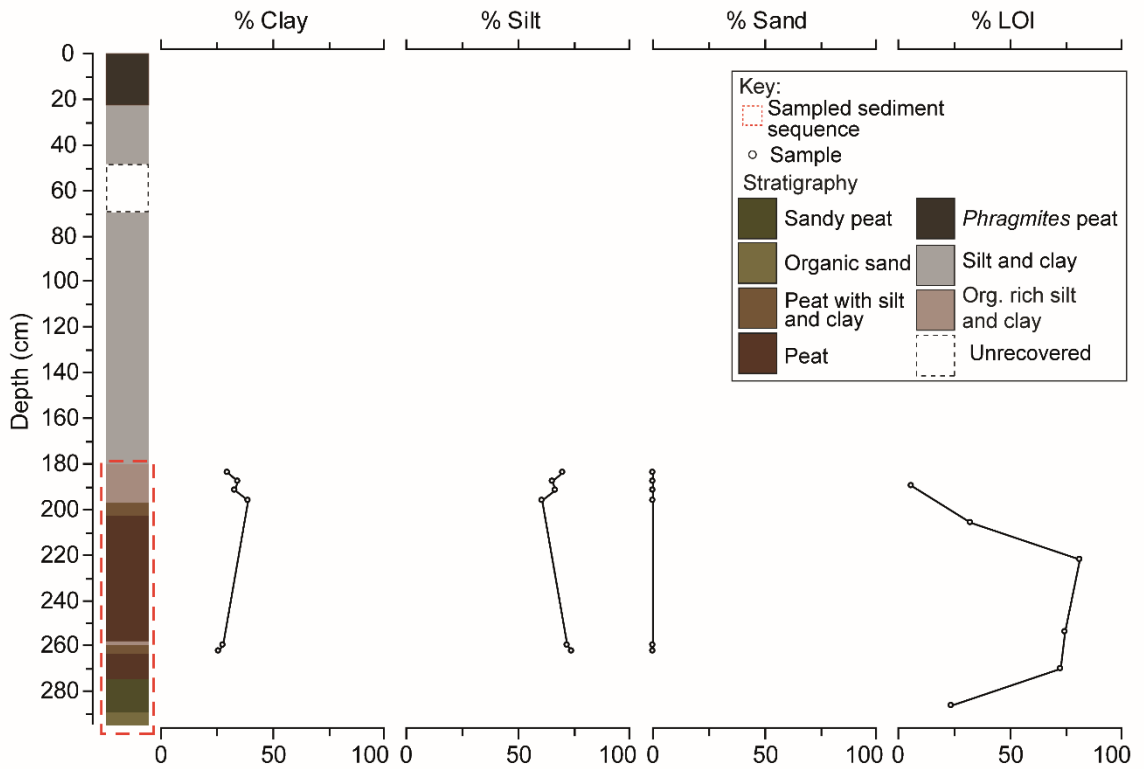
Figure 5.5: Stratigraphy, particle size and LOI for sampled sequence from MN-16-2. The boundaries for the clay, silt and sand fraction are defined by Wentworth (1922).
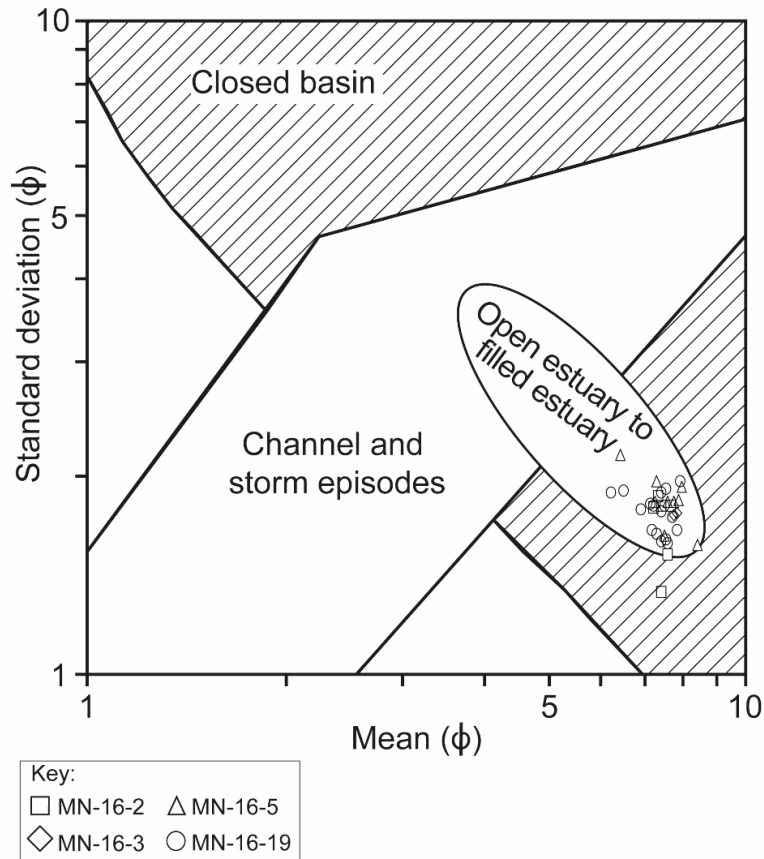
Figure 5.6: Bivariate plot of mean against standard deviation (phi) for MN-16-2 (square), MN-16-5 (triangle), MN-16-3 (diamond) and MN-16-19 (circle). The graphic sedimentary domains determined by Tanner (1991a; 1991b), and later modified by Lario et al., (2002), are overlain onto this plot. Permission to reproduce this figure has been granted by Elsevier.

5.3.2 MN-16-3

MN-16-3 contains five main sediment units (Table 5.2); sandy peat (191 cm to 178 cm); peat (178 cm to 140 cm); organic clayey silt (140 cm to 104 cm); clayey silt (104 cm to 14 cm); *Phragmites* peat (14 cm to 0 cm). The sediment sequence was sampled between 191 cm and 135cm, collecting the basal peat and transition from peat to organic clayey silt at 140 cm.

Particle size was analysed for two samples in the MN-16-3 sampled sediment sequence (Figure 5.7). Both samples (138 cm and 136 cm) are comprised of ~ 44 % clay and ~ 56 % silt. The sediments from MN-16-3 (Figure 5.6) plot in the graphic sedimentary domain indicative of open to filled estuary on the bivariate plot, the sediments are poorly sorted with a mean particle size in the fine silt fraction.

The organic content for MN-16-3 was determined for seven samples, at a 16 cm resolution (Figure 5.7). The organic content increases steadily from 3 % at 188 cm peaking at 80 % at 148 cm. Following which it declines to 12 % by 138 cm.

Table 5.2: Description of main sediment units identified in MN-16-3 and associated Troels-Smith (1955) *classification.*

Unit depth (cm)	Description	Troels-Smith log
0-14	*Phragmites* peat	Sh3+ Th^{1}1 Th^{0}phrag+ Ga+ As+ nig 3+ strat 0+ elas 2 sicc 3 lm.sup N/A
14-104	Clayey silt	As3+ Ag1 Ga+ Lf+ Th^2+ nig 2+ strat 0 elas 0 sicc 3 lm.sup 0
104-140	Organic clayey silt with shell fragments	Ag3 As1 Ptm+ Sh+ Th^1++ nig 2+ strf 0 sicc 2+ elas 0 lm sup N/A
140-178	*Phragmites* peat	Sh3 Th^0+ Th^{2}1 As+ nig 4 strf 0 sicc 3+ elas 0 lm 2
178-191	Sandy *Phragmites* peat	Sh2+ Gmin1 Gmaj+ Th^{2}1 Anth+ nig 4 strf 0 sicc 3+ elas 0 lm 0
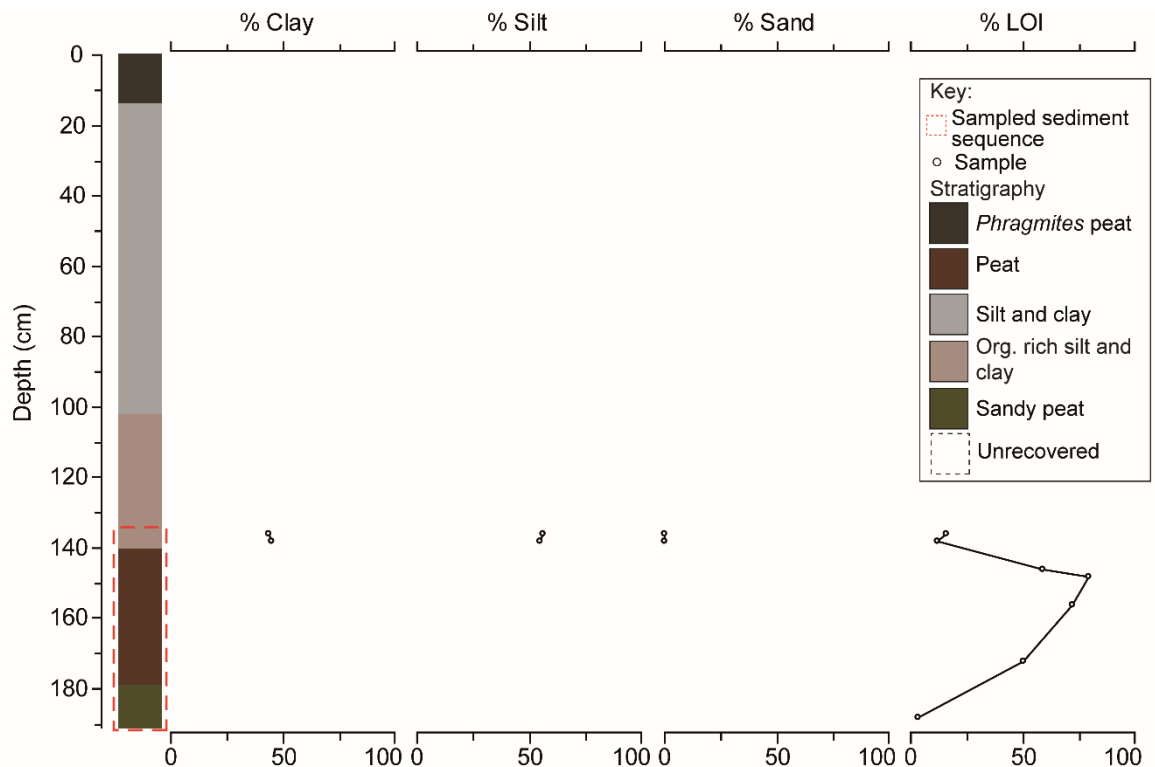
Figure 5.7: Stratigraphy, particle size and LOI for sampled sequence from MN-16-3. The boundaries for the clay, silt and sand fraction are defined by Wentworth (1922).

5.3.3 MN-16-5

The MN-16-5 sampled sequence contains six main units (Table 5.3); organic sand (126 cm to 120 cm); sandy peat (120 cm to 114 cm); minerogenic peat (114 cm to 110 cm); organic silt and clay (110 cm to 60 cm); silty clay (60 cm to 15 cm); *Phragmites* peat (15 cm to 0 cm).

Table 5.3: Description of main sediment units identified in MN-16-5 and associated Troels-Smith (1955) *classification.*

Unit depth (cm)	Description	Troels-Smith log
0-15	Top soil	As2 Ag1 Sh1 Th^0+ Lf+ nig 3 strat 0 elas 0 sicc 3 lm.sup N/A
15-60	Silty clay	As3 Ag1 Lf1 Gmin+ Th^0+ Sh+ nig 2+ strat 0+ elas 0 sicc 2+ lm.sup 0
60-110	Organic silt and clay	Ag1+ As1+ Sh2 Th$^{1/2}$+ Th^{phrag}+ nig 2+ strf 0+ sicc 2 elas 0 lm N/A
110-114	Peat with trace of clay, silt and sand	Sh2+ Gmin+ Ag+ As1+ nig 3 strf 0 sicc 2+ elas 0 lm 0
114-120	Sandy peat	Gmin1+ Sh2+ Th1 nig 3 strf 0 sicc 2+ elas 0 lm 0
120-126	Organic sand	Gmin3 Sh1+ Gmaj+ nig 3 strf 0 sicc 2+ elas 0 lm 0

Particle size analysis was completed for nine samples in core MN-16-5 at a 16 cm resolution (Figure 5.8). The clay fraction varies significantly in the samples analysed between 92 cm and 76 cm. The silt fraction remains steady between 108 cm and 84 cm, after which, this fraction fluctuates between 43 % (76 cm) and 69 % (68 cm). A peak in the sand fraction (12 %) occurs at 92 cm, with sand near absent in the other samples analysed. The sediments from MN-16-5 (Figure 5.6) plot in the graphic sedimentary domain indicative of open to filled estuary on the bivariate plot and are very poorly sorted with a mean particle size in the fine silt.

Seven samples, at a minimum resolution of 16 cm, were analysed to determine changes in organic content for MN-16-5 (Figure 5.8). The organic content increases from 5 % at the base to a peak of 42 % (116 cm), following which it declines to 14 % at 108 cm, which is sustained until 44 cm.
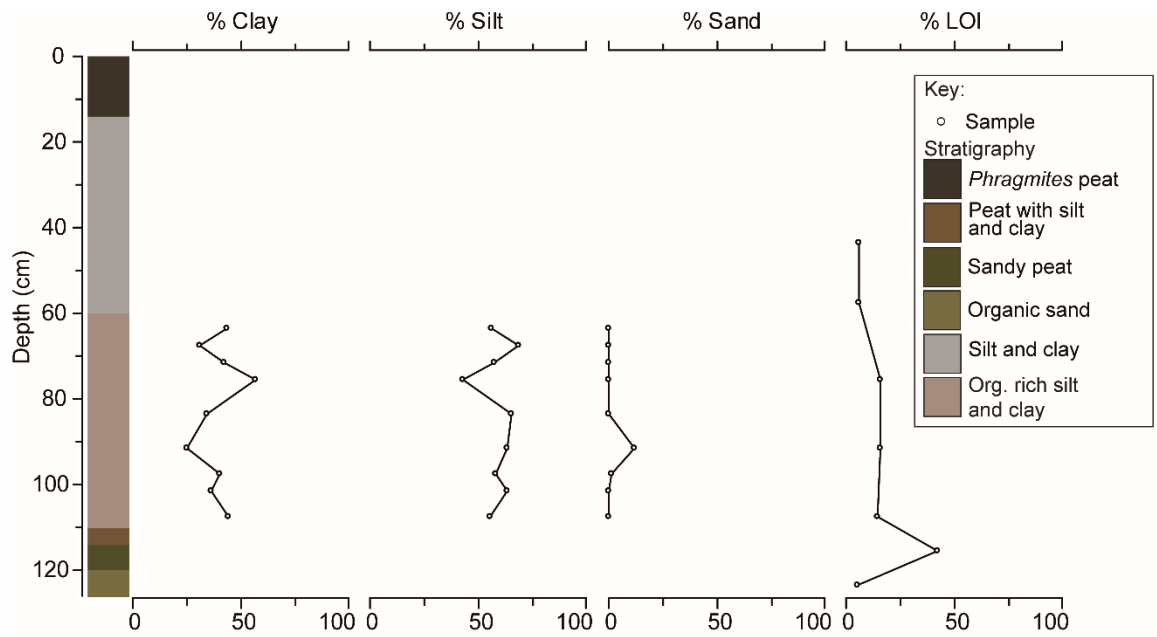
Figure 5.8: Stratigraphy, particle size and LOI for sampled sequence from MN-16-5. The boundaries for the clay, silt and sand fraction are defined by Wentworth (1922).

5.3.4 MN-16-19

The main sediment units for MN-16-19, located further inland (Figure 5.1B), are outlined in Table 5.4. Organic sedimentation dominates the sediment sequence until 417 cm, after which a transition to organic rich silt occurs. A return to peat sedimentation occurs at 355 cm, remaining until the onset of organic clayey silt sedimentation at 237 cm. Minerogenic sedimentation, with varying degrees of organics, dominates the sediment sequence until near the surface, with a 10 cm band of peat present at 143 cm.

The particle size data set for MN-16-19 contains 17 samples between 415 cm and 332 cm and 224 cm and 216 cm, at a minimum resolution of 8 cm (Figure 5.9). An initial upwards coarsening trend, between 415 cm and 400 cm, is replaced by an upwards fining until 366 cm. The particle size between 366 cm and 216 cm is variable, with the dominating size fraction fluctuating between clay and silt. The upwards coarsening trend from 366 cm is associated with a subordinate sand component (2 %) at 348 cm.

The bivariate plot of mean particle size against standard deviation for MN-16-19 illustrates that the analysed sediments plot in the open to filled estuary sedimentary domain (Figure 5.6). These sediments are poorly sorted with a predominantly fine to medium silt mean particle size.

Table 5.4: Description of main sediment units identified in MN-16-19 and associated Troels-Smith (1955) *classification.*

Unit depth (cm)	Description	Troels-Smith log
0-50	Clayey top soil	
50-133	Organic silty clay	Sh1+ Ag1 As2 nig 2+ strf 0 sicc 3 elas 0 lm N/A
133-143	Peat	Sh4 Th^1+ Ag+ As+ nig 4 strf 0 sicc 3 elas 0 lm 3
143-152	Organic clayey silt	Ag2 As1 Sh1+ Ptm+ Th^1+ nig 2+ strf 0 sicc 3 elas 0 lm 3
152-226	Clayey silt with very irregular organics	Ag3 As1 Sh+ Th^1+ nig 2 strf 0 sicc 3 elas 0 lm 0
226-232	Peat with clay and silt	Sh2+ Th^{phrag}+ Th^{1}2 As+ Ag+ nig 3+ strf 0 sicc 3 elas 0 lm 1
232-237	Organic clayey silt	Ag3 As+ Sh1 Th^1+ nig2+ strf 0 ela s0 sicc 2+ lm 2
237-260	Peat with clay and silt	Sh2+ Th^{phrag}+ Th^{1}2 As+ Ag+ nig 3+ strf 0 sicc 3 elas 0 lm 1
260-288	Peat	Sh2+ Th^{3}2 Th^{phrag}++ nig 4 strf 0 sicc 2 elas 0 lm N/A
288-355	Peat with silt and clay	Sh3 Th^{3}1+ Ag+ As+ nig 4 strf 0 sicc 2 elas 0 lm 0
355-417	Organic silt	Ag2+ Sh1 Ag1+ Th^2+ Th^{phrag}2+ nig 2+ sicc 2 elas 0 strf 0 lm N/A
417-515	Peat with wood and rootlets	Sh3 Th^{2}1 Dl+ nig 4 strat 0 sicc 3+ elas 0 lm N/A
515-620	Well humified peat	Sh4 Th^2+ nig 4 strat 0 sicc 2+ elas 0 lm N/A
620-624	Peat with silt and clay	Sh2 Th^2+ Ag1 As1 nig3 strat 1 sicc 3 elas 0 lm 4
624-655	Well humified peat	Sh4 Th^2+ nig 4 strat 0 sicc 2+ elas 0 lm 2
650-785	Well humified peat with silt	Sh4 Th^3+ Ag+ nig 4 strat 0 sicc 2+ elas 0 lm N/A
785-797	Organic sand	Gmin3 Sh1 Dl+ Th^3+ nig 4 strat 0 elas 0 sicc 2+ lm.sup 0

Figure 5.9: Stratigraphy, particle size and LOI for sampled sequence from MN-16-19. The boundaries for the clay, silt and sand fraction are defined by Wentworth (1922).

End-member mixing analysis identified two end-members that account for 97 % of the variance in the MN-16-19 particle size data. Changes in the proportional down-core distribution of each end-member is shown in Figure 5.10. EM1 is poorly sorted and is comprised of silt (61 %) and clay (39 %). The poorly sorted EM2, in contrast, is dominated by silt (82 %), with a clay (17 %) and minor sand component (1 %). The particle size data set for MN-16-19 is predominantly explained by EM1 however at 352 cm EM2 is solely present.

The organic content for MN-16-19 was determined at a 16 cm resolution for 42 samples (Figure 5.9). The organic content remains high, at ~ 85 %, until 422 cm with minor peaks below this trend occurring at 742 cm and 502 cm for example. A sharp decline, to 11 % occurs between 422 cm and 406 cm, following which, the organic content gradually increases, peaking at 80 % at 262 cm. The organic content decreases to 10 % by 214 cm, remaining steady until an increase from 150 cm.
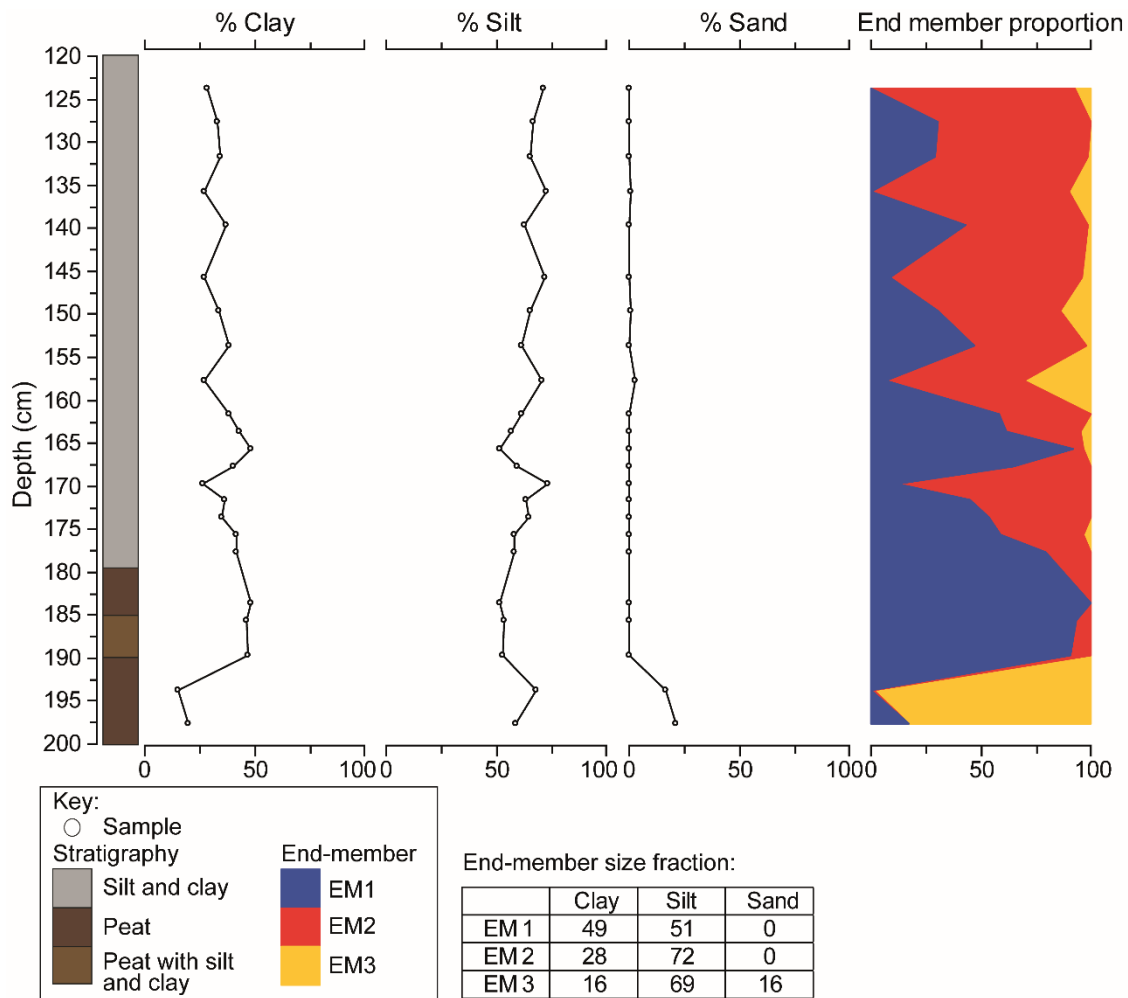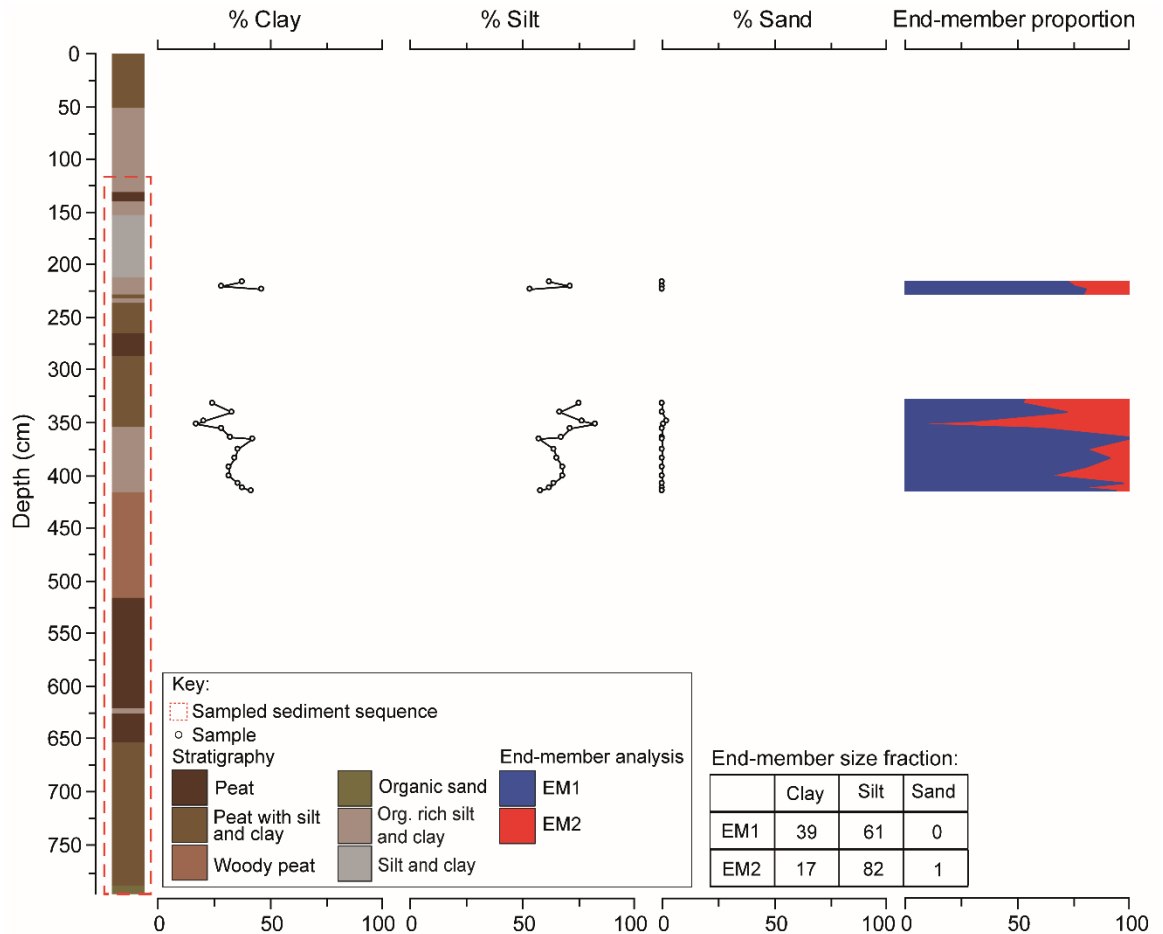
Figure 5.10: The proportional down-core distribution of end-members determined from MN 16-19 particle size data using the end-member analysis algorithm developed by Paterson and Heslop (2015)*. The stratigraphy and clay silt and sand fractions (defined by* (Wentworth, 1922)*) are plotted alongside this for comparison.*

5.4 Biostratigraphy

5.4.1 MN-16-2

Diatom analysis completed for the sampled sediment sequence (294 cm - 180 cm) from MN-16-2 identified 265 species in seven samples (raw counts are presented in Appendix 13). Diatom preservation was problematic in the organic units (290 cm to 205 cm) of this core, with diatoms only preserved at 240 cm, 204 cm and 200 cm (Figure 5.11). Two zones were identified between 294 cm and 180 cm, based on lithostratigraphy and diatom flora (Figure 5.11 and 5.12). Brackish-marine taxa dominate the diatom assemblage of Zone 1 (294 cm to 198 cm). However, these are decreasing in this zone whilst the freshwater component is increasing. Zone 2 (198 cm to 180 cm) is defined by a sharp increase in marine and brackish taxa combined with a decrease in the freshwater component of the assemblage.
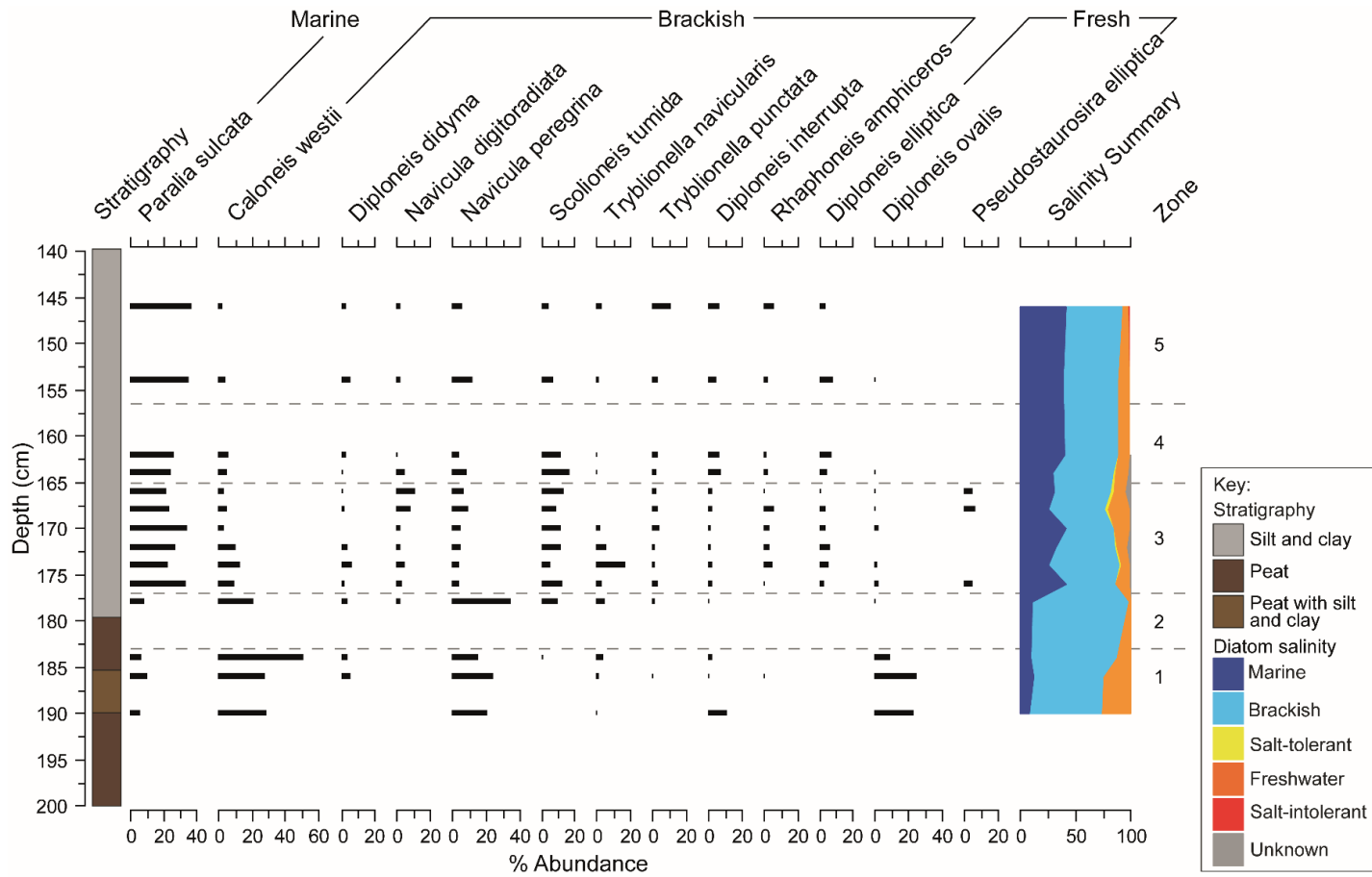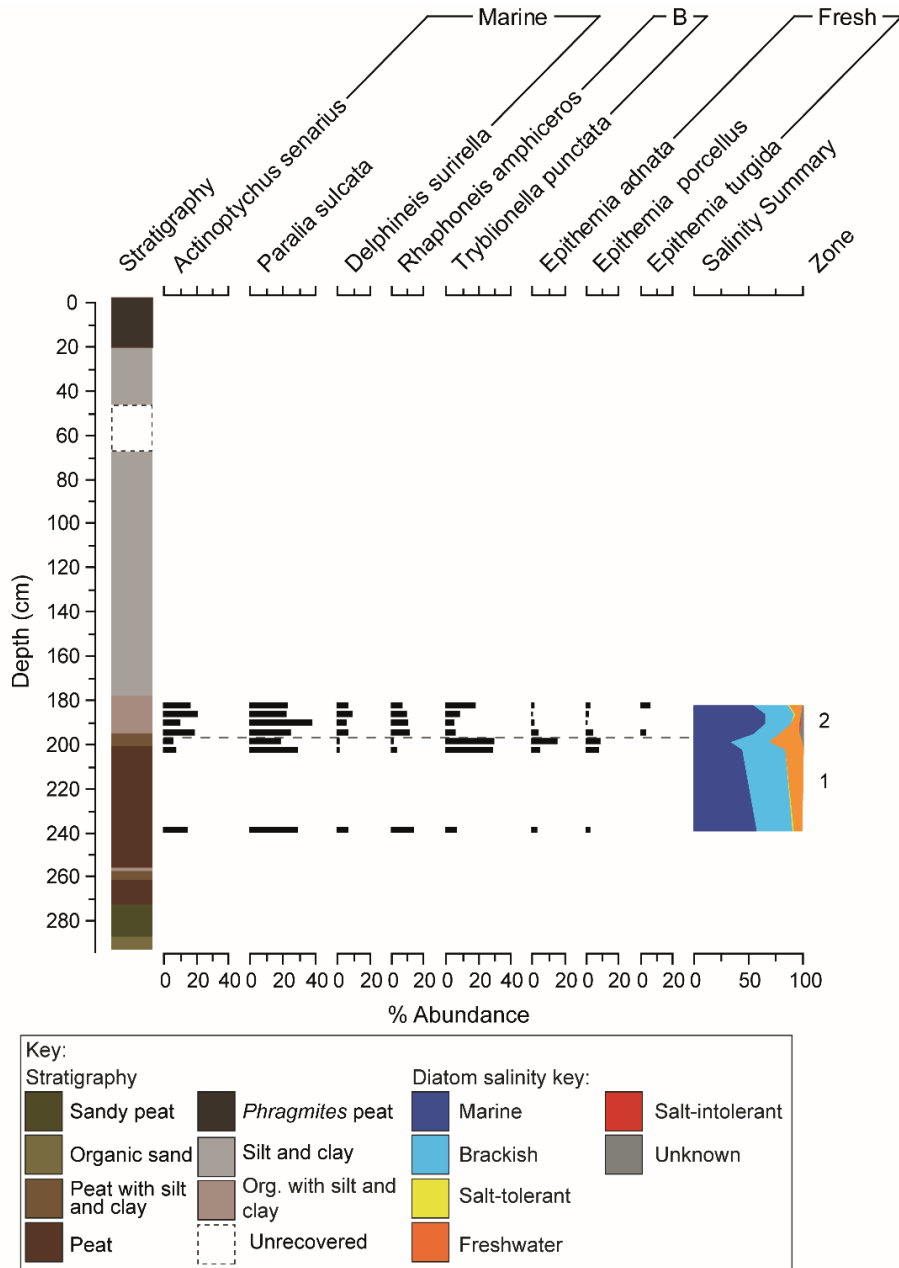
Figure 5.11: Diatom assemblage for MN-16-2; species shown exceed 5 % of the total count. Diatoms are grouped based on their salinity tolerance using the halobian classification (Hustedt, 1953).

Marine planktonic taxa initially account for nearly half of the diatom assemblage for Zone 1, with *Paralia sulcata* particularly abundant. The brackish and freshwater component increases by 204 cm, with brackish and freshwater epipelic taxa, such as *Tryblionella punctata* and *Epithemia adnata* respectively, becoming abundant. The transition from

Zone 1 to Zone 2, at 198 cm, is denoted by a sharp increase in marine and brackish taxa as well as the decrease of freshwater taxa. Marine planktonic taxa, such as *Actinoptychus senarius* and *Paralia sulcata*, increase in abundance across the transition from Zone 1 to 2, dominating the later zone. In contrast, freshwater epipelic taxa, such as *Epithemia adnata* and *Epithemia porcellus* decrease in Zone 2, with freshwater conditions decreasing to 6 % of the total count in this zone.
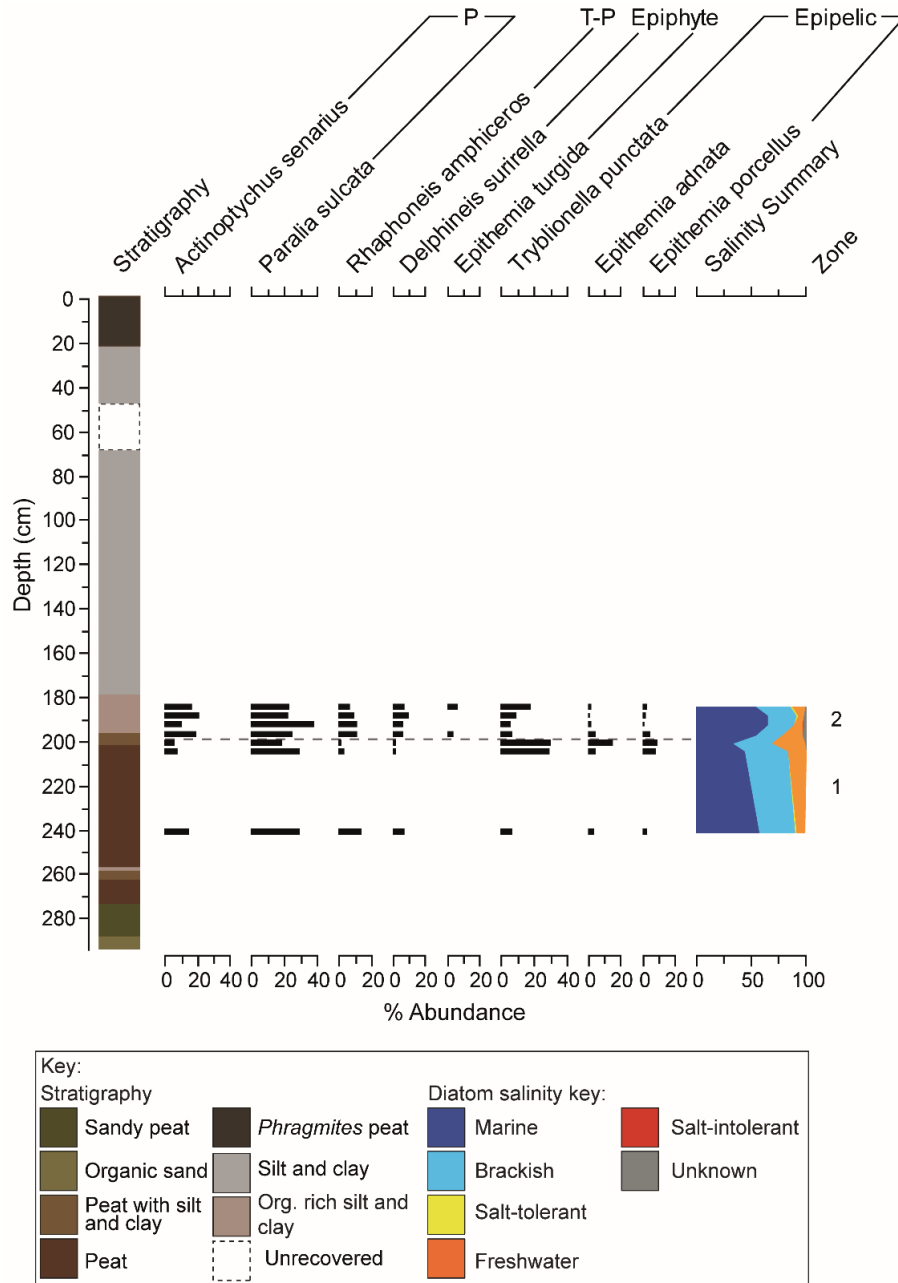
Figure 5.12: Diatom assemblage for MN-16-2; species shown exceed 5 % of the total count. Diatoms are grouped based on their life form using Vos and De Wolf (1988; 1993).

5.4.2 MN-16-3

Diatom preservation for the sampled sediment sequence (191 cm to 135 cm) for MN-16-3 was poor, with diatoms not preserved in the organic units of this core (191 cm to 140 cm). Diatom analysis completed for two samples identified 170 species (raw counts presented in Appendix 14). A zone boundary was identified at 140 cm, based on lithostratigraphy. Diatoms were not preserved in Zone 1 (191 cm to 140 cm) whilst Zone 2 (140 cm to 135 cm) is characterised by a predominantly marine planktonic diatom assemblage, with *Paralia sulcata* particularly abundant (Figure 5.13 and 5.14).
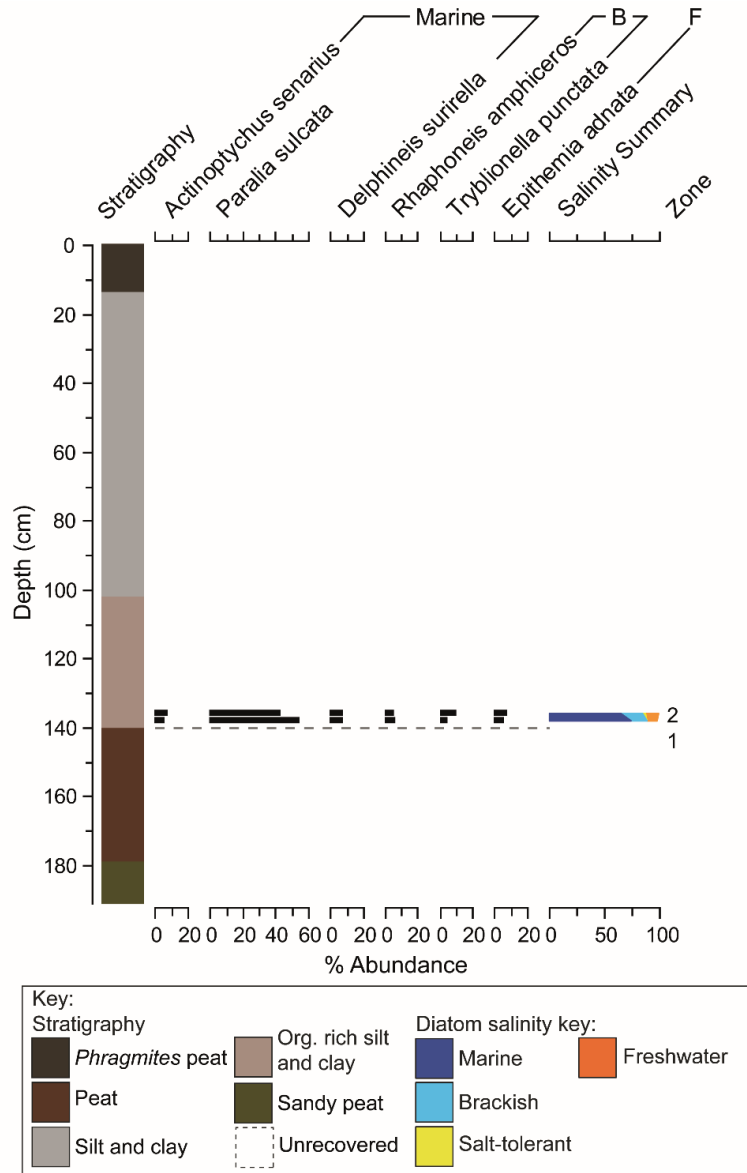
Figure 5.13: Diatom assemblage for MN-16-3; species shown exceed 5 % of the total count. Diatoms are grouped based on their salinity tolerance using the halobian classification (Hustedt, 1953).
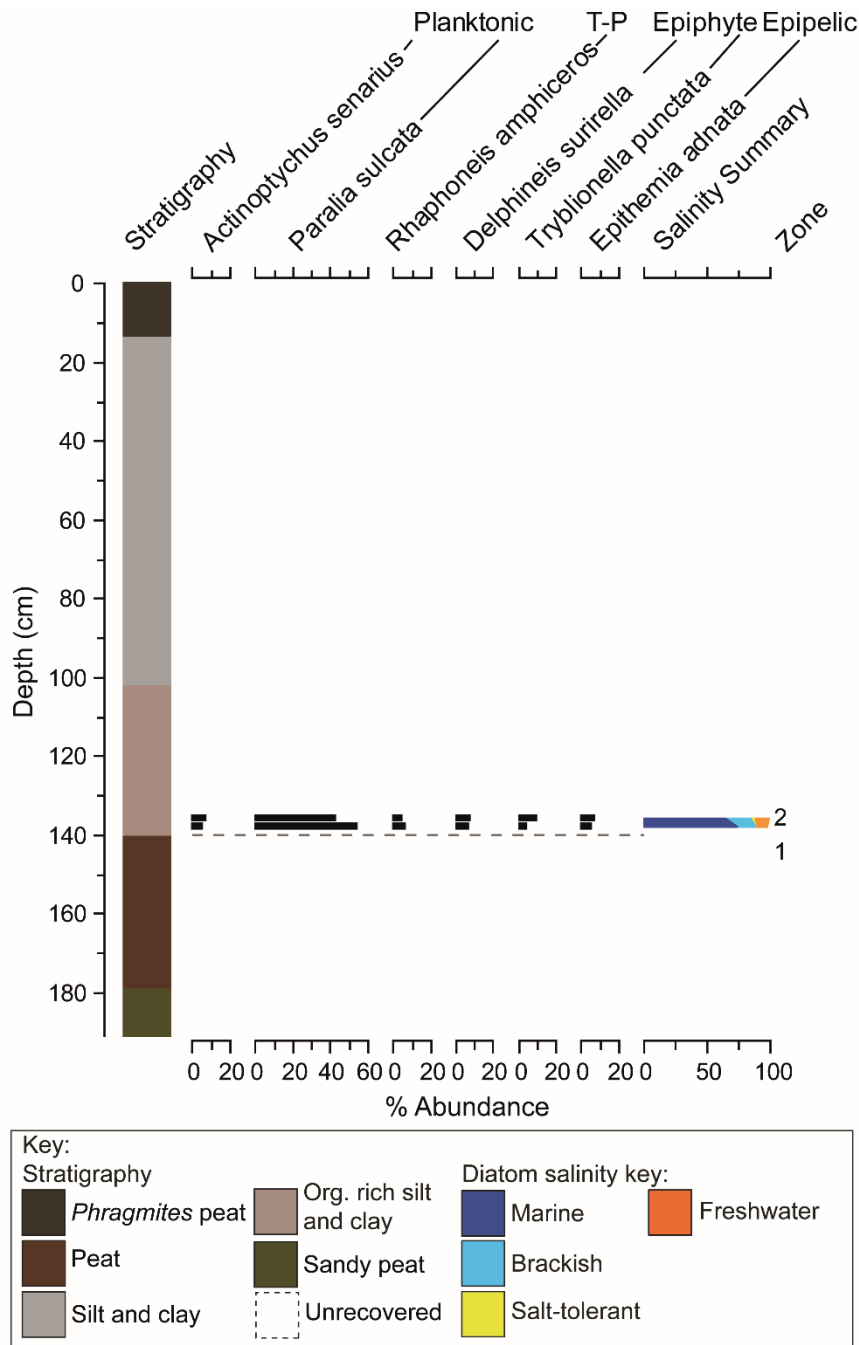
Figure 5.14: Diatom assemblage for MN-16-3; species shown exceed 5 % of the total count. Diatoms are grouped based on their life form using Vos and De Wolf (1988; 1993).

5.4.3 MN-16-5

A diatom assemblage of 253 taxa was identified from eight samples for MN-16-5 (raw counts presented in Appendix 15) was identified for MN-16-5 (Figure 5.15 and 5.16). Diatom preservation was poor in the top 72 cm of the sediment sequence. Four zones, based on lithostratigraphy and diatom flora, were identified. A brackish-marine zone (Zone 1: 126 cm to 114 cm) is replaced by a freshwater-brackish zone, which occurs between 114 cm and 106 cm (Zone 2). A sharp increase in the brackish-marine components occurs

in Zone 2 and is sustained for Zone 3 (106 cm to 80 cm), following which the freshwater component increases (Zone 4: 80 cm to 0 cm).
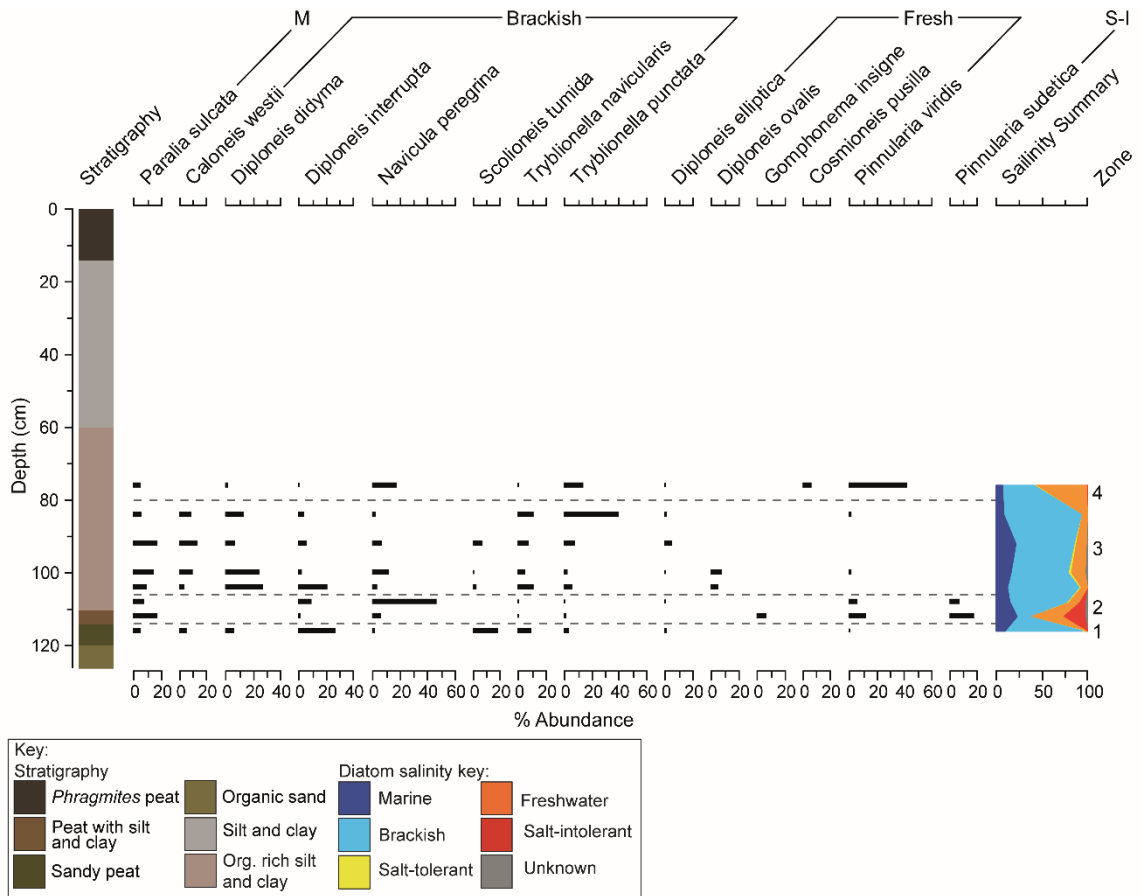
Figure 5.15: Diatom assemblage for MN-16-5; species shown exceed 5 % of the total count. Diatoms are grouped based on their salinity tolerance using the halobian classification (Hustedt, 1953).

Zone 1 is dominated by brackish taxa, which account for over 80 % of the total count. However, this zone is only comprised of a single diatom sample, with the brackish aerophilous taxa, *Diploneis interrupta*, particularly abundant.

The transition from Zone 1 to 2 is denoted by a sharp decrease in the brackish component to 11 % by 112 cm, however this component increases in abundance once more following this decrease. The decreased brackish component at the beginning of Zone 2 is combined with an increase in the freshwater component as well as the occurrence of salt-intolerant taxa. Freshwater and salt-intolerant aerophilous taxa, such as *Pinnularia viridis* and *Pinnularia sudetica* respectively, are particularly abundant at the beginning of Zone 2.

A peak in the brackish component marks the onset of Zone 3 at 106 cm, which accounts for over 60 % of the total diatom assemblage. This dominance of brackish taxa, combined

with a small freshwater component, is sustained for most of this zone. Brackish epipelic taxa, such as *Diploneis didyma*, *Tryblionella punctata* and *Tryblionella navicularis* are particularly abundant in this zone.

Brackish taxa begin to decrease in abundance at the culmination of Zone 3, reaching 35 % of the total count by 76 cm. The freshwater component increases in Zone 4, with the aerophilous diatom *Pinnularia viridis* dominating. However, Zone 4 is only comprised of one diatom sample.
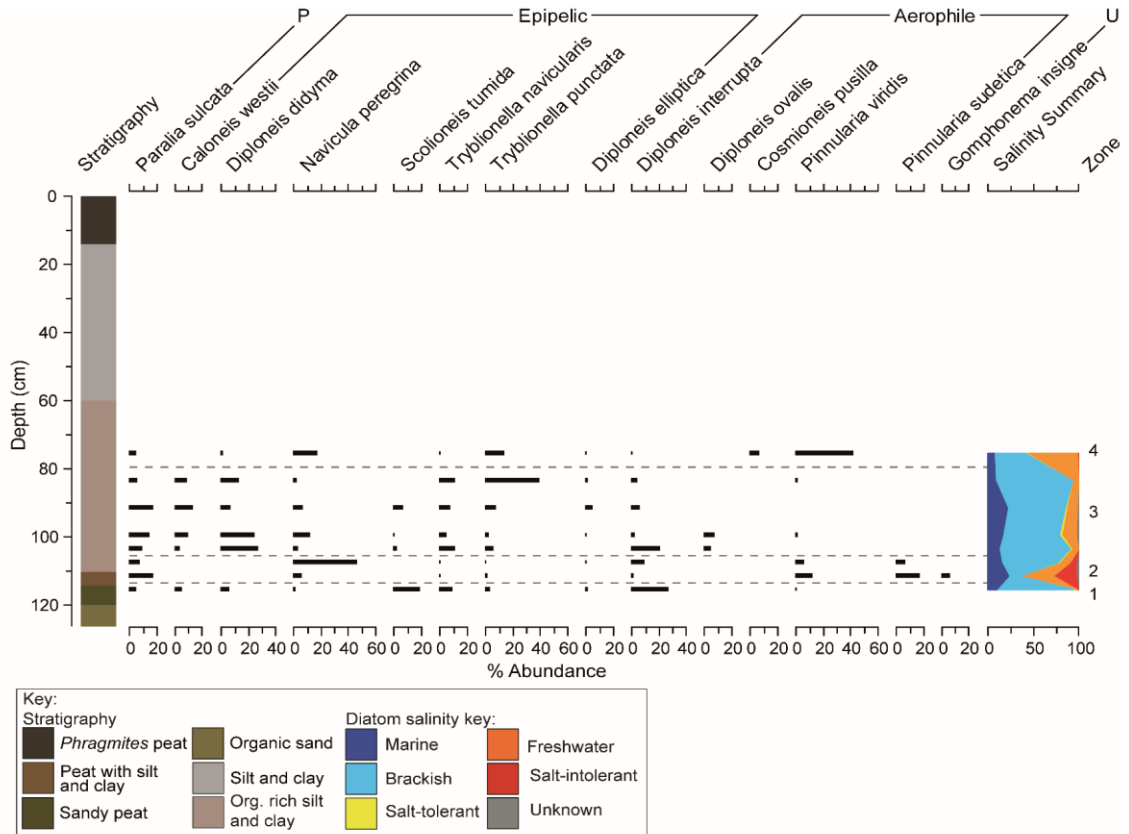
Figure 5.16: Diatom assemblage for MN-16-5; species shown exceed 5 % of the total count. Diatoms are grouped based on their life form using Vos and De Wolf (1988; 1993).

5.4.4 MN-16-19

Diatom analysis completed for core MN-16-19 (797 cm to 120 cm) identified 249 taxa in 22 samples (raw counts presented in Appendix 16). Diatom preservation was variable in the organic units of the sampled sequence (Figure 5.17 and 5.18). Five zones were identified, based on lithostratigraphy and diatom flora: a brackish-freshwater zone (Zone 1: 797 cm to 447 cm), a brackish-marine zone (Zone 2: 447 cm to 397 cm), a freshwater zone with variable brackish influence (Zone 3: 397 cm to 300 cm), a freshwater-brackish zone (Zone 4: 300 cm to 223 cm) and a brackish marine zone (Zone 5: 223 cm to 120 cm).

Freshwater taxa dominate Zone 1, until 686 cm, when the brackish component increases from 39 % to 64 % of the total diatom assemblage. By 462 cm, the freshwater component has increased, with taxa such as the epipelic *Epithemia porcellus* and epiphytic *Fragilaria vaucheriae* abundant.

The transition from Zone 1 to Zone 2 is denoted by a sharp increase in and dominance of brackish taxa. Brackish epipelic taxa, such as *Tryblionella navicularis*, *Tryblionella punctata* and *Scolioneis tumida*, are particularly abundant in this zone. Marine taxa also increase in Zone 2, peaking at 39 % at 412 cm, with *Paralia sulcata* dominating this component.

The onset of Zone 3 is marked by fluctuations between the brackish and freshwater components, with a peak in brackish conditions occurring at 366 cm, following which freshwater conditions dominate by 360 cm. Epipelic taxa, such as the freshwater *Cocconeis placentula* and salt-tolerant *Cocconeis pediculus,* are abundant in Zone 3. Diatoms were not preserved for the remainder of Zone 3 and are absent at the onset of Zone 4.

Freshwater taxa, such as the tychoplanktonic *Staurosira construens* and epipelic *Staurosirella lapponica*, initially dominate the upper section of Zone 4. A shift in dominance, from freshwater to brackish taxa, occurs prior to the transition to Zone 5 (223 cm), with brackish epipelic taxa, such as *Navicula peregrina*, dominating at the culmination of Zone 4.

A sharp increase in brackish taxa occurs at the onset of Zone 5. Brackish epipelic taxa, such as *Scolioneis tumida* and *Tryblionella navicularis*, dominate this zone, with the former reaching 50 % of the total diatom assemblage. Marine taxa, such as *Paralia sulcata*, are also present whilst the freshwater component is subordinate.
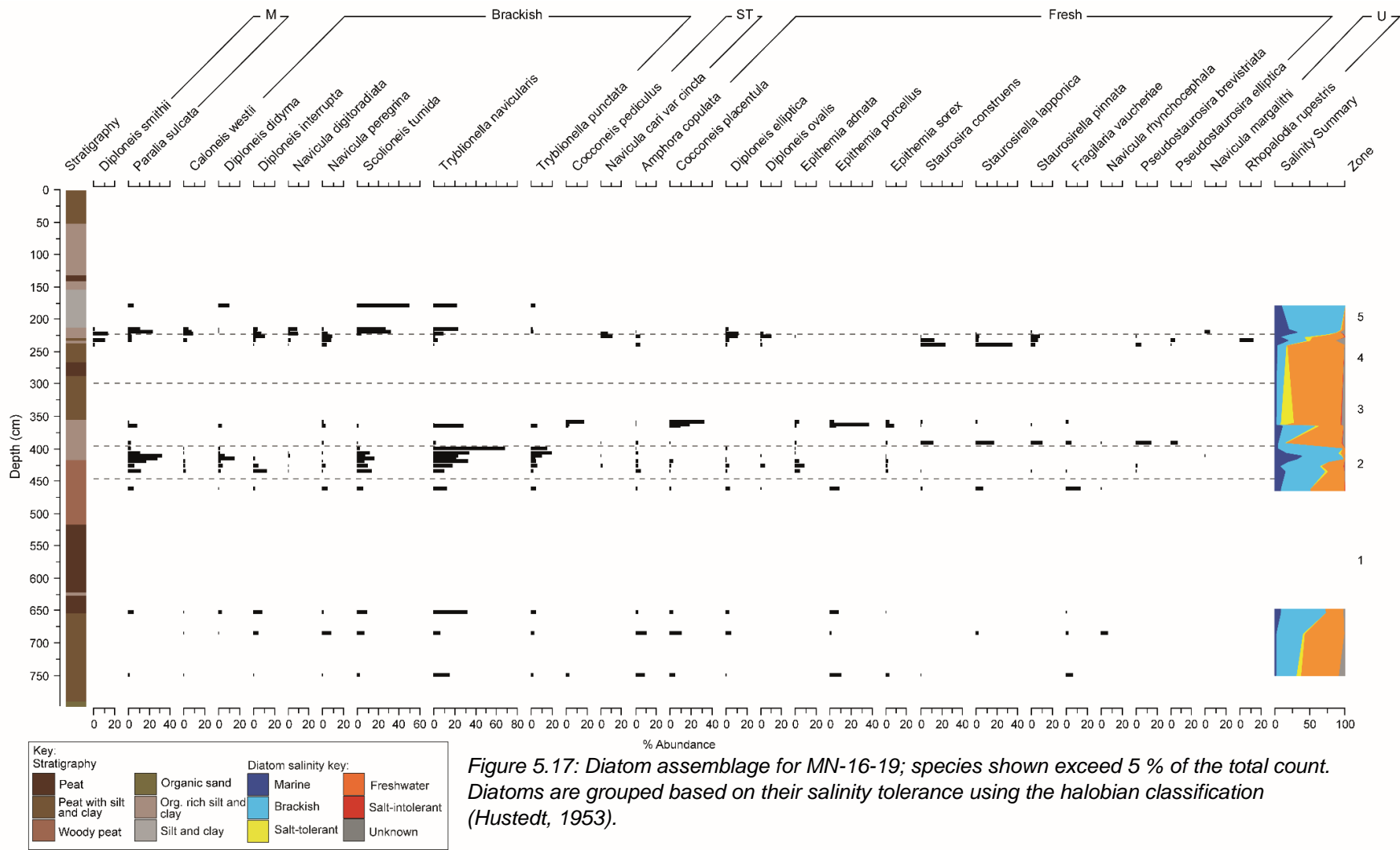
Figure 5.17: Diatom assemblage for MN-16-19; species shown exceed 5 % of the total count. Diatoms are grouped based on their salinity tolerance using the halobian classification (Hustedt, 1953).
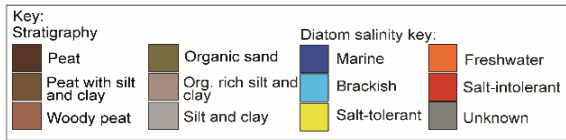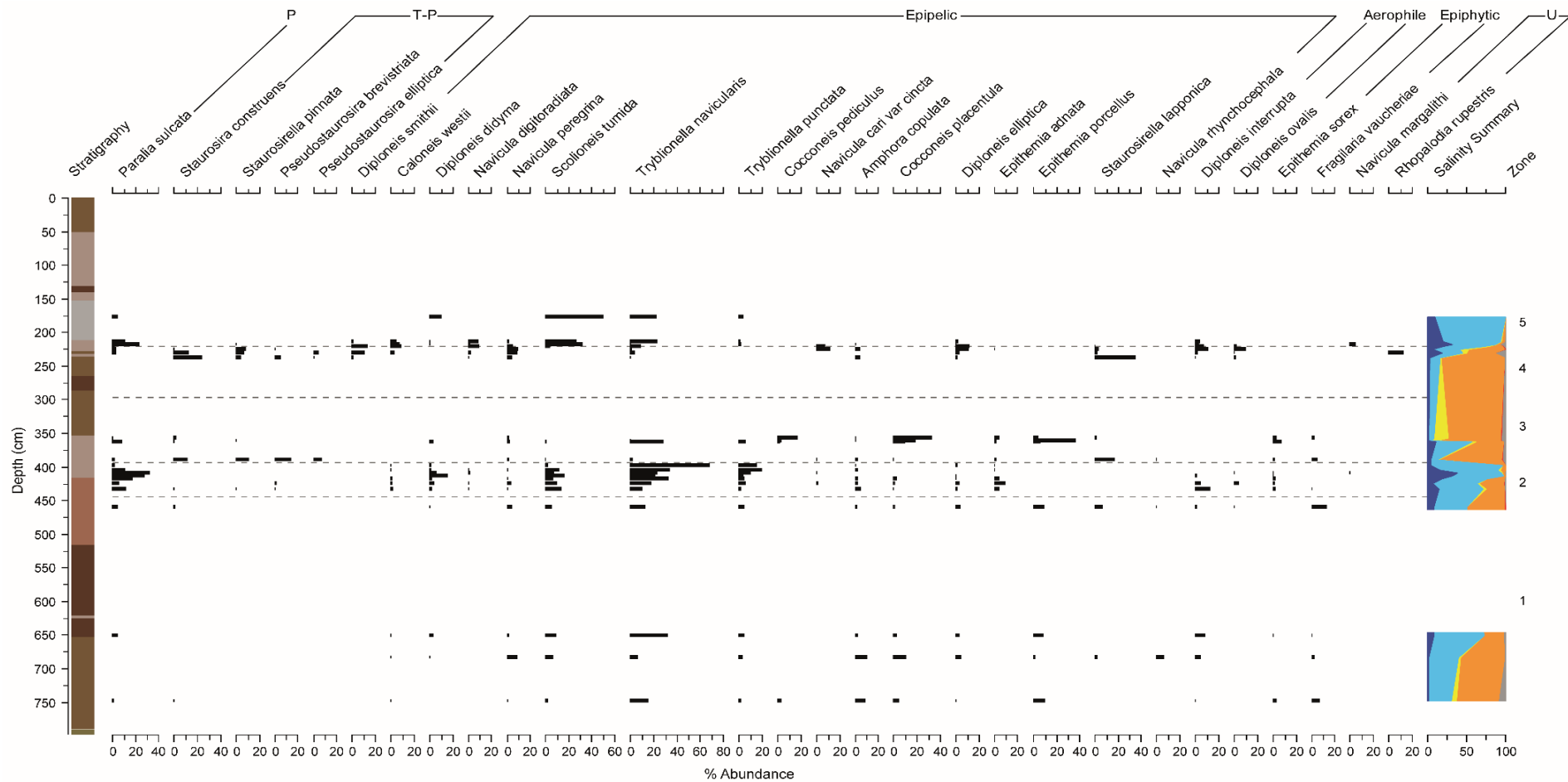
Figure 5.18: Diatom assemblage for MN-16-19; species shown exceed 5 % of the total count. Diatoms are grouped based on their life form using Vos and De Wolf (1988; 1993).

5.5 Chronology

AMS radiocarbon dating was used to determine the chronology for sections of the sampled Minsmere transect (Figure 5.4), with all sampled material dated at the NERC Radiocarbon Facility, East Kilbride (Allocation number: 2075.1017). The uncalibrated and calibrated ages for all dated material is presented in Table 5.5.

5.4.1 MN-16-1

A basal sample from the most coastal point of the Minsmere transect, MN-16-1, was submitted for AMS radiocarbon dating to constrain the timing of the onset of peat deposition at this location and rising regional ground water level. Plant macrofossils and seeds, such as *Poaceae* remains and *Carex*, sampled from 358 cm (-5.62 m OD) date the onset of peat deposition to 4816-4447 cal BP (Laboratory code: SUERC-79046). Diatoms were absent at the base of the core, which along with the stratigraphic context, indicates the radiocarbon date is freshwater limiting. Comparatively, this date is considerably older than others of a similar altitude (Figure 5.4) and consideration will be given to the validity of this radiocarbon date in Chapter 7.

5.4.2 MN-16-3

The onset of organic clayey silt sedimentation in MN-16-3 at 140 cm (-3.69 m OD) is associated with marine-brackish conditions. Plant macrofossils (e.g. *Poaceae* remains) sampled from 142 cm (-3.71 m OD) dated the transition from peat to organic clayey silt to 2101-1880 cal BP (Laboratory code: SUERC-79047).

5.4.3 MN-16-5

Diatom analysis of MN-16-5 identified the disappearance of salt-intolerant taxa across the transition from minerogenic peat to organic silty clay (110 cm; -3.03 m OD). AMS radiocarbon analysis of plant macrofossils and seeds (e.g. *Poaceae* remains *and Brassicaceae* seed) sampled from 112.5 cm (-3.05 m OD) date this transition to 1265-1065 cal BP (Laboratory code: SUERC-79048).

5.4.4 MN-16-19

The timing of the onset of peat deposition and rising regional ground water level for MN-16-19, the most landwards sampled sequence, was constrained by a basal bulk peat sample. An additional error of ± 100 ^{14}C is applied to this sample since it is based on bulk peat (Hu, 2010; Hijma et al., 2015). Material sampled from 793 cm (-9.28 m OD) dates to 6310-5670 cal BP (Laboratory code: SUERC-79055). The stratigraphic context of this sample, in addition to the absence of diatoms at the base of the core, indicates this radiocarbon date is freshwater limiting.

The transition from woody peat to organic rich silt in MN-16-19 at 417 cm (-5.52 m OD) is associated with increased brackish conditions. Plant macrofossils and seeds (e.g. *Carex* and *Brassicaceae* seeds) sampled from 419 cm (-5.54 m OD) date this transition to 1966-1738 cal BP (Laboratory code: SUERC-79054).

A sample for AMS radiocarbon dating was submitted to constrain the sedimentation shift from clayey silt to organic rich silt, associated with increasing freshwater conditions at 364 cm (-4.99 m OD) in MN-16-19. Plant macrofossils and seeds sampled from 363 cm (-4.98 m OD) date this transition to 1592-1408 cal BP (Laboratory code: SUERC-79053).

A sedimentation shift, from minerogenic peat to organic clayey silt, occurs at 226 cm (-3.61 m OD) in MN-16-19. Marine and brackish conditions increase across this transition whilst freshwater conditions decrease. Plant macrofossils (e.g. *Poaceae* remains) sampled at 228.5 cm (-3.63 m OD) date this transition to 917-743 cal BP (Laboratory code: SUERC-79052).

Table 5.5: AMS radiocarbon dates produced for Minsmere. All samples were radiocarbon dated at NERC Radiocarbon Facility, East Kilbride (Allocation number: 2075.1017). The radiocarbon date for MN-16-19 -9.28 m OD is based on a bulk peat sample therefore a 'bulk error' of ± 100 ^{14}C is included for this sample (Hu, 2010; Hijma et al., 2015).

Site	Sample ID	Laboratory code	^{14}C ± 1σ BP	Cal. age (BP)- 2σ range	
				Max	Min.
	MN-16-1 -5.62 m OD	SUERC-79046	4099 ± 39	4816	4447
	MN-16-3 -3.71 m OD	SUERC-79047	2014 ± 38	2101	1880
	MN-16-5 -3.05 m OD	SUERC-79048	1231 ± 38	1265	1065
Minsmere	MN-16-19 -3.63 m OD	SUERC-79052	909 ± 37	917	743
	MN-16-19 -4.98 m OD	SUERC-79053	1613 ± 35	1592	1408
	MN-16-19 -5.54 m OD	SUERC-79054	1920 ± 38	1966	1738
	MN-16-19 -9.28 m OD	SUERC-79055	5266 ± 140	6310	5670

5.6 Palaeoenvironmental interpretation

The stratigraphic transect extending landwards from the coast at Minsmere identified sequences dominated by minerogenic sedimentation nearest the coast, with dominance decreasing with distance inland. In central sections of the transect, thick peat deposits with wood are consistently present, documenting the dominance of freshwater and brackish wetland deposits. The transect documents the migration of tidal influence landwards from the coast during the late Holocene with silt and clay sedimentation intercalated with more organic deposits in the central section.

5.6.1 MN-16-2

The transition from silty peat to organic clayey silt in MN-16-2 at 198 cm (-4.07 m OD) is associated with decreasing organic content and an upwards coarsening, indicative of increasing depositional energy (Figure 5.19). The shift in sedimentation is associated with sediments transitioning from the closed basin envelope of the bivariate plot to the open and filled estuary envelope. The occurrence of marine and brackish diatom taxa in the peat unit indicate that the site was already tidally influenced. A gradual decline in organic content from 222 cm is interpreted as a transition from a high to low marsh environment. The lithostratigraphic and biostratigraphic results indicate a further decrease in position of the site in the tidal frame and shift in depositional energy from 198 cm (-4.07 m OD). *Paralia sulcata*, a marine planktonic taxa, dominates the assemblage of the organic clayey silt unit with other taxa indicative of tidal inlets and large tidal channels (e.g. *Delphineis surirella* and *Rhaphoneis amphiceros*) also present (Vos and De Wolf, 1988). Despite this, freshwater epipelic and epiphytic taxa are present in the organic clayey silt unit therefore indicating an intertidal flat environment.
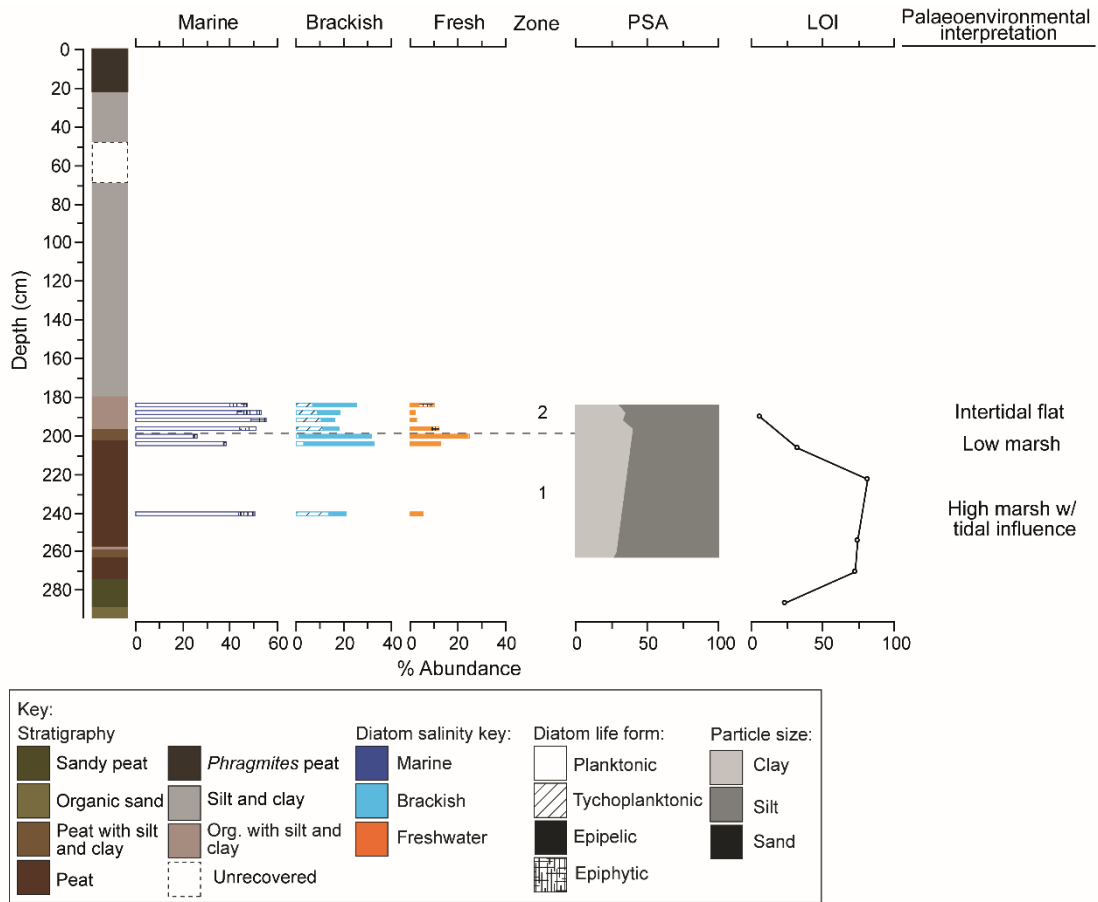
Figure 5.19: Summary diagram of results produced for MN-16-2 with palaeoenvironmental interpretation. Stratigraphy, particle size, organic content and the diatom summary, illustrating changes in salinity and life form, are presented.

5.6.2 MN-16-3

Poor diatom preservation hinders palaeoenvironmental interpretation. The onset of organic rich clayey silt sedimentation in MN-16-3 at 140 cm (-3.69 m OD) is associated with low organic content and a diatom assemblage dominated by marine planktonic taxa, with marine epiphytic taxa also present (Figure 5.20). The dominance of marine littoral taxa (e.g. *Paralia sulcata* and *Delphineis surirella*) is indicative of subtidal areas, notably large tidal channels and tidal inlets (Vos and De Wolf, 1988). Freshwater epipelic diatoms are present following the onset of the organic rich clayey silt unit, despite the dominance of marine planktonic taxa. The presence of freshwater diatom taxa and nature of sedimentation therefore indicates an intertidal flat environment, rather than subtidal channels (Vos and De Wolf, 1988).
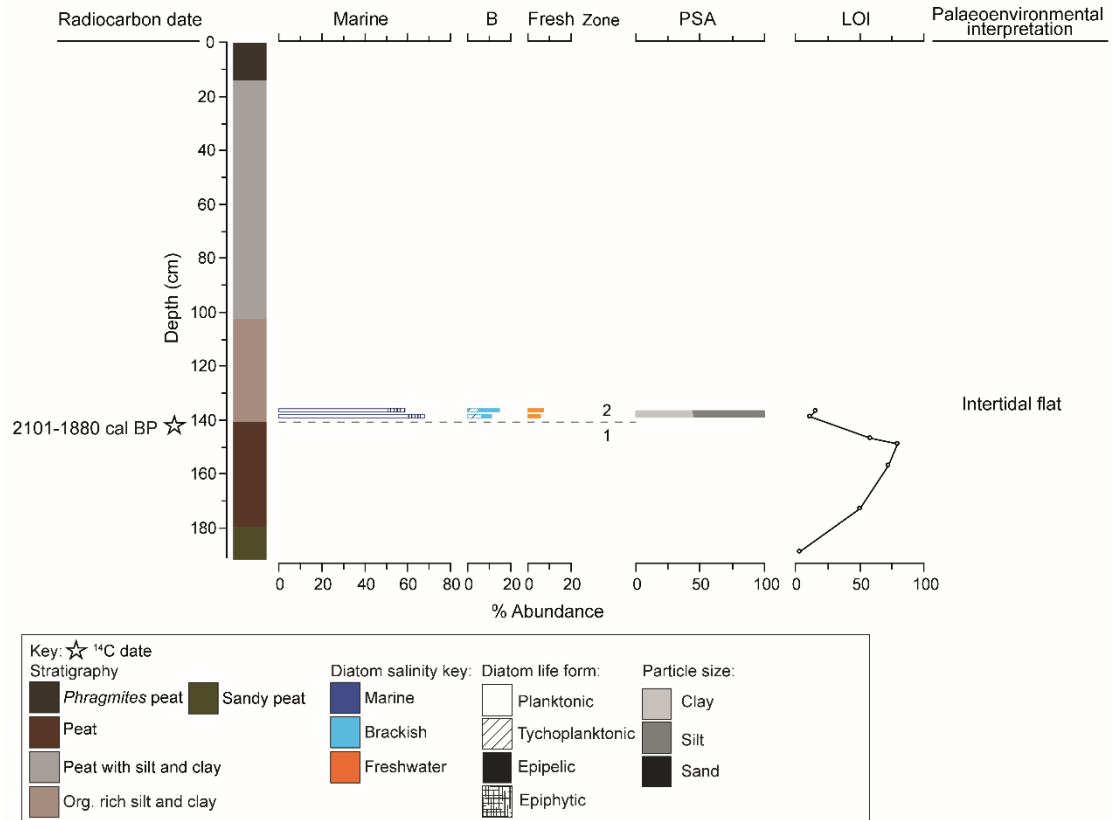
Figure 5.20: Summary diagram of results produced for MN-16-3 with palaeoenvironmental interpretation. Stratigraphy, particle size, organic content and the diatom summary, illustrating changes in salinity and life form, are presented

5.6.3 MN-16-5

The shift from peat with silt and sand to organic silt and clay in MN-16-5 at 110 cm (-3.03 m OD) coincides with an upwards coarsening, following which a peak in sand occurs, indicating an increasing depositional energy (Figure 5.21). The variable particle size associated with the organic silt and clay sedimentation may indicate the site was dynamic, with variable tidal influence. The sedimentation shift at 110 cm is associated with the disappearance of salt-intolerant taxa, with brackish epipelic taxa (e.g. *Diploneis didyma*, *Navicula peregrina* and *Tryblionella punctata*) dominating. The dominance of these taxa indicate that the organic silt and clay unit is associated with marine subtidal basins and intertidal mudflats. The decreasing occurrence of *Diploneis interrupta*, a brackish aerophilous taxa indicative of salt marsh environments, after 106 cm, further indicates that the position of the site in the tidal frame is decreasing. The depositional energy and position in the tidal frame from 110 cm (- 3.03 m OD) indicates the existence of an intertidal flat environment.
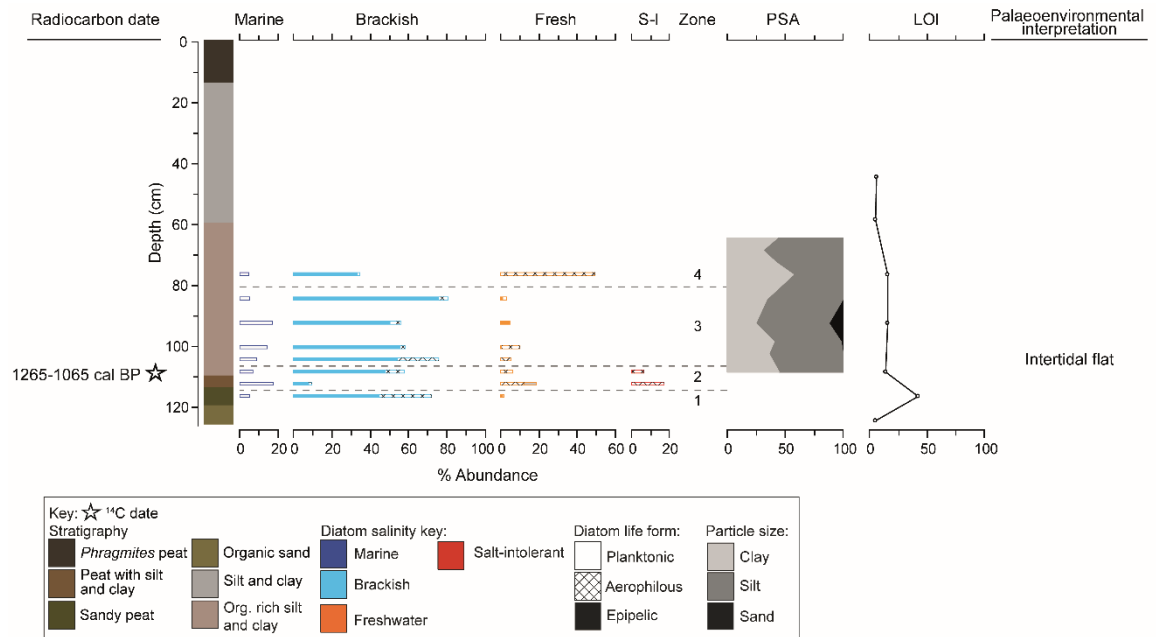
Figure 5.21: Summary diagram of results produced for MN-16-5 with palaeoenvironmental interpretation. Stratigraphy, particle size, organic content and the diatom summary, illustrating changes in salinity and life form, are presented

5.6.4 MN-16-19

A summary of the lithostratigraphic and biostratigraphic results from MN-16-19 are presented in Figure 5.22. Peat sedimentation dominates between 6310 and 1738 cal BP with a transition from minerogenic peat through to wood peat occurring during this time. The diatom taxa associated with initial sedimentation at MN-16-19 are predominantly brackish-freshwater with a subordinate marine planktonic component indicating tidal influence that is potentially marginal. Diatoms were not preserved in the peat (655-515 cm) or wood peat (515-417 cm) unit, which along with the stratigraphic context, indicates a freshwater context located above direct tidal influence.

The sharp decrease in organic content between 422 cm and 406 cm is associated with the transition from well rooted woody peat to organic rich silt at 417cm. This shift in sedimentation is also associated with an increasing dominance of brackish epipelic and marine planktonic diatom taxa, in addition to the freshwater component of the assemblage becoming subordinate. The dominating brackish epipelic taxa (e.g. *Tryblionella navicularis*) are indicative of intertidal to lower supratidal mudflats and creeks, as well as subtidal marine basins and lagoons (Vos and De Wolf, 1988). The onset of organic rich silt sedimentation is associated with a slight upwards coarsening (415 cm and 400 cm), indicating a gradual change in depositional energy. The changes in the diatom

115

assemblage, associated with the sedimentation shift (417 cm; - 5.52 m OD), indicates a high marsh environment which is experiencing increasing tidal influence from 1966-1738 cal BP. The increasing abundance of marine planktonic taxa following the onset of organic rich silt sedimentation at 417 cm indicates tidally influenced hydrodynamic conditions. In addition, the occurrence of these taxa has been linked with tidal inlets opening (Bao et al., 1999; Freitas et al., 2002) as well as barrier breaching (Sáez et al., 2018).
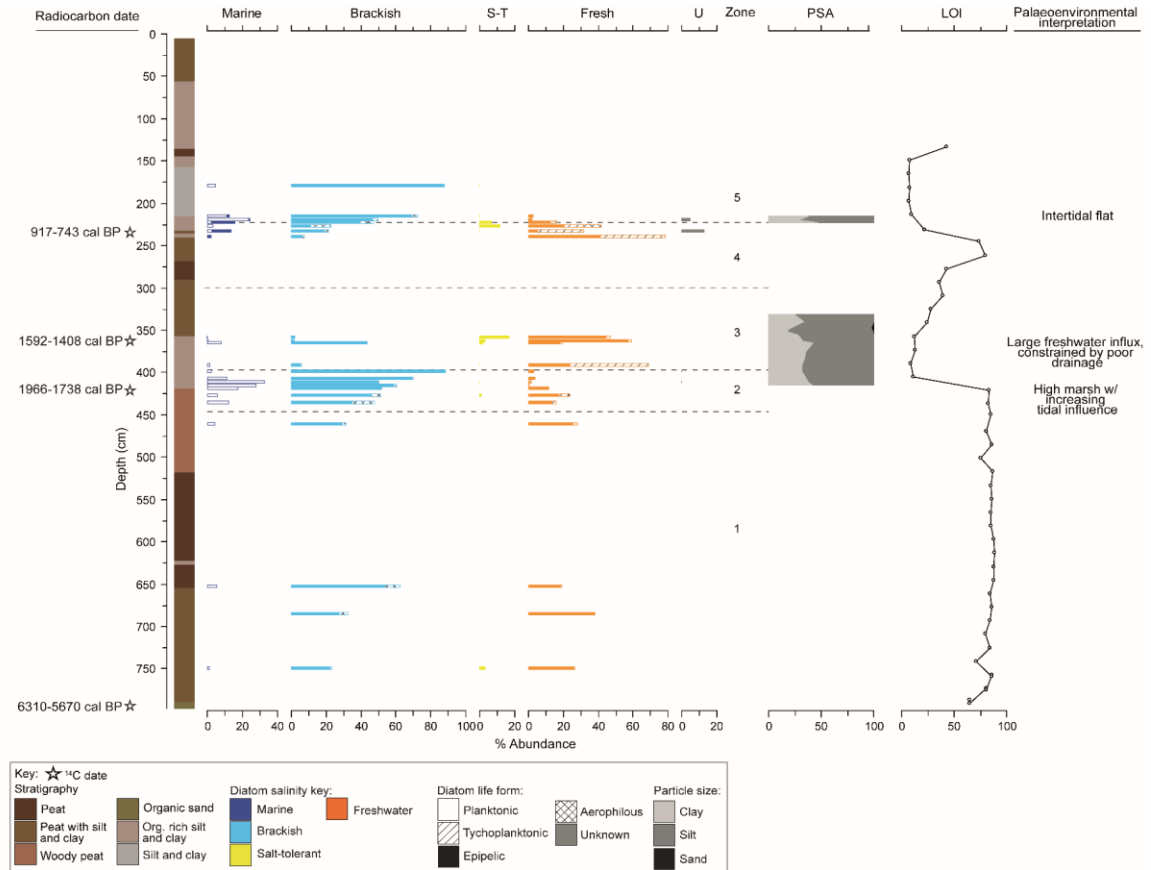
Figure 5.22: Summary diagram of results produced for MN-16-19 with palaeoenvironmental interpretation. Stratigraphy, particle size, organic content and the diatom summary, illustrating changes in salinity and life form, are presented

The onset of organic rich silt sedimentation at 417 cm is initially associated with a brackish epipelic dominated diatom assemblage, however, from 392 cm until 360 cm this sedimentation is dominated by a freshwater epipelic and tychoplanktonic assemblage. Marine planktonic and brackish epipelic taxa are, however, still present in this unit. Freshwater dominated diatom assemblages, which also contain a small brackish component, have been previously associated with shallow lagoon environments with slightly brackish water, low-energy hydrodynamic conditions and aquatic vegetation growth (Bao et al., 1999). The association of a freshwater dominated diatom assemblage

with minerogenic sedimentation is interpreted to indicate a large freshwater influx, constrained by poor drainage.

The transition from *Phragmites* peat with trace of silt and clay to organic clayey silt at 237 cm (- 3.72 m OD) is associated with a changing diatom assemblage. This sedimentation shift coincides with increasing marine planktonic and brackish epipelic taxa in addition to the decline, and eventual disappearance, of freshwater taxa. This shift to a brackish dominated diatom assemblage indicates increasing tidal influence and lowering of the position of the site in the tidal frame. The transition to organic clayey silt sedimentation is also associated with a gradual decline in organic content, with lower values sustained until 150 cm. The changes in diatom assemblage and organic content associated with this sedimentation shift at 237 cm indicate a transition to an intertidal flat environment.

Chapter 6: Results and interpretation- Sizewell Marshes

This chapter presents the results for the Sizewell Marshes, following an overview of changes in coastal configuration and human land use on this section of the Suffolk coast. A description of the site and survey is provided prior to the results, which are subdivided into the lithostratigraphy and sedimentology, biostratigraphy, chronology and resulting palaeoenvironmental interpretation.

6.1 Study area background

The Sizewell Marshes are situated between Minsmere and Aldeburgh, 8 km south of Dunwich, and have national, and international, importance for nature conservation as well as infrastructure. The Sizewell Marshes has been designated a SSSI and AONB for their lowlands and unimproved wet meadows which provide habitats for a wide range of birds, invertebrates and nationally rare plants (Natural England, 2013). One of the UK's largest nuclear power complexes, Sizewell B, and the planned Sizewell C nuclear new build, is also situated on this section of the Suffolk coast (Figure 6.1).

Historical evidence suggests that a considerable settlement existed at Sizewell during the medieval period (Good and Plouviez, 2007). The minutes from the annual Hethewamoot meeting, relating to washed up goods, fishing rights and contracts, between 1378 and 1481 note that significant fishing fleets were present during the 14th and 15th century at Sizewell however boats had to be small enough to be dragged on to the beach (Bailey, 1990). Sizewell is believed to have suffered the same fate as Dunwich, with most of the settlement now lost to the sea by erosion (Good and Plouviez, 2007; Alison Farmer Associates, 2012). Good and Plouviez (2007) note that Leiston Common, situated on the western boundary of Sizewell Marshes, was enclosed at the beginning of the 19th century. A drainage dyke has extended from the Sizewell Marshes northwards to the Minsmere sluice since the early 19th century (Pye and Blott, 2006). Historical maps (e.g. Hodskinson, 1783) indicates a previous link between the Sizewell Marshes and Minsmere, illustrating that the area drained northwards into the broads at Minsmere (Figure 5.2). Sizewell Marshes may have previously drained directly into the sea given the location of this low-lying area however there is no documentary evidence to indicate this (Pye and Blott, 2006).

6.2 Site description and survey

The Sizewell Marshes is comprised of reedbeds and grazing marshes, segmented by drainage dykes and wet woodland, neighbouring forested heathland. Traditional management practices, such as maintaining a high-water table, are still used in the Sizewell Marshes (Williamson, 2005). A narrow, steep shingle bank extends along the coastline at Sizewell and is backed by a narrow belt of dunes (Pye et al., 2007; Alison Farmer Associates, 2012). An artificial clay embankment underlies sections of these dunes on the Sizewell frontage to provide extra flood protection (Pye et al., 2007).
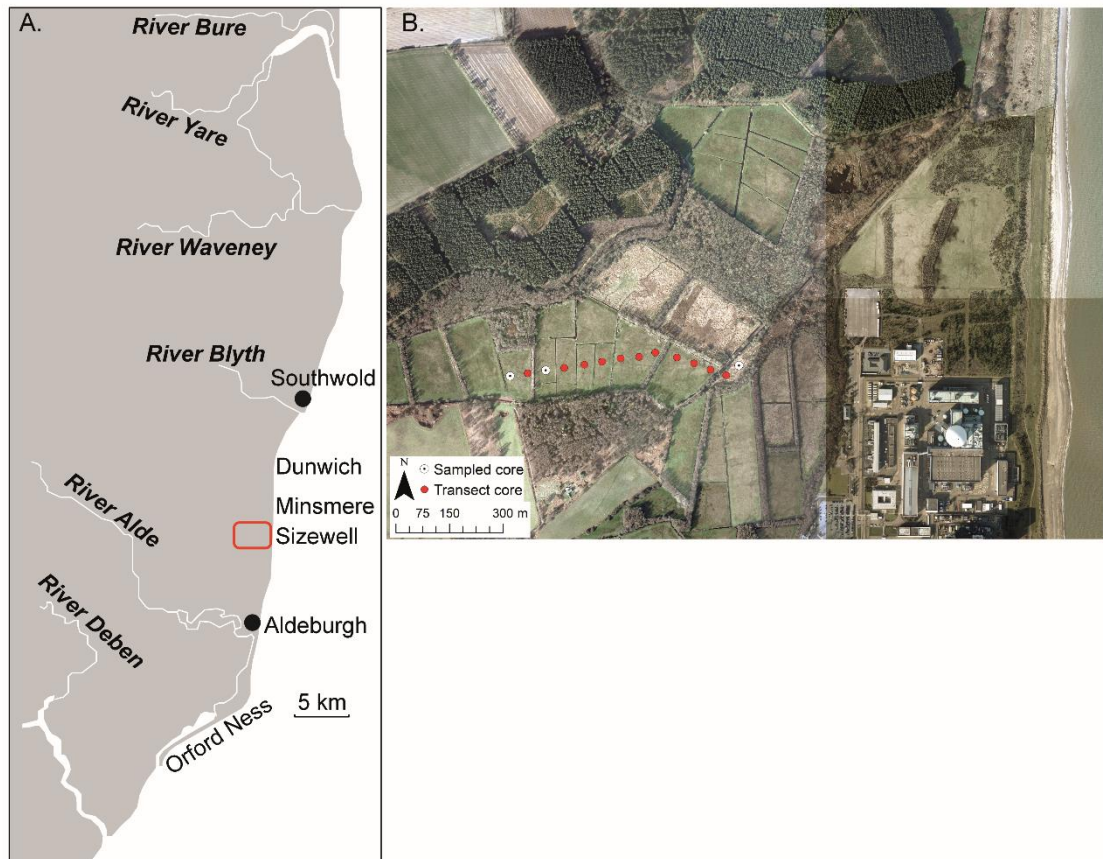
Figure 6.1: A. Suffolk coast with the Sizewell Marshes highlighted in red. B. Stratigraphic transect completed at Sizewell Marshes. The red filled circles represent gouge cores and the white filled circles denote the sediment sequences sampled for analysis. The dome of Sizewell B and nuclear power station complex is visible on the southern portion of the coast. Aerial imagery: © Getmapping Plc.

A transect extending west to east was completed on the grazing marshes and wetland situated behind the Sizewell B complex (Figure 6.1). Proximity to the drainage dykes bisecting the grazing marshes was kept to a minimum, to avoid anthropogenic disturbance to the stratigraphy. The stratigraphy was investigated every 25 m, using a gouge core, and a sample for sedimentological and biostratigraphical analysis was taken using a Russian

corer at the most easterly point in the transect, SW-17-13 (Figure 6.1). Basal peats were sampled at a range of altitudes from SW-17-1, SW-17-3 and SW-17-13 (-2.99 m OD, -4.07 m OD and -6.92 m OD respectively) to constrain the timing of the onset of peat deposition and rising regional ground water level. Additional points, extending northeast from the final point in the transect, were planned pre-fieldwork however this was not possible due to overgrown vegetation and open water from the overflowing drainage channels.

6.3 Lithostratigraphy and sedimentology

Organic sedimentation dominates the stratigraphic transect completed at Sizewell with a band of minerogenic sedimentation occurring in the cores nearest the coast (Figure 6.2). The primary sampled core, SW-17-13, contains six main units outlined in Table 6.1. Sandy peat (600 cm to 570 cm) is overlain by very well rooted woody peat (570 cm to 195 cm), well rooted silty peat (195 cm to 180 cm), silt with variable organic content (180 cm to 161 cm), peat with silt trace (161 cm to 75 cm) and peat with sand (75 cm to 0 cm). Only the top 3 m of the core, in addition the bottom section (530-580 cm) were sampled for analysis due to homogeneity in the peat unit between 577 cm and 305 cm.

Particle size analysis was completed for nine samples, at a resolution of 4 cm, in the minerogenic units between 195 cm and 161 cm (Figure 6.3). The clay and silt fraction is variable, with dominance fluctuating between these fractions in the samples analysed. End-member mixing analysis could not be completed for the sampled sequence due to the AnalySize software requiring over 10 samples to ensure geological context (Weltje and Prins, 2007; Paterson and Heslop, 2015).

The SW-17-13 sediments plot in, and on the boundary of, the graphic sedimentary domain associated with environments ranging from open to filled estuary (Figure 6.4) according to Tanner (1991a; 1991b) Lario et al. (2002). The samples analysed are poorly sorted with a mean particle size in the fine silt fraction.

The organic content was determined for 15 samples at a 16 cm resolution (Figure 6.3). The organic content remains stable, exceeding 70 % between 289 cm and 209 cm. The organic content decreases to 16 % at 177cm and with low values sustained until 161 cm, after which it increases gradually to 70 % by 145 cm. Organic content of ~ 70 % occurs between 145 cm and 97 cm after which it begins to decrease due to the presence of sand from 81 cm.
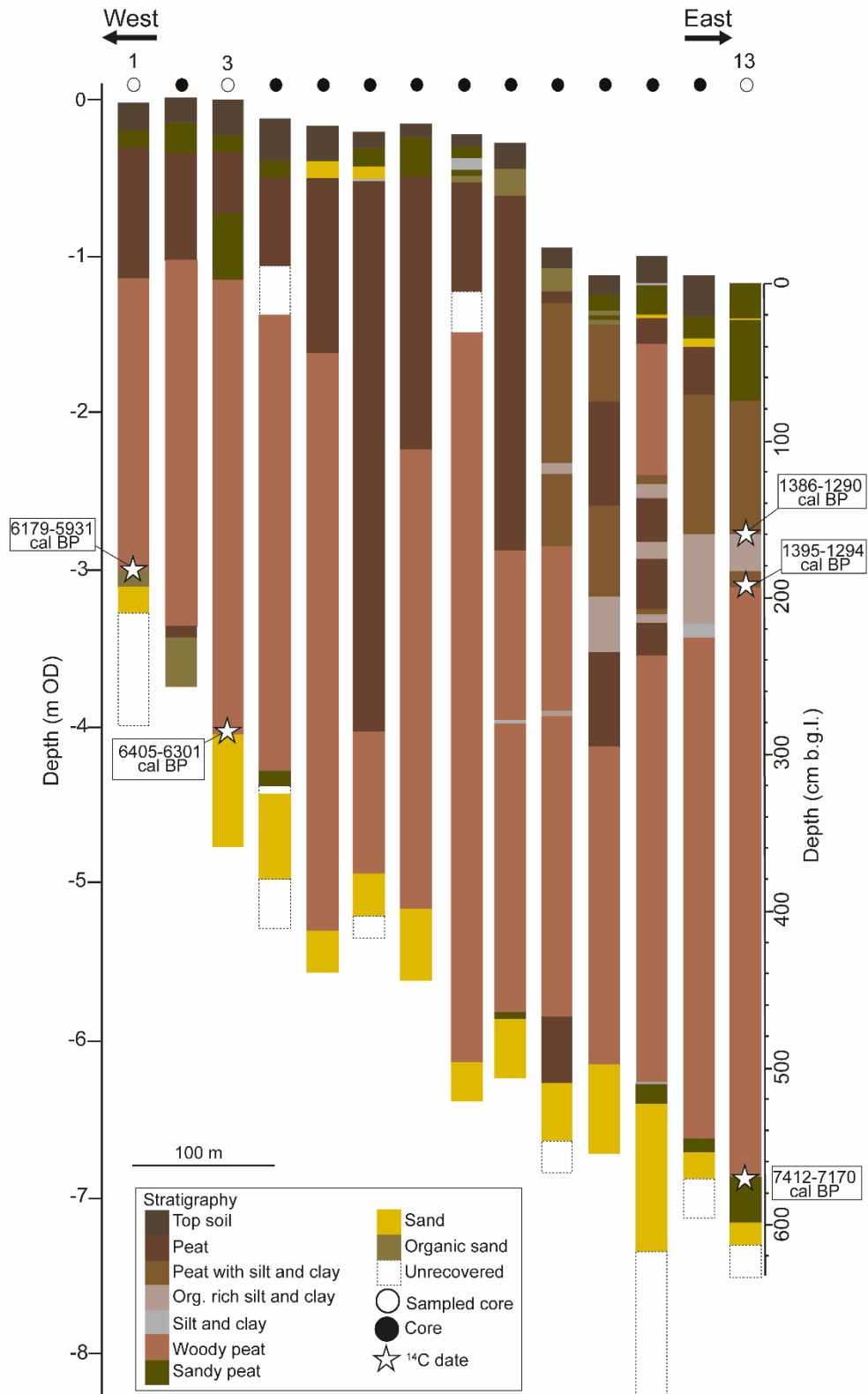
Figure 6.2: Stratigraphic transect completed at Sizewell Marshes, with associated radiocarbon dates for sampled sediment sequences. See Figure 6.1 for the location of Sizewell Marshes and the stratigraphic transect, in relation to other sections of the coastline. The depth (cm) below ground level is provided for the primary sampled sediment sequence, SW-17-13.

Table 6.1: Description of main sediment units identified in SW-17-13 and associated Troels-Smith (1955) *classification.*

Unit depth (cm)	Description	Troels-Smith log
0-75	Peat with rootlets, irregular wood and sand trace.	Sh3+ Th^{0}1 Th$^{0\ phrag}$ + Dl+ Gmin+ nig 3 strat 0 sicc 3 elas 0
75-161	Peat with rootlets, *Phragmites* rhizomes, irregular wood and silt trace.	Sh2+ Th^{1}1 Th^{phrag}1 Ag+ Th$^{0\ phrag}$+ nig 3+ strat 0 elas 0 sicc 3 lm 0
161-180	Silt with rootlets and *Phragmites* rhizomes throughout.	Ag3+ Sh+ Th^{1}1 Th$^{1\ phrag}$+ nig 2+ strat 0 sicc 3 elas 0 lm 3
180-195	Well rooted silty peat with *Phragmites* rhizomes.	Sh2+ Ag1 Th^{1}1+ Th$^{2\ phrag}$+ nig 3 strat 0 sicc 3 elas 0 lm 1/2
195-570	Peat with rootlets, *Phragmites* rhizomes and wood.	Sh3 Th^{2}1 Th^{0phrag}+ Dl+ nig 3++ strat 0 sicc 2 elas 0 lm.sup 0
570-600	Well humified peat with trace of sand and irregular rootlets.	Sh4 Th^2+ Gmin+ nig 4 strat 0 sicc 1 elas 0 lm 0

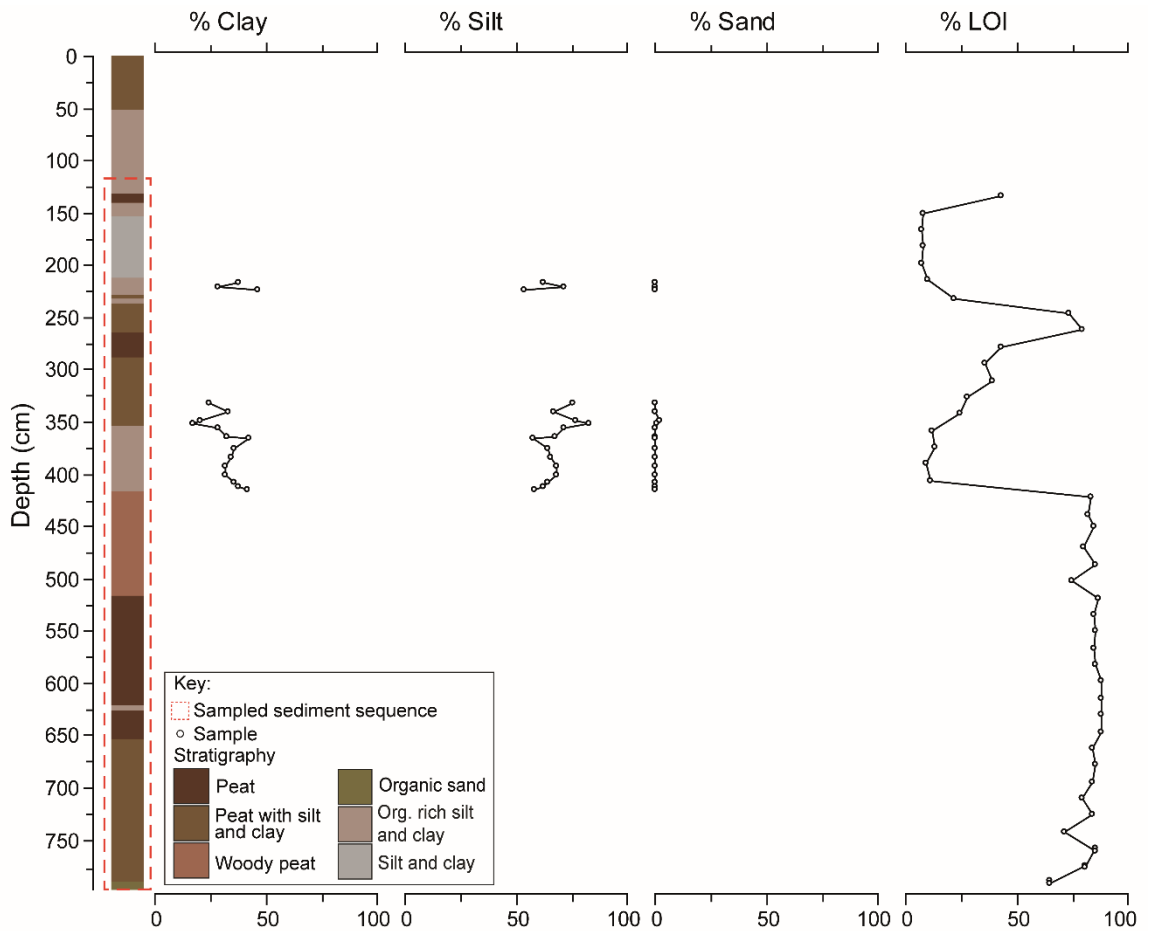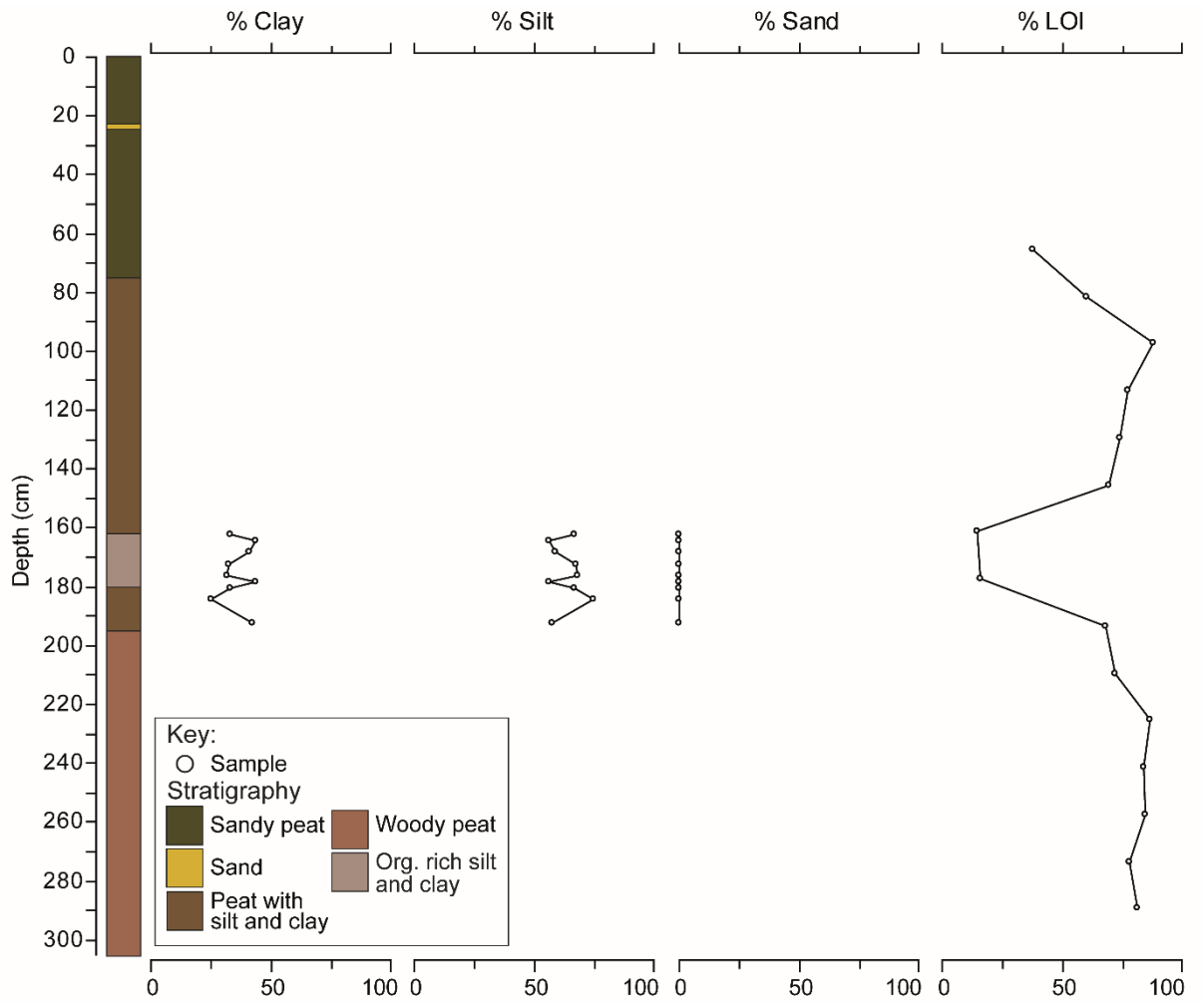*Figure 6.3: Stratigraphy, particle size and LOI for SW-17-13. The boundaries for the clay, silt and sand fraction are defined by* Wentworth (1922).
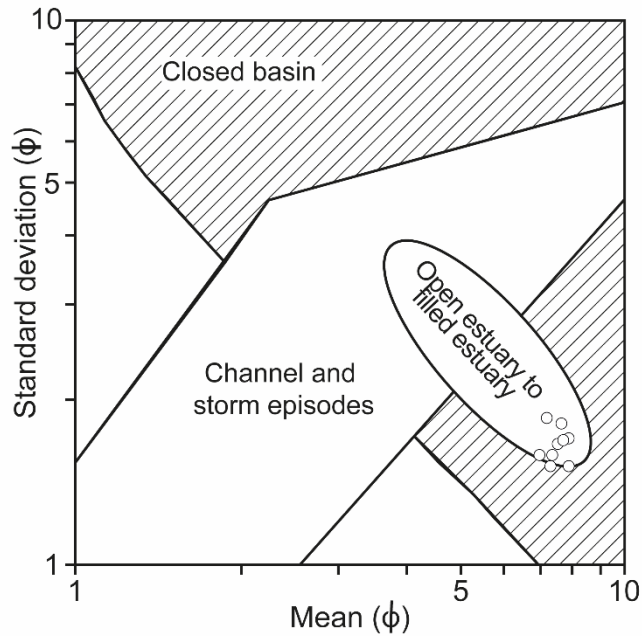
Figure 6.4: Bivariate plot of mean against standard deviation (phi) for SW-17-13. The graphic sedimentary domains determined by Tanner (1991a; 1991b)*, and later modified by* Lario et al. (2002) *are overlain onto this plot. Permission to reproduce this figure has been granted by Elsevier.*

6.4 Biostratigraphy

Diatoms were not preserved in the sampled core from Sizewell therefore foraminifera were counted, resulting in the identification of five agglutinated taxa in 10 samples (Figure 6.5). Up to 140 tests were counted per sample, with raw counts presented in Appendix 17. The foraminiferal assemblage is divided into four zones based on visual inspection of the clear changes in dominant taxa: Zone 1 (305 cm to 225 cm), Zone 2 (225 cm to 272.5 cm), Zone 3 (172.5 cm to 122 cm) and Zone 4 (122 cm to 0 cm).

Jadammina macrescens is dominant throughout SW-17-13. The single sample of Zone 1 (271 cm) is comprised entirely of *Jadammina macrescens*. No foraminifera were present in the sample counted at 231 cm in Zone 1. The dominant species in Zone 2 varies between *Jadammina macrescens* and *Miliammina fusca*, which peak at 80 % and 57 % respectively. *Trochammina inflata* and *Haplophragmoides spp* are also present, peaking at 15 % and 16 % respectively. Zone 3 is dominated by *Jadammina macrescens,* which exceeds 80 % of the total count. *Haplophragmoides spp* is also present in Zone 3, along with subordinate components of *Miliammina fusca* and *Trochammina inflata*. No foraminifera were present in a sample at 125 cm. *Jadammina macrescens* exceeds 78 % of the total count of Zone 4, whilst *Trochommina inflata* increases to 17 % of the total count.
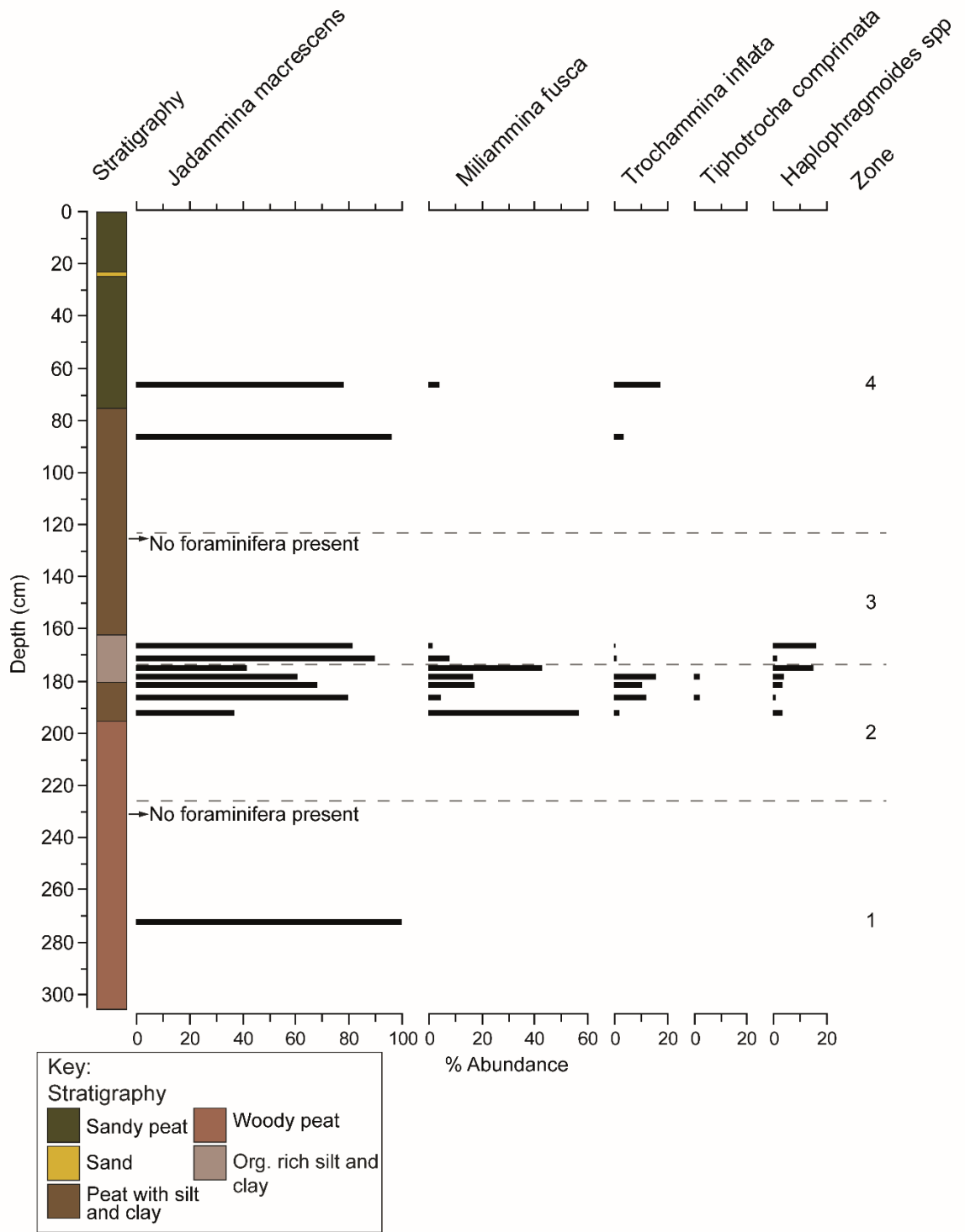
Figure 6.5: Foraminifera assemblage for SW-17-13.

6.5 Chronology

All radiocarbon samples from the Sizewell Marshes (Table 6.2, Figure 6.2) were analysed at the NERC Radiocarbon Facility, East Kilbride (Allocation number: 2112.0418). Basal samples comprising plant macrofossils and twig (SW-17-1) and plant macrofossils (SW-17-3 and SW-17-13) were submitted for AMS radiocarbon dating. Foraminifera were not

present at the base of SW-17-1, SW-17-3 and SW-17-13 therefore the radiocarbon dates are freshwater limiting. The onset of peat deposition is constrained to 6179-5931 cal BP (Laboratory code: SUERC-80965), 6405-6301 cal BP (Laboratory code: UCIAMS-210609) and 7412-7170 cal BP (Laboratory code: SUERC-80968) at the base of SW-17-1, SW-17-3 and SW-17-13 respectively.

The timing of the shift from very well rooted peat to well rooted silty peat at 195 cm (-3.12 m OD) and disappearance of foraminifera in SW-17-13 was constrained using AMS radiocarbon dating. Plant macrofossils and seeds sampled at 195.5 cm (-3.13 m OD) were submitted and dating this transition to 1395-1294 cal BP (Laboratory code: SUERC-80967).

Foraminiferal analysis across the transition from well-rooted silt to *Phragmites* rich peat at 161 cm (SW-17-13 -2.78 m OD) identified the presence of agglutinated species with *Jadammina macrescens* dominating. Plant macrofossils were sampled at 159.5 cm (-2.77 m OD), dating this shift to organic sedimentation to 1386-1290 cal BP (Laboratory code: SUERC-80966).

Table 6.2: AMS radiocarbon dates produced for the Sizewell Marshes. All samples were radiocarbon dated at NERC Radiocarbon Facility, East Kilbride (Allocation number: 2112.0418).

Site	Sample ID	Laboratory code	^{14}C ± 1σ BP	Cal age (cal BP)- 2σ range	
				Max	Min.
	SW-17/1 -2.99 m OD	SUERC-80965	5263 ± 38	6179	5931
	SW-17/13 -2.77 m OD	SUERC-80966	1431 ± 37	1386	1290
Sizewell	SW-17/13 -3.13 m OD	SUERC-80967	1444 ± 37	1395	1294
	SW-17/13 -6.92 m OD	SUERC-80968	6339 ± 35	7412	7170
	SW 17/3 -4.07 m OD	UCIAMS-210609	5570 ± 30	6405	6301

6.6 Palaeoenvironmental interpretation

A summary of the lithostratigraphic and biostratigraphic results from the Sizewell Marshes core are presented in Figure 6.6. The occurrence and disappearance of foraminifera recorded in the sediment sequence sampled at SW-17-13 records increases and decreases in marine influence at this site. The five agglutinated species identified are indicative of either a saltmarsh or brackish lagoon environment, commonly dominating high to mid- marsh environments throughout the UK, whilst *Miliammina fusca* is also present in low marsh environments (e.g. Horton et al., 1999; Lloyd and Evans, 2002; Horton and Edwards, 2005; Massey et al., 2006). At 191.5 cm (-3.09 m OD), 3.5 cm above the transition from very well-rooted peat to well-rooted silty peat, *Jadammina macrescens* and *Miliammina fusca* dominate the foraminifera assemblage, remaining abundant throughout the well-rooted silt unit (190 cm to 161 cm). Samples nearest the regressive contact (161

cm) are predominantly comprised of *Jadammina macrescens* (exceeding 80 % of the total count). The dominance of this species is indicative of a position near to High Water Extreme Spring Tide, a narrow zone identified as the best palaeo sea-level indicator (Scott and Medioli, 1978). Only agglutinated taxa, associated with the highest portion of the intertidal zone, occur in SW-17-13 between 1395-1294 cal BP and 1386-1290 cal BP, indicating marginal tidal influence. Minerogenic sediments only occurred in the section of the stratigraphic transect closest to the coast whilst analysed samples plot close to, or on, the boundary between the open to filled estuary and closed basin sedimentary domains of the bivariate plot, also suggesting that tidal influence was variable.

A prolonged period of peat sedimentation dominates the stratigraphic transect completed indicating that this section of the coastline was stable, and the back-barrier environments protected, during the Holocene. The lithostratigraphic evidence is strongly indicative of predominantly *Phragmites* marsh with occurrence of wood suggesting fen carr environment. The isolated occurrences of high-marsh foraminifera, predominantly *Jadammina macrescens*, in the organic rich units of SW-17-13 (Zone 1 and 4 of the foraminifera assemblage) are therefore interpreted as more isolated irregular periods of tidal inundation associated with the highest tidal levels.

A stratigraphically comparable sediment sequence was sampled by Lloyd et al. (2008) ~ 1 km northeast of SW-17-13 at Goose Hill (Appendix 1). Organic rich clay sedimentation, between 2470-2330 cal BP and 1820-1600 cal BP at Goose Hill (GH08-04) was associated with a foraminifera assemblage dominated by *Miliammina fusca*. The dominance of this mid- to lower marsh foraminifera indicates that Goose Hill, situated north-northeast of SW-17-13, was lower in the intertidal zone during part of the late Holocene than SW-17-13. The shift to organic clay sedimentation at Goose Hill predates the transition recorded at SW-17-13.

The dominance of peat sedimentation in the Sizewell Marshes transect and high-marsh foraminifera in the SW-17-13 core indicate that the coastal barrier has been stable in this location since 7412-7170 cal BP and that tidal influence was marginal to this section of the Suffolk coast. The onset of quiet water conditions at Goose Hill from 2470-2330 cal BP were interpreted by Lloyd et al. (2008) as indicating that the source of marine inundation was further north and that tidal influence had penetrated southwards behind the barrier system, rather than inundation by barrier breach at Sizewell. The results presented from the Sizewell Marshes as part of this thesis support the interpretation made by Lloyd et al. (2008), that tidal influence originated from further north and migrated behind the coastal barrier rather than breaching through it.
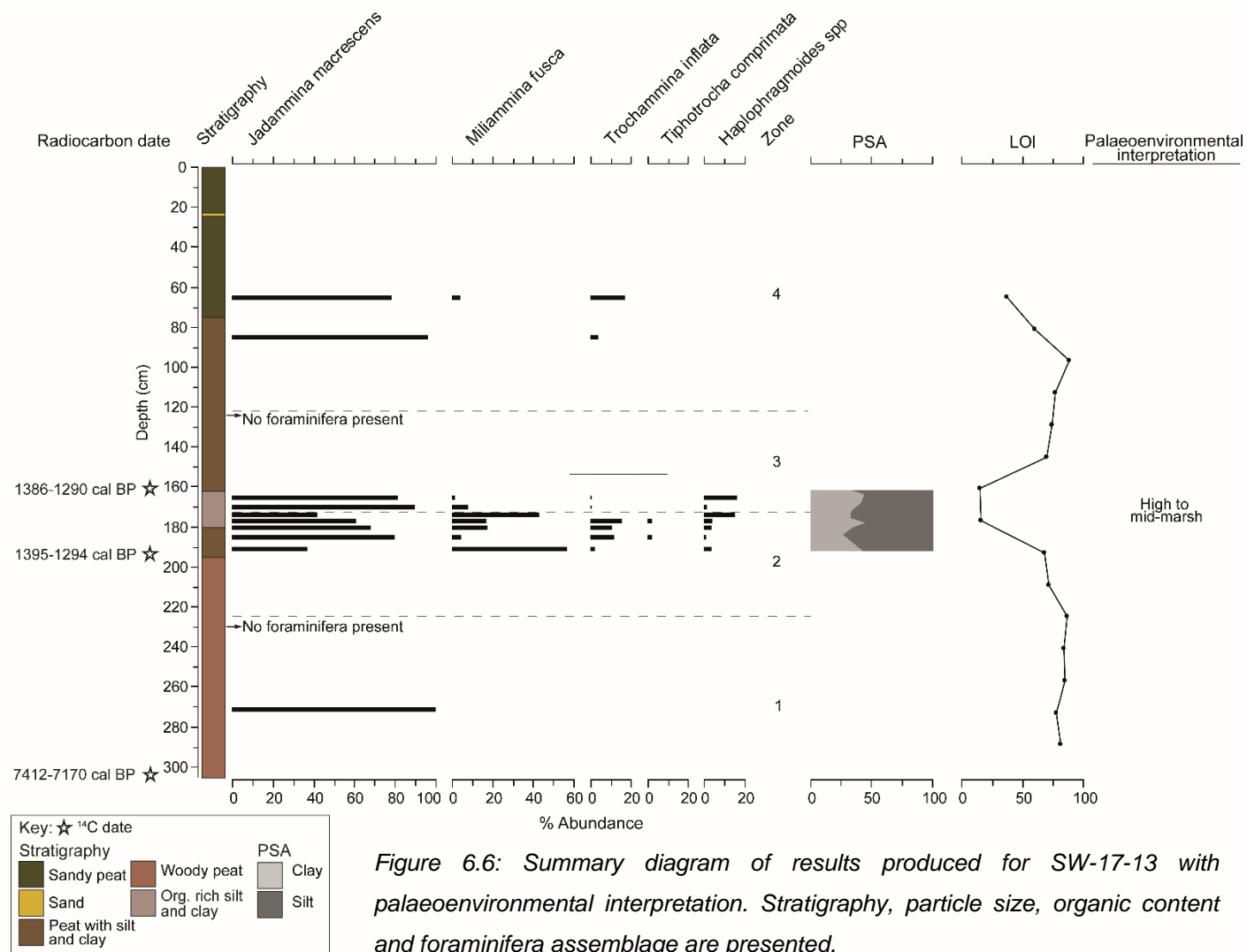
Figure 6.6: Summary diagram of results produced for SW-17-13 with palaeoenvironmental interpretation. Stratigraphy, particle size, organic content and foraminifera assemblage are presented.

128

Chapter 7: Synthesis

This chapter initially integrates the results presented for Walberswick NNR (Chapter 4), Minsmere (Chapter 5) and Sizewell (Chapter 6). The new sea-level index points resulting from this thesis are presented, with comparison made to the existing data and GIA model predictions of RSL change for the region. Consideration is given to the mechanisms driving Holocene coastal evolution which are then evaluated with respect to the influence of RSL change, sediment supply and barrier dynamics.

7.1 Comparison of new Holocene palaeoenvironmental records for Suffolk

The sediment sequences sampled from each of the five sites investigated are shown in Figure 7.1. Changes in sediment type with depth are given in both m OD and cm below ground level (b.g.l.) to enable inter-site comparisons of the sedimentation patterns and altitude of the main stratigraphic changes. Figure 7.2 provides a timeline of the main changes identified by bio- and litho-stratigraphic analyses and determined by AMS radiocarbon dating to investigate inter-site variability in the timing of stratigraphic and biostratigraphic changes.

7.1.1 Comparison of sedimentation patterns and associated palaeoenvironments

Figure 7.1 highlights the variable Holocene sedimentation pattern that occurs in a 15 km section of the Suffolk coast for the five sites investigated, indicating the influence of local factors. Transects investigated at Westwood Marsh, Oldtown Marsh and Great Dingle Hill were completed proximal (~ 2 km) to each other. Despite this, the resulting sediment sequences reveal very different patterns of sedimentation. Peat sedimentation dominates the sediment sequence sampled from Westwood Marsh (WM-15-6), with a unit comprised of silty clay, indicative of intertidal mudflats dominating the upper half. In contrast, an intercalated sequence of organic and minerogenic units occurs at Oldtown Marsh (OTM-16-13) whilst minerogenic sedimentation is dominant at Great Dingle Hill (GDH-16-2). The sediment sequence from Great Dingle Hill (GDH-16-2) is comparable to other sequences sampled close to the coast (MN-16-1, MN-16-2, MN-16-3, MN-16-5). The pattern of alternating organic and minerogenic sedimentation, associated with intertidal and freshwater environments, separated by transitional saltmarsh deposits, at Oldtown Marsh (OTM 16-13) is comparable to the inland sequence sampled at Minsmere (MN-16-19). Both sediment sequences are comprised of three phases of peat sedimentation separated by minerogenic units indicative of intertidal environments. In contrast, further south, at Sizewell peat sedimentation dominates, with the occurrence of a band of minerogenic sedimentation, indicative of a high- to mid-marsh environment, occurring only in the cores nearest the coast. The influence of proximity to the coast, for example, is evident from the

sediment sequences sampled at Minsmere. The transect evidences the migration of tidal environments landwards, with minerogenic sedimentation associated with intertidal flats environment nearest the coast and shallow lagoon environments inland.
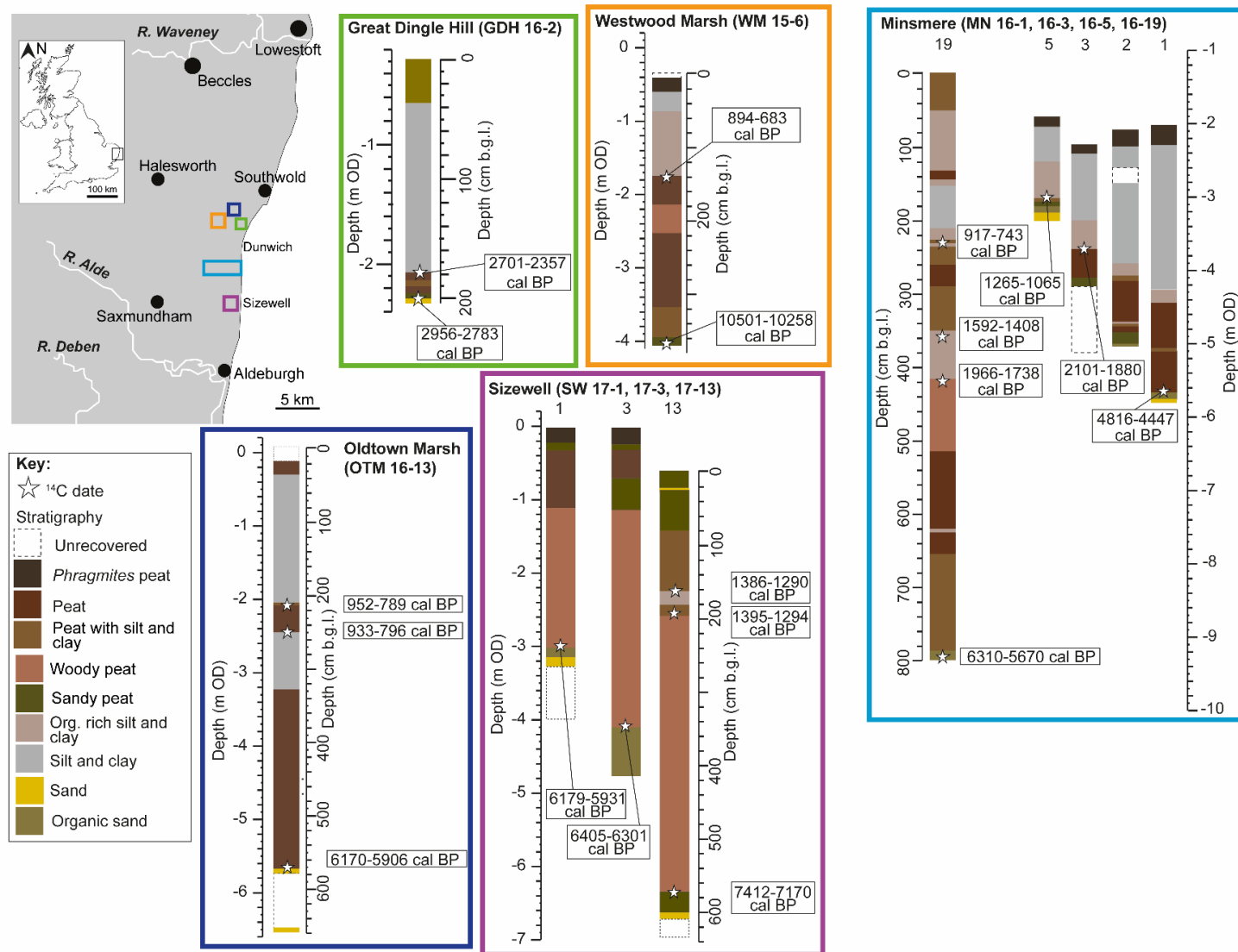
Figure 7.1: Sampled sediment sequences from sites investigated as part of this thesis, with radiocarbon dates constraining the onset of peat deposition or changes in sea-level tendency determined from bio- and litho-stratigraphic analysis. Sample depth is provided in m OD and cm below ground level (b.g.l.). The full results for each site, including the complete sediment transect, is presented in Chapters 4 (Westwood Marsh, Oldtown Marsh and Great Dingle Hill), 5 (Minsmere) and 6 (Sizewell).

7.1.2 Comparison of chronology and altitude for main stratigraphic changes

A chronological, inter-site comparison of the litho- and bio-stratigraphic changes is presented in Figure 7.2, demonstrating clear chronological coincidence, as well as difference, between the sites. A comparison of the altitude (m OD) of each chronologically constrained data point is illustrated in Figure 7.3. Samples from Minsmere and Sizewell constraining the timing of changes in sea-level tendency are consistently altitudinally lower than changes from the other sites. The sediment records from Minsmere (8 m) and Sizewell (6 m) contain peat deposits up to 2 m and 4 m thick respectively, and the intercalated nature of these sequences, in addition to the thickness of the peat deposits, makes them more susceptible to post-depositional lowering (Jelgersma, 1961; Kaye and Baghoorn, 1964; Shennan and Horton, 2002; Horton et al., 2013).

The onset of peat deposition and rising regional ground water level at Oldtown Marsh (OTM-16-13) at 6170-5906 cal BP is similar in timing to the onset of peat accumulation at Minsmere (MN-16-19) and Sizewell (SW-17-1, SW-17-3) dated to 6310-5670 cal BP (MN 16-19), 6179-5931 cal BP (SW-17-1) and 6405-6301 cal BP (SW-17-3) (Figure 7.2.). Despite their chronological coincidence, the altitudinal position for the onset of peat accumulation is very different between these sites, occurring at -9.28 m OD (MN-16-19), -2.99 m OD (SW-17-1), -4.07 m OD (SW-17-3) and -5.64 m OD (OTM-16-13). Inland at Sizewell (SW-17-13) and at Westwood Marsh (WM-15-6) peat sedimentation pre-dates these sites, beginning at 7412-7170 cal BP and 10501-10258 cal BP respectively.

In the minerogenic-dominated cores situated nearest the coast, the onset of peat deposition and rising regional ground water level is dated to 4816-4447 cal BP (MN-16-1) and 2956-2783 cal BP (GDH-16-2). A transition from sandy peat to silty clay, associated with an increase in marine planktonic diatom taxa, occurs at Great Dingle Hill at 2701-2357 cal BP (- 2.09 m OD). There is, however, no litho- or bio-stratigraphic evidence of such an event at neighbouring sites (OTM-16-13 and WM-15-6) or at other sites proximal to the coast (e.g. MN-16-1, MN-16-3, MN-16-5). At Minsmere, the onset of silt and clay sedimentation near the coast post-dates the similar transition at Great Dingle Hill, occurring at 2101-1880 cal BP and 1265-1065 cal BP for MN-16-3 and MN-16-5 respectively.

The stratigraphic changes between c. 2000 and 1000 cal BP vary between sites (Figure 7.2). Isolated transitions from organic to minerogenic sedimentation, and vice-versa, are recorded in the stratigraphic sequence from several sites with limited chronological overlap.
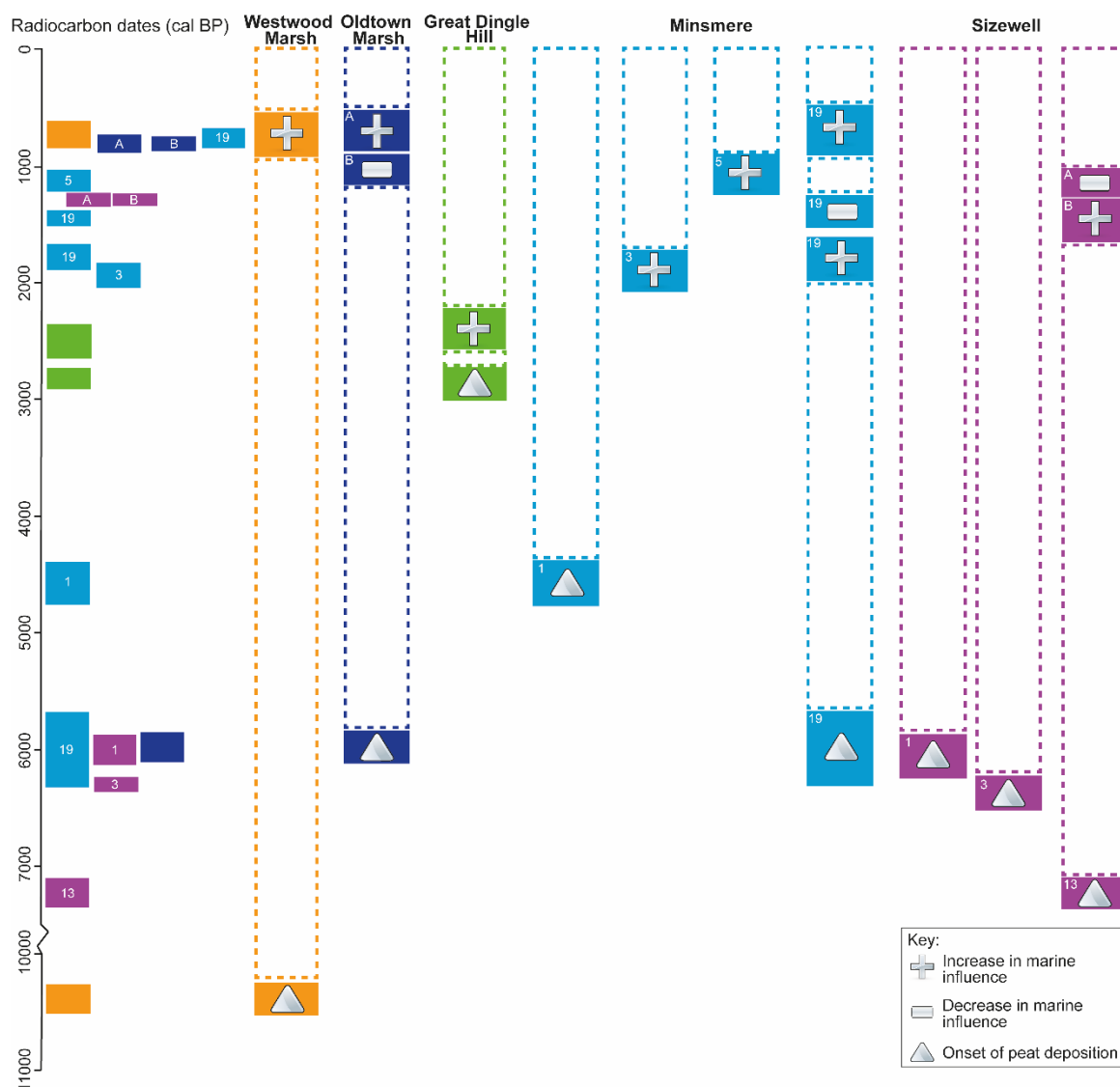
Figure 7.2: A chronological, between site, comparison of the dated litho- and bio-stratigraphic changes. The coloured bars for the radiocarbon dates are site specific, i.e. dates for Westwood Marsh are represented by orange boxes, with numbers added for sites were multiple cores were sampled.

Organic sedimentation dominants the Holocene sequence further south at Sizewell until 1395-1294 cal BP (- 3.13 m OD) when a short-lived phase of organic-rich silt sedimentation occurs until 1386-1290 cal BP (- 2.77 m OD). Coinciding transitions, from organic to minerogenic sedimentation, associated with an increase in marine planktonic and brackish epieplic diatom taxa, occur at Westwood Marsh, Oldtown Marsh and Minsmere, dated to 894-683 cal BP (WM-15-6), 952-789 cal BP (OTM-16-13) and 917-743 cal BP (MN-16-

19). The altitude of the organic to minerogenic transition varies across these sites, despite chronological coincidence (WM-15-6 -1.77 m OD; OTM-16-13 -2.03 m OD; and MN-16-19 -3.63 m OD).
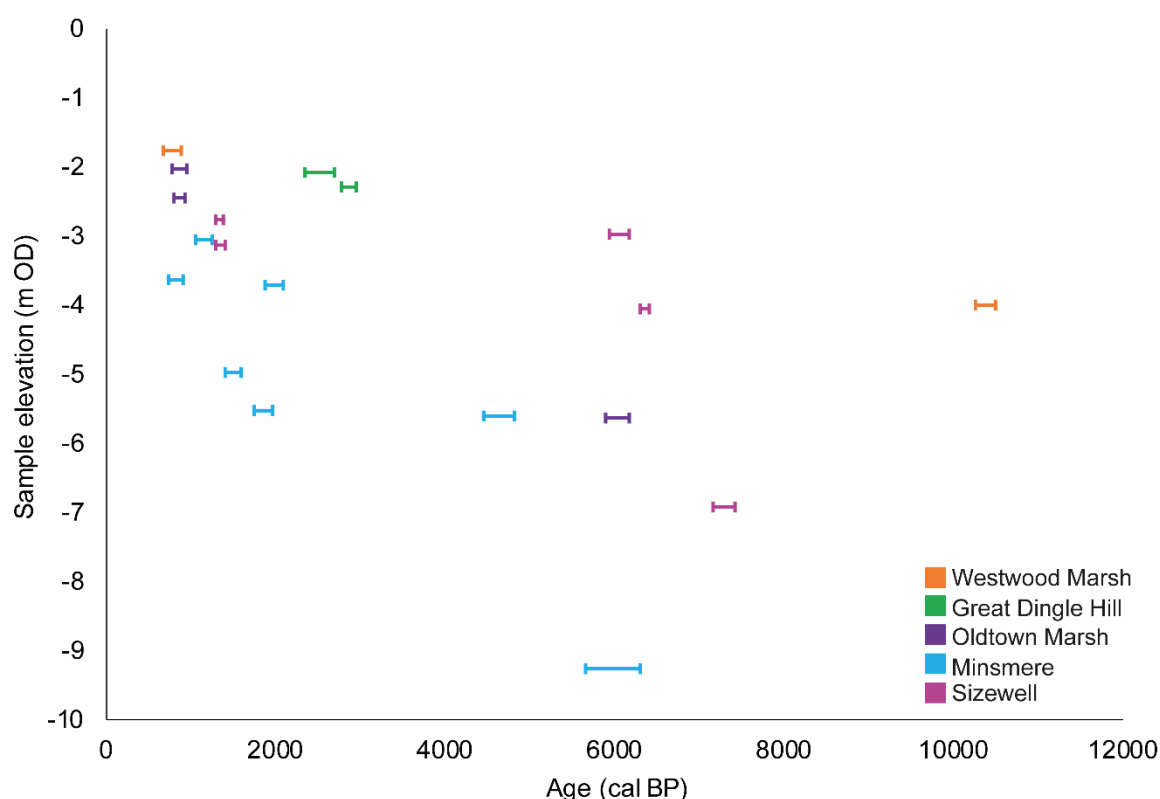
Figure 7.3: Altitudinal comparison of the sample elevation (m OD) of the AMS radiocarbon dated samples from Westwood Marsh, Oldtown Marsh, Great Dingle Hill, Minsmere and Sizewell.

7.2 RSL change

7.2.1 Reconstructions of changes in RSL from Suffolk

Changes in sea-level tendency, i.e. increases (positive tendency) or decreases (negative) in marine influence, were determined from bio- and lithostratigraphic analysis of AMS radiocarbon dated intercalated peat samples, outlined in Chapters 4, 5 and 6. These changes in tendency indicate that palaeo sea level may have controlled the origin of these intercalated peat samples. Basal peats, in addition to the intercalated peat samples, can be used to estimate vertical movements in RSL by producing sea-level index points, outlined below. This section will make comparisons with the regional dataset and GIA model predictions to evaluate if the identified changes in sea-level tendency formed due to RSL change. The horizontal and vertical errors associated with reconstructing changes in RSL are also considered.

The sea-level index point attributes from this study (location, age, elevation and tendency) are outlined for each sea-level indicator in Table 7.1. Changes in tendency will be considered in order to evaluate the new RSL data (e.g. Shennan, 1986; Long, 1992; Shennan et al., 2018). A consistent direction of sea-level tendency should be recorded over a wider area and be greater than local significance if RSL change is the driving mechanism of coastal evolution at a time and location (Shennan, 1986; Shennan et al., 2018). The elevation attribute, termed the indicative meaning, is the vertical relationship between a chosen contemporaneous tide level and a dated sea-level indicator, determined by the present day vertical tidal range over which a sea-level indicator occurs (indicative range), measured relative to an assigned tide level (reference water level) (Shennan, 1986; 2015; van de Plassche, 1986; Horton et al., 2013). Chapter 2 provides further information relating to the indicative meaning.

Freshwater peat samples that do not show a direct relationship to a contemporaneous tide level cannot be used as sea-level index points to reconstruct the altitude of RSL in the past (Brooks and Edwards, 2006; Shennan et al., 2018). However, these samples can be used as freshwater limiting data, as they must have formed above the upper limit of marine influence, indicating that local RSL was below the elevation at which they are found at the time of deposition (Brooks and Edwards, 2006; Shennan et al., 2018). Freshwater peat samples which do not show a direct relationship with a contemporaneous tide level are assigned a reference water level of (MTL + HAT)/2 here (Shennan et al., 2018). The indicative meaning of basal peats that accumulated when conditions were more saline, such as GDH-16-2 -2.29 m OD, can be far better constrained. The reference water level therefore for this sample is MHWST + 0.2 m (Brooks and Edwards, 2006).

Increases in marine influence (positive sea-level tendency) recorded in the diatom and, or, foraminifera assemblage for each site are associated with a shift from organic to minerogenic sedimentation (Table 7.1 and 7.2). These transitions from herbaceous or *Phragmites* peat to tidal marsh deposits are associated with a reference water level of MHWST – 0.2 m (Shennan, 1986; Brooks and Edwards, 2006; Shennan et al., 2018). Reductions in marine influence (negative sea-level tendency) were recorded at Oldtown Marsh, Minsmere and Sizewell as a transition from minerogenic to organic sedimentation, and the absence of foraminifera and, or, dominance of freshwater diatoms. The shift to woody peat sedimentation at Oldtown Marsh (OTM 16-13 -2.45 m OD) is associated with the occurrence of foraminifera. This high to freshwater marsh transition from wood peat to tidal marsh deposits is indicative of a M[1] reference water level (Shennan et al., 2018). The shift from organic silt sedimentation to peat with silt and clay inland at Minsmere (MN 16-19 -4.98 m OD) is associated with a transition from a brackish and marine dominated

diatom assemblage to freshwater dominated one, and is associated with a reference water level of MHWST + 0.6 m (Brooks and Edwards, 2006). The onset of *Phragmites* peat with irregular wood at Sizewell (SW 17-13 -2.77 m OD) and occurrence of foraminifera indicates a reference water level of M^1- 0.2 m, determined by the transition from tidal marsh deposit to *Phragmites* peat (Shennan, 1986; Shennan et al., 2018).

The sea-level index points and freshwater limiting data produced for the sites investigated cover the last c. 10500 cal BP (Table 7.2, Figure 7.4). Freshwater limiting data for the early and mid-Holocene constrain the position of RSL below an altitude at a given time. Freshwater limiting data from Minsmere (MN-16-19), Oldtown Marsh and Sizewell (SW-17-1 and SW-17-3) overlap chronologically despite altitude dissimilarity, at -9.97 m OD, -6.63 m OD and -3.68 m OD respectively, raising questions relating to their validity which are discussed in section 7.2.3. The sea-level index points extending from 3000 to 750 cal BP are all based on intercalated peat samples, except for the basal sample from Great Dingle Hill (2956-2783 cal BP; -3.49 m). The elevation of the index points ranges from -6.58 to -2.83 m for this c. 2000 yr period, providing inconsistent evidence of the changes in RSL during the late Holocene (Figure 7.4). For example, two intercalated index points from Oldtown Marsh (OTM-16-13) record a positive sea-level tendency at -2.83 m for 952-789 cal BP and a negative sea-level tendency at -3.64 m for 933-796 cal BP. In the following sections consideration will be given to the influence of local factors on Holocene sedimentation, and comparisons made with sea-level index points from East Anglia and GIA model predictions of RSL in order to determine the suitability and validity of the RSL data presented in Figure 7.4.

Table 7.1: Sea-level index point attributes for Great Dingle Hill (GDH), Oldtown Marsh (OTM), Westwood Marsh (WM), Minsmere (MN) and Sizewell (SW). The reference water level (RWL) is given as a mathematical expression of tidal parameters ± an indicative difference. The tidal parameters include mean high water spring tide (MHWST), mean tide level (MTL), highest astronomical tide (HAT) and M^1 ((MHWST+HAT)/2). The indicative range (IR) is the most probable vertical range in which the sample formed. All ^{14}C ± 1σ dates are calibrated using Calib 7.1 (Stuiver et al., 2018), using the 95 % confidence limits. The radiocarbon date for MN-16-19 -9.28 m OD is based on a bulk peat sample therefore a 'bulk error' of ± 100 ^{14}C is included for this sample (Hu, 2010; Hijma et al., 2015).

| Sample ID | Location | | | | Age | | | Tendency | Elevation | |
	Site	Latitude	Longtitude		Radiocarbon age ± 1σ (^{14}C BP)	Calibrated radiocarbon age (cal BP)			RWL (m)	IR (± m)
GDH-16-2 -2.09 m OD	Great Dingle Hill	52°18'0.00"N	1°38'34.00"E		2440 ± 35	2701	2357	+	MHWST-0.2	0.2
GDH-16-2 -2.29 m OD	Great Dingle Hill	52°18'0.00"N	1°38'34.00"E		2775 ± 37	2956	2783	B	MHWST+0.2	0.8
OTM-16-13 -2.03 m OD	Oldtown Marsh	52°18'22.80"N	1°38'43.50"E		965 ± 39	952	789	+	MHWST-0.2	0.2
OTM-16-13 -5.64 m OD	Oldtown Marsh	52°18'22.80"N	1°38'43.50"E		5209 ± 35	6170	5906	B	(MTL+HAT)/2	(MTL to HAT)/2
OTM-16-13 -2.45 m OD	Oldtown Marsh	52°18'22.80"N	1°38'43.50"E		970 ± 30	933	796	-	M^1	0.2
WM-15-6 -1.77 m OD	Westwood Marsh	52°18'1.57"N	1°36'57.86"E		836 ± 35	894	683	+	MHWST-0.2	0.2
WM-15-6 – 4.01 m OD	Westwood Marsh	52°18'1.57"N	1°36'57.86"E		9220 ± 40	10501	10258	B	(MTL+HAT)/2	(MTL to HAT)/2
MN-16-1 -5.62 m OD	Minsmere	52°14'14"N	1°37'24"E		4099 ± 39	4816	4447	B	(MTL+HAT)/2	(MTL to HAT)/2
MN-16-3 -3.71 m OD	Minsmere	52°14'14"N	1°37'24"E		2014 ± 38	2101	1880	+	MHWST-0.2	0.2
MN-16-5 -3.05 m OD	Minsmere	52°14'14"N	1°37'24"E		1231 ± 38	1265	1065	+	MHWST-0.2	0.2
MN-16-19 -3.63 m OD	Minsmere	52°14'14"N	1°37'24"E		909 ± 37	917	743	+	MHWST-0.2	0.2
MN-16-19 -4.98 m OD	Minsmere	52°14'14"N	1°37'24"E		1613 ± 35	1592	1408	-	MHWST+0.6	0.4
MN-16-19 -5.54 m OD	Minsmere	52°14'14"N	1°37'24"E		1920 ± 38	1966	1738	+	MHWST-0.2	0.2
MN-16-19 -9.28 m OD	Minsmere	52°14'14"N	1°37'24"E		5266 ± 140	6310	5670	B	(MTL+HAT)/2	(MTL to HAT)/2
SW-17-1 -2.99 m OD	Sizewell	52°13'04"N	1°36'34"E		5263 ± 38	6179	5931	B	(MTL+HAT)/2	(MTL to HAT)/2
SW-17-13 -2.77 m OD	Sizewell	52°13'04"N	1°36'34"E		1431 ± 37	1386	1290	-	M^1-0.2	0.2
SW-17-13 -3.13 m OD	Sizewell	52°13'04"N	1°36'34"E		1444 ± 37	1395	1294	+	MHWST-0.2	0.2
SW-17-13 -6.92 m OD	Sizewell	52°13'04"N	1°36'34"E		6339 ± 35	7412	7170	B	(MTL+HAT)/2	(MTL to HAT)/2
SW-17-3 -4.07 m OD	Sizewell	52°13'04"N	1°36'34"E		5570 ± 30	6405	6301	B	(MTL+HAT)/2	(MTL to HAT)/2

Table 7.2: Reconstruction of RSL, relative to local MSL. The reference water level was calculated using the tidal parameters from Southwold (Admiralty Tide Tables, 2016), situated at most 12 km from the sites investigated. RSL (m) was calculated by subtracting the reference water level from the sample elevation, relative to local MSL. The contribution of the individual sources to the total vertical error (E_t) is outlined in Table 7.3.

Sample ID	Altitude (m OD)	Indicative meaning			RSL (relative to MSL)	RSL 2σ Uncertainty	
		RWL (m)	RWL (m)	IR (± m)		+ (m)	- (m)
GDH-16-2 -2.09 m OD	-2.09	MHWST-0.2	1	0.2	-2.89	0.23	0.22
GDH-16-2 -2.29 m OD	-2.29	MHWST+0.2	1.4	0.8	-3.49	0.81	0.81
OTM-16-13 -2.03 m OD	-2.03	MHWST-0.2	1	0.2	-2.83	0.23	0.22
OTM-16-13 -5.64 m OD	-5.64	(MTL+HAT)/2	0.89	(MTL to HAT)/2	-6.33	0.71	0.70
OTM-16-13 -2.45 m OD	-2.45	M[1]	1.39	0.2	-3.64	0.23	0.22
WM-15-6 -1.77 m OD	-1.77	MHWST-0.2	1	0.2	-2.57	0.23	0.22
WM-15-6 – 4.01 m OD	-4.01	(MTL+HAT)/2	0.89	(MTL to HAT)/2	-4.7	0.70	0.70
MN-16-1 -5.62 m OD	-5.62	(MTL+HAT)/2	0.89	(MTL to HAT)/2	-6.31	0.70	0.70
MN-16-3 -3.71 m OD	-3.71	MHWST-0.2	1	0.2	-4.51	0.23	0.23
MN-16-5 -3.05 m OD	-3.05	MHWST-0.2	1	0.2	-3.85	0.23	0.23
MN-16-19 -3.63 m OD	-3.63	MHWST-0.2	1	0.2	-4.43	0.23	0.23
MN-16-19 -4.98 m OD	-4.98	MHWST+0.6	1.8	0.4	-6.58	0.42	0.41
MN-16-19 -5.54 m OD	-5.54	MHWST-0.2	1	0.2	-6.34	0.24	0.23
MN-16-19 -9.28 m OD	-9.28	(MTL+HAT)/2	0.89	(MTL to HAT)/2	-9.97	0.72	0.70
SW-17-1 -2.99 m OD	-2.99	(MTL+HAT)/2	0.89	(MTL to HAT)/2	-3.68	0.70	0.70
SW-17-13 -2.77 m OD	-2.77	M[1]-0.2	1.19	0.2	-3.76	0.23	0.22
SW-17-13 -3.13 m OD	-3.13	MHWST-0.2	1	0.2	-3.93	0.23	0.22
SW-17-13 -6.92 m OD	-6.92	(MTL+HAT)/2	0.89	(MTL to HAT)/2	-7.61	0.71	0.70
SW-17-3 -4.07 m OD	-4.07	(MTL+HAT)/2	0.89	(MTL to HAT)/2	-4.76	0.70	0.70

Tidal parameters for Southwold: Highest Astronomical Tide (HAT) 1.58 m, Mean High Water Spring Tide (MHWST) 1.2 m, Mean Tide Level (MTL) 0.2 m, Mean Sea Level (MSL) 0.2 m
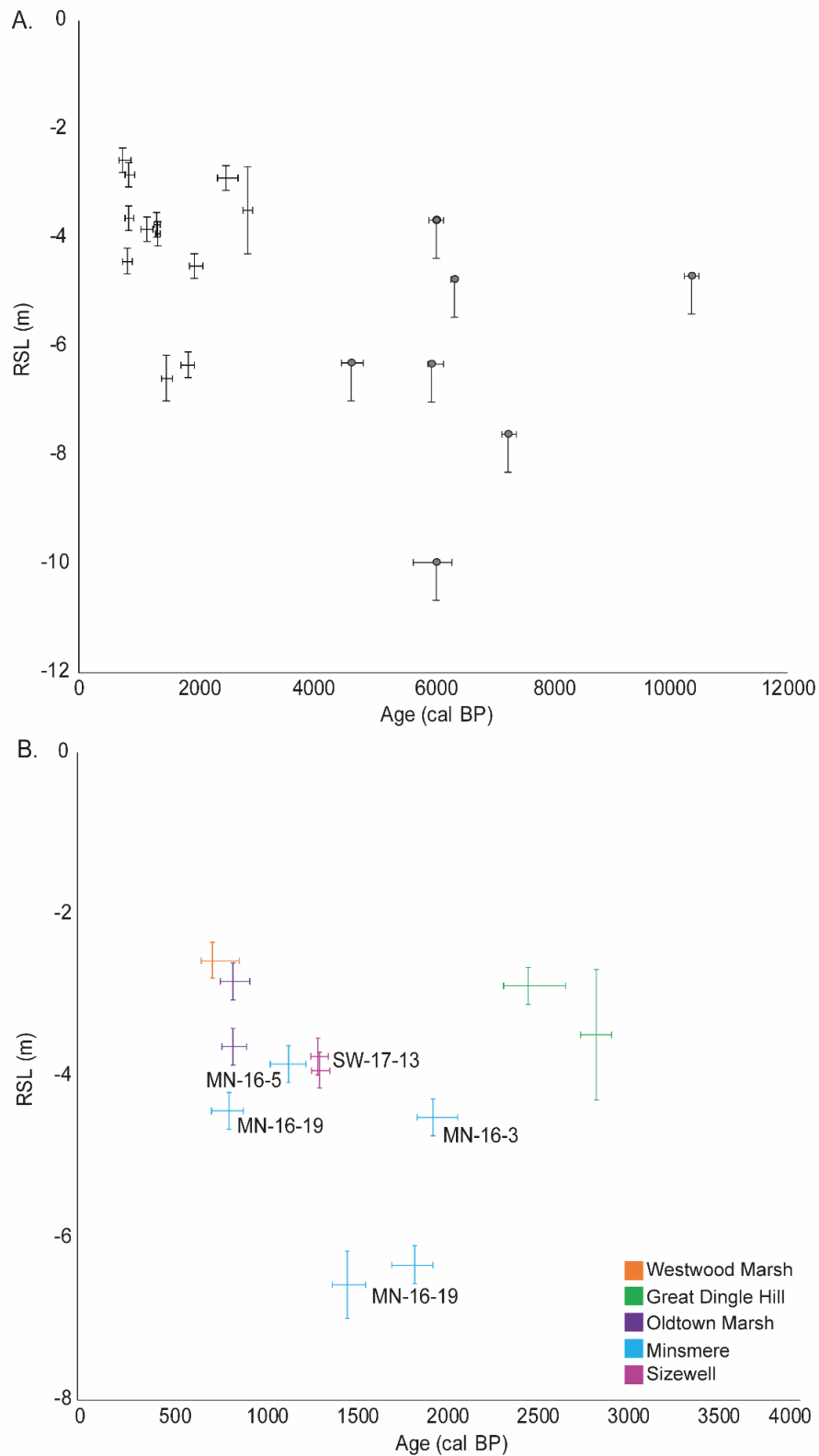
Figure 7.4: A. Age-elevation plot of sea-level index points and limiting data (circles) produced as part of this thesis. The median age of each sample (cal BP) is plotted with the 2σ age uncertainty. B. Sea-level index points, resulting from intercalated peat samples, for the late Holocene. The associated site is denoted by the colour with labels added for sites were multiple cores were sampled.

7.2.2 Errors associated with RSL reconstruction

Estimation of standardised errors

The total error (E_t) is the total of all quantified errors and is determined as $\sqrt{(e_1^2 + e_2^2 + e_3^2 + \ldots + e_n^2)}$ were $e_1 \ldots e_n$ are individual sources of error (Preuss 1979; Shennan 2015). Table 7.3 outlines the individual sources of error quantified or estimated for each sea-level index point. Standardised errors estimate the error sources relating to the indicative meaning, sampling and elevation measurement (Hijma et al., 2015). The indicative range and sample thickness error equates to half of the indicative range and sample thickness respectively. A sampling error of ± 0.01 m is included to account for errors arising when measuring sample depth (Shennan, 1986; Hijma et al., 2015). Core shortening can be substantial, depending on the coring equipment used, with shortening of up to 30 % possible in less than a 1 m section of a core (Morton and White, 1997). Using a Russian core sampler minimises the impact of core shortening and is associated with an error of ± 0.01 m (Woodroffe, 2006; Hijma et al., 2015). Non-vertical drilling results in a greater sample depth than the true depth (Hijma et al., 2015). Törnqvist et al., (2004) concluded that this can cause an error of 0.02 m per metre depth of hand coring. This error is unidirectional, therefore only affecting the upper portion of the total vertical error. A standard levelling error (± 0.1 m) associated with the use of a dGPS has additionally been included.

Accuracy of the indicative meaning

Consideration must be given to the accuracy of the indicative range, and tide level it refers to, when interpreting RSL data. Shennan (1982; 1986) originally compiled the indicative meanings with the aim of reconstructing RSL change in Fenland. Applying the indicative meaning, which is dependent on the stratigraphic context, to other study areas is equivocal as the vertical range over which an indicator formed will vary with tidal range (Horton et al., 2000). In addition, the calculation of the indicative meaning assumes that the tidal regime has remained constant with time (Shennan, 1982; 1986). The errors associated with tidal range, and therefore the determination of the indicative meaning, will be greatest for coastlines with large tidal ranges, which have experienced significant spatial variations in tide level, such as estuaries (Horton, 1997). Zong (1993) illustrated this for Morecambe Bay, when an indicative range of 0.6 m was determined for a *Phragmites* or monocot peat overlain by a minerogenic saltmarsh unit, 0.4 m greater than that proposed by Shennan (1982; 1986) and attributed to differences in tidal amplitude between Morecambe Bay (~ 10.5 m) and Fenland (~ 8.5 m) (Horton et al., 2000). The accuracy of the indicative meaning is of greater importance in macro-, rather than micro-, tidal areas (Shennan, 1986). Despite these uncertainties, estimates of the indicative meaning determined by

Shennan (1980; 1982; 1986) have been used for the various iterations of the geological RSL database created for the UK and Ireland to establish a relationship between the elevation of a sea-level indicator and a reference tide level (Shennan and Horton, 2002; Brooks and Edwards, 2006; Shennan et al., 2018). These are adopted here to ensure a consistent basis for the analysis of changes in RSL.

Table 7.3: Individual sources of error quantified or estimated for each sea-level index point (Table 7.2 and Figure 7.4). The total error (E_t) was calculated as $\sqrt{(e_1^2 + e_2^2 + e_3^2 + \ldots + e_n^2)}$ were $e_1 \ldots e_n$ are error components (Preuss, 1979; Shennan, 2015).

Sample ID	IR (m)	Sample thickness (m)	Sampling (m)	Core stretching/shortening (m)	Non-vertical drilling (m)	Levelling (m)	RSL 2σ Uncertainty (m) +	RSL 2σ Uncertainty (m) -
GDH-16-2 -2.09 m OD	0.20	0.01	0.01	0.01	0.04	0.10	0.23	0.22
GDH-16-2 -2.29 m OD	0.80	0.01	0.01	0.01	0.04	0.10	0.81	0.81
OTM-16-13 -2.03 m OD	0.20	0.01	0.01	0.01	0.04	0.10	0.23	0.22
OTM-16-13 -5.64 m OD	0.69	0.01	0.01	0.01	0.11	0.10	0.71	0.70
OTM-16-13 -2.45 m OD	0.20	0.01	0.01	0.01	0.05	0.10	0.23	0.22
WM-15-6 -1.77 m OD	0.20	0.01	0.01	0.01	0.03	0.10	0.23	0.22
WM-15-6 – 4.01 m OD	0.69	0.02	0.01	0.01	0.07	0.10	0.70	0.70
MN-16-1 -5.62 m OD	0.69	0.02	0.01	0.01	0.07	0.10	0.70	0.70
MN-16-3 -3.71 m OD	0.20	0.02	0.01	0.01	0.03	0.10	0.23	0.22
MN-16-5 -3.05 m OD	0.20	0.03	0.01	0.01	0.02	0.10	0.23	0.23
MN-16-19 -3.63 m OD	0.20	0.03	0.01	0.01	0.05	0.10	0.23	0.23
MN-16-19 -4.98 m OD	0.40	0.02	0.01	0.01	0.07	0.10	0.42	0.41
MN-16-19 -5.54 m OD	0.20	0.02	0.01	0.01	0.08	0.10	0.24	0.22
MN-16-19 -9.28 m OD	0.69	0.01	0.01	0.01	0.16	0.10	0.72	0.70
SW-17-1 -2.99 m OD	0.69	0.02	0.01	0.01	0.06	0.10	0.70	0.70
SW-17-13 -2.77 m OD	0.20	0.01	0.01	0.01	0.03	0.10	0.23	0.22
SW-17-13 -3.13 m OD	0.20	0.01	0.01	0.01	0.04	0.10	0.23	0.22
SW-17-13 -6.92 m OD	0.69	0.02	0.01	0.01	0.12	0.10	0.71	0.70
SW-17-3 -4.07 m OD	0.69	0.01	0.01	0.01	0.08	0.10	0.70	0.70

Compaction

Compaction introduces uncertainties into estimates of the rate and magnitude of RSL change, as the original elevation of the sediment is lowered post-deposition, affecting sediment volume and distorting stratigraphy (Kaye and Baghoorn, 1964; Allen, 2000; Brain, 2006; 2015). It therefore results in a considerable altitudinal uncertainty for highly compressible peats and fine-grained minerogenic sediments (Allen, 2000; Baeteman et al., 2011). Whilst consideration of compaction is important for determining the original altitude of a sea-level indicator, it is of greater importance if it is a causal factor in producing intercalated Holocene sequences (Shennan, 1986). Sediment compaction is minimal for basal peats and does not require consideration for samples taken from the base of basal peat, reducing the altitudinal uncertainty when reconstructing RSL using these index points (Horton and Shennan, 2009; Brain, 2015).

 An initial assessment of compaction can be made by comparing the altitude of basal, base of basal and intercalated index points (Figure 7.5). Of the 19 newly constructed sea-level index points, 11 are intercalated, with 7 of the 8 basal index points freshwater limiting (Figure 7.5). The intercalated index points from the inland core at Minsmere (MN-16-19) plot consistently below the intercalated index points from the other sites. The Holocene sequence from MN-16-19 is thick (~ 8 m) and comprised of intercalated fine-grained minerogenic and thick peat (up to 3.68 m) units. Several intercalated index points plot at altitudes ranging from -2.57 m OD to -4.43 m OD between 1400 and 700 cal BP potentially indicating that compaction is significant for these sites. Compaction is unlikely to account for the attitudinally dissimilarity in freshwater limiting data from Minsmere (MN-16-19 -9.97 m OD), Oldtown Marsh (OTM-16-13 -6.63 m OD) and Sizewell (SW-17-1 -3.68 m OD and SW-17-3 –4.07 m OD) as they are based on basal peats sampled close to the base of the Holocene sequence, meaning that compaction was not significant. Consideration is given to the horizontal errors associated with these freshwater limiting data in section 7.2.3.

Horton and Shennan (2009) regard the effect of compaction for intercalated index points to be dependent on the thickness of the Holocene sequence, thickness of overburden sediment and depth of sediment to the base of the Holocene sequence. Quantitative assessment identified an empirical relationship between these parameters and elevation residuals (reconstructed RSL- modelled RSL) for the sediment sequences from this thesis (Figure 7.6 and Table 7.4). A statistically significant correlation was identified between elevation residuals, overburden thickness and total thickness of the Holocene sequence for the dataset presented as part of this thesis. A strong correlation exists between the thickness of the overburdening sediment and the elevation residuals (r = 0.76). The altitudinal comparison (Figure 7.6A) and significant correlation between the elevation

residuals, depth of overburden and sediment thickness at the 5% significance level (Table 7.4) indicates that sediment compaction has had an impact on the late Holocene intercalated index points. Failure to account for the effects of sediment compaction results in estimates of the late Holocene RSL rate being overestimated, with the inclusion of intercalated index points resulting in an overestimation of 0.1-0.4 mm yr^{-1} for the east coast of England (Horton and Shennan, 2009).
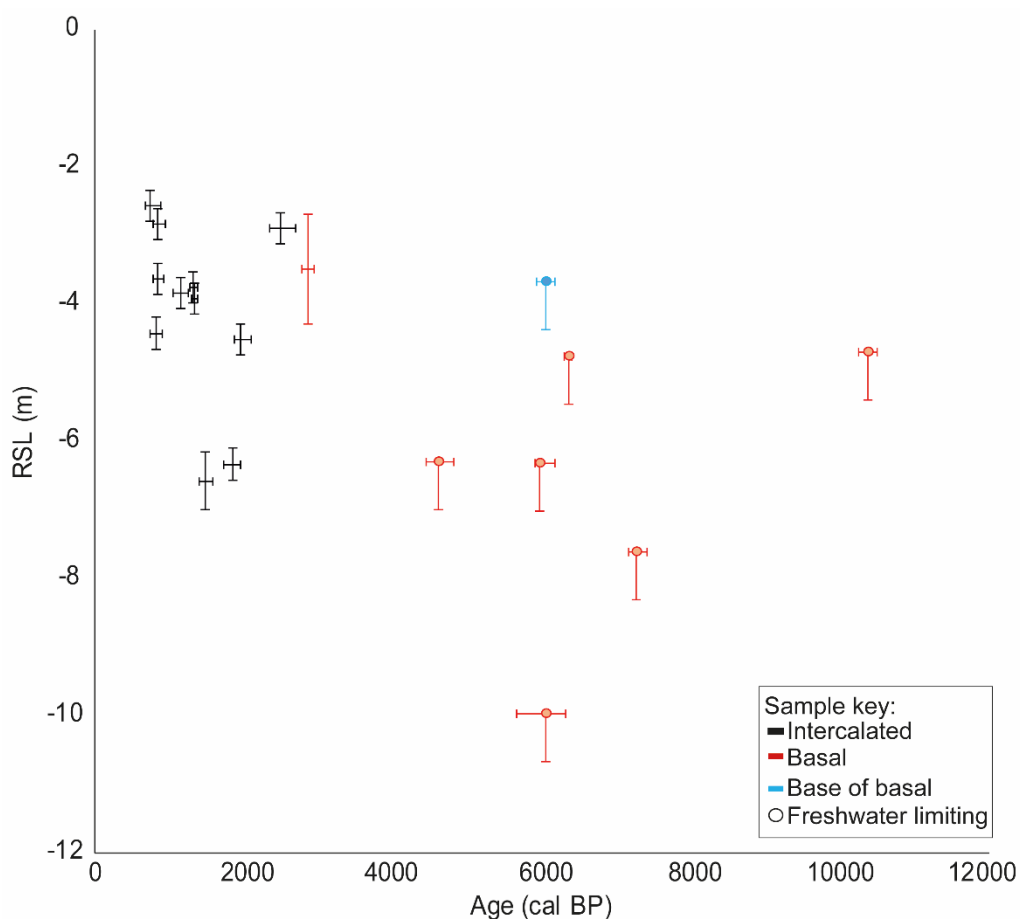
Figure 7.5: Comparison of intercalated (black), basal (red) and base of basal (blue) sea-level index points for Great Dingle Hill, Oldtown Marsh, Westwood Marsh, Minsmere and Sizewell showing median age with the 2σ age uncertainty and altitude error estimates.
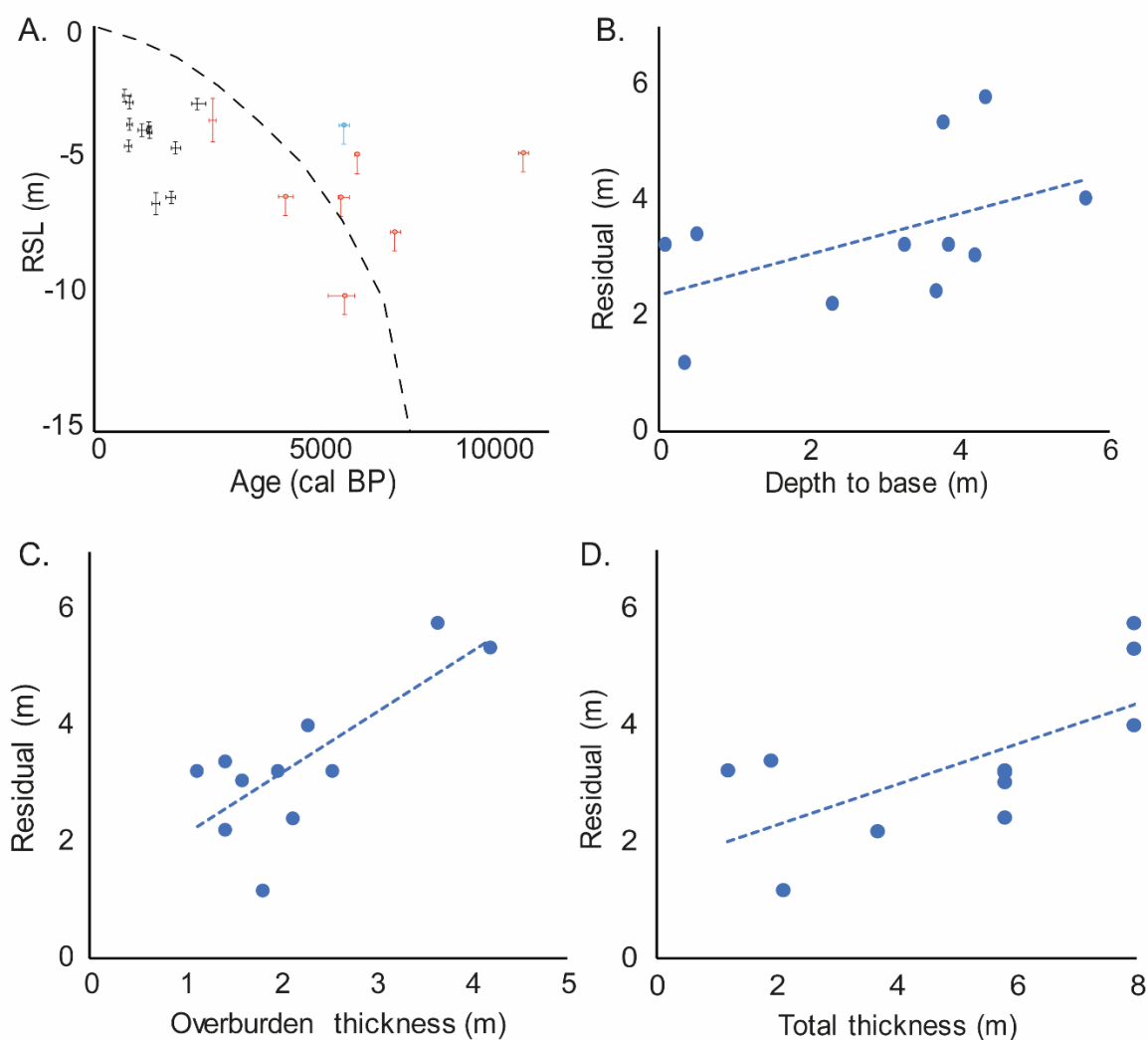
Figure 7.6- A. Intercalated (black), basal (red) and base of basal (blue) index points from Great Dingle Hill, Oldtown Marsh, Westwood Marsh, Minsmere and Sizewell showing median age with the 2σ age uncertainty and altitude error estimates. The dashed line shows the most recent GIA model RSL predictions for East Anglia (Bradley, personal communication 2019). B. Scatter plots for intercalated sea-level index points showing relationship between residuals (observed RSL-modelled RSL) and depth to base, (C) overburden thickness and (D) total thickness of Holocene sequence, in addition to linear best-fit rate.

Table 7.4- Pearson's product-moment correlation coefficients (r) of overburden thickness, depth to base of Holocene sequence and total thickness of Holocene sequence. Values in bold exceed the critical value at the 0.05 significance level.

	Number of intercalated index points	Critical value	Depth to overburden (r value)	Depth to base (r value)	Total thickness (r value)
All sites	11	0.60	**0.76**	0.50	**0.66**

Tidal range changes

Changes in tidal range were not quantified despite being regarded as a significant uncertainty associated with sea-level index points (Brooks and Edwards, 2006; Baeteman et al., 2011; Griffiths and Hill, 2015). For example, a greater early Holocene tidal range would result in the reference water level of a deposit being higher than the modern equivalent therefore reconstructing the position of RSL lower. Horton et al. (2013) determined that failing to account for Holocene changes in palaeotidal range underestimated RSL by ~ 0.5 m in New Jersey. Modelling the physics of the tidal system remains a challenge, with dynamic global models unable to provide the accuracy of coastal tides required for RSL studies (Griffiths and Hill, 2015). Tidal evolution modelling for the northwest European shelf seas has indicated that the tidal amplitude for the east coast of Britain has remained close to its present day size since 8 ka BP (Gehrels et al., 1995; Uehara et al., 2006; Ward et al., 2016). However, coastlines fronted by a wide shallow shelf or semi-enclosed (e.g. North Sea) are more susceptible to changes in tidal range through time (Gehrels et al., 1995; Uehara et al., 2006; Ward et al., 2016).

Palaeotidal models indicate that changes in tidal range were minimal at the open coast (Shennan et al., 2003), with changes in tidal range, and therefore errors, affecting coastal areas that have experienced significant changes in geometry through time (Brooks and Edwards, 2006; Horton and Shennan, 2009). Shennan et al. (2000a) modelled the position of MHWST relative to MTL in the western North Sea for the Holocene and predicted an increase of ~ 0.8 m between 8 and 6 ka BP, with < 0.2 m of change occurring from 6 ka BP to present (Shennan et al., 2003). More recently, changes during the last 8 ka for east England have been modelled to be minimal in comparison with changes during the early Holocene and late glacial period (Ward et al., 2016). Despite this, changes in tidal range must be given consideration when interpreting RSL data as alterations to water depth and shelf width, resulting from RSL change, will cause tidal range change and vice versa (Griffiths and Hill, 2015). In addition, changes in tidal range will have implications for estimates of RSL change, given that the contemporaneous tide levels that sea-level indicators are related to will have varied with tidal amplitude, which in turn is influenced by RSL (Gehrels et al., 1995; Shennan et al., 2000b; Uehara et al., 2006; Neill et al., 2010; Ward et al., 2016).

7.2.3 Regional comparison of RSL data and GIA model predictions for East Anglia

The regional database for East Anglia contains 39 published (Coles and Funnell, 1981; Devoy, 1982; Alderton, 1983; Brew et al., 1992; Horton et al., 2004) and 7 unpublished (Lloyd et al., 2008), data points, which will be referred to as the existing RSL data for East Anglia (Figure 7.7). The unpublished data were produced by Lloyd et al. (2008) for

Minsmere-Sizewell area (Appendix 1). The chronology of this unpublished data was determined using bulk peat samples, with no additional 'bulk' error included prior to calibration or wider age error margin added post calibration. Estimates of ground altitude were also made for several sample cores (Goose Hill and Coney Hill). The existing RSL data for East Anglia extends from Somerton Holmes, east Norfolk, to Aldeburgh, an area extending ~ 36 km north and 20 km south of Southwold (Figure 7.7). They are considered appropriate to group based on similar distances from former ice loads and similar GIA effects (Shennan et al., 2018). The existing data for the East Anglia region covers the last 10 ka and documents a gradually rising RSL from -20 m to -0.69 m during the Holocene, comparable with the general trend of the most recent GIA model predictions for the region (Figure 7.8; Bradley, personal communication 2019). The sea-level index point attributes for the existing data for East Anglia, published and unpublished, in addition to that presented as part of this thesis are outlined in Appendix 18.
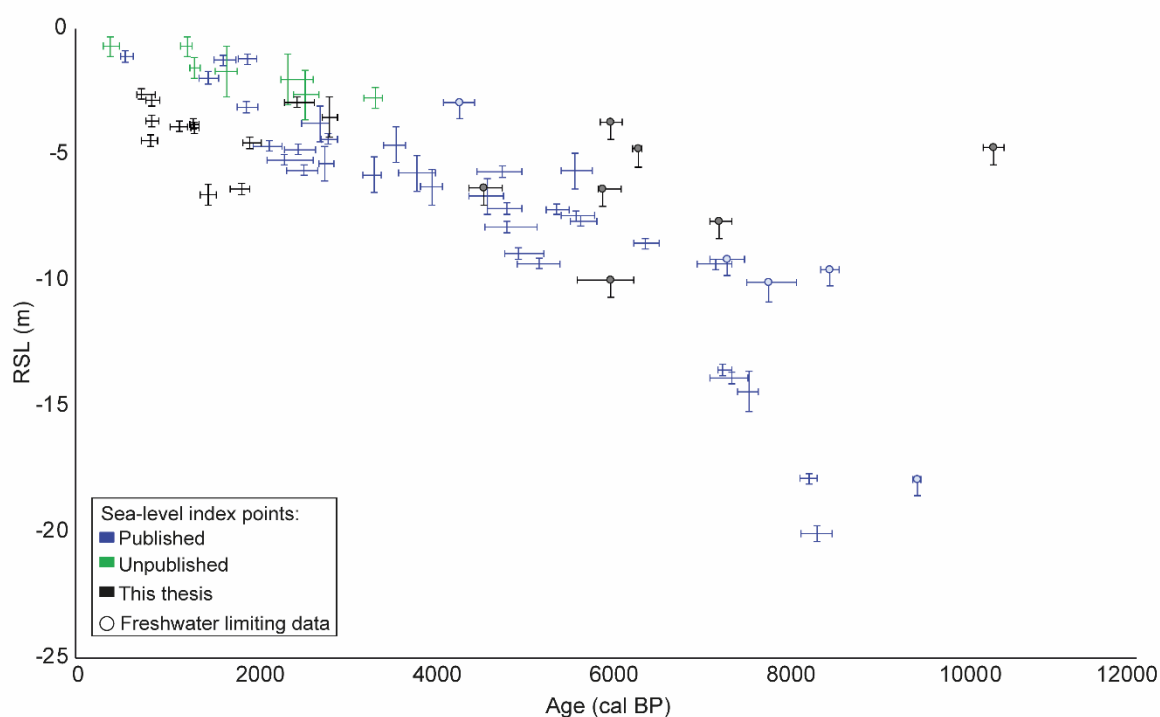
Figure 7.7: Published, in blue (Coles and Funnell, 1981; Devoy, 1982; Alderton, 1983; Brew et al., 1992; Horton et al., 2004), and unpublished, in green (Lloyd et al., 2008), sea-level index points for East Anglia plotted alongside new sea-level index points (black) produced as part of this thesis.
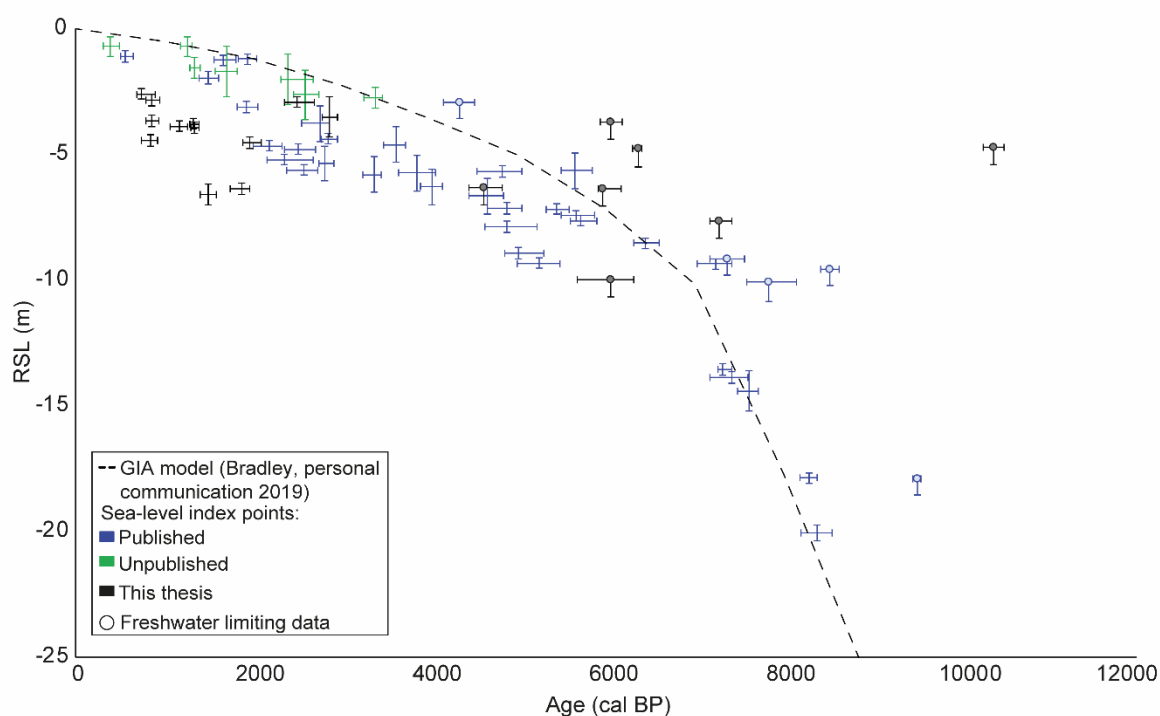
Figure 7.8: Existing sea-level data, published (blue) and unpublished (green), for East Anglia (Coles and Funnell, 1981; Devoy, 1982; Alderton, 1983; Brew et al., 1992; Horton et al., 2004; Lloyd et al., 2008) *plotted alongside new sea-level index points produced as part of this thesis (black) and the most recent GIA model predictions of RSL (dashed line) for the region (Bradley, personal communication 2019).*

Freshwater limiting data

The freshwater limiting data from Minsmere (MN-16-1 and MN-16-19) contrasts with the GIA model predictions and existing RSL data for East Anglia. Basal freshwater peats from MN-16-1 and MN-16-19 constrain RSL to beneath -6.31 m (4816-4447 cal BP) and -9.97 m (6310-5670 cal BP) respectively. Existing sea-level index points, accepted in the current RSL database for further analysis (Shennan et al., 2018), constrain RSL above the elevation of these freshwater limiting data from Minsmere, questioning their validity. The AMS radiocarbon date for MN-16-19 is based on a bulk peat sample, and may therefore have been influenced by the downwards reworking of humic acids and rootlets (Balesdent, 1987). Shennan et al. (2008) noted a significant difference in AMS radiocarbon dates based on macrofossils and bulk samples from the same peat unit. Freshwater limiting dates from comparable altitudes from east Norfolk (Alderton, 1983) and south Suffolk (Devoy, 1982) range from 8626 to 7172 cal BP. Therefore, the freshwater limiting date from MN-16-19 is omitted from further analysis due to uncertainty associated with the AMS radiocarbon date. The freshwater limiting date from MN-16-1 contrasts with multiple sea-level index points accepted in the Shennan et al. (2018) RSL database. MN-16-1 is

chronologically comparable with intercalated index points from the lower reaches of the Blyth (Brew et al., 1992), which constrain the transition from peat to clay and document the landwards progression of tidal influence. One of these resulting sea-level index points for the Blyth plots beneath the MN-16-1 freshwater limiting date, whilst the other above (Figure 7.8). The freshwater limiting date from MN-16-1 is omitted based on the Blyth index points being consistent stratigraphically and chronologically and accepted by the current RSL database (Shennan et al., 2018). Coring ~ 400 m west of MN-16-1 identified shallow sediment sequences, less than 0.5 m deep, comprised of sand dominated soil with sub-angular or sub-rounded gravels and underlain by a gravel platform (Hamilton, 2017). The bottom of the sampled MN-16-1 sequence may be a continuation of this feature, erroneously interpreted as the underlying geology. Similar gravel lenses are encountered in the upper stratigraphy of the Romney Marsh depositional complex associated with the redistribution of barrier sediments during late-Holocene inundation (Long et al., 2006a).

The freshwater limiting date from Westwood Marsh, 10501-10258 cal BP, plots considerably higher than expected, with an elevation residual exceeding 20 m, comparison with other sites indicates that this date does not constrain the rise of regional ground water level in response to RSL (Figure 7.7). It is believed to have been influenced by older carbon, potentially due to reworking of the palaeoground surface or the erroneous inclusion of plant macrofossils (e.g. *Potamogeten spp.*) that are susceptible to absorbing older carbon, and it is therefore discounted.

Intercalated sea-level index points

The existing RSL data plot below the GIA model predictions, particularly for the mid- and late Holocene (Figure 7.8). Shennan et al. (2018) attributes the scatter of index points beneath the GIA predictions, in part, to compaction. Similarly, the new data points also plot beneath the GIA model predictions, with greater disparity for the late Holocene compared with the existing RSL data. A correction for post-depositional lowering has not been applied to the published or unpublished RSL data for East Anglia, often as it has not been considered (e.g. Coles and Funnell, 1981; Alderton, 1983; Brew et al., 1992; Lloyd et al., 2008). Conversely, Devoy (1982) adjusted for compaction but did not provide numerical values of the estimates used, meaning that the correction could not be included in the current RSL database for the UK and Ireland (Shennan et al., 2018). A comparison of limiting data, intercalated and basal index points for east Norfolk (Coles and Funnell, 1981; Alderton, 1983; Shennan and Horton, 2002; Horton et al., 2004) and northern Suffolk (Brew et al., 1992) concluded that the influence of compaction may be significant for this area (Horton et al., 2004).

Post-depositional lowering of the index points from their original elevation is likely to account for a proportion of the difference between the GIA model prediction and the RSL data (both existing and newly presented) for East Anglia. The elevation residuals (difference between reconstructed and predicted RSL) for the intercalated index points from Westwood Marsh, Oldtown Marsh, Minsmere (MN-16-5 and MN-16-19) and Sizewell (SW-17-13) are particularly large, ranging from ~ 2 to 6 m for the late Holocene. The Holocene sequence associated with each of these index points contains thick peat units, ranging from 2.30 m (Westwood Marsh) to 4.05 m (Sizewell).   Compaction can be considerable for sequences comprised of peat intercalated between thick Holocene minerogenic sediments, with the extremely porous structure of highly organic material resulting in volume decreases of up to 90 % (Jelgersma, 1961; Kaye and Baghoorn, 1964; Haslett et al., 1998; Shennan and Horton, 2002; Horton et al., 2013). These intercalated index points from Westwood Marsh, Oldtown Marsh, Minsmere (MN-16-5 and MN-16-19) and Sizewell (SW-17-13) also contrast with the elevation of existing RSL data for the late Holocene, plotting up to 6 m below index points from the upper valley of the Bure-Yare-Waveney estuary (Coles and Funnell, 1981; Alderton, 1983), inland at Minsmere and Sizewell (Lloyd et al., 2008). In particular, the sediment sequences sampled as part of this thesis at Minsmere were considerably thicker (~ 3 m), with thicker individual peat units, than those sampled by Lloyd et al. (2008). Post-depositional lowering of the index points produced for this thesis from the Minsmere-Sizewell area is therefore likely to be greater due to the total thickness of the Holocene sediment sequence and peat units.

Spit development and barrier dynamics were identified as influential for Holocene coastal evolution and the sediment record, in the Blyth estuary, northern Suffolk (Brew et al., 1992) and east Norfolk (Coles and Funnell, 1981; Alderton, 1983; Boomer and Godwin, 1993). The sediment infilling of large estuaries and local morphological change may result in non-trivial changes in local tides (Griffiths and Hill, 2015; Shennan et al., 2018). Small open coast estuaries previously existed prior to the Middle Ages on the Suffolk coast at Dunwich and Minsmere, and have since been blocked by shingle and sand barriers (Pye and Blott, 2006). A degree of the mismatch between the intercalated index points from Westwood Marsh, Oldtown Marsh, Minsmere (MN-16-5 and MN-16-19) and Sizewell (SW-17-13) and the model predictions of RSL for the late Holocene is likely to relate to local changes in tidal range resulting from changes in the configuration of the coast. A tidal range smaller than present, due to the influence of barrier features and the size and shape of estuaries, would equate to reference water levels smaller than the modern equivalents and therefore RSL would be higher, thus reducing the altitudinal offset observed in the data.

Lastly, the difference between the new intercalated index points presented, and GIA model predictions and existing RSL data may be due to the sea-level indicator not being primarily controlled by RSL rise. For example, Holocene sediment sequences could be modified by a compaction mechanism, with high compaction of organic sediments leading to surface lowering, marine incursion and inorganic sedimentation, resulting in changes in sea-level tendency in the sediment sequence (Devoy, 1982). The driving mechanisms responsible for the changes in sea-level tendency presented as part of this thesis will be discussed in section 7.2.4 and 7.3.1.

7.2.4. Evaluation of RSL as a primary driver of coastal advance/retreat

RSL change and resultant coastal change is a function of processes operating from global to local spatial scales. It is therefore of vital importance to consider the relevant temporal and spatial scales of these processes when reconstructing changes in RSL (Shennan et al., 2002; Shennan, 2015). RSL, by definition, varies spatially and temporally, and is a function of: the time-dependent eustatic sea level, the total isostatic effect of the glacial rebound process, the tectonic effect, the total effect of local processes within the coastal system, and the sum of unknown or unquantified factors (Shennan et al., 2012; Shennan, 2015). Further detail on reconstructing changes in RSL is provided in Chapter 2. All regional plots of RSL change for the UK show a scatter of sea-level data, attributed to either underestimation of error terms, differential GIA, underestimation of local scale factors or evidence of unquantified factors (Shennan et al., 2018). Tendency analysis of a sea-level indicator can help to distinguish between the controlling processes operating at different spatial and temporal scales. A consistent direction of sea-level tendency should be recorded over a wider area and be greater than local significance if regional processes are responsible for RSL change at a time and location (Shennan, 1986; Shennan et al., 2018). Analysis by Shennan et al. (2018) concluded that local-scale processes, rather than decimetre- and centennial- scale oscillations in sea level, significantly control the temporal pattern of sea-level tendency and horizontal changes in coastal environments.

Long (1992) undertook an alternative tendency analysis to that completed by Shennan et al. (2018). The probability of a sample dating to a time range was determined using CALIB, with the cumulative probability distribution of positive and negative sea-level tendencies calculated by adding the probability values for each yearly interval (Long, 1992). This form of analysis is advantageous as it considers the full 2σ calibrated age, rather than just the median age, and identifies periods in a time range when there were significant changes in tendency. Changes in sea-level tendency based on lithostratigraphy will lag behind changes based on biostratigraphy, as biological indicators will respond faster to

environmental change (Long, 1992; Allen, 1995). However, a chronology based on biostratigraphic changes is complicated by the uncertain elevation relationship between change in the altitude of the sea and change in the height of the water table (Long, 1992). There are therefore advantages and disadvantages of both, with selection dependent on the research question.

Suffolk (Figure 7.9A) and east Norfolk (Figure 7.9C) demonstrate a continuous RSL rise trend during the Holocene, the rate of which is gradually declining (e.g. Shennan et al., 2018). RSL in East Anglia rose by ~ 15 m between 8400 and 5000 cal BP, and ~ 6 m since 5000 cal BP (Figure 7.9), indicating RSL change was a more important control for sedimentation during the early and mid-Holocene (Coles and Funnell, 1981; Alderton, 1983; Brew et al., 1992; Horton et al., 2004; Lloyd et al., 2008; this thesis). The proportion of positive versus negative sea-level tendencies for the Holocene was considered at 250 year intervals for Suffolk (Figure 7.9B) and east Norfolk (Figure 7.9D) to produce a simplified pattern of changes in tendency. Two distinctive phases of sea-level tendency are identified for Suffolk, at 8000 to 2500 cal BP, and 2500 cal BP to present. The changes in sea-level tendency associated with each phase are discussed below for Suffolk, with comparisons made with the pattern of tendency recorded in east Norfolk.

Phase 1 (8000-2500 cal BP)

The Suffolk sediment record is dominated by positive sea-level tendencies from 8000 to 2500 cal BP (Figure 7.9B), with periods of minerogenic sedimentation, associated with intertidal and saltmarsh environments, recorded in the lower reaches of the Blyth, Minsmere, Great Dingle Hill and Sizewell (Brew et al., 1992; Lloyd et al., 2008; this thesis). A short-lived, isolated, phase of negative sea-level tendency is also recorded in the lower reaches of the Blyth (Brew et al., 1992), where high intertidal sedimentation is replaced by peat sedimentation from 5467 to 4847 cal BP (Brew et al., 1992). The pattern of sea-level tendency for Suffolk between 8000 and 2500 cal BP is comparable with east Norfolk, where positive sea-level tendencies also dominate, with a period of negative tendency from c. 6000 - 5000 cal BP.

The consistent pattern of sea-level tendency in Suffolk and east Norfolk is further evidence of the importance of the rate of RSL rise for the coastal evolution of the southern North Sea basin during the early and mid-Holocene (van de Plassche, 1982; Long and Innes, 1993; Denys and Baeteman, 1995; Beets and van der Spek, 2000; Baeteman et al., 2002). The period of negative sea-level tendency recorded at east Norfolk and Suffolk between 5750 and 4750 cal BP (Figure 7.9) has also been identified in the Fens and north Norfolk (Coles, 1977; Funnell, 1979; Coles and Funnell, 1981; Alderton, 1983; Shennan, 1986;

Brew et al., 1992). It is likely that the regional similarity of this period of negative sea-level tendency corresponds to a decrease in the rate of RSL rise in these areas of southeast England.

Phase 2 (2500 cal BP- present day)

Sea-level tendency for the last 2500 cal BP on the Suffolk coast varies spatially and temporally, with short-lived phases of positive and negative tendency (Figure 7.9B). Changes in sea-level tendency tend to be isolated to distinct sections of the Suffolk coast, the location of which changes through time. Between c. 2500 and 750 cal BP changes are isolated to the Minsmere-Sizewell area, overlapping slightly with changes in tendency in the Walberswick NNR between c. 1000 and 500 cal BP. This variability may, in part, be an artefact of an unequal pattern of RSL data, resulting from the varying research initiatives of individuals (Long, 1992). Positive sea-level tendency occurs in the Walberswick NNR at Oldtown Marsh prior to 933-796 cal BP, the timing of which has not been constrained due to the erosive nature of the contact. Greater chronological overlap of changes in sea-level tendency between sections of the Suffolk coast is likely had a date been obtained for this transition.

Changes in sea-level tendency in Suffolk and east Norfolk do not co-vary from 2500 cal BP to present (Figure 7.9 B and D), despite the altitude vs time record for Holocene changes in RSL being comparable (Figure 7.9A and C). If RSL change is the driving mechanism of coastal evolution, a consistent direction of sea-level tendency should be recorded over a wider area (Shennan, 1986; Shennan et al., 2018). No consistent pattern in sea-level tendency is recorded over a spatial extent of less than 13 km for the late Holocene, thus indicating that RSL change is not the over-riding driver of coastal change at this time. Instead, the temporally variable pattern of sea-level tendency indicates that local factors controlled coastal advance or retreat during the late Holocene. The variability in changes of late Holocene sea-level tendency is therefore thought to reflect the influence of sediment-driven mechanisms, including the interplay between sediment availability and RSL rise, and the resulting impact on barrier dynamics, in addition proximity to the coast, natural preconditions (e.g. coastal plain extent) and human influence are also contributory factors. Consideration is given to the influence sediment-driven mechanisms in section 7.3.1.
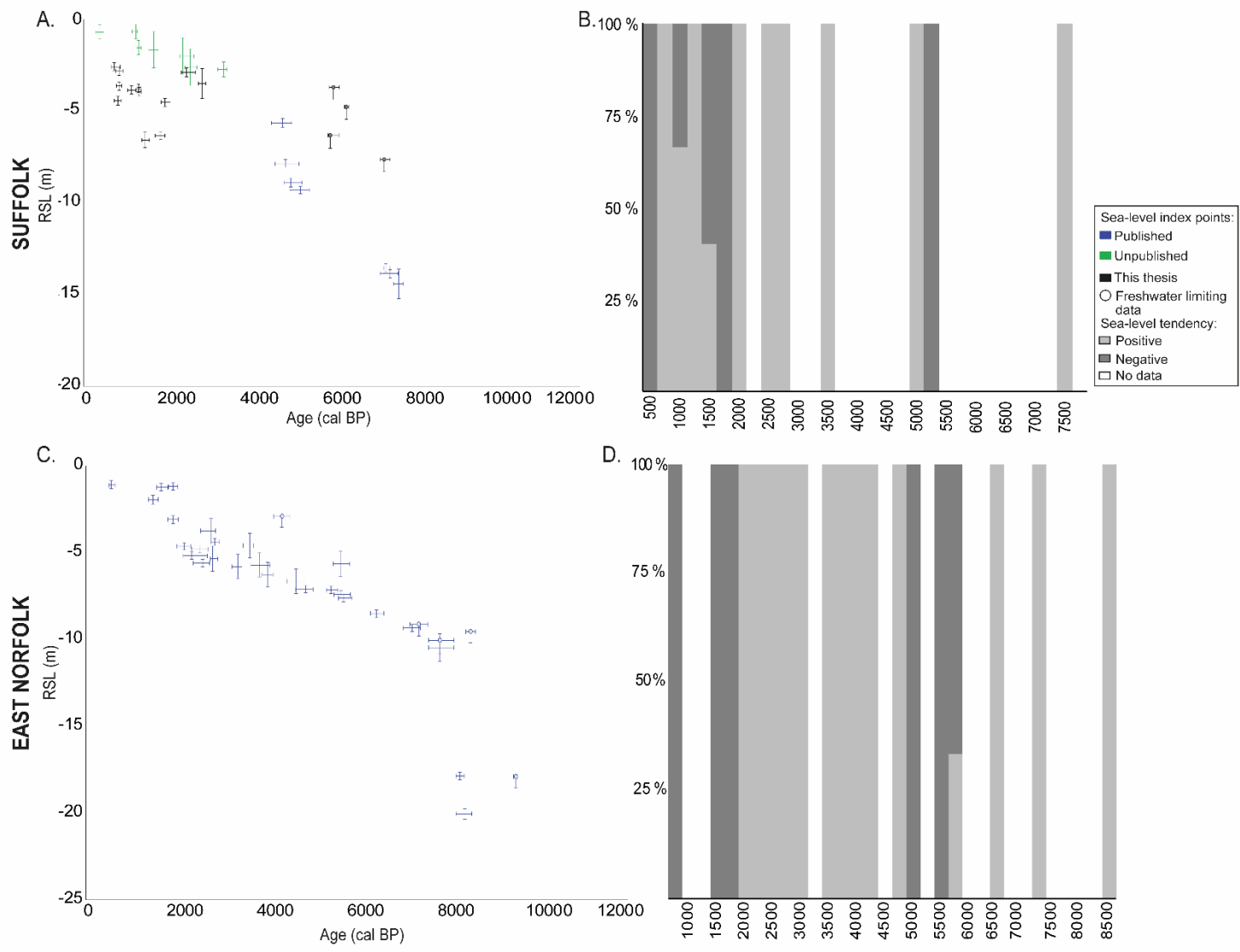
Figure 7.9: A and C. Age-altitude plot of sea-level index points and freshwater limiting data for Suffolk (Brew et al. 1992; Lloyd et al. 2008; this thesis) and east Norfolk (Alderton 1983; Coles and Funnell 1981; Horton et al. 2004) respectively. Freshwater limiting data for WM-15-6, MN-16-1 and MN-16-19 is omitted, see section 7.2.3 for more information. B and D. Proportion of positive and negative sea-level tendencies for Suffolk and east Norfolk respectively in 250 year intervals. Age labels indicate the upper limit of the 250 year interval, which was assigned by the index point median age with no consideration of the 2σ age uncertainty. Note differences in scale.

7.3 Sediment supply and barrier dynamics

The Suffolk coastline alternates between cliffs formed from soft unconsolidated Quaternary sediments and low-lying wetlands, separated from the sea by a narrow beach-barrier system. The cliffs have historically exhibited spatially and temporally variable change in position and height over decadal timescales, affecting sediment supply for East Anglia's sediment budget (Cambers, 1973; 1975; Robinson, 1980; Carr, 1981; McCave, 1987; Brooks and Spencer, 2010; Burningham and French, 2017). The sediment supply to the beach-barrier system is, at present, insufficient to ensure coastline resilience to storms, with studies recording shoreward movement of the barrier during periods of RSL rise and increased storminess (Haskoning, 2009), increasing the susceptibility of back-barrier environments to tidal inundation. Substantial spits, such as Orford Ness and Landguard Point, are extant features of the Suffolk coast, with evidence indicating that they existed historically. Small open coast estuaries existed on the coastline prior to the Middle Ages, but became blocked by gravel and sand barriers between the 14th and 18th century (Chant, 1974; Parker, 1978; Comfort, 1994; Pye and Blott, 2006). In addition, a protective barrier is thought to have existed at Orford Ness since the late Holocene, due to the dominance of peat sedimentation in the sediment records of the adjacent marshes (Carr and Baker, 1968; Carr, 1970). An abundant sediment supply would have been required to form these features and maintain landform integrity. Dynamic offshore bank systems, such as the Sizewell-Dunwich bank complicate regional sediment transport, with the potential to act as a sediment sink and morphologically influence the wave climate and tidal currents (Lees, 1983; Brooks and Spencer, 2010). These elements of coastal and nearshore geomorphology and sediment supply will be explored further in the following sections of this chapter.

Changes in sea-level tendency recorded in the sediment sequences from this thesis cluster during the late Holocene, a period when globally the rate of RSL rise was low (Woodworth et al., 2009; Cazenave et al., 2018). Late Holocene rates of 0.67 ± 0.06 mm yr^{-1} and 0.61 mm yr^{-1} have been estimated for the northern coast of Norfolk (Horton et al., 2004) and East Anglia (Shennan and Horton, 2002) respectively. Due to this low rate of RSL rise during this period, local sedimentological and morphological factors are likely to have been more influential for the reconfiguration of the Suffolk coast than vertical changes in RSL. The absence of synchronous changes in sea-level tendency for East Anglia during the late Holocene (see section 7.2.4) indicates the influence of local factors, such as topography of pre-Holocene basement, proximity to the coast, variation in sediment supply, influence of river catchments and barrier presence and status (Beets et al., 1992; Beets and van der Spek, 2000; Baeteman and Declercq, 2002; Pierik et al., 2017).

7.3.1 Evaluation of sediment supply and barrier dynamics as primary drivers of coastal advance/retreat

Existing stratigraphic research on the Suffolk coast concluded that the development of barrier and spit features, and therefore sediment availability, might have been influential for the evolution of the Suffolk coast (Brew et al., 1992; Lloyd et al., 2008). Barrier building and the creation of discrete sedimentary basins in estuaries is thought to have occurred in the late Holocene, with spit development and barrier dynamics acting as primary controls of Holocene coastal evolution and the resulting sediment record in the Blyth estuary (Brew et al., 1992). Lloyd et al. (2008) suggested the presence, absence and evolution of barrier features as an explanation for the changes in sea-level tendency preserved in the late Holocene sediment sequence from the Minsmere-Sizewell area. Holocene sediment sequences from Westwood Marsh, Oldtown Marsh, Great Dingle Hill, Minsmere and Sizewell indicate that sediment supply and barrier dynamics were important driving mechanisms for the evolution of the Suffolk coast during the late Holocene. In this section, consideration will be given to the sediment-driven factors that may have influenced changes in sea-level tendency at the investigated sites. Comparison of the pattern of sea-level tendency for the Suffolk coast in section 7.2.4 identified a temporally variable spatial pattern of tendency through the late Holocene, with changes confined to a section of the coast, the location of which changes with time. Changes in sea-level tendency were identified for the Minsmere-Sizewell area between c.3500 and 750 cal BP, with changes at the Walberswick NNR occurring between c. 1000 and 500 cal BP. The influence of sediment supply and barrier dynamics as drivers of late Holocene coastal change is considered chronologically in this section therefore separating these areas of the coast.

Minsmere-Sizewell area

Analysis by Lloyd et al. (2008) on the north side of the New Cut (Figure 7.10- SM) identified an isolated positive sea-level tendency, indicating marginal tidal influence at 3459-3253 cal BP. This change in sea-level tendency is recorded only in the sampled sequence, located in close proximity to the Minsmere Old River, which drained the Minsmere Levels prior to the construction of the New Cut at the beginning of the 19th century. This isolated increase in marine influence indicates an influence of local, potentially morphological and/or sedimentological, factors such as the widening of tidal inlets, further landwards extension of existing tidal influence or barrier overwash.

Coinciding positive sea-level tendencies were recorded at Coney Hill (Figure 7.10- CH) and Great Dingle Hill (Chapter 4- Walberswick NNR) at 2745-2458 cal BP and 2701-2357 cal BP respectively, despite inter-site differences in the nature of coastal sedimentation.

The onset of minerogenic sedimentation at Coney Hill is associated with sand and foraminifera indicative of a high marsh or low salinity lagoon, whilst sand is absent at Great Dingle Hill, and diatom taxa indicate intertidal-subtidal mudflats. Reduced barrier integrity, enabling tidal ingress, is a plausible explanation for the onset of tidal influence at Coney Hill and Great Dingle Hill. A breach in the barrier could have been created by a high magnitude event whilst, alternatively, a restricted sediment supply could have led to sediment reworking and increased barrier instability and permeability. Evidence of a high magnitude event is absent at the onset of minerogenic sedimentation in the stratigraphic transect at Great Dingle Hill.

The dominance of brackish conditions prior to the change in sedimentation at Great Dingle Hill indicates that the site was already tidally influenced, potentially via channel inlets through the barrier. A sufficient sediment supply would have stabilised the barrier position at these sites, halting the landwards migration of tidal environments, due to the low rate of RSL rise at this time. However, the results indicate this was not the case, suggesting that sediment supply was insufficient during this time. Coney Hill and Great Dingle Hill are proximal to sections of the present-day barrier that have been susceptible to breach and overwash in the recent past (Pye and Blott, 2009). Evidence indicates that barrier breaching, or further reduced barrier integrity, is the most likely explanation for the positive sea-level tendencies recorded at both sites. Following this, a positive sea-level tendency is recorded by Lloyd et al. (2008) at Goose Hill, Sizewell from 2678-2318 cal BP, with the sedimentation associated with a brackish lagoon environment indicating marginal tidal influence that may have migrated southwards from Minsmere behind the barrier system (Lloyd et al., 2008).
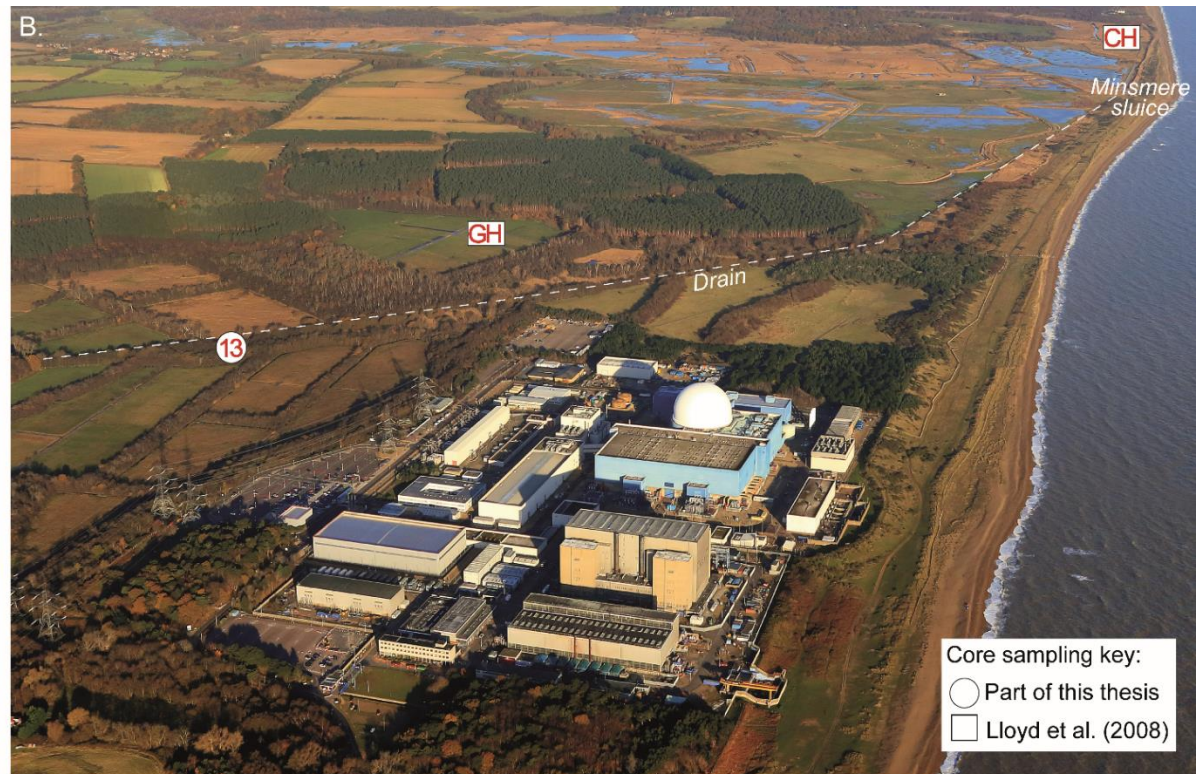
Figure 7.10: Map showing the location of sediment cores analysed by Lloyd et al. (2008) and as part of this thesis in the Minsmere-Sizewell area. Permission to reproduce aerial images has been granted by Mike Page.

Sediment sequences sampled by Lloyd et al. (2008) and this thesis document a landwards movement of tidal influence at Minsmere between 3450-3330 cal BP and 1400-1290 cal BP. This period of positive sea-level tendency is recorded only at Minsmere. Changes in sea-level tendency record the onset of subtidal sedimentation nearest the coast (MN-16-3) at 2101-1880 cal BP, with intertidal flats (SM) and shallow lagoon (MN-16-19) environments forming inland by 1810-1560 and 1966-1738 cal BP respectively (Figure 7.10). A prolonged period (1810-300 cal BP) of fine grained, marine, sedimentation is recorded north of the New Cut at SM (Lloyd et al., 2008).

Further south, at Sizewell, SW-17-13 records a positive sea-level tendency (1395-1294 cal BP), stratigraphically proceeded by a negative tendency (1386-1290 cal BP). Shennan (1986) states that chronologically coincident sea-level tendencies from proximal transgressive and regressive overlaps in the same core should not be smoothed as it indicates the operation of a different balance of processes. The asymptotic relationship between minerogenic marsh/mudflat accretion rates and time, in addition to the influence of barrier dynamics, promotes deposition of regressive stratigraphies, resulting in negative sea-level tendencies (Jennings et al., 1995). In addition, negative sea-level tendencies can result from high rates of sediment deposition, counterbalancing rising RSL (Gerrard et al., 1984). The submergence and emergence of the marsh surface, resulting in positive and negative tendencies, may therefore be a response to increased tidal influence, rather than a signal of RSL rise and fall.

Regionally synchronised evidence is required for RSL rise to be associated with marsh submergence and RSL fall with emergence (Shennan, 1986). In addition, compaction/consolidation mechanisms can alter the pattern of coastal sedimentation, with compaction of organic sediments resulting in marine incursion and minerogenic sedimentation (positive sea-level tendency), and a decline in the rate of RSL rise enabling plants to recolonise (negative sea-level tendency) these sediments (Devoy, 1982). The isolated nature of the chronologically overlapping positive and negative sea-level tendency recorded at Sizewell (SW-17-13) indicates the influence of local sedimentological factors rather than a RSL rise and subsequent fall. A chronologically overlapping record of positive and negative sea-level tendency found inland at Minsmere (Figure 7.10- MM), also indicates an influence of local sedimentological factors (Lloyd et al., 2008).

A return to organic sedimentation is recorded at MN-16-19 at 1592-1408 cal BP. Given that a coincident change in sea-level tendency is not recorded in the Minsmere cores situated closest to the coast, this negative sea-level tendency is not thought to reflect a decrease in tidal influence, due to the closure or narrowing of tidal inlets for example. In

addition, Lloyd et al. (2008) document tidal influence to be migrating further landwards (Figure 7.10- MM), with a positive sea-level tendency recorded ~ 2.3 km northwest of MN-16-19 at 1398-1291 cal BP. Diatom evidence in MN-16-19 records a large freshwater influx in the organic silt unit, prior to the onset of peat sedimentation at 1592-1408 cal BP, thought to be constrained by poor drainage. Evidence therefore indicates that this change in tendency is due to local factors.

Positive sea-level tendencies in MN-16-5 and MN-16-19 at 1265-1065 cal BP and 917-743 cal BP respectively, coincide with similar changes recorded further north at Westwood and Oldtown Marsh. On the north side of the New Cut, marine minerogenic sedimentation is sustained until 500-300 cal BP, meaning that Minsmere remains tidally influenced when the positive sea-level tendencies, associated with tidal flat sedimentation, are recorded at MN-16-5 and MN-16-19. Tidal flat sedimentation at MN-16-19 is associated with an increase, and subsequent decline, of marine planktonic taxa, with brackish epipelic taxa dominating. These positive sea-level tendencies may therefore indicate the expansion of tidal influence, potentially due to the widening of existing tidal inlets or expansion of creek development (Allen, 2000). The changes in sea-level tendency identified in this thesis in the Minsmere-Sizewell area indicate that tidal influence is dominant between c. 3500 and 750 cal BP. Lloyd et al. (2008) propose that, given the dominance of tidal influence, but absence of synchronous changes in tendency, Minsmere was open to the sea during this period, protected by a partial barrier, similar to that proposed by Pye and Blott (2006) for the Blyth. The results presented in this thesis for the Minsmere-Sizewell area support this conclusion, indicating that sediment supply and barrier dynamics were influential for back-barrier sedimentation during the late Holocene.

Historical maps and documents illustrate the influence of barrier dynamics on the coast at Minsmere. 'The Butlery Cartulary', a document dated to 1237, in addition to Saxton's 1575 and Kirby's 1737 map, illustrate that a small open coast estuary existed at Minsmere during these times (Steers, 1927; Axel and Hosking, 1977; Parker, 1978; Pye and Blott, 2006). Hodskinson's 1783 map illustrates that a barrier had developed, blocking the mouth of the estuary (Axel and Hosking, 1977; Pye and Blott, 2006; Rea Price and Robb, 2015). Reproductions of the coastal configuration relating to these maps are presented in Chapter 5. The results presented as part of this thesis for Sizewell do not dispute the hypothesis proposed by Lloyd et al. (2008), that tidal influence to this area migrated south from Minsmere behind the barrier system. The sedimentological transect at Sizewell is dominated by organic sedimentation, with a narrow organic-rich silt band associated with marginal tidal influence occurring only at its eastwards end.

Southwold-Dunwich area

Between Southwold and Dunwich, the southwest migration of tidal influence is documented by coincident positive sea-level tendencies from Oldtown Marsh (952-789 cal BP; 1161-998 cal AD) and Westwood Marsh (894-683 cal BP; 1267-1056 cal AD). In addition, a positive sea-level tendency, associated with the onset of marine saltmarsh and estuarine mud sedimentation is recorded on Dingle Marshes, neighbouring Dunwich, at c. 1100 AD (Sear et al., 2015). The nature of sedimentation at Oldtown and Dingle Marshes (Sear et al., 2015) differs, despite the coinciding positive sea-level tendencies, potentially reflecting differing proximities to the coast. Changes in sedimentation recorded on Dingle Marshes were attributed to storms breaching a gravel barrier or spit (Sear et al., 2015). However, there is no sedimentological evidence to indicate that the coincident positive sea-level tendency at Oldtown Marsh is attributable to a high magnitude event, with the onset of mudflat sedimentation associated with highly dynamic conditions with variable, and initially marginal, tidal influence.

Positive sea-level tendencies are also recorded further south at Minsmere during this time. This phase of positive sea-level tendency coincides with a period of coastal reorganisation between Southwold and Dunwich. Conceptual palaeogeographical reconstructions for this period (Figure 2.9) depict the Blyth River diverted south by Kingsholme spit which is estimated to have developed between c. 1500 and 700 AD, forming an estuary during Roman times (Gardner, 1754; Steers, 1927; Chant, 1974; Parker, 1978; Comfort, 1994; Pye and Blott, 2006). Storms during the 13th and 14th century halted spit development, blocking the entry to the haven and connecting the distal point of the spit with the Dunwich cliffs (Steers, 1927). A sufficient sediment supply would have been required for the development of Kingsholme spit, with increased supply necessary for continued southwards progradation. If insufficient, sediment recycling within the barrier system would create points of weakness, susceptible to breaching and the creation of tidal inlets, which would in turn influence the back-barrier sediment record. The interplay between sediment supply and spit development is therefore likely to have influenced the back-barrier sediment record, with an insufficient sediment supply increasing the risk of spit/barrier breach. The Domesday Book notes that over 50 % of the taxable farm land situated near Dunwich was lost to the sea between 1066 and 1086 AD, coinciding with the onset of minerogenic sedimentation at Westwood, Oldtown and Dingle Marshes (Gardner, 1754; Comfort, 1994; Sear et al., 2011).

Human impact on the back-barrier environments is likely to have been influenced by sediment availability and resulting barrier dynamics, with sediment sequences indicating that populations neighbouring Dunwich attempted to maintain access to the sea by

creating artificial breaches in the spit following the choking of the haven in the 14th century (Comfort, 1994). Records from the 18th century note that sand spreading was carried out to improve land drainage, and a thin layer of poorly sorted sand absent of marine indicators, is common at ~ 0.3 m on the north side of the New Cut at Minsmere (Lloyd et al., 2008). The timing of the cessation of tidal influence on the north side of the New Cut at Minsmere (500-300 cal BP) may indicate early manipulation of the environment by humans or may indicate the southwards extension of a pre-existing barrier across tidal inlets, however there is no evidence to differentiate between these. Further north, the enclosure of Westwood Marsh by a sea wall at the end of the 16th century left a distinctive signature on the upper sediment record at this site, with a return to peat sedimentation seen in the top 0.3 m.

East Anglia region

Existing stratigraphic research from the east Norfolk and northern Suffolk coast concluded that changes in sedimentation are not solely due to RSL and subsidence, and that local physiographical changes are important (Coles and Funnell, 1981; Brew et al., 1992; Boomer and Godwin, 1993). Barrier dynamics, and therefore sediment supply, have been identified as influential for the Holocene evolution of the Bure-Yare-Waveney estuary system (Coles and Funnell, 1981; Boomer and Godwin, 1993). The onset of peat sedimentation in this estuary system at c. 4.5 ka is interpreted to have formed when a barrier sealed the estuary mouth (Coles and Funnell, 1981). A return to minerogenic sedimentation by c. 2 ka, succeeded by sandy sediment containing estuarine and estuarine channel foraminifera, is associated with sheltered, followed by open, estuarine conditions (Coles and Funnell, 1981). This transition, and the strong incursion of marine water, is attributed to the destruction of an existing barrier, with the sustainment of peat sedimentation from c. 1.5 ka associated with the growth of the present day Great Yarmouth spit (Coles and Funnell, 1981; Brew, 1990; Boomer and Godwin, 1993). In northern Suffolk, the onset of clay sedimentation at 7605-7175 cal BP is associated with deposition of a brackish/marine shelly horizon, caused by a rapid incursion of marine influence due to the breach of a barrier or spit feature (Brew et al., 1992).

The analysis presented as part of this thesis, alongside existing findings, indicates that local sedimentological and morphological factors were more influential for the late Holocene configuration of the East Anglian coast than vertical changes in RSL, due to the low rate of RSL rise at this time (Shennan et al., 2018). These findings cover a larger spatial extent than the existing analysis, and most of the mid- and late Holocene. The variability of the sedimentary response on the east Norfolk and Suffolk coast indicates the importance of sediment supply to enable late Holocene barrier building, or breakdown, and

the creation of discrete sedimentary basins in the estuaries (Brew et al., 1992). Barrier development and the creation of small open coast estuaries were features of the Suffolk coast historically (Pye and Blott, 2006). The absence of a sufficient sediment supply for barrier development would increase the susceptibility of back-barrier environments to inundation (e.g. Carter et al., 1990; Kraus, 2004). In the southern North Sea basin, insufficient sediment supply has been proposed as a mechanism to explain the culmination of late Holocene peat growth (Beets et al., 1992; 1994; Baeteman, 1999).

7.4 Driving mechanisms of Holocene coastal evolution of the Suffolk coast

Reconstructions of the Holocene coastal evolution of the Suffolk coast, and comparisons with existing research for the East Anglia region, as part of this thesis have identified that the relative dominance of the driving mechanism for coastal change has varied temporally. This reflects existing research for the southern North Sea basin, which has determined spatial and temporal variations in the driving mechanisms of coastal change (van de Plassche, 1982; Long and Innes, 1993; Denys and Baeteman, 1995; Beets and van der Spek, 2000; Baeteman and Declercq, 2002).

The pattern of sea-level tendency for the East Anglian coast is regionally consistent for the mid-Holocene and is consistent with the change in the position of RSL during this period (Figure 7.9 A and C). This regionally consistent sea-level tendency indicates that the changes in sedimentation during the mid-Holocene were RSL-driven. This contrasts with the late Holocene, when sea-level tendency is inconsistent across East Anglia. In addition, the change in the position of RSL with time contrasts with the highly variable pattern of sea-level tendency for this period, indicating an influence of local factors. The sediment sequences presented as part of this thesis indicate that sediment supply and barrier dynamics were the primary driving mechanisms of late Holocene back-barrier sedimentation in Suffolk. RSL change during the late Holocene was only a secondary control on coastal sedimentation, exerting a minimal control on the significant changes in coastal evolution recorded in back-barrier sediments. The sediment record from the Blyth estuary also indicated that spit development and barrier dynamics were the primary controls of Holocene coastal evolution (Brew et al., 1992). The late Holocene is therefore associated with barrier building and the creation of distinct sedimentary basins in estuaries (Brew et al., 1992), with an increased sediment supply required to develop and maintain these features. Thus variations in sediment availability are likely to have been highly influential for the late Holocene evolution of the Suffolk coast.

Changes in sea-level tendency are recorded in isolation at different sections of the Suffolk coast i.e. occurring in the Walberswick NNR between c. 1000 and 500 cal BP, with

changes at Minsmere preceding this at c. 3500 to 750 cal BP whilst changes in tendency in the lower reaches of the Blyth are constrained to the mid-Holocene, with minerogenic sedimentation sustained throughout the late Holocene (Brew et al., 1992). The data presented for the late Holocene therefore indicate that a series of sediment release and supply pathways have existed on the Suffolk coast since at least 3 ka, the location of which changes through time. Figure 7.11 depicts the influence of changes in sediment release and supply pathways on back-barrier environments through time. Sedimentation changes recorded at a location may therefore reflect temporal changes in this spatial pattern of sediment release and storage, through erosion and deposition.
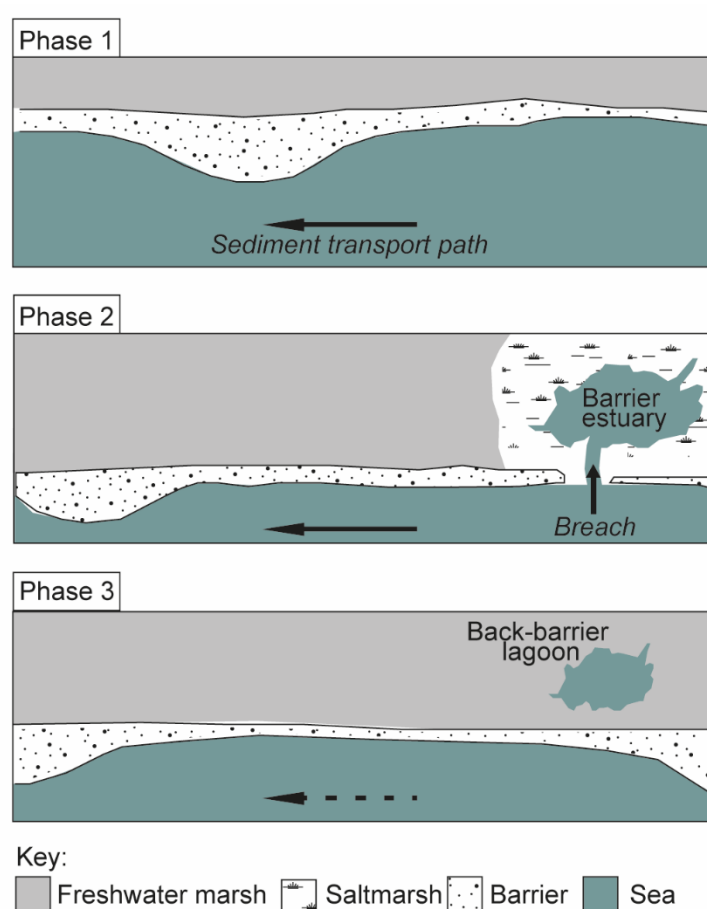
Figure 7.11: Schematic illustrating the spatially and temporally variable pattern of sediment release and supply pathways identified from the late Holocene data presented as part of this thesis. Phase 1 and 2 show the southwards movement of a sediment supply pathway. The limited sediment supply increases the vulnerability of sections of the barrier. Phase 2 shows the barrier breach that has resulted from a weak point in the barrier, creating a barrier estuary. Phase 3 shows a shift in the spatial pattern of sediment release and supply. The breach has annealed due to temporal changes in the spatial pattern of sediment release and storage, resulting from erosion and deposition.

Analysis of the instrumental record has identified that the evolution of the cliffs and shoreline on the Suffolk coast is spatially and temporally variable. Multiple modes of shoreline change have been identified for the Suffolk coast from cluster analysis of the relative position of the shoreline (1881-2015) and metrics of shoreline change, indicating the importance of sediment budget variations as a driver of multi-decadal coastal behaviour (Burningham and French, 2017). Analysis of the sediment release behaviour of the Suffolk cliff system identified a switching of states, between on, off and no change (Brooks and Spencer, 2012). The late Holocene data presented as part of this thesis, in addition to historical and instrumental data, suggest that the vulnerability of the Suffolk coast varies spatially and is dependent on a site's location relative to the pattern of sediment release and supply at a given time.

Attributing changes in sedimentation, from organic to minerogenic and vice-versa, to changes in RSL can oversimplify the interpretation of the sediment record and fail to give consideration to the complex interplay between sediment supply, barrier dynamics, rate of RSL rise and accommodation space, in addition to temporal variations in their relative importance. Adopting a regional approach is vital for distinguishing between sediment-driven and RSL-driven changes recorded in coastal sediments as these can result in similar sediment signatures (Gerrard et al., 1984; Jennings et al., 1995). Changes from marine to terrestrial conditions, and vice-versa, preserved in sediments from back-barrier environments have been shown to not necessarily reflect changes in RSL (Duffy et al., 1989). Barrier dynamics, including initiation, establishment and breakdown, is one example which will influence the back-barrier environment and have implications for the type of depositional environments formed (Orford et al., 1991). Compaction, whilst a significant vertical uncertainty associated with reconstructing RSL change, is of greater importance for coastal and RSL change if it is a causal factor in producing intercalated Holocene sequences (Shennan, 1986). Consideration must therefore be given to compaction as a driving mechanism of changes in sea-level tendency preserved in sediment sequences. Compaction is an ongoing process that lowers the sediment surface relative to the tidal frame resulting in the creation of accommodation space additional to that created by RSL rise (Devoy, 1982; Jennings et al., 1995; Long et al., 2006b). Long et al. (2006b) identified compaction as a key driving mechanism of late Holocene coastal change at Romney Marsh, with peat surface lowering of at least 3 m identified. The loading of a peat surface by sediment and water, following initial inundation of a site, would result in a positive feedback cycle whereby the accommodation space created by RSL rise would lead to compaction, additional accommodation space and further inter- and subtidal

sedimentation (Long et al., 2006b). This positive feedback cycle would result in sediment-driven changes in tendency to be preserved in the sediment record.

The substantially spatially and temporally variable sediment response preserved in the back-barrier records investigated in this thesis highlights the interplay between sediment availability, barrier dynamics and the rate of RSL change, in addition to local factors such as proximity to the coast and pre-Holocene topography. Inter-regional comparisons are necessary to differentiate between the multifactorial processes driving the Holocene evolution of a coastal system. The importance of local factors is demonstrated by the fact that whilst sediment records from east Norfolk and Suffolk contain similar patterns of coastal sedimentation, sea-level tendency for the late Holocene displays large differences in chronology (Coles and Funnell, 1981; Alderton, 1983; Brew et al., 1992; Horton et al., 2004). The major changes in coastal evolution occur predominantly during the late Holocene on the Suffolk coast, a period when the rate of RSL rise was low, making distinction between sediment-driven and RSL-driven changes in coastal sedimentation clearer.

The sediment sequences sampled and analysed as part of this thesis did not identify evidence of high magnitude events. However, storms are known to have influenced this coastline historically and in recent decades. The most notable example is Dunwich, where historical records indicate that storms have had a catastrophic impact during the last 1000 years, with 90 % of this medieval port settlement now submerged due to coastal recession (Sear et al., 2011). In addition, rates of erosion are documented to have been high (up to 4.5 m yr^{-1}) throughout the 20th century (Cambers, 1975; Carr, 1981; Brooks and Spencer, 2010; 2012). Sediment records containing evidence of high magnitude events may therefore be situated offshore of the present-day coast or have been lost due to coastal erosion and recession.

Chronological constraint for major coastal behavioural changes identified in this thesis, using microfossil and stratigraphic analyses, focussed on transitional contacts. This sampling strategy is common however the bias against eroded abrupt contacts may result in lithological signatures of sudden events being overlooked. Long and Innes (1995) highlight the difficulty of determining episodes of barrier breakdown and the associated erosion of back-barrier sediments from sediment records. Two schools of thought, gradualism and catastrophism, exist in studies of Holocene back-barrier environments (Spencer et al., 1998). For example, the significance of local processes such as barrier breakdown for sedimentation in the Romney marsh area have been debated (Tooley and Switsur, 1988; Jennings and Smyth, 1990). The Suffolk coastline may have had greater

geomorphological resilience to storms in the past. Research undertaken at Dungeness highlighted the inherent dynamism of resilient coastlines and their capacity for internal readjustment to changes in RSL, sediment supply and storms (Long et al., 2006a). In addition, the storms on the Suffolk coast may simply not have been large enough, as research indicates that large storms are very difficult to generate on the Suffolk coast (Pye and Blott, 2009). Storms may only have been able to act alongside the background control of sediment supply and/or erosion during the late Holocene.

Historical land use practices, such as drainage, reclamation, and peat cutting have resulted in land subsidence due to the loss, decay and consolidation of sediments (Allen, 1993; Hoeksema, 2007). This is a significant problem in the Netherlands, where a third of the land is situated below mean sea level and 65 % would be submerged at high tide without dunes, dikes and pumps (Hoeksema, 2007). Allen (1993) notes that the reclamation of estuaries and tidal embayments (e.g. the Fenland and the Severn Estuary) has resulted in ground surface elevational differences. In the Severn Estuary reclamation age is a primary control for the spatially variable elevation differences in the estuary (Allen, 1993). Ground surface elevation changes, resulting from land use practices, are likely to have occurred in Suffolk where ~ 11000 ha of saltmarsh have been reclaimed since the Roman period (Doody, 1996). Land use practices may explain the variable ground surface elevations at Minsmere (Figure 5.4), which show correspondence with the location of drainage ditches, representing land partitioning at different times.

Other methods, such as pollen and geochemical (elemental, molecular or isotope) analyses, may have provided additional insight into the driving mechanisms of Holocene coastal change in this thesis. Geochemical signatures in coastal sediments are a powerful tool for reconstructing environmental change during the Holocene, particularly when combined with micropalaeontological and sedimentological proxies (e.g. Dellwig et al., 1999; Dezileau et al., 2011; Kylander et al., 2011; Dinelli et al., 2012; McCloskey and Liu, 2012; Sparrenbom et al., 2013). Elemental profiles of sediment sequences have been used for the identification of extreme events due to their geochemically distinct signatures (Dezileau et al., 2011; Kylander et al., 2011; McCloskey and Liu, 2012). Elemental indicators can be subdivided into terrestrial (e.g. iron, titanium and chromium) and marine (bromine and chlorine) metals, providing evidence to aid the determination of barrier conditions (e.g. McCloskey and Liu, 2012). In addition, the abundance of particular elements is indicative of the energy of the environment. Zirconium and titanium, for example, are indicative of high-energy environments due to their association with the heavy mineral fraction (Dellwig et al., 1999). Litho- and bio-stratigraphic analysis did not identify evidence of high magnitude events. However, the non-destructive x-ray

fluorescence (XRF) core scanning technology would confirm if there is a geochemical signature of high magnitude events due to elemental concentrations being determined at a resolution of less than 0.5 cm (Croudace et al., 2006).

Problematic diatom preservation restricted palaeoenvironmental interpretation of the sampled peat deposits. Pollen analysis has been previously used to reconstruct vegetation communities in Holocene sea-level research (e.g. Godwin, 1940; Waller, 1994), with particular uses including the differentiation of peat types, such as salt versus freshwater peat (Bernhardt and Willard, 2015). In addition, pollen analysis can generate a 'skeleton of radiocarbon dates' (Moore et al., 1991), providing an overview of the relative age of the changes in sea-level tendency identified from diatom analysis. The pioneering research by Godwin (1940) used changes in the relative abundance of specific plant taxa from sediment cores to determine age control for reconstructions of Holocene sea-level change for the East Anglian Fenland. In sea-level research, changes in the abundance of a particular pollen taxa, such as the *Ulmus* decline during the mid-Holocene and the increased frequencies of *Pinus* pollen in southern England during the last c. 300 years (Long et al., 1999), have been associated with a specific age to produce chronohorizons (Bernhardt and Willard, 2015).

In addition, carbon stable isotope geochemistry ($\delta^{13}C$) and the ratio of organic carbon to total nitrogen (C/N ratio) are being increasingly used to reconstruct coastal environments and overcome issues encountered with microfossil preservation (Lamb et al., 2006; Khan et al., 2015a). $\delta^{13}C$ and C/N ratios have been previously used to determine the provenance of organic matter from coastal archives (Khan et al., 2015b; Wilson, 2017; Kemp et al., 2019), as these methods can distinguish between the isotopically distinct C_3 (e.g. *Phragmites australis*) and C_4 (e.g. *Spartina patens*) vegetation, as well as freshwater and marine organic matter. More recently, compound-specific $\delta^{13}C$ analysis (e.g. from specific n-alkanes that are known to originate from specific types of vegetation) has been used to refine organic matter provenance, as algae and bacteria present in bulk samples can affect the ability to differentiate between organic matter sources; thus hindering the identification of vegetation zones (Lamb et al., 2006; Kemp et al., 2010; Tanner et al., 2010). In addition, developments in dating methodologies since the end of the 20th century allows radiocarbon dating of compound-specific isotopes of lacustrine and marine sediments (e.g. Eglinton et al., 1997; Ohkouchi and Eglinton, 2008; Yamane et al., 2014). This dating technique has not been used in the field of sea level and coastal research but would provide a means to extend chronological constraint to transitional clastic units in which plant macrofossils for radiocarbon dating are limited or absent.

Determining a given site's future vulnerability or resilience is complicated by the existence of multiple sediment release and supply pathways and their spatial variance through time (Figure 7.11). The rate of RSL rise was low during the late Holocene, when a temporally variable spatial pattern of sediment release and supply is proposed as an important control on coastal evolution. However, coastal systems such as Suffolk, and elsewhere in the southern North Sea basin, are currently responding to a faster rate of RSL rise than that identified for the mid- and late Holocene (Defra, 2006; Church et al., 2013; Burningham and French, 2017; Cazenave et al., 2018). Global mean sea level during the late Holocene rose at an average rate comparable with the mid-to-late 19th century and 20th century (~1.2 to 1.9 mm yr^{-1}) (Woodworth et al., 2009; Cazenave et al., 2018). However, satellite altimetry has determined a global mean sea level rise rate of 3.1 ± 0.3 mm yr^{-1} for the last 25 years (Cazenave et al., 2018), exceeding the late Holocene average. The future response of an anthropogenically modified coastline to a temporally variable spatial pattern of sediment release and supply pathways, whilst RSL is rising, is uncertain and requires careful consideration and incorporation into coastal management strategies. Interventions previously effective for ensuring resilient coastlines may no longer be appropriate, as outcomes are likely to differ due to the increase in rate of RSL rise. At present, sediment supply and coastal erosion are the most important drivers of coastal change however, these factors will be secondary to RSL rise in the future, particularly as rates of RSL rise comparable with the early Holocene become increasingly common during the 21st century.

Chapter 8: Conclusion

This thesis aimed to reconstruct Holocene coastal evolution, using the Suffolk coast as a case study, to improve understanding of long-term (millennial) coastal behaviour. The objectives of this research were to (1) reconstruct changes in RSL, (2) identify variations in sediment supply and the influence of barrier dynamics on back-barrier sedimentation and (3) determine the behaviour of barrier and back-barrier environments in response to (1) and (2).

Extensive stratigraphic investigation demonstrated significant spatial and temporal differences in sedimentation at sites on the Suffolk coast. A multiproxy approach, comprising sedimentological, bio- and chronostratigraphic methods, identified and constrained the timing of major phases of coastal change. Inter-regional comparisons with existing stratigraphic data aided the determination of the potential driving mechanisms responsible for these changes.

8.1 Key findings

1. Pattern, chronology and altitude of sedimentation

Stratigraphic transects completed in a 12 km section of the Suffolk coast, at Westwood Marsh, Oldtown Marsh, Great Dingle Hill, Minsmere and Sizewell, identified both similar and contrasting sedimentation patterns. Sedimentation at Oldtown Marsh was characterised by three periods of freshwater peat sedimentation separated by brackish-marine minerogenic sedimentation, comparable to sequences identified inland at Minsmere (MN-16-19). However, further south, organic sedimentation dominates the Holocene sediment sequences at Sizewell, with a single unit of minerogenic sedimentation only found nearest the coast. Levelling (to m OD) of the stratigraphic data and AMS radiocarbon dating of the sample cores identified inter-site variability in the altitude and chronology of sediment changes, irrespective of comparability of sedimentation patterns. For example, the cessation of the first phase of marine-brackish sedimentation occurred at 1592-1408 cal BP inland at Minsmere (MN-16-19), c. 700 cal BP prior to a similar transition at Oldtown Marsh. Stratigraphy also identified intra-site variability. At Minsmere, minerogenic sedimentation dominated the Holocene sequence nearest the coast, whereas 1 km inland, the dominance of minerogenic sedimentation decreases, revealing a peat infilled basin which, following inundation, was later drained.

The stratigraphic data in this thesis has identified clear evidence for inter- and intra-site variability in sedimentation. In addition, stratigraphically comparable Holocene sequences across all sites did not necessarily equate to altitudinal or chronological similarity. These

findings indicate that local factors (e.g. sedimentological or morphological) have influenced coastal sedimentation at the investigated sites during the Holocene.

2. Palaeoenvironmental reconstructions

A combination of sedimentological and biostratigraphic methods were used to reconstruct palaeoenvironmental change preserved in the sampled cores. This multiproxy method is employed extensively in coastal evolution and RSL change research (e.g. Zong and Tooley, 1999; Freitas et al., 2002; Long et al., 2006b; Bao et al., 2007), and provides an independent means of determining the mechanisms driving sedimentation, in addition to reconstructing changes in RSL. Basal peats constrained the onset of peat deposition and rising regional ground water level (Törnqvist et al., 1998) whilst changes in sea-level tendency, determined from biostratigraphic analysis, were associated with transitions from freshwater or saltmarsh to intertidal environments, and vice-versa.

Sedimentological and biostratigraphic analysis enabled changes in sea-level tendency to be identified and provided valuable evidence relating to the occurrence of phases of paludification, terrestrialisation, compaction and the nature of the depositional environment (e.g. Gehrels et al., 2001; Plater et al., 2015). The ecological classification of diatoms, based on life form and salinity with associated sedimentary environment (Vos and De Wolf, 1988; 1993), produced interpretations exceeding that gained from assessing salinity changes in isolation. The chronology presented as part of this thesis was crucial in allowing inter- and intra- site comparisons to be made, in order to determine whether regional or local factors were driving Holocene coastal change. It also improves constraint for RSL change during the last 4000 years, filling a temporal gap in the RSL history of the Suffolk coast.

3. RSL change as a driving mechanism of coastal change

The 16 new sea-level index points (11 intercalated peat and 5 basal peat samples) support the gradual RSL rise reconstructed by published RSL data for southeast England (Shennan et al., 2018). Freshwater limiting data constrain the position of RSL beneath -3.68 m between c. 7400 and 6000 cal BP, with the sea-level index points, resulting from intercalated peat samples, documenting the position of RSL since c. 3000 cal BP.

The altitude of the sea-level index points varies, from -6.58 m to -2.57 m, during the late Holocene. In particular, chronologically overlapping index points from Westwood Marsh, Oldtown Marsh and Minsmere indicate that that the position of RSL varies by 2 m in a c. 200 year period. A strong correlation was identified between elevation residuals (reconstructed RSL-predicted RSL), overburden thickness and total thickness of the Holocene sequence, indicating that compaction had a significant effect on the new

intercalated index points, potentially explaining a proportion of their scatter throughout the late Holocene. Other explanations could include changes in tidal range or an underestimation of the age and/or elevation error (Shennan et al., 2018).

The existing RSL database for East Anglia contains 39 published and 7 unpublished sea-level index points (Coles and Funnell, 1981; Devoy, 1982; Alderton, 1983; Brew et al., 1992; Horton et al., 2004; Lloyd et al., 2008). These cover the last 10000 cal BP, documenting a gradual rise of RSL from -20 m to -0.69 m by 400 cal BP, consistent with regional GIA model predictions (Bradley, personal communication 2019). The late Holocene sea-level index points resulting from this thesis fills temporal gaps in our understanding of RSL during this period, particularly for the last 2000 years. The existing sea-level index points, in addition to those presented as part of this thesis, plot beneath the GIA model predictions of RSL. However, the elevation residuals for the index points presented in this thesis are greater (up to 6 m) than those for existing index points (up to 4 m) for the late Holocene despite compaction being quantified for neither. Index points for Minsmere from this thesis plot RSL up to 5 m lower than those produced by Lloyd et al. (2008), despite chronological overlap. The disparity between the new sea-level index points, existing points and GIA model predictions may be due to increased compaction from the new Minsmere sequences, or changes in tidal range. Changes in coastal configuration is known to result in significant changes in local tides (Griffiths and Hill, 2015; Shennan et al., 2018), and historical evidence indicates that small open coast estuaries existed on the Suffolk coast, and have since been blocked by shingle and sand barriers (Pye and Blott, 2006). The position of sea-level index points would be too high if palaeotidal range had been larger, as the reference water level of a deposit would be higher than the modern equivalent therefore reconstructions of RSL would be lower.

The pattern of sea-level tendency for the East Anglia region was consistent for the mid-Holocene, with predominantly positive changes recorded, whilst during the late Holocene the pattern was substantially variable. In addition, the changes in sea-level tendency during the mid-Holocene were consistent with the change in the position of RSL for this period whilst this comparison for the late Holocene identified a contrast with the position of RSL. The pattern of sea-level tendency for the East Anglia region indicates that the primary driving mechanism of coastal change has varied temporally during the Holocene. The regionally consistent pattern during the mid-Holocene indicates that coastal sedimentation was controlled by RSL, whereas the variability in the late Holocene indicates that local factors influenced coastal sedimentation, with RSL acting only as a background control.

Regional comparisons of sea-level tendency are essential due to the depositional equifinality of RSL- and sediment-driven changes in sediment records. The identified changes in sea-level tendency during the last c. 3000 cal BP display asynchronies both inter-site and with existing research from east Norfolk and Suffolk. Given their localised nature, it is unlikely that these changes are RSL-driven, as this would form a regionally synchronous record (Shennan et al., 2018). These changes occurred during the late Holocene, when the rate of RSL rise was low in comparison to the early and mid-Holocene (Shennan and Horton, 2002; Horton et al., 2004). This means that local sedimentological and morphological factors, as opposed to vertical changes in RSL, primarily controlled the nature of back-barrier sedimentation, with sediment availability, and associated barrier dynamics, controlling the resilience of back-barrier environments to tidal inundation as RSL rose gradually.

4. Barrier dynamics and sediment supply as driving mechanisms of coastal change

The variable inter-site sediment response identified as part of this thesis indicates an influence of local factors such as marsh accretion response, compaction, topography, morphology of the underlying geology, proximity to the coast and human influence, which must be given due consideration. Factors such as this have been identified as important for the evolution of the southern North Sea basin area during the late Holocene (Vos and van Heeringen, 1997; Baeteman et al., 2002; Pierik et al., 2017). In addition, existing stratigraphic research completed on the east Norfolk and Suffolk coast identified barrier and spit development, and therefore sediment availability, as influential for late Holocene coastal change (Coles and Funnell, 1981; Brew et al., 1992; Lloyd et al., 2008).

Changes in sea-level tendency during the late Holocene occur in phases, isolated to different sections of the Suffolk coast. Changes in sea-level tendency are predominantly recorded in the Minsmere-Sizewell area from c. 3500 to 750 cal BP, whereas changes occur near the Walberswick NNR after c. 1000 cal BP. This variability in sea-level tendency reflects variations in sediment supply and the resulting influence of barrier dynamics, with its temporally and spatially variable nature attributed to variation in the location of sediment pathways during the last 3000 years.

Contemporary, analysis of the coastal changes of the Suffolk coast has identified the importance of sediment budget variations as a driver of multi-decadal coastal behaviour (Burningham and French, 2017), with multiple modes of sediment release behaviour identified for the Suffolk cliff system (Brooks and Spencer, 2012), a major input for East Anglia's sediment budget. Historical and instrumental data, in addition to the late Holocene

data presented as part of this thesis, indicate that the vulnerability of the Suffolk coast has varied spatially, dependent on the location of a site relative to the pattern of sediment release and supply at a given time. Based on this concept, determining the vulnerability or resilience of a given site would be difficult due to the stochastic nature of changes in this spatial pattern through time.

5. Storm influence on coastal change

Evidence of high-magnitude events was not identified at any of the sites investigated in this thesis. However, given that coastal erosion is well documented on the coastline (Cambers, 1975; Carr, 1981; Brooks and Spencer, 2010; 2012), a sediment record of storm occurrence may now be offshore. Chronologically overlapping changes in sea-level tendency were identified near Dunwich at Dingle Marshes (Sear et al., 2015) and at Oldtown Marsh (this thesis) at c. 1100 AD. The nature of the sedimentation varies at these sites, with the onset of minerogenic sedimentation associated with sand at Dingle Marshes but not at Oldtown Marsh. The positive sea-level tendency at Dingle Marshes is attributed by Sear et al. (2015) to storms breaching a gravel barrier or spit. The coincident changes at these sites, despite differences in sedimentation, may indicate the influence of proximity to the coast, topography and/or availability of sand. At present, both sites are proximal to the coast, with Oldtown Marsh sheltered by surrounding high relief and Dingle Marshes more exposed behind the coastal barrier.

The absence of storm signatures in the back-barrier sediment sequences may be because the Suffolk coast had greater geomorphological resilience to high-magnitude events during the Holocene. This hypothesis is discounted for the late Holocene because local sedimentological and morphological factors were the primary driving mechanisms of coastal evolution. Changes in sedimentation may have been influenced by high-magnitude events, but the signature was not recorded due to the influence of local factors (e.g. Pierik et al., 2017) or the storms not being large enough. In addition, high magnitude events may have influenced the creation of tidal inlets through the barrier system, with a reduction in resilience linked to a limited sediment supply.

6. Anthropogenic influence on coastal change

The record of natural coastal change can be modified by anthropogenic activity that has occurred across the coast. Therefore, the negative sea-level tendencies identified as part of this thesis, cannot be conclusively attributed to sediment-driven processes. Consideration must be given to human activities and the resulting back-barrier signatures they would cause. Coastal environments in Suffolk were important for the coastal populations' economy (Rippon, 2000). The configuration of the Suffolk coast, including

the development of Kingsholme spit (1500 and 700 AD), is known to have impacted nearby coastal populations. Further, the configuration of the coast between Southwold and Dunwich is documented to have been crucial in Dunwich becoming one of the most important cities in Suffolk by Saxon times (Chant, 1974; Comfort, 1994). In addition, the blockage of Dunwich harbour by the 14th century, due to storms and the southwards growth of Kingsholme spit, led to Dunwich's decline (Sear et al., 2011) and resulted in neighbouring populations creating artificial breaches in the spit to try and maintain access to the sea (Comfort, 1994).

Further alteration of back-barrier environments, through embanking, drainage and reclamation, occurred at an accelerated from the 16th and 17th century in Suffolk (Williamson, 2005). Recent (1970s) attempts to manage the Suffolk coast have included the bulldozing of sand and shingle from the seawards side of the barrier to create a flood defence to prevent washover at Dunwich (Pye and Blott, 2009). The utilisation and management of coastal wetlands by humans has left distinctive signatures on the landscape and in the sediment records, such as sand layers indicating drainage improvements (Lloyd et al., 2008).

7. Implications for future coastal change and resilience

Suffolk and other coastal systems in the southern North Sea basin are currently responding to a rate of RSL rise faster than that identified for the mid- and late Holocene (Defra, 2006; Church et al., 2013; Burningham and French, 2017; Cazenave et al., 2018). The future resilience of an anthropogenically modified coastline to a temporally variable spatial pattern of sediment release and supply pathways, whilst RSL is rising, requires consideration and incorporation into coastal management strategies. The future response of coastlines is likely to differ due to the increase in RSL rise therefore coastal managers may need to reassess previously 'successful' practice, as previous interventions may be rendered ineffective. Future RSL rise will result in sediment supply and coastal erosion becoming secondary drivers of coastal change, particularly as RSL rise rates comparable with the early Holocene become increasingly common during the 21st century.

8.2 Future research

Statistical analysis indicated that compaction had a significant effect on the new intercalated index points produced as part of this thesis due to the thickness of the overall Holocene sediment sequence and individual peat units. The post-depositional lowering of these intercalated index points from their original elevation introduces uncertainties into estimates of the rate and magnitude of late Holocene RSL change (Kaye and Baghoorn, 1964; Brain, 2015). A geotechnical model (e.g. Paul and Barras, 1998; Van Asselen, 2011;

Brain et al., 2012) could be used to decompact the sampled sediment sequences, correcting the elevation of sea-level index points to their original depositional altitude. However, compaction is difficult to quantify and rarely accounted for (Baeteman et al., 2011; Shennan et al., 2018).

Given the high rates of erosion the Suffolk coast has experienced (Cambers, 1975; Carr, 1981; Brooks and Spencer, 2010), a proportion of the record of Holocene coastal change will be preserved offshore of the present day coast. Tying the onshore and offshore records together would provide a more complete picture of coastal evolution in Suffolk. Improving understanding of the offshore sand bank and bar features, including their relationship with the adjacent coastline, sediment budget and wave climate, would be beneficial as these dynamic features are likely to be influential for sediment transport on this coast. The extension of the Sizewell banks, its coalescence with the Dunwich Bank in the 1920s, and their landwards movement offshore of the Dunwich-Minsmere cliffs (Carr, 1979) is well documented. However, the transport of sediment in the nearshore system and the interaction with the offshore banks is greatly debated (Carr, 1981), with contradictory evidence on whether they acted as sediment sinks or morphologically influenced wave climate and tidal currents (McCave, 1978; Lees, 1983; Brooks and Spencer, 2010). The sediment gained on the Sizewell-Dunwich bank between 1824 and 1965 has been equated to the volume of sediment eroded from the Suffolk coast during this time (Carr, 1979; 1981; Brooks and Spencer, 2010). A slowing of cliff retreat between Dunwich and Minsmere and a period of growth of the Sizewell-Dunwich Bank system since 1925, has been attributed to sediment input from the rapidly eroding Covehithe, Easton and Benacre cliffs, in northern Suffolk, to the banks (Pye and Blott, 2006; Brooks and Spencer, 2010). In addition, the current stability of the coast at Dunwich, despite the narrow, sediment limited beach, has led to suggestions of a sheltering effect from the Sizewell-Dunwich bank (Robinson, 1980; Brooks and Spencer, 2010).

Ongoing research being undertaken as part of the BLUEcoast project, led by University of Liverpool and the National Oceanography Centre, will improve understanding of the offshore system on the Suffolk coast. A marine radar survey undertaken at Minsmere aims to gather continuous bathymetric data for the Dunwich-Sizewell bank and subtidal nearshore bars, providing information relating to offshore morphology and sediment migration patterns. The palaeoenvironmental dataset could be enhanced by studying sediment provenance to investigate further the series of sediment release and supply pathways proposed for the late Holocene. In addition, geophysical survey techniques might enable a more rapid and spatially extensive determination of stratigraphy to inform core sampling.

Appendices

Appendix 1

Sediment sequences sampled by Lloyd *et al.* (2008) *at Minsmere and Sizewell with radiocarbon dates and palaeoenvironmental interpretation. Location of each sampled and analysed core is noted on the associated map. Adapted from* Lloyd *et al.* (2008)*.*

The figure originally presented here cannot be made freely available via LJMU E-Theses Collection because copyright permissions have been unattainable. The data in the figure was sourced from Lloyd, J.M., Zong, Y., Woods, A., 2008. Preliminary investigation of the relative sea-level and inundation history of the Sizewell and Minsmere coastline, Suffolk, British Energy Estuarine and Marine Studies. Technical Report 07/08 no. 015.

Appendix 2

Common sediment types, humicity, physical properteries and bondary conditions for coastal sediments (Long *et al.*, 1999) *based on the Troels-Smith classification scheme* (Troels-Smith, 1955) *with moderations (*) by* Aaby and Berglund (1986)*.*

Name	Code	Sediment type	Field characteristics
Argilla steatodes	As	Clay < 0.002 mm	May be rolled into a thread < or = 2 mm diameter without breaking. Plastic when wet, hard when dry.
Argilla granosa	Ag	Silt 0.06-0.002 mm	Will not roll into thread without splitting. Will rub into dust on drying (such as on hands). Gritty on back of teeth.
Grana minora*	Gmin	Fine, medium and coarse sand (0.06-2.0 mm)	Crunchy between teeth. Lacks cohesion when dry. Grains visible to the naked eye.
Grana majora*	Gmaj	Fine, medium and coarse gravel (2-60 mm)	
Testae (molluscorum)	Tm	Whole mollusc shells	
Particulae testarum (molluscorum)	Ptm	Shell fragments	
Substantia humosa	Sh	Humified organics beyond identification	Full disintegrated deposit lacking macroscopic structure, usually dark brown or black.
Turfa herbacea	Th$^{0-4}$	Roots, stems and rhizomes of herbaceous plants	Can be seen vertically aligned or matted within sediment in growth position.
Turfa bryophytica	Tb$^{0-4}$	The protonema, rhizods, stems, leaves etc. of mosses	Can be seen vertically aligned or matted within sediment in growth position.
Turfa lignosa	Tl$^{0-4}$	The roots and stumps of woody plants and their trucks, branches and twigs	Can be seen vertically aligned or layered within sediment in growth position.
Detritus lignosus	Dl	Detrital fragments of wood and bark > 2 mm	Non-vertical or random alignment. May be laminated, not in growth position.
Detritus herbosus	Dh	Fragments of stems and leaves of herbaceous plants > 2 mm	Non-vertical or random alignment. May be laminated, not in growth position.
Detritus granosus	Dg	Woody and herbaceous humified plant remains < 2 mm > 0.1 mm that cannot be separated	Non-vertical or random alignment. May be laminated, not in growth position.
Limus detrituosus	Ld$^{0-4}$	Fine detritus organic mud(particles < 0.1 mm)	Homogeneous, non-plastic, often becomes darker on oxidation and will shrink on drying. Most shades of colour.
Limus ferrugineus	Lf	Mineral and/or organic iron oxide	Forms mottled staining. Can be crushed between fingers. Often in root channels or surrounding Th.

Anthrax	Anth	Charcoal	Crunchy black fragments.
Stirpes	Stirp	Tree stump	
Stratum confusum	Sc	Disturbed stratum	

Humicity	Comment
0	Plant structure fresh. Yields colourless water on squeezing.
1	Plant structure well-preserved. Squeezing yields dark coloured water. 25 % deposit squeezes through fingers.
2	Plant structure partially decayed though distinct. Squeezing yields 50 % deposit through fingers.
3	Plant structure decayed and indistinct. Squeezing yields 75 % deposit through fingers.
4	Plant structure discernible or absent. 100 % passes through fingers on squeezing

Nigor (Degree of darkness)	
0	The shade of quartz sand
1	The shade of calcareous clay
2	The shade of grey clay
3	The shade of partly decomposed peat
4	The shade of black, fully decomposed peat

Stratificatio (Degree of stratification)	
0	Complete herterogeneity: breaks equally in all directions
1	Intermediate between 0 and 4
2	Intermediate between 0 and 4
3	Intermediate between 0 and 4
4	Very thin horizontal layers that split horizontally

Siccitas (Degree of dryness)	
0	Clean water
1	Thoroughly saturated, very wet
2	Saturated
3	Not saturated
4	Air dry

Elasticitas (degree of elasticity)	
0	Totally inelastic, plastic
1	Intermediate between 0 and 4
2	Intermediate between 0 and 4
3	Intermediate between 0 and 4
4	Elastic

Limes superior (boundary)	
0	> 1 cm boundary area- *diffusus*
1	< 1cm and > 2 cm- *conspicuus*
2	< 2 mm and > 1 mm- *manifestus*
3	< 1 mm and > 0.5 mm- *acutus*
4	< 0.5 mm

Appendix 3

Selection procedure used to determine the appropriate number of end-members

The coefficient of determination (r^2) and angular differences between the original particle size data and reconstructions were used to determine the goodness of fit and the optimal number of end-members (q). The coefficient of determination (Figure A1.1A) equates to the proportion of variance within the observed data set which can explained by a model with q end-members. The inflection point of the curve, when the number of end-members is plotted against r^2, was used to identify the optimal number of end-members. The angular deviation (Figure A1.1B) indicates the degree to which the observed data set can be explained by q end-members. The smaller the angular difference, the stronger the correlation between the observed data set and q end-members. In the example below (Figure A1) the optimal number of end-members was 2, based primarily on the high R^2 value and low linear correlation between end-members.
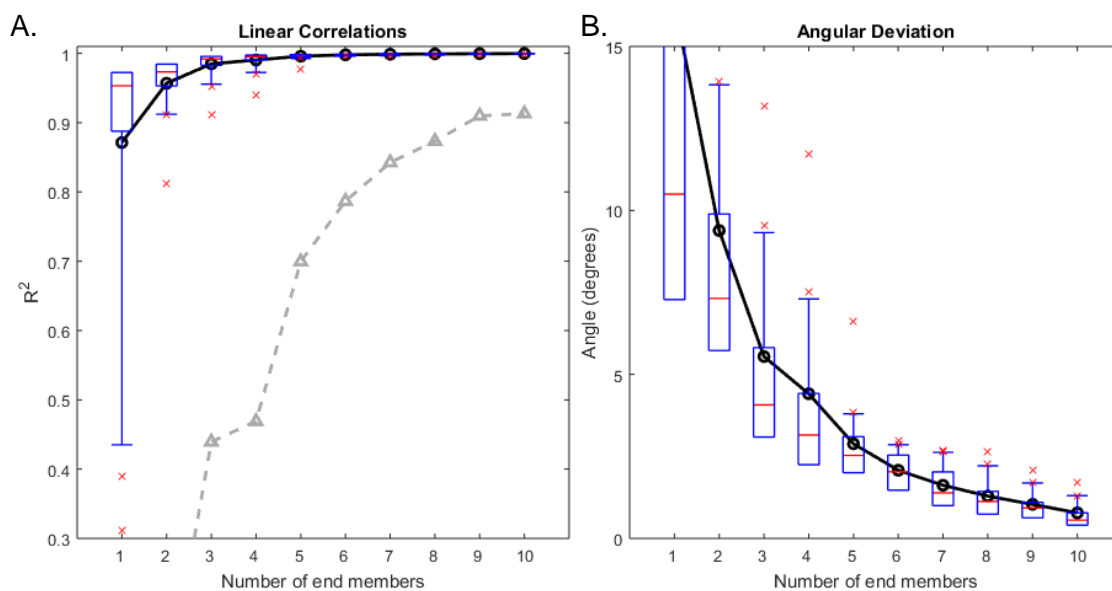
Figure A1.1: A. The squared linear correlations are displayed as a function of the number of end members. B. The angular deviation equates to the angular differences (in degrees) between the reconstructed and observed data sets as a function of the number of end members. In both plots the solid black lines and circles are the model misfit to the whole data set, the blue box and whiskers represent the values determined from individual specimens. The red bars are the median values, the blue boxes are the interquartile range, and the blue whiskers mark out the one-sided 95th percentiles (i.e., the 95% coverage interval). The red crosses represent outlying specimens (i.e., specimens that lie outside of the 95% coverage interval). The grey dashed line and triangles on the left hand plot is the maximum squared linear correlation between the different fitted end members. This is a measure of the linear independence of the end members.

Appendix 4

Methodology for diatom preparation (Palmer and Abbott 1986; Battarbee 1986)

A sample weighing approximately 0.5 cc was placed into a beaker and 20 ml of hydrogen peroxide (400 ml of 30 % weight of volume hydrogen peroxide topped up to 2 litres with de-ionized water) was added to digest organic material. The organic material was removed to ensure optimum visibility when identifying the microfossils. These beakers were placed on a hot plate to aid digestion. Digestion was complete once the solution had turned clear. Hydrogen peroxide was removed using a vacuum pump, following which they were topped up to 25 ml with distilled water.

Microscope slides were prepared by pipetting drops of the sample onto cover slips after which drops of distilled water were added. When the cover slips were dry, slides were labelled and drops of Naphrax added to each, to mount the cover slips. The cover slips were inverted and placed on top of the Naphrax and the slides were then placed on the hot plate. The slides remained on the hot plate until the toluene solvent was removed from the Naphrax.

Appendix 5

Methodology for picking foraminifera (Scott and Medioli, 1980)

Samples were wet sieved between 63 μm and 500 μm and the subsample exceeding 63 μm collected in a beaker. A Pastuer pipette was used to transfer a portion of the sediment into a counting tray for identification and picking. Samples were counted under a binocular microscope, at 32 times magnification, and foraminifera found were counted and identified. Once investigated, samples were stored wet in centrifuge tubes and kept refrigerated.

Appendix 6

Methodology for picking plant macrofossils and sample pretreatment prior to radiocarbon dating (Mauquoy and Van Geel, 2007)*.*

Sample added to beaker with 10 % NaOH and topped up to 100 ml with deionised water and left overnight to disaggregate the sample. Samples were sieved though 500 µm and 250 µm sieve. The 500 µm fraction was wet picked and the 250 µm sieve was checked for identifiable macrofossils. Identified macrofossils (C. Hunt, personal communication) were stored in vials with deionised water and several drops of 10 % HCl to acidify the sample.

Upon arrival at the NERC Radiocarbon Dating Facility (East Kilbride, Scotland) samples were digested in 2M HCl (80°C, 8 hours), washed free from mineral acid with deionised water, dried and homogenised. The total carbon in a known weight of the pre-treated sample was recovered as CO_2 by combustion with CuO in a sealed quartz tube. The gas was converted to graphite by Fe/Zn reduction.

Samples analysed at Beta Analytic underwent the acid-alkali-acid pretreatment method prior to radiocarbon dating. Gently crushed samples were dispersed in deionized water, washed with hot HCL acid to remove carbonates, following which an alkali wash (NaOH) was completed to remove secondary organic acids and a final acid rinse neutralises the solution prior to drying. The total carbon in a known weight of the pre-treated sample was recovered as CO_2 by combustion in an oxygen stream or through direct reaction with reduced CuO. The Bosch reaction between carbon dioxide and hydrogen was used to produce elemental carbon (graphite), water and heat.

Appendix 7

Samples submitted and resulting radiocarbon dated, conventional and calibrated, for all sites

Site	Sample ID	Latitude	Longitude	Lab. Code	NERC Allocation number	^{14}C ± 1σ BP	Cal age (cal BP)- full 2σ range	
							Max	Min.
Great Dingle Hill	GDH-16-2 -2.11 m OD	52º18'0.00"N	1º38'34.00"E	SUERC-72912	2037.1016	2440 ± 35	2701	2357
Great Dingle Hill	GDH-16-2 -2.29 m OD	52º18'0.00"N	1º38'34.00"E	SUERC-76469	2037.1016	2775 ± 37	2956	2783
Oldtown Marsh	OTM-16-13 -2.03 m OD	52º18'22.80"N	1º38'43.50"E	SUERC-72907	2037.1016	965 ± 39	952	789
Oldtown Marsh	OTM-16-13 -5.64 m OD	52º18'22.80"N	1º38'43.50"E	SUERC-72911	2037.1016	5209 ± 35	6170	5906
Oldtown Marsh	OTM-16-13 -2.45 m OD	52º18'22.80"N	1º38'43.50"E	BETA-498399	NA	970 ± 30	933	796
Westwood Marsh	WM-15-6 -1.77 m OD	52º18'1.57"N	1º36'57.86"E	SUERC-72906	2037.1016	836 ± 35	894	683
Westwood Marsh	WM-15-6 -4.01 m OD	52º18'1.57"N	1º36'57.86"E	BETA-512111	NA	9220 ± 40	10501	10258
Minsmere	MN-16-1 -5.62 m OD	52º14'14"N	1º37'24"E	SUERC-79046	2075.1017	4099 ± 39	4816	4447
Minsmere	MN-16-3 -3.71 m OD	52º14'14"N	1º37'24"E	SUERC-79047	2075.1017	2014 ± 38	2101	1880
Minsmere	MN-16-5 -3.05 m OD	52º14'14"N	1º37'24"E	SUERC-79048	2075.1017	1231 ± 38	1265	1065
Minsmere	MN-16-19 -3.63 m OD	52º14'14"N	1º37'24"E	SUERC-79052	2075.1017	909 ± 37	917	743

Site	Sample ID	Latitude	Longitude	Lab. Code	NERC Allocation number	^{14}C ± 1σ BP	Cal age (cal BP)- full 2σ range	
							Max	Min.
Minsmere	MN-16-19 -4.98 m OD	52º14'14"N	1º37'24"E	SUERC-79053	2075.1017	1613 ± 35	1592	1408
Minsmere	MN-16-19 -5.54 m OD	52º14'14"N	1º37'24"E	SUERC-79054	2075.1017	1920 ± 38	1966	1738
Minsmere	MN-16-19 -9.28 m OD	52º14'14"N	1º37'24"E	SUERC-79055	2075.1017	5266 ± 140	6310	5670
Sizewell	SW-17-1 -2.99 m OD	52º13'04"N	1º36'34"E	SUERC-80965	2112.0418	5263 ± 38	6179	5931
Sizewell	SW-17-13 -2.77 m OD	52º13'04"N	1º36'34"E	SUERC-80966	2112.0418	1431 ± 37	1386	1290
Sizewell	SW-17-13 -3.13 m OD	52º13'04"N	1º36'34"E	SUERC-80967	2112.0418	1444 ± 37	1395	1294
Sizewell	SW-17-13 -6.92 m OD	52º13'04"N	1º36'34"E	SUERC-80968	2112.0418	6339 ± 35	7412	7170
Sizewell	SW-17-3 -4.07 m OD	52º13'04"N	1º36'34"E	UCIAMS-210609	2112.0418	5570 ± 30	6405	6301

Appendix 8

Sediment supply and barrier dynamics as driving mechanisms of Holocene coastal change for the southern North Sea basin.

Christine A. Hamilton[a*], Jason R. Kirby[a], Timothy P. Lane[a], Andrew J. Plater[b], Martyn P. Waller[c]

[a]*School of Natural Sciences and Psychology, Liverpool John Moores University, Byrom Street, Liverpool, L3 3AF, UK*

[b]*Department of Geography, University of Liverpool, Roxby Building, Liverpool L69 7ZT, UK*

[c]*Department of Geography and Geology, Kingston University London, Penrhyn Road, Kingston upon Thames, Surrey, KT1 2EE, UK*

*Corresponding author: C.A.Hamilton@2015.ljmu.ac.uk/christine.hamilton246@gmail.com

Abstract

The combined effects of climate change and human impact lead to regional and local coastal responses that pose major challenges for the future resilience of coastal landscapes, increasing the vulnerability of communities, infrastructure and nature conservation interests. Using the Suffolk coast, southeast England, as a case study, we investigate the importance of sediment supply and barrier dynamics as driving mechanisms of coastal change throughout the Holocene. Litho-, bio- and chronostratigraphic methods are used to decipher the mechanisms of coastal change from the record preserved within coastal stratigraphy. Results suggest that local coastal configuration and sediment supply were the most influential in determining coastal change during the mid- and late Holocene, against a background control of sea-level rise. The importance of sedimentological and morphological factors in shaping Holocene coastal changes in the southern North Sea basin must therefore be considered when using the database of evidence from this region as an analogue for future change under accelerated sea-level rise.

Keywords

Sediment supply; Barrier dynamics; Holocene; Coastal environments; Stratigraphy; Diatoms

1. Introduction

The rate of relative sea-level (RSL) rise increased at the end of the 20th century and this is projected to continue in future climate change scenarios (AR5-RCPs) (Church et al., 2013), putting the future resilience of coastal landscapes, and their associated communities, infrastructure and nature

conservation interests at risk. Resilient coastlines have the capacity to respond and evolve to forcing by natural and anthropogenic processes and are the desired outcome of coastal management strategies (Nicholls and Branson, 1998; Long et al., 2006). Coastal resilience is best framed by understanding the local coastal response to global forcing mechanisms and how this fits within the regional setting. Understanding the role of coastal configuration and sediment supply in moderating coastal change is essential for informing coastal management strategies. Extending understanding beyond the instrumental era enables the relative importance of the driving mechanisms of coastal evolution, and their spatial and temporal variability, to be investigated, aiding the production of informed management strategies (Plater et al., 2009). The Holocene record of coastal geomorphological change preserved within coastal stratigraphy can help with evidence based management decision-making of barrier coasts by improving understanding of the complex behaviour of barrier systems and their response to climate and geomorphic change. The southern North Sea Basin is an ideal site for exploring this for the mid- to late Holocene, when morphological and sedimentological factors are likely to be at their most influential for coastal evolution due to low background rates of RSL rise. This paper aims to establish the extent to which variations in sediment supply and barrier dynamics can be determined from the Holocene back-barrier stratigraphic record. Using the Suffolk coast as a case study, litho-, bio- and chronostratigraphic methods are utilised to establish driving mechanisms of coastal change and understand their relative importance for Holocene coastal evolution.

Barrier coasts form approximately 15 % of the world's coastline and protect sensitive back-barrier wetlands and adjacent coastal environments from the direct impacts of storms and erosion (Cooper et al., 2018). Barrier and back-barrier evolution are controlled by; RSL change, sediment supply, barrier grain-size, substrate gradient, geological inheritance, wave and tidal energy (Roy, 1984; Roy et al., 1994; Cooper et al., 2018). The interconnected nature of these processes requires investigation in unison, as they can result in a range of responses, dependent on the geomorphological character of the coast (Carter and Woodroffe, 1994). For example, sea-level rise could manifest itself through a range of responses, such as barrier overtopping, overwashing or breaching, dependent on the ability of the coast to accommodate geomorphic stress (Carter and Woodroffe, 1994).

Back-barrier sediments can be utilised to identify variation in barrier coherence and determine the mechanisms controlling barrier evolution (e.g. Spencer et al., 1998; Lario et al., 2002; Clarke et al., 2014). Tidal inlets are dynamic features of barrier coastlines that allow tidal waters to penetrate landwards each tidal cycle, providing a connection between the ocean and back-barrier environments (Fitzgerald et al., 2002; 2008). The morphology and sedimentary structure of tidal inlets is continually altered by the complex interactions of waves, tides and currents (Fitzgerald et al., 2002; 2008; Long et al., 2006; Mellett et al., 2012). The location of tidal inlets relative to a barrier coastline influences sediment input to the coastal system and as a result, the pattern of sediment processing (Long et al., 2006). Sediment supply directly influences the importance of RSL rise for barrier (e.g. barrier rollover, overstepping or erosion) and back-barrier evolution (Carter, 1988; Carter et al., 1989; Forbes et al., 1995; Jennings et al., 1998; Rosati, 2005; Fitzgerald et al., 2008;

Plater and Kirby, 2011). A reduced sediment supply can result in sediment reworking and thinning, weakening barrier architecture and increasing the likelihood of tidal inundation to back-barrier environments (Orford et al., 1991). In contrast, an adequate sediment supply, coupled with a low or stable rate of RSL rise, can cause barrier stabilisation or progradation, protecting back-barrier environments from tidal inundation (Roy et al., 1994).

2. Study Site

2.1 Suffolk coast, United Kingdom

The Suffolk coast, southeast England (Fig. 1) is on the northwestern boundary of the southern North Sea basin (Fig. 1A). The region has high conservation value with large portions protected by the Suffolk Coast and Heaths Area of Outstanding National Beauty (AONB), the Suffolk Coast National Nature Reserve, the Minsmere-Walberswick Heaths and Marshes Site of Special Scientific Interest (SSSI), the Minsmere-Walberswick Heaths and Marshes Special Area of Conservation (SAC), Minsmere-Walberswick Special Area of Protection (SPA), and the Minsmere-Walberswick Ramsar. The coastline alternates between cliffs formed from soft unconsolidated Quaternary sediments and low-lying wetlands, separated from the sea by a narrow beach-barrier system. The study area (Fig. 2) is a region of low-lying brackish and freshwater marshes containing shallow lagoons and extensive drainage channels behind a narrow barrier ridge of coarse sand and gravel which is susceptible to breaching and overtopping during storm surges (Steers, 1953; Pye and Blott, 2009). The tidal regime on the Suffolk coast is semi-diurnal with an average mean spring tidal range between Southwold and Minsmere of c. 2 m. The wave regime is bimodal, with waves approaching predominantly from the north and northeast or south and southwest, and moderate, with 76 % of the waves not exceeding 2 m (Pye and Blott, 2006; 2009; Brooks and Spencer, 2010). The underlying geology is a sandstone containing shells (Coralline Crag, Norwich Crag, and Red Crag) dating from the Pliocene and Pleistocene (Hamblin et al., 1997).

The current stability of the Suffolk coast is significantly compromised by long-term subsidence (Shennan and Horton, 2002), RSL rise, and a lack of sediment supply (Pye and Blott, 2006; Haskoning, 2009). The coastline is particularly vulnerable to storms, experiencing high rates of erosion (up to 4.5 m a[-1]) throughout the 20th century (Cambers, 1975; Carr, 1981; Brooks and Spencer, 2010; 2012). Historical records evidence the catastrophic impact storms have had on the coast of Suffolk over the last 1000 years, with over 90 % of the medieval port settlement of Dunwich now submerged due to coastal recession (Sear et al., 2011). Adaptive and sustainable strategies are necessary to manage the coast effectively due to the significant infrastructure (e.g. Sizewell B nuclear power station and the planned Sizewell C nuclear new build) as well as high conservation value.

Data points and associated glacial isostatic adjustment model output from East Anglia, in addition to Fenland, North Norfolk and Essex, record a predominantly continuous RSL rise trend during the Holocene, although the rate of RSL rise declined gradually throughout this period (e.g. Shennan et al., 2018). Global mean sea level rose at a rate of 1.2 to 1.9 mm yr^{-1} between the mid-to-late 19th century and 20th century, a rate comparable with the late Holocene period (Woodworth et al., 2009;

Cazenave et al., 2018). However, satellite altimetry has determined a global mean sea level rise rate of 3.1 ± 0.3 mm yr^{-1} for the last 25 years (Cazenave et al., 2018), exceeding the late Holocene average.

Information on the existing Holocene stratigraphy of the Suffolk coast is spatially and temporally limited, hindering an understanding of the system's long-term behaviour. Existing research has focused on Norfolk and Essex, to the north and south of Suffolk respectively, revealing large stratigraphic differences between the two regions. Research completed in northern Suffolk (Bure-Yare-Waveney estuary and Blyth estuary) identified lithostratigraphic similarities with the Holocene sequence of intercalated peat horizons from east Norfolk (Coles and Funnell, 1981; Alderton, 1983; Brew et al., 1992; Boomer and Godwin, 1993; Horton et al., 2004) but contrasts with southern Suffolk. Here, clastic estuarine sedimentation dominates and peat is limited or absent (Brew et al., 1992). Reconstructions of palaeogeography in central Suffolk, between the Southwold and Sizewell, are primarily based upon historical records (e.g. Pye and Blott, 2006). The resulting conceptual models reconstruct small open coast estuaries, which existed along this coast prior to the Middle Ages but were blocked and enclosed by gravel and sand barriers between the 14th and 18th century (Chant, 1974; Parker, 1978; Comfort, 1994; Pye and Blott, 2006).

2.2 Driving mechanisms of coastal change in southern North Sea basin

Back-barrier stratigraphy contains a complex record of the driving mechanisms of coastal change, which varies through space and time, modulated by coastal processes. Research investigating the evolution of the coastal plains of the Netherlands, Belgium and southern England during the Holocene has shown that the driving mechanisms of coastal change vary spatially and temporally. The rate of RSL rise, for example, greatly influenced the southern North Sea depositional record during the early and mid-Holocene. Minerogenic sedimentation, representative of tidal environments, dominates the early Holocene depositional history of the southern North Sea basin as high rates of RSL rise resulted in landward advancement of the coast. For example, RSL rose by over 20 m OD between 8.8-5 ka in southeast England (Long and Innes, 1993) whilst on the Belgian and Holland coast the RSL rise rate decreased from over 7 mm yr^{-1} to less than 3 mm yr^{-1} after 7 ka (van de Plassche, 1982; Denys and Baeteman, 1995; Beets and van der Spek, 2000; Baeteman and Declercq, 2002). The relative dominance of a driving mechanism will also vary spatially and temporally. Thus, in the southern North Sea basin the transition from the early to mid-Holocene is denoted by a shift in the relative importance of RSL rate vs sediment supply. The decline in RSL rise rate after 7 ka enabled sediment supply to balance, and eventually surpass, the creation of accommodation space, halting the landwards migration of tidal sedimentary environments and stabilising the shoreface, resulting in shoreline progradation (Beets and van der Spek, 2000; Baeteman and Declercq, 2002). By 5.5-4.5 ka, freshwater marsh and peat sedimentation dominated the majority of the Belgian coastal plain (Beets and van der Spek, 2000; Baeteman and Declercq, 2002) whilst the central section of the Dutch coast prograded nearly 10 km between c. 5 ka and 2 ka (Beets and van der Spek, 2000).

Local factors, such as variation in sediment supply, morphology of the pre-flooded surface, barrier presence and status, and the influence of river catchments, modulate how the sedimentological

signal is recorded (Beets et al., 1992; Beets and van der Spek, 2000; Baeteman and Declercq, 2002; Pierik et al., 2017). The late Holocene is characterised by a return to minerogenic, tidal sedimentation and the culmination of a 2000-3000 year period of peat accumulation. The mechanisms responsible for the cessation of peat sedimentation are likely to be various. Local factors have been suggested as potential explanations; inadequate conditions for the preservation of organic sedimentation (Long et al., 2000); coastal barrier breach and the formation of drainage networks, enhanced by digging and excavating for industrial purposes (Vos and van Heeringen, 1997); creation of accommodation space caused by the compaction of the peat following reclamation and drainage (Baeteman et al., 2002; Mrani-Alaoui and Anthony, 2011) and the influence of natural preconditions, i.e. the geological setting such as coastal plain extent and sediment delivery (Pierik et al., 2017).

3. Methods

Stratigraphy across each site was investigated using a 30 mm diameter Eijkelkamp gouge corer and sediments logged following the Troels-Smith (1955) classification scheme. The Crag underlying the region is composed mainly of sand with thinner sandy gravel units and occasional silty-clay laminae. All cores bottomed-out in saturated, irrecoverable sand or Crag. Sampled cores for laboratory analysis were collected using a 50 mm diameter Russian corer, wrapped in cling film, placed in plastic tubing and refrigerated in the dark at 4° C. All cores were surveyed relative to the UK Ordnance Datum (OD) using a Topcon differential GPS (10 cm precision).

Palaeoenvironmental reconstruction of cores is based on diatom analysis, supported by particle size analysis, sediment organic content, and identification of foraminifera. Diatom distribution is strongly controlled by salinity (e.g. Kolbe, 1927; Hustedt, 1953; Kjemperud, 1981), enabling marine, brackish and freshwater palaeoenvironments and the boundary between these to be characterised (Palmer and Abbott, 1986; Vos and De Wolf, 1993; Denys and De Wolf, 1999). Diatom preparation followed the standard method summarised by Palmer and Abbott (1986) and Battarbee (1986). A minimum of 250 diatoms were counted per slide and species identification followed Van der Werff and Huls (1958-1974), Krammer and Lange-Bertalot (1991; 1997) and Hartley et al. (1996). Diatoms were classified based on their life-form (Vos and De Wolf, 1988; 1993) and salinity tolerance, using the Halobian classification scheme (Kolbe, 1927; Hustedt, 1953; Simonsen, 1962; Schuette and Schrader, 1981). Species greater than 5 % of the total diatom valves counted are presented graphically using C2 (Juggins, 2003) and grouped using the halobian classification (Hustedt, 1953) and lifeform (Vos and De Wolf, 1988; 1993). The count sheet for diatom species exceeding 5 % of the total diatom valves counted are presented for each core in the Supplementary Material. Diatoms assemblages are zoned based on stratigraphically constrained cluster analysis using the constrained incremental sum of squares (CONISS) software in TILIA (Grimm, 1987). Foraminifera identification followed the method summarised by Scott and Medioli (1980) at stratigraphic transitions where diatoms were not preserved. Where possible, a minimum of 100 foraminifera were counted per sample.

A Beckman Coulter LS13320 granulometer was used for particle size determination and identified the dimensions of particles ranging from 0.04 to 2000 μm using the laser diffraction method. The aggregating effects of organics were avoided using the hydrogen peroxide digestion method (Kunze and Dixon, 1987) and Calgon was added to deflocculate particles prior to analysis. The bivariate plot of mean grain size against standard deviation was used to determine the depositional energy of a sediment sample using the environment specific graphic envelopes identified by Tanner (1991a; 1991b) and later modified by Lario et al. (2002). Mean grain size and standard deviation are hydraulically controlled, therefore positively correlated with the energy of the environment and degree of sediment processing, i.e. transportation and deposition processes (Tanner, 1991a; 1991b; Long et al., 1996; Lario et al., 2002; Priju and Narayana, 2007). Organic content was determined using the loss-on-ignition (LOI) methodology (Ball, 1964; Plater et al., 2015). Approximately 5 g of sediment was dried overnight at 105 °C and weighed to two DP. The sample was ignited at 550 °C for 4 hours and reweighed after being cooled in a desiccator (Heiri et al., 2001). Organic content was calculated as the percentage weight of the original sample. AMS radiocarbon dating of plant macrofossils provided a chronology for the sampled material. Horizontally aligned plant macrofossils and seeds were selected for analysis for all samples, excluding the basal sample from OTM-16-13 which is based on wood. Radiocarbon measurements were completed at the Natural Environmental Research Council (NERC) Radiocarbon Facility in East Kilbride, Scotland and BETA Analytic, Miami. Dates were calibrated using CALIB Radiocarbon Calibration (Stuiver et al., 2018) and the IntCal13 calibration curve (Reimer et al., 2013) and are presented as μ ± 2σ cal BP within the text. The uncalibrated and calibrated ages for all material radiocarbon dated are presented in Table 1.

4. Results

Results are presented for two sites Great Dingle Hill and Oldtown Marsh (Fig. 2), situated within the Walberswick National Nature Reserve between Southwold and Dunwich (Fig. 1B).

4.1 Great Dingle Hill

Representative stratigraphy at the site consists of five main sediment units outlined in Table 2, with corresponding Troels-Smith (1955) log, for the sampled core (GDH-16-2; TM48486 73145). GDH-16-2 contains a well humified sandy peat unit (200-196 cm), lower well humified peat unit (196-179 cm) subdivided by a silty clay peat unit (190-185 cm), overlain by a mottled silty clay unit (179 cm to 36 cm) and an upper unit comprised of organic-rich sand (36 cm to 0 cm) (Fig. 3). Organic content decreases from 40 % near the base (190 cm) to 8 % (128 cm) in the upper sampled section, with a minor peak below the overall trend at 199 cm (23 %) due to the proximity to basement substrate (Fig. 4). The sediments from GDH-16-2 plot within the graphic sedimentary domain defined by Lario et al. (2002) as indicative of open to closed estuarine environments (Fig. 5).

Five diatom assemblage zones are identified based on the diatom flora and lithostratigraphy (Fig. 4). Brackish epiepelic diatom taxa dominate Zone 1, indicating a marine influence. The peat unit contains an increase in minerogenic content between 190 cm and 185 cm, associated with the presence of brackish diatom taxa in Zone 1. The onset of peat deposition has been constrained to

2870 ± 87 cal BP. Brackish epipelic diatoms dominate Zone 2 whilst Zone 3 is delineated by an increase in marine planktonic species. This increase in marine conditions coincides with a transition from well-humified peat to silty clay peat and is associated with a decrease in organic content and gradual coarsening upwards. The increase in planktonic taxa across the transition coincides with the near disappearance of brackish aerophilous species. The increase in marine species at the transgressive contact is constrained to 2530 ± 172 cal BP. Brackish-marine species, with planktonic and epipelic ecology, continue to dominate the assemblage for Zone 4 and 5, with the organic content remaining consistently between 8 to 14 %.

4.2 Oldtown Marsh

The stratigraphy at Oldtown Marsh contains a series of alternating organic and minerogenic units (Fig. 6), very similar to the Holocene sequence found further north in the Blyth estuary (Brew et al., 1992). Sample core OTM-16-13 (TM48610 73838) consists of seven main sediment units (Table 3): an organic sand (580-572 cm) a lower, variably humified, peat unit with occasional wood fragments (572- 332.5 cm); overlain by an organic clayey silt unit (332.5-254 cm); a fibrous woody peat unit (254-216 cm); silty peat unit (216-210 cm); a clayey silt unit (210- 45 cm); and an upper fibrous peat unit (45 cm to 0 cm).

Diatom preservation was variable throughout OTM-16-13 (Fig. 7). As a result, where diatom preservation was poor, foraminifera were counted. Five diatom assemblage zones are identified between 300 and 170 cm based on diatom flora and lithostratigraphy.

At 330 cm (-3.21 m OD), 2.5 cm above the sharp transition from variably humified peat to organic clayey silt, *Jadammina macrescens*, a high-marsh foraminifera species occurs (Fig. 7), recording marine inundation at this site (Gehrels, 2002). LOI values decrease sharply from 88 % to 7 % between 334 and 326 cm, indicating that this is an erosive contact. Diatom analysis within the organic clayey silt unit (332.5-254 cm) identified brackish epipelic and marine planktonic species, with the former dominating Zone 1. Particle size analysis identified an upwards fining within Zone 1 that is initially gradual and increases more rapidly in Zone 2, after 278 cm, coincident with a similar trend in organic content.

Jadammina macrescens is abundant at the upper boundary of the organic clayey silt unit (258 cm) in Zone 3 (Fig. 7). Organic content values ranging from 60 - 80 % at the upper and lower boundary of the organic clayey silt and middle fibrous peat units, respectively, indicate a transitional shift in sedimentation within Zone 3. The timing of this shift in sedimentation and occurrence of high-marsh foraminifera is constrained to 860 ± 69 cal BP. Organic content decreases to 45 % by 213 cm following the onset of deposition of the middle peat unit. Freshwater tychoplanktonic diatoms dominate Zone 4, with a brackish epipelic component also present.

The transition to silty clay sedimentation (214.5 cm) (870 ± 82 cal BP), correlates with the near disappearance of fresh tychoplanktonic diatoms and increasing dominance of marine planktonic and brackish epipelic species at the transition from Zone 4 to 5. Marine taxa gradually increase in abundance into Zone 5 and organic content remains very low. Brackish epipelic and marine planktonic diatoms dominate the clayey silt unit, whilst freshwater epiphytes disappear within this

zone. Marine planktonic diatoms peak in abundance at 202 cm, followed by a shift to brackish epipelic species. Particle size analysis reveals an initial, highly variable, upwards fining associated with the onset of minerogenic sedimentation at 211 cm, succeeded by a shift to upwards coarsening at c. 190 cm into the silty clay unit. When plotted, a cluster of the sediments sampled (c. 204 – 172 cm) plot within the closed- basin domain of the bivariate plot (Fig. 5).

5. Discussion

5.1. Palaeoenvironmental interpretation- Great Dingle Hill

Minerogenic sedimentation dominates the stratigraphic transect completed at Great Dingle Hill. The onset of minerogenic sedimentation in GDH-16-2 is associated with a sustained increase in marine conditions after 2530 ± 172 cal BP, indicating that Great Dingle Hill was tidally influenced throughout the late Holocene. Reduced barrier integrity, enabling tidal ingress, is a likely explanation for the continued dominance of marine and brackish conditions. A high magnitude event could have created a breach in the barrier whilst alternatively a restricted sediment supply could have led to sediment reworking and increased barrier instability and permeability. The onset of minerogenic sedimentation within the stratigraphic transect is not associated with the presence of sand or, indeed, other indicators of a high magnitude event.

The brackish epipelic taxa dominating the diatom assemblage of the peat unit are associated with intertidal to lower supratidal mudflats and creeks, and subtidal marine basins and lagoons (Vos and De Wolf, 1988; 1993). Marine and brackish planktonic taxa, characteristic of sub-tidal areas or large tidal channels (Vos and De Wolf, 1988; 1993; Zong and Tooley, 1999), increase in abundance at 176 cm (Fig. 4). The slight upwards coarsening, associated with the shift to minerogenic sedimentation, indicates an increase in depositional energy. The changes in diatom ecology (i.e. salinity and life form) associated with this sedimentation shift indicate an increase in tidal influence during the late Holocene. The increased input of planktonic species, previously identified as allochthonous (Simonsen, 1969; Vos and De Wolf, 1993), strongly indicates tidally influenced hydrodynamic conditions. Increases in these taxa have been previously attributed to episodes of barrier breaching (Sáez et al., 2018) and the opening of tidal inlets (Bao et al., 1999; Freitas et al., 2002).

Barrier breaching, or further reduced barrier integrity, is identified as the most likely cause for the transition from organic to minerogenic sedimentation at 2530 ± 172 cal BP. The dominance of brackish epipelic taxa prior to this indicates that Great Dingle Hill was already tidally influenced, potentially via channel inlets through the barrier. The return to minerogenic sedimentation associated with marine conditions by 2530 ± 172 cal BP could be explained by RSL rise, and the associated creation of accommodation space outpaced organic accumulation, however this is unlikely as the rate of RSL rise decreased during the mid- to late Holocene (Shennan et al., 2018). Particle size, and the bivariate plot (Fig. 5), do not record coarse sedimentation followed by a fining upwards sequence, which would be indicative of a high-magnitude event and subsequent recovery. Sediment supply would have become more important for driving coastal change as the rate of RSL decreased during the Holocene. If sufficient, the sediment supply would stabilise the position of the

barrier and halt the landwards movement of tidal environments however the results indicate this was not the case.

5.2.   Palaeoenvironmental interpretation- Oldtown Marsh

Peat sedimentation initially dominates the seaward end of the stratigraphic transect at Oldtown Marsh, indicating that the coastline was stable and the back-barrier environments initially protected. The onset of the lower minerogenic unit (332.5-254 cm) in OTM-16-13 is associated with high marsh foraminifera, succeeded by a dominance of brackish epipelic diatoms and the occurrence of marine planktonic taxa, indicative of a tidal mudflat environment. The upwards fining and increasing organic content within the organic clayey silt unit (from c. 278 cm) reflects a decrease in the depositional energy and gradual increase in position within the tidal frame, interpreted as a transition from intertidal mud flat to salt marsh.

Vertical changes in sea level are unlikely to be responsible for this initial marine inundation due to the low RSL rise rate during the mid- and late Holocene (Shennan et al., 2018). Possible explanations include impeded drainage (Baeteman, 1981), or repeated reactivation of tidal channels resulting in peat dewatering (Spencer et al., 1998), surface lowering and landward migration of tidal influence (Baeteman and Denys, 1995). Similar shifts in sedimentation throughout the southern North Sea basin have been attributed to imbalances in sediment budget (e.g. Beets et al., 1992; 1994; Baeteman, 1999; Brew et al., 2000). The erosive nature of this contact (332.5 cm) may have occurred post-deposition, due to rapid inundation, possibly caused by peat dewatering and collapse or by barrier breakdown.

Freshwater tychoplanktonic taxa (e.g. *Staurosira construens* and *Pseudostaurosira elliptica*) dominate the diatom assemblage of the peat (254 cm to 214.5 cm) (Vos and De Wolf, 1993) and when combined with a small brackish component can be associated with a shallow fresh to brackish water lagoon environment, low-energy hydrodynamic conditions and aquatic vegetation (Bao et al., 1999). The organic content however initially remains high, following the transition to fibrous peat (254 cm), indicating a gradual transition from a high-marsh environment. The gradually decreasing organic content and upwards coarsening may indicate gradual barrier breakdown, enabling an increasing tidal ingress into a barrier estuary. Diatoms are not preserved at the lower boundary of the middle fibrous peat, so it is not possible to determine if tidal influence is increasing within this unit.

The reduced marine influence and onset of peat accumulation (254 cm) may have been strongly influenced by barrier dynamics from 860 ± 69 cal BP, especially since there is no evidence in the available RSL record, or any plausible mechanism for a sea-level driven process at this time (Shennan et al., 2018). An adequate sediment supply is a prerequisite for a stable barrier position, as a barrier with an abundant sediment supply will have better capabilities for internal reorganisation and growth. Back-barrier environments will accrete sediment rapidly when sediment supply exceeds the accommodation space created by RSL rise resulting in less frequent tidal inundation (Baeteman et al., 2011). With time, salt marsh environments replace mud flat and peat begins to accumulate due to the asymptotic relationship between sediment accretion rates and time if sediment supply is sufficient (Jennings et al., 1995). Therefore, it is most likely that local factors

(e.g. sedimentological or morphological) were responsible for the deposition of the middle peat unit recorded within the stratigraphic transect.

Particle size data indicate that the site was highly dynamic, with variable tidal influence, following the onset of clayey silt sedimentation at 214 cm. Marine planktonic taxa increase in abundance, indicating that the site's position within the tidal frame was lowering or that the widening of a barrier opening was enabling tidal influence to penetrate further landwards. The diatom and particle size analysis indicate a mud flat environment experiencing an increasing tidal influence. The absence of full marine conditions and occurrence of freshwater taxa until 206 cm indicates that the tidal influence on this site was initially marginal. The dominance of brackish epipelic taxa from 202 cm indicates that tidal influence is decreasing and is coincident with an initial coarsening and consistent particle size, indicating an initial increase in depositional energy followed by a stabilisation of the environment. The model of Tanner (1991a; 1991b) supports this interpretation as sedimentation transitions from an estuarine environment to a closed basin by 204 cm, until 172 cm. The decreasing tidal influence may indicate that a tidal inlet or previous barrier breach is annealing. Diatoms are not preserved in the top 1.5 m of the Oldtown Marsh core, hampering interpretations for the upper core section.

The timing of the upper transgressive contact at Oldtown Marsh coincides with a period of coastal reorganisation between Southwold and Dunwich. Conceptual palaeogeographical reconstructions, based on historical evidence, depict the Blyth River diverted south by a spit, Kingsholme, estimated to have developed between c. 1500 and 700 AD, to form an estuary from Roman times (Gardner, 1754; Steers, 1927; Chant, 1974; Parker, 1978; Comfort, 1994; Pye and Blott, 2006). Spit development was halted during the 13th and 14th century due to storms (1287 and 1328) which blocked the entry to the haven, connecting the distal point with the Dunwich cliffs (Steers, 1927). An insufficient sediment supply to the barrier system would have resulted in sediment recycling within the spit, creating points of weakness and eventually leading to progressive breakdown, which in turn would influence the back-barrier sediment record. Litho- and bio-stratigraphic research on nearby Dingle Marshes, neighbouring Dunwich, identified an environmental shift in a freshwater retting pit to marine saltmarsh and estuarine mud at c. 1100 AD, attributed to storms breaching a gravel barrier or spit (Sear et al., 2015). There is no sedimentological evidence to attribute marine inundation at Oldtown Marsh at 870 ± 82 cal BP (1080 ± 82 cal AD) to a high magnitude event. The differences in sedimentary record between Oldtown and Dingle Marshes (Sear et al., 2015) may reflect differing proximities to the coast. Additionally, the populations of Dunwich, Walberswick and Blythburgh are likely to have influenced the back-barrier sediment record as they attempted to maintain access to the sea by creating artificial breaches in the spit, for example following the choking of the haven in the 14th century (Comfort, 1994).

5.3.   Regional perspectives on Holocene coastal evolution

Comparisons of the late Holocene sediment record from Great Dingle Hill and Oldtown Marsh with northern Suffolk (Blyth estuary) and eastern Norfolk (Bure-Yare-Waveney estuary and Horsey) illustrate substantial variability in sedimentary response between sites with the same regional pattern of sea-level tendency. For example, the shift from organic to minerogenic sedimentation in

the Blyth estuary is constrained to 4920 ± 292 cal BP (Brew et al., 1992). In contrast, the onset of minerogenic sedimentation further north, in the Bure-Yare-Waveney estuary system, occurs later, at 3000-2000 cal BP (Coles and Funnell, 1981; Alderton, 1983; Horton et al., 2004). The timing of this transition in the Bure-Yare-Waveney estuary system is comparable with Great Dingle Hill, where minerogenic sedimentation associated with the development of an intertidal mudflat environment is sustained from 2530 ± 172 cal BP until near present-day.

At Oldtown Marsh, however, a prolonged period of minerogenic sedimentation only occurs from 870 ± 82 cal BP, overlapping with the transition to marine saltmarsh and estuarine mud at Dingle Marshes, Dunwich (Sear et al., 2015). Local factors (e.g. sedimentological and morphological) are likely to have had a greater influence on the reconfiguration of the coast during the late Holocene than vertical changes in sea level due to the low rate of RSL rise (Shennan et al., 2018). This is clearly supported by the variable sedimentary response across Suffolk and Norfolk, highlighting the importance of sediment supply to facilitate late Holocene barrier building (or barrier breakdown) and the creation of discrete sedimentary basins within the estuaries (Brew et al., 1992). Sediment availability and barrier dynamics are hypothesised to have been highly influential for the evolution of the Suffolk coast during the late Holocene. The susceptibility of the back-barrier to inundation would have increased during the late Holocene if the sediment supply was not sufficient for barrier development and the southwards progradation of Kingsholme spit. Insufficient sediment supply was one mechanism proposed to explain the culmination of late Holocene peat growth elsewhere in the southern North Sea basin (Beets et al., 1992; 1994; Baeteman, 1999).

5.4 Sediment supply and barrier dynamics as driving mechanisms of Holocene coastal change
Analysis of the sediment sequences from Oldtown Marsh and Great Dingle Hill indicate that sediment supply and barrier dynamics were key driving mechanisms of Holocene back-barrier sedimentation in Suffolk. RSL change, however, was only a background control when the back-barrier record was deposited at these sites, exerting a minimal control on the significant changes in coastal evolution reported here. Attributing shifts from organic to minerogenic sedimentation, and vice-versa, to changes in sea level can result in the oversimplification of the sediment record and often fails to consider the complex interplay between sediment supply, barrier dynamics, accommodation space and the rate of RSL rise, in addition to temporal variations in their relative importance. This simplified approach can lead to erroneous interpretations – for example in Germany where intercalated peats within Holocene marine sediment were attributed to a regression, reflecting a falling sea level (Behre, 2007), is at best equivocal when errors are fully considered and other processes explored (Baeteman et al., 2011). Mid- to late Holocene analogues from the southern North Sea basin therefore give a false impression with regard to future coastal change under accelerated sea-level rise. The importance of a regional approach when distinguishing between sediment-driven and RSL-driven changes recorded in the sediment record has been previously highlighted (Jennings et al., 1995). Changes in marine and terrestrial conditions preserved in back-barrier palaeoenvironmental records have been shown to not necessarily reflect changes in sea level (Duffy et al., 1989). For example, barrier dynamics,

including its initiation, establishment and breakdown, will influence the back-barrier environment and have implications for the depositional environments formed (Orford et al., 1991).

The late Holocene was associated with barrier building and the creation of discrete sedimentary basins within estuaries (Brew et al., 1992). Spit development and barrier dynamics were identified as primary controls of the Holocene coastal evolution, and resulting sediment record, in the Blyth estuary (Brew et al., 1992). The development of these features would have placed increased demands on the sediment supply required to maintain landform integrity. Variations in sediment supply are therefore likely to have been highly influential to the evolution of the Suffolk coast during this period.

Throughout the instrumental era, a limited and temporally and spatially variable sediment supply has greatly influenced the evolution of the Suffolk coast. At present, the sediment supply to Suffolk's gravel beaches is insufficient to ensure the coastline is resilient to storms. Studies have indicated that during periods of RSL rise and increased storminess, the barrier moves shoreward in places in order to evolve in response to forcing (Haskoning, 2009). Suffolk's cliffs, a major input into East Anglia's sediment budget, have exhibited high rates of spatially and temporally variable historical change, over decadal timescales, highlighting a well-defined north-south trend of cliff retreat (Cambers, 1973; 1975; Robinson, 1980; Carr, 1981; McCave, 1987; Brooks and Spencer, 2010; Burningham and French, 2017). Dynamic offshore bank systems complicate regional sediment transport, potentially acting as a sediment sink and morphologically influencing the wave climate and tidal currents (Lees, 1983; Brooks and Spencer, 2010). Research into the evolution of the Sizewell-Dunwich Bank system, situated offshore of the Dunwich-Minsmere cliffs, map the extension of the Sizewell Bank, its coalescence with the Dunwich Bank in the 1920s, and their landwards movement (Carr, 1979). Substantial spits, such as Orford Ness and Landguard Point, are also current features of the Suffolk coastline.

Cluster analysis of the relative position of the shoreline (1881-2015), combined with metrics of shoreline change, identified multiple modes of shoreline change on the Suffolk coast and noted the importance of sediment budget variations as a driver of multi-decadal coastal behaviour (Burningham and French, 2017). Predictions of future shoreline retreat also identified that the sediment release behaviour of the Suffolk cliff system exhibits a switching of states, between on, off and no change (Brooks and Spencer, 2012). The late Holocene data presented in this paper indicates that a series of sediment release and supply pathways, which change their location through time, have existed on this coastline since at least 3 ka. Fig. 8 illustrates this concept, depicting the influence of changes in sediment release and supply pathways through time on back-barrier environments. Transitions between organic and minerogenic sedimentation in a given location may reflect temporal changes in this spatial pattern of sediment release and storage, due to erosion and deposition. The late Holocene data presented, in addition to historical and instrumental data, suggest that the vulnerability of the Suffolk coast has varied spatially, dependent on the location of a site relative to the pattern of sediment release and supply at a given time. The

vulnerability or resilience of a given site, based on this concept, would therefore be difficult to determine due to changes in this spatial pattern through time.

6. Conclusions

Sediment supply and barrier dynamics have been identified as key driving mechanisms moderating the coastal evolution of the Suffolk coast during the mid- and late Holocene. Our findings illustrate that a temporally variable spatial pattern of sediment release and supply was an important control on coastal evolution through the late Holocene, a period when the rate of RSL change was low. Coastal systems throughout the southern North Sea basin, including Suffolk, are now responding to a rate of RSL rise which is faster than that identified for the mid- and late Holocene (Defra, 2006; Church et al., 2013; Burningham and French, 2017; Cazenave et al., 2018). The future response of anthropogenically modified coastal landscapes to a temporally variable spatial pattern of sediment release and supply pathways, whilst RSL is rising, is an uncertainty which requires consideration and incorporation into coastal management strategies. Coastal managers must therefore be cautious in advocating 'successes' from recent past practice. Future outcomes for the Suffolk coast will differ due to the increase in sea-level rise and this may result in the failure of previously effective interventions.

The difficulty of teasing apart the driving mechanisms of coastal change and the interplay between sediment availability, barrier dynamics and the rate of RSL change from back-barrier sediment records has been highlighted by the substantially variable sedimentary response preserved. Inter-regional comparisons are required to distinguish between the multifactorial processes driving the Holocene evolution of a coastal system. Sediment records from northern Suffolk and southern Norfolk contain similar patterns; however, the chronologies differ, indicating the importance of local processes (e.g. Coles and Funnell, 1981; Alderton, 1983; Brew et al., 1992; Horton et al., 2004). Stratigraphic data are limited between Dunwich and Aldeburgh and expanding the study area further south may help to explain the differing records of coastal geomorphological change preserved.

7. Figures and Tables
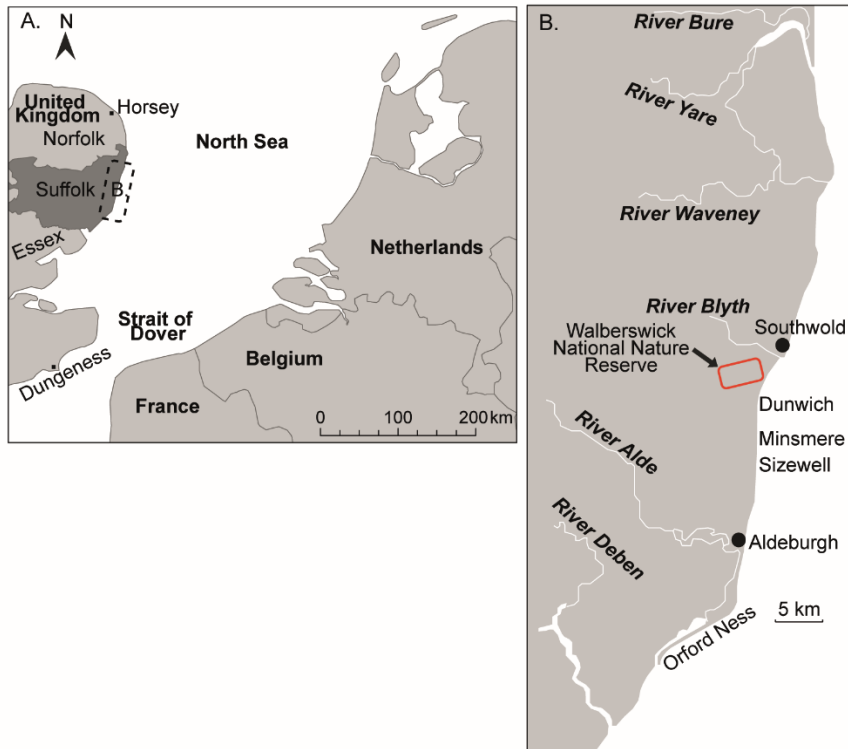
Fig. 1- A. Map of southern North Sea basin with the county of Suffolk highlighted in dark grey and outline of Fig. 1B highlighted by the dashed box. B. Suffolk coast with locations mentioned in the text included. The red box highlights the location of the Walberswick National Nature Reserve, which contains Oldtown Marsh and Great Dingle Hill.

Fig. 2 - Stratigraphic transects completed at Oldtown Marsh and Great Dingle Hill. The white filled circles denote the sediment sequences sampled for analysis whilst the red circle represent gouge cores. Aerial imagery: © Getmapping Plc.
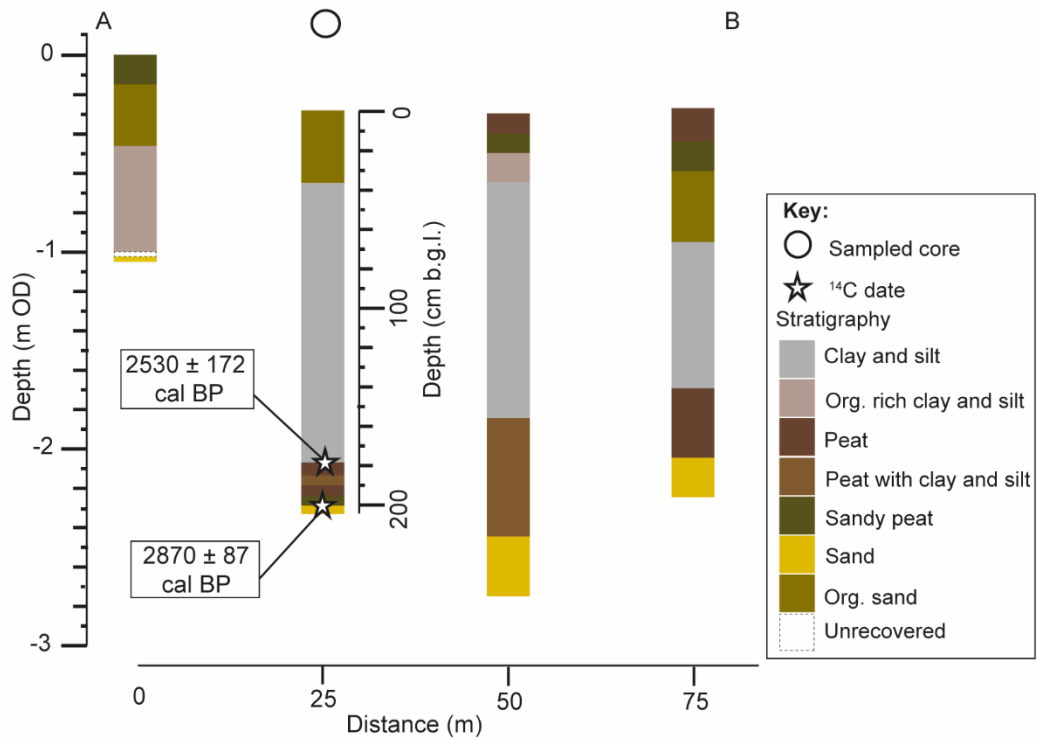
Fig. 3 - Stratigraphic transect from Great Dingle Hill, including radiocarbon dates from sampled sediment sequence.
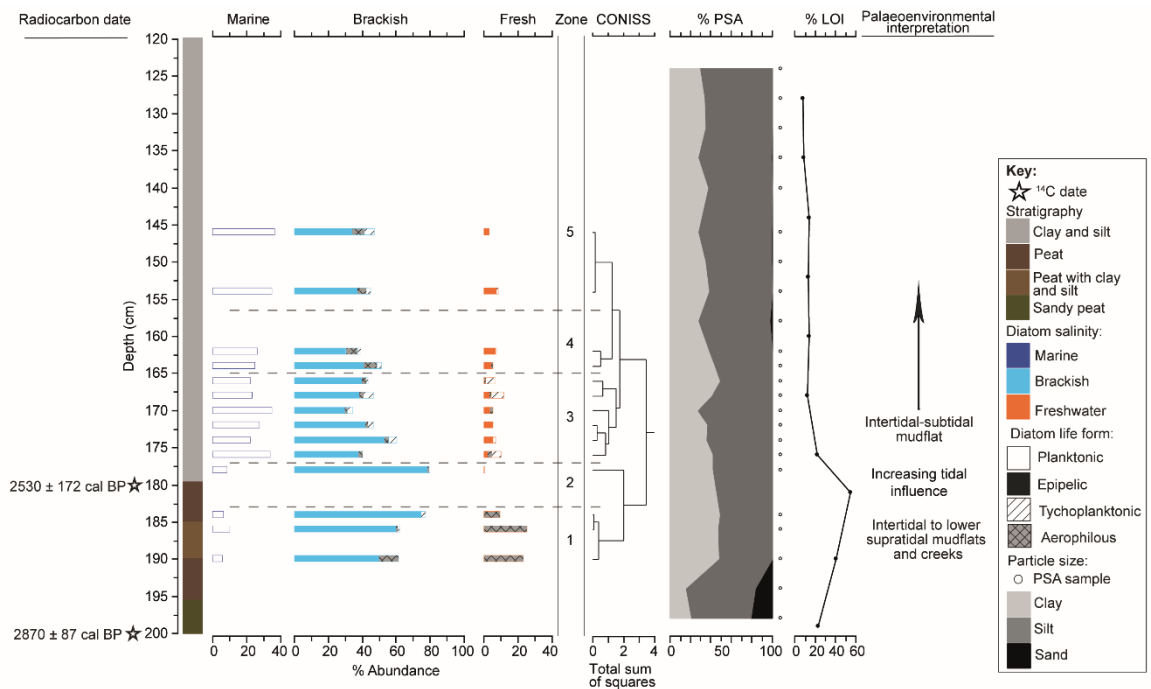
Fig. 4 - Lithostratigraphy, organic content and particle size (PSA), and summary diatom data from the sampled sediment sequence from Great Dingle Hill (GDH-16-2). The diatom summary is based on taxa exceeding 5 % of the total valves counted and are grouped using the halobian classification (Hustedt 1953) and subdivided by lifeform (Vos and De Wolf 1988; 1993).
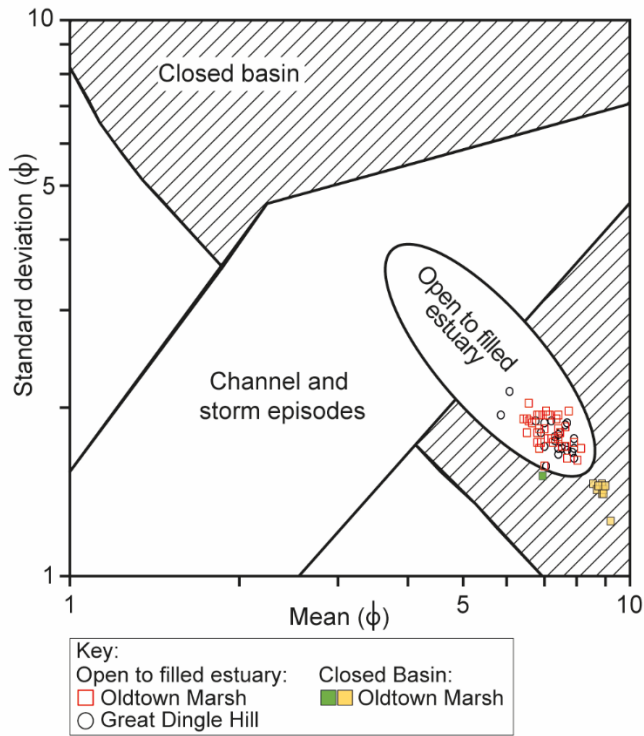
Fig. 5 - Bivariate plot of mean against standard deviation (phi) for sediments from Great Dingle Hill (GDH-16-2) and Oldtown Marsh (OTM-16-13). The graphic sedimentary domains determined by Tanner (1991), and later modified by Lario et al. (2002) are overlain onto this plot. The particle size sample location for Great Dingle Hill and Oldtown Marsh is shown on Figure 4 and 7 respectively. The stratigraphic position of samples from Oldtown Marsh that plotted in the closed basin sedimentary domain is illustrated on Figure 7.
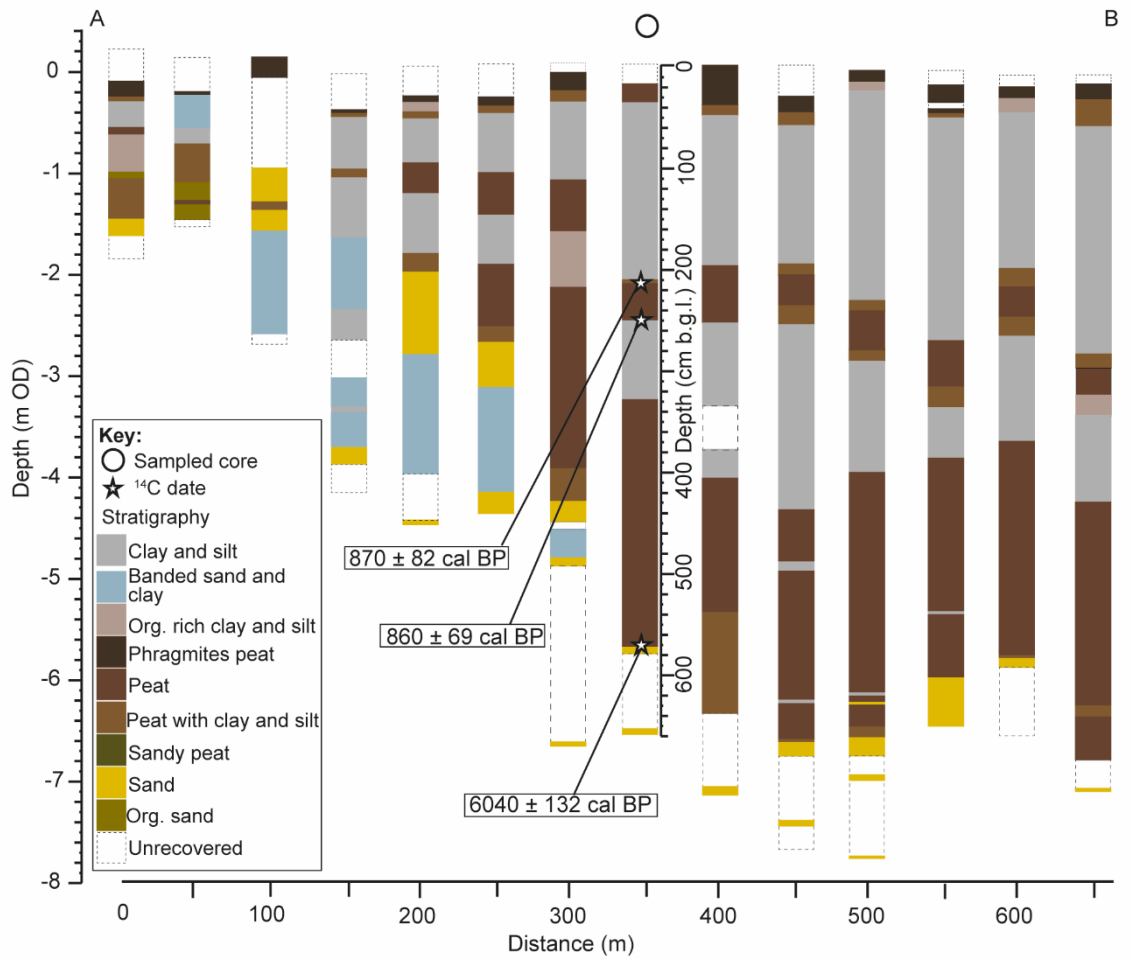
Fig. 6 - Stratigraphic transect from Oldtown Marsh, including radiocarbon dates from sampled sediment sequence.
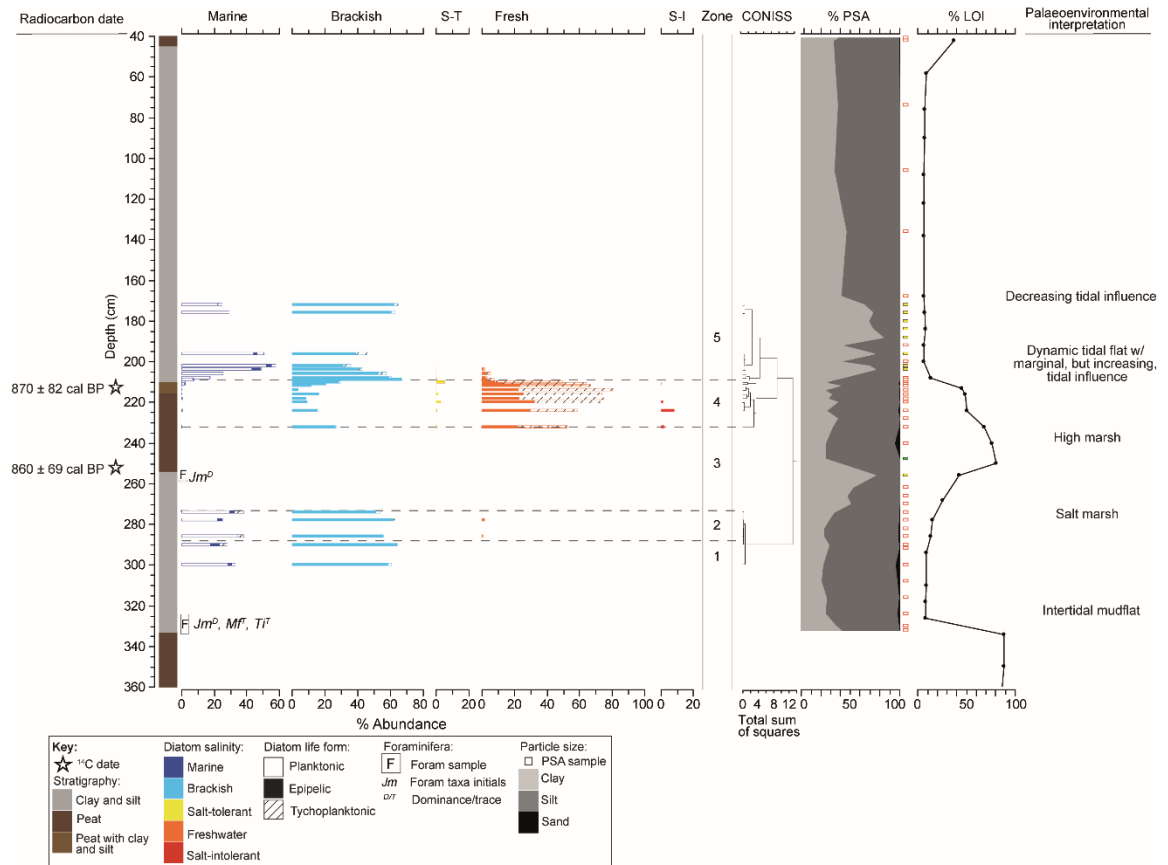
Fig. 7 - Lithostratigraphy, organic content and particle size (PSA), foraminifera (Jm- Jadammina macrescens, Mf- Miliammina fusca, Ti- Trochammina inflata) and summary diatom data from the sampled sediment sequence from Oldtown Marsh (OTM-16-13). The abundance (D- dominance, T- trace) of foraminifera species is noted for each sample. The diatom summary is based on taxa exceeding 5 % of the total valves counted and are grouped using the halobian classification (Hustedt 1953) and subdivided by lifeform (Vos and De Wolf 1988; 1993). The basal radiocarbon date for OTM-16-13 is shown in Fig. 6.
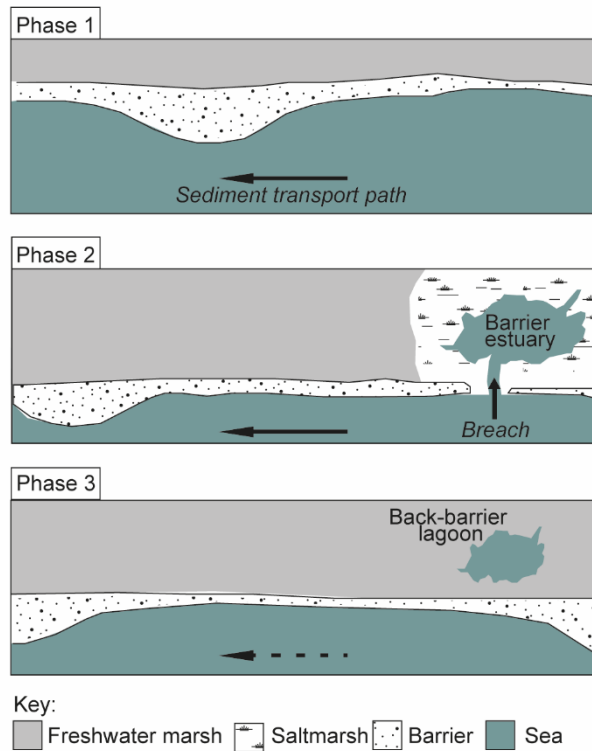
Fig. 8 – Schematic illustrating the temporally and spatially variable pattern of sediment release and supply pathways identified from the late Holocene data presented in this paper. Phase 1 and 2 show a southwards migration of a sediment supply pathway. The vulnerability of sections of the barrier is increased due to the sediment supply being limited. Phase 2 shows the barrier breach which has resulted from a weak point in the barrier, creating a barrier estuary. Phase 3 shows a shift in the spatial pattern of sediment release and supply. The breach has annealed as a result of temporal changes in the spatial pattern of sediment release and storage, resulting from erosion and deposition.

Table 1: AMS radiocarbon dates produced for Great Dingle Hill and Oldtown Marsh.

Site	Laboratory code	^{14}C age (1σ) BP	Calibrated age (2σ) BP	Calibrated age (2σ) AD/BC	Stratigraphic context	Altitude (m OD/cm)	
Great Dingle Hill	SUERC-72912	2440 ± 35	2701-2357	752-408 cal BC	Well humified peat with irregular rootlets	-2.09	180
	SUERC-76469	2775 ± 37	2956-2783	1006-834 cal BC	Basal peat	-2.29	200
Oldtown Marsh	SUERC-72907	965 ± 39	952-789	1161-998 cal AD	Silty peat with clay trace	-2.03	212
	BETA-498399	970 ± 30	933-796	1154-1017 cal AD	Woody peat	-2.45	253.5
	SUERC-72911	5209 ± 35	6170-5906	4221-3957 cal BC	Basal peat	-5.64	573

Table 2: Description of main sediment units identified within the sampled sediment sequence from Great Dingle Hill (GDH-16-2) and associated Troels-Smith (1955) classification.

Unit depth (cm)	Description	Troels-Smith log
0-36	Organic-rich sand	Ga2 Sh1 As1 Th^1+ Th^0+ nig 3+ strat 0 elas 0 sicc 2+
36-179	Silty clay with black mottling and occassional rootlets which increase with depth	As3 Ag1 Sh+ Th^1+ nig 2+ strat 0 elas 0 sicc 2+ lm.sup 1
179-185	Well humified, crumbly peat with irregular rootlets and trace of clay	Sh4 Th^1+ Th^0+ As+ nig 4 strat 0 elas 0+ sicc 1+ lm.sup 3
185-190	Silty clay peat with irregular rootlets and black mottling	As1+ Ag1 Sh2 Th^1+ Th^0+ nig 2+ strat 0 elas 0 sicc 2 lm.sup 2
190-196	Well humified, crumbly peat with irregular rootlets and trace of clay	Sh4 Th^1+ Th^0+ As++ nig 4 strat 0 elas 0+ sicc 1+ lm.sup 1
196-200	Well humified sandy peat	Sh2 Ga2 Th^0+ Th^1+ As+ nig 3++ strat 0 elas 0+ sicc 1+ lm.sup 0

Table 3: Description of main sediment units identified within the sampled sediment sequence from Oldtown Marsh (OTM-16-13) and associated Troels-Smith (1955) classification.

Unit depth (cm)	Description	Troels-Smith log
0-45	Fibrous peat with abundant phragmites	Sh2 Th^{0}2 Ag+ nig 3 strat 0 elas 1 sicc 1+
45-210	Clayey silt with increasing traces of organics with depth	Ag2+ As2 Th^0+ Th^1+ Sh+ nig 2+ strat 0 elas 0 sicc 2+ lm.sup 2
210-216	Silty peat	Sh3 Ag1+ Th^0+ Th^1+ As+ nig strat 0 elas 0 sicc 2+ lm.sup 1
216-254	Fibrous woody peat	Sh2 Th^{1}2 Th^0+ Dl++ As+ Ag+ nig 3+ strat 0 elas 1 sicc 1+ lm.sup 0
254-332.5	Clayey silt with abundant rootlets and patches of organics	Ag2+ As2 Th^1+ Th^2+ Sh+ nig 2+ strat 0 elas 0 sicc 2+ lm.sup 0
332.5-572	Peat with rootlets, traces of silt and clay and sections of wood throughout	Sh2 Th^{1}1 Th^{2}1 As+ Ag+ Dl+ nig 4 strat 0 elas 0+ sicc 1+ lm.sup 4
572-580	Organic sand	Ga4 Sh++ Gmaj+ As+ Ag+ Dl+ nig 2 strat 0 elas 0 sicc 2+ lm.sup 0

Appendix 9

Raw diatom counts for Westwood Marsh.

Salinity key		Lifeform key	
Category	Code	Category	Code
Marine	A	Plankton	A
Brackish	B	Benthos (unknown)	B1
Salt tolerant	C	Benthos (epipsammic)	B2
Fresh	D	Benthos (epipelic)	B3
Salt intolerant	E	Epiphytes	C
Unknown	U	Aerophile	D
		Eu-terrestrial	E
		Unknown	U

Diatom species	Salinity	Depth (cm): Life-form	Q26	124	128	132	134	136	138	140	270
Actinoptychus senarius	A	A	0	4	22	30	4	11	7	2	7
Auliscus sculpta	A	B1	0	0	0	1	0	0	0	0	0
Cocconeis disculoides	A	C	0	0	0	0	0	0	0	0	1
Cocconeis scutellum	A	C	0	0	0	0	0	1	2	1	0
Delphineis surirella	A	C	0	0	2	3	1	3	10	0	0
Diploneis crabro	A	B1	0	0	0	0	5	4	0	0	0
Diploneis smithii	A	B1	2	2	7	3	1	0	0	0	3
Grammatophora oceanica	A	C	0	0	0	0	0	0	3	0	0
Pseudopodosira westii	A	B1	2	1	3	4	0	0	1	4	7

Species											
Navicula bottnica	A	B1	0	0	0	0	1	3	0	0	0
Navicula forcipata	A	B1	0	0	0	1	0	0	1	0	0
Paralia sulcata	A	B1	8	35	50	101	43	120	86	95	62
Podosira stelligera	A	A	0	0	3	12	1	0	0	0	0
Psammodictyon panduriforme	A	B1	0	0	0	0	1	0	0	0	0
Rhabdonema arcuatum	A	U	0	0	0	0	0	1	0	0	0
Surirella comis	A	U	0	0	0	0	0	0	0	0	1
Surirella fastuosa	A	B1	0	2	2	1	13	1	0	0	6
Thalassiosira leptopa	A	U	0	1	0	6	0	0	0	0	0
Trachyneis aspera	A	B1	0	7	34	1	14	0	0	0	11
Triceratium favus	A	A	1	0	0	2	0	0	0	0	0
Achnanthes brevipes	B	C	0	0	0	0	0	0	0	1	0
Anomoeoneis spaerophora var sculpta	B	B1	0	0	0	1	0	0	0	0	1
Caloneis westii	B	B1	1	32	21	43	19	4	31	40	40
Diploneis didyma	B	B1	75	127	77	36	64	9	5	7	118
Diploneis interrupta	B	B1	0	0	1	3	7	0	4	3	14
Navicula digitoradiata	B	B1	0	1	0	0	0	0	2	2	0
Navicula peregrina	B	B1	0	2	6	0	0	0	1	7	1
Nitzschia sigma	B	B1	0	0	1	0	11	15	4	0	1
Petroneis marina	B	U	0	0	0	2	0	1	0	3	2
Rhaphoneis amphiceros	B	U	0	2	4	11	10	11	6	0	3
Rhopolodia musculus	B	C	0	0	0	1	0	0	0	0	0
Scolioneis tumida	B	B1	0	6	5	53	28	44	58	16	13
Synedra fasciculata	B	C	0	0	0	0	0	1	0	0	0
Tryblionella acuminata	B	U	0	5	2	2	5	3	1	0	5
Tryblionella navicularis	B	B1	5	29	1	35	2	6	7	49	11
Tryblionella punctata	B	U	2	9	11	21	0	11	7	19	6
Cyclostephanos dubius	C	U	0	0	0	0	0	1	0	0	0

209

Species											
Cocconeis disculus	D	C	0	0	0	1	0	0	1	0	0
Cymbella heteropleura	D	C	0	0	0	0	0	0	0	0	2
Cymbella microcephala	D	C	0	0	0	0	0	0	0	0	1
Diploneis elliptica	D	D	0	1	10	2	23	4	0	0	6
Diploneis ovalis	D	D	0	0	0	0	0	0	18	10	0
Epithemia sorex	D	C	0	0	0	0	0	1	0	0	1
Staurosira construens	D	A	0	0	0	0	0	0	0	0	1
Pseudostaurosira brevistriata	D	A	0	0	0	0	0	0	0	0	2
Fragilaria construens var binodis	D	U	0	0	0	0	1	0	0	0	0
Staurosirella pinnata	D	C	0	0	0	0	0	0	0	0	1
Hantzschia amphioxys	D	D	4	0	0	0	0	0	0	0	0
Nitzschia paleacea	D	U	0	0	0	0	0	0	0	0	1
Pinnularia intermedia	D	D	2	0	0	0	0	0	0	0	0
Cymatosira lorenziana	U	U	0	0	0	0	0	1	0	0	0
Achnanthes angustata	U	U	0	1	0	0	0	0	0	0	0
Cyclotella dubius	U	U	0	0	0	1	0	0	0	0	0
Total # of species:			102	267	262	377	254	256	255	259	328

Appendix 10

Foraminifera counts for Oldtown Marsh.

Depth (cm):	249	258	264	270	276	324	328	330	334
Foraminifera species									
Jadammina macrescens	0	156	0	1	1	83	44	32	0
Miliammina fusca	0	0	0	0	0	1	0	0	0
Trochammina inflata	1	12	0	0	0	2	0	0	0
Total # of species:	1	168	0	1	1	86	44	32	0

Appendix 11

Diatom counts for Oldtown Marsh. See Appendix 9 for salinity and life-form key.

Diatom species	Salinity	Life-form	172	176	196	202	204	206	208	209	210	211	212	214	216	218	220	224	232	274	278	286	290	300
Actinoptychus senarius	A	A	4	5	16	3	5	7	2	2	0	0	0	0	0	1	0	0	0	3	3	3	2	4
Cocconeis costata	A	C	0	0	0	0	0	0	0	0	0	0	0	0	0	1	0	0	0	0	0	0	0	0
Cocconeis scutellum	A	C	0	0	1	0	0	0	2	0	1	2	0	0	0	0	0	0	0	1	0	0	0	0
Cymatosira belgica	A	A	0	0	0	0	0	0	0	2	0	0	0	0	0	0	0	0	0	0	0	0	0	0
Delphineis surirella	A	C	0	0	0	0	0	7	6	0	3	0	0	1	0	0	0	0	0	0	0	0	0	0
Diploneis crabro	A	B1	0	0	0	0	2	0	0	0	0	0	0	0	0	0	0	0	0	0	0	0	0	0
Dimerogramma minor	A	C	0	0	0	0	0	2	0	0	1	0	0	0	0	0	0	0	0	0	0	0	0	0
Grammatophora oceanica	A	C	0	0	0	0	0	1	3	0	0	0	0	0	0	0	0	0	0	0	0	0	0	0
Pseudopodosira westii	A	B1	3	0	5	3	1	0	1	0	0	0	0	0	0	0	0	0	0	6	1	4	5	2
Navicula forcipata	A	B1	0	0	0	0	0	0	5	0	3	0	0	2	0	0	0	0	0	0	0	0	0	0
Navicula marina	A	B1	0	0	0	0	0	1	0	0	0	0	0	0	0	0	0	0	0	0	0	0	0	0
Paralia sulcata	A	B1	20	28	42	54	104	59	46	17	8	5	2	2	2	2	0	3	1	27	20	35	17	26
Podosira stelligera	A	A	3	3	0	1	5	0	0	0	0	0	0	0	0	0	0	0	0	1	5	3	4	0
Psammodictyon panduriforme	A	B1	0	0	0	0	0	0	2	0	0	0	1	1	0	1	0	0	0	0	0	0	0	0
Raphoneis surirella	A	C	0	0	0	0	0	0	0	8	0	2	0	0	0	0	0	0	0	0	0	0	0	0
Surirella fastuosa	A	B1	1	0	0	0	0	0	0	0	0	0	0	0	0	0	0	0	0	0	1	0	0	0

Species																								
Thalassiosira leptopa	A	U	0	1	1	0	0	0	0	1	0	2	0	0	0	0	0	0	0	2	0	0	1	2
Thalassiosira oestrupii	A	A	0	1	0	0	0	0	0	0	0	0	0	0	0	0	0	0	0	0	0	0	0	0
Trachyneis aspera	A	B1	0	0	1	2	13	0	0	1	0	2	0	0	0	0	0	0	0	0	0	0	0	0
Triceratium favus	A	A	2	1	1	0	0	0	0	0	0	0	0	0	0	0	0	0	0	0	1	1	1	1
Tryblionella granulata	A	B1	0	0	2	1	0	0	0	0	0	0	0	0	0	0	0	0	0	3	3	0	6	3
Achnanthes delicatula	B	C	0	1	0	0	0	0	0	0	3	2	7	1	3	5	5	4	0	0	0	0	0	0
Amphora commutata	B	B1	0	0	0	0	0	0	0	0	0	0	0	0	0	0	0	0	1	0	0	0	0	0
Amphora exigua	B	B1	0	0	0	0	0	0	0	0	0	0	0	0	0	1	0	0	0	0	0	0	0	0
Amphora holsatica	B	B1	0	0	0	0	0	0	0	0	0	0	1	0	0	0	0	0	0	0	0	0	0	0
Caloneis westii	B	B1	0	0	2	1	8	21	20	9	11	0	0	0	0	1	0	0	0	0	0	0	0	0
Campylodiscus echeneis	B	B1	1	0	0	0	0	0	0	0	0	0	0	0	0	0	0	0	0	4	6	2	3	2
Diploneis didyma	B	B1	3	13	14	15	24	5	0	0	0	0	0	0	0	0	0	0	0	4	2	4	4	4
Diploneis interrupta	B	B1	2	0	0	0	2	1	0	0	0	0	0	1	1	0	0	1	0	1	0	0	1	0
Diploneis pseudovalis	B	U	0	0	0	0	0	0	0	0	0	0	0	0	0	0	0	1	0	0	0	0	0	0
Fallacia pygmaea	B	B3	0	0	0	0	0	0	0	1	0	3	0	0	0	10	8	13	0	0	0	0	0	0
Frustulia creuzbergensis	B	B1	0	0	0	0	0	0	0	1	0	2	0	0	0	0	0	0	0	0	0	0	0	0
Mastogloia elliptica	B	B1	0	0	0	0	0	0	0	0	0	0	0	0	0	1	3	0	0	0	0	0	0	0
Navicula arenaria	B	U	0	0	0	0	0	0	0	0	1	0	1	0	0	0	0	0	0	0	0	0	0	0
Navicula digitoradiata	B	B1	0	0	0	0	0	18	49	40	12	13	3	0	0	0	1	1	1	0	0	0	0	0
Navicula elegans	B	B1	0	0	0	0	0	0	0	0	0	0	0	3	0	0	1	1	0	0	0	0	0	0
Navicula peregrina	B	B1	1	0	1	0	1	5	8	8	21	26	27	11	41	13	14	26	65	0	0	0	0	0
Navicula pygmea	B	B1	0	0	0	0	0	0	0	0	0	0	9	9	0	0	0	0	0	0	0	0	0	0
Navicula salinarum	B	B1	0	0	0	0	0	0	0	0	0	0	2	2	0	0	0	0	0	0	0	0	0	0

Species																								
Nitzschia scalaris	B	B1	0	0	0	0	0	1	2	0	1	1	1	1	1	0	0	0	3	0	0	0	0	0
Nitzschia sigma	B	B1	0	0	0	0	0	0	9	6	6	0	1	1	3	0	0	0	0	0	0	0	0	0
Nitzschia vitrea	B	B1	0	0	0	0	0	0	0	0	0	0	0	0	0	0	0	0	1	0	0	0	0	0
Petroneis marina	B	U	0	1	0	3	0	0	0	0	0	0	0	0	0	0	0	0	0	0	0	0	0	1
Rhaphoneis amphiceros	B	U	3	2	9	5	6	12	5	0	2	0	1	0	0	0	2	0	1	3	1	1	0	2
Scolioneis tumida	B	B1	55	51	14	8	15	79	82	113	40	12	0	0	1	0	0	0	0	0	0	0	0	0
Synedra pulchella	B	C	0	0	0	0	0	0	0	0	0	5	0	3	0	0	2	4	2	0	0	0	0	0
Tryblionella acuminata	B	U	0	0	0	0	0	0	2	1	0	0	2	1	0	0	0	0	1	0	0	0	0	0
Tryblionella navicularis	B	B1	4	3	17	9	46	6	1	0	0	0	0	0	0	0	0	0	1	2	2	2	2	1
Tryblionella punctata	B	U	3	1	3	1	8	1	0	0	0	0	1	0	1	0	1	1	0	42	54	52	59	55
Amphora veneta	C	B1	0	0	0	0	0	0	0	0	0	0	0	0	0	0	0	0	3	0	0	0	0	0
Anomoeoneis sphaeophora	C	B1	0	0	0	0	0	0	0	1	0	0	0	0	0	0	0	0	0	0	0	0	0	0
Navicula avenacea	C	B1	0	0	0	0	0	0	0	0	0	0	0	0	0	4	1	0	0	0	0	0	0	0
Navicula capitata var hungarica	C	U	0	0	0	0	0	0	0	0	0	0	0	1	0	0	0	0	0	0	0	0	0	0
Navicula cari var cincta	C	D	0	0	0	0	0	0	0	0	0	0	0	0	0	2	4	1	0	0	0	0	0	0
Navicula cincta	C	D	0	0	0	0	1	1	2	3	17	0	2	1	4	1	8	3	2	0	0	0	0	0
Navicula cryptocephala	C	B1	0	0	0	0	0	0	0	0	0	0	0	0	0	1	0	0	0	0	0	0	0	0
Navicula recens	C	U	0	0	0	0	0	0	0	1	0	0	0	0	0	0	0	0	0	0	0	0	0	0
Nitzschia frustulum	C	B1	0	0	0	0	0	0	0	0	0	0	0	1	0	0	0	0	0	0	0	0	0	0
Rhopalodia brebissonii	C	U	0	0	0	0	0	0	0	4	6	2	1	0	1	0	0	0	0	0	0	0	0	0
Stauroneis producta	C	B1	0	0	0	0	0	0	0	0	0	0	0	0	1	0	3	1	0	0	0	0	0	0

Species																								
Surirella brebissonii	C	U	0	0	0	0	0	0	0	0	0	0	0	0	1	1	1	0	0	0	0	0	0	0
Achnanthes minutissima	D	C	0	0	0	0	0	0	0	0	0	0	0	0	0	0	1	0	0	0	0	0	0	0
Amphora copulata	D	U	0	0	0	0	0	2	1	0	0	0	2	1	1	0	1	4	6	0	0	0	0	0
Amphora ovalis	D	B1	0	0	0	0	0	0	0	0	0	0	0	1	0	0	1	1	0	0	0	0	0	0
Caloneis bacillum	D	D	0	0	0	0	0	0	0	3	0	1	0	0	0	0	0	0	0	0	0	0	0	0
Cocconeis disculus	D	C	0	0	0	0	1	0	0	0	0	1	0	0	0	0	0	0	0	0	0	0	0	0
Cocconeis placentula	D	C	0	0	0	1	0	1	0	0	0	0	0	0	0	0	0	0	0	0	0	0	0	0
Cymbella aspera	D	D	0	0	0	0	0	0	0	0	0	0	0	0	1	0	0	0	0	0	0	0	0	0
Cymbella cymbiformis	D	C	0	0	0	0	0	0	0	0	0	0	0	0	0	0	0	0	0	0	1	0	0	0
Cymbella microcephala	D	C	0	0	0	0	0	0	0	0	0	0	0	0	0	0	2	1	0	0	0	0	0	0
Diatoma hymale	D	C	1	0	0	1	0	0	0	0	0	0	0	0	0	0	0	0	2	0	0	0	0	0
Diploneis elliptica	D	D	0	0	0	0	1	0	1	1	1	3	6	3	6	4	6	8	16	0	2	1	0	0
Diploneis ovalis	D	D	0	0	0	0	0	1	1	0	2	2	0	0	0	4	1	2	8	0	0	0	0	0
Epithemia adnata	D	U	0	0	1	0	0	0	0	0	0	0	0	0	0	0	0	0	0	0	1	0	0	1
Epithemia argus	D	C	0	0	0	0	1	0	0	0	0	0	0	0	0	0	0	0	0	0	0	0	0	0
Fragilaria capucina	D	C	0	0	0	0	0	0	0	0	0	0	1	0	0	0	0	0	0	0	0	0	0	0
Staurosira construens	D	A	0	0	0	0	0	3	2	4	20	29	47	47	76	55	33	23	19	0	0	0	0	0
Staurosirella pinnata	D	C	0	0	0	0	1	3	0	7	0	6	10	58	10	30	29	19	21	0	0	0	0	0
Gomphonema insigne	D	U	0	0	0	0	0	0	0	0	0	0	0	0	0	0	0	0	1	0	0	0	0	0
Gomphonema olivaceum	D	C	0	0	0	0	0	0	3	0	0	0	0	0	0	0	0	0	0	0	0	0	0	0
Gyrosigma acuminatum	D	B1	0	0	0	0	0	0	0	0	0	1	1	0	0	0	0	0	0	0	0	0	0	0
Mastogloia smithii	D	B1	0	0	0	0	0	0	0	0	2	0	0	0	0	1	0	0	0	0	0	0	0	0

Species																							
Navicula cari	D	B1	0	0	0	0	0	0	0	8	0	0	0	0	0	1	0	0	0	0	0	0	0
Navicula dicephala	D	B1	0	0	0	0	0	0	0	0	0	0	0	0	0	1	0	0	0	0	0	0	0
Navicula gracilis	D	B1	0	0	0	0	0	0	0	0	0	0	0	0	1	0	0	0	0	0	0	0	0
Navicula placentula	D	B1	0	0	0	0	0	0	0	0	0	0	1	0	0	0	2	4	0	0	0	0	0
Cosmioneis pusilla	D	B1	0	0	0	0	0	0	0	0	0	0	0	1	0	0	0	0	0	0	0	0	0
Navicula rhynchocephala	D	D	0	0	0	0	0	0	0	2	0	3	21	13	0	2	16	15	7	0	0	0	0
Nitzschia amphibia	D	D	0	0	0	0	0	0	0	0	0	0	0	0	0	0	1	0	0	0	0	0	0
Pinnularia major	D	U	0	0	0	0	2	0	0	0	0	1	2	0	0	2	2	1	3	0	0	0	0
Pinnularia viridis	D	D	0	0	0	0	0	3	0	0	0	0	0	0	0	1	0	0	0	0	0	0	0
Placoneis elginensis	D	U	0	0	0	0	0	0	0	0	0	0	0	0	0	1	0	0	0	0	0	0	0
Stauroneis anceps	D	U	0	0	0	0	0	0	0	0	0	0	0	0	0	1	0	0	0	0	0	0	0
Stauroneis phoenicenteron	D	B1	0	0	0	0	0	0	0	0	0	2	0	0	0	0	0	0	0	0	0	0	0
Pseudostaurosira elliptica	D	A	0	0	0	0	0	1	1	2	101	95	56	42	38	57	42	32	0	0	0	0	0
Staurosirella lapponica	D	C	0	0	0	0	3	8	6	6	25	28	34	41	61	57	62	55	32	0	0	0	0
Stephanodiscus rotula	D	U	0	0	0	0	0	0	0	0	0	0	0	0	0	0	0	0	0	0	0	0	1
Surirella brightwelli	D	B1	0	0	0	0	0	0	1	0	0	0	0	0	0	0	0	0	0	0	0	0	0
Pseudostaurosira brevistriata	D	A	0	0	0	0	0	0	0	0	0	2	0	0	0	0	4	22	5	0	0	0	0
Pinnularia nobilis	E	B1	0	0	0	0	0	0	0	0	0	0	0	0	0	0	0	0	37	0	0	0	0
Tabellaria flocculosa	E	C	0	0	0	0	0	0	0	0	0	0	0	0	0	0	0	0	2	0	0	0	0
Cocconeis guttata	U	U	0	0	0	0	0	2	0	0	0	0	4	0	0	0	0	0	0	0	0	0	0
Rhopalodia gibberula	U	U	0	0	0	0	0	0	0	0	0	0	0	0	0	0	1	0	0	0	0	0	0
Stauroneis alpina	U	U	0	0	0	0	0	0	4	0	2	0	3	0	0	2	0	1	0	0	0	0	0

Pinnunavis elegans	U	U	0	0	0	0	0	0	0	0	0	1	2	2	0	0	0	0	0	0	0	0	0	0
Cavinula variostriata	U	U	0	0	0	0	0	0	0	0	0	0	1	0	0	0	0	0	0	0	0	0	0	0
Pinnularia neglecta	U	U	0	0	0	0	0	0	0	0	0	0	1	0	0	0	0	0	0	0	0	0	0	0
Fragilaria schulzii	U	U	0	0	0	0	0	0	0	0	0	0	2	0	0	0	0	0	0	0	0	0	0	0
Nitzschia amphiplectans	U	U	0	0	0	0	0	0	0	0	0	0	0	1	0	0	0	0	0	0	0	0	0	0
Navicula florinae	U	U	0	0	0	0	0	2	0	0	0	0	0	0	0	0	0	0	0	0	0	0	0	0
Martyana martyi	U	U	0	0	0	0	0	1	0	0	0	0	0	0	0	0	0	0	0	0	0	0	0	0
Synedra pulchella	U	U	0	0	0	0	0	0	0	0	0	1	0	0	4	0	0	0	0	0	0	0	0	0
Gyrosigma sp	U	U	0	0	0	0	0	0	3	0	0	0	0	0	0	0	0	0	0	0	0	0	0	0
Tabularia fasisculata	U	U	0	0	0	0	0	0	0	0	0	2	4	0	5	0	0	0	0	0	0	0	0	0
Caloneis subsalina	U	U	0	0	0	0	0	0	0	0	0	0	0	0	1	0	0	0	0	0	0	0	0	0
Navicula toulaae	U	U	0	0	0	0	0	0	0	0	0	0	0	0	1	0	0	0	0	0	0	0	0	0
Caloneis crassa	U	U	0	0	0	0	0	0	0	0	0	0	0	0	0	4	0	0	0	0	0	0	0	0
Encyonenon paucistriatum	U	U	0	0	0	0	0	0	0	0	0	0	0	0	0	2	0	0	0	0	0	0	0	0
Navicula simplex	U	U	0	0	0	0	0	0	0	0	0	0	0	0	0	0	4	0	0	0	0	0	0	0
Epithemia cistula	U	U	0	0	0	0	0	0	0	0	0	0	0	0	0	0	0	1	0	0	0	0	0	0
Rhopalodia rupestris	U	U	0	0	0	0	0	0	0	0	0	0	0	0	0	0	0	6	0	0	0	0	0	0
Cymbella cornuta	U	U	0	0	0	0	0	0	0	0	0	0	0	0	0	0	0	1	0	0	0	0	0	0
Navicula fasciculata	U	U	0	0	0	0	0	0	0	1	0	0	0	0	0	0	0	0	0	0	0	0	0	0
Rhopolodia rupestris	U	U	1	0	0	0	0	0	0	0	0	0	0	0	0	0	0	0	0	0	0	0	0	0
Total # of species:			107	111	130	108	250	254	270	253	289	254	259	252	258	273	258	257	250	101	103	108	105	105

Appendix 12

Raw diatom counts for Great Dingle Hill. See Appendix 9 for salinity and life-form key.

Diatom species	Salinity	Depth (cm): Life-form	146	154	162	164	166	168	170	172	174	176	178	184	186	190
Achnanthes longipes	A	C	0	0	0	0	0	0	2	1	0	0	0	0	0	0
Actinoptychus senarius	A	A	4	7	4	0	4	5	3	5	2	3	0	0	1	1
Caloneis liber	A	B1	0	0	1	0	0	0	0	0	0	0	0	0	0	0
Cerataulous radiatus	A	U	0	0	1	0	0	0	0	0	0	0	0	0	0	0
Cocconeis costata	A	C	0	0	0	0	0	0	0	0	1	0	0	0	0	0
Cocconeis peltoides	A	C	0	0	0	1	1	0	0	1	0	0	0	0	0	0
Cocconeis scutellum	A	C	2	0	5	0	3	0	0	0	1	0	0	2	0	0
Delphineis surirella	A	C	0	0	11	7	8	0	4	0	0	3	3	2	0	1
Diploneis bombus	A	B1	0	0	0	0	0	0	2	0	0	0	0	0	0	0
Diploneis crabro	A	B1	0	0	2	0	1	0	0	0	2	0	0	0	0	0
Dimerogramma minor	A	C	0	1	0	0	0	0	0	0	0	1	0	0	0	0
Grammatophora oceanica	A	C	0	0	2	0	1	0	0	0	0	1	0	0	0	0
Pseudopodosira westii	A	B1	0	0	0	0	0	0	0	0	0	3	2	0	1	3
Navicula bottnica	A	B1	0	0	2	1	0	0	0	0	0	0	0	0	0	0
Navicula forcipata	A	B1	0	0	1	0	2	0	0	0	0	2	1	0	0	0
Navicula humerosa	A	B1	0	0	0	0	0	0	0	0	0	1	0	0	0	0
Paralia sulcata	A	B1	96	90	69	63	58	61	88	75	60	86	23	18	27	16
Pleurosigma normanii	A	B1	0	0	1	0	0	0	0	0	0	0	0	0	0	0
Podosira stelligera	A	A	0	1	2	0	0	0	1	0	0	0	0	0	0	0

Species															
Psammodictyon panduriforme	A	B1	2	0	0	0	0	0	0	0	0	2	0	0	0	0
Rhabdonema arcuatum	A	U	0	0	0	0	0	0	0	1	0	0	0	0	0	0
Surirella fastuosa	A	B1	0	0	1	0	0	0	0	0	0	0	0	0	0	0
Thalassiosira leptopa	A	U	0	0	0	0	0	0	1	0	0	0	0	0	0	0
Thalassiosira oestrupii	A	A	0	0	0	2	1	0	0	0	0	0	0	0	0	0
Trachyneis aspera	A	B1	2	0	0	0	0	0	1	3	1	1	0	2	1	0
Tryblionella granulata	A	B1	0	0	0	0	0	0	2	0	0	0	0	0	0	0
Achnanthes brevipes	B	C	0	0	0	0	0	1	0	0	0	3	2	0	0	0
Achnanthes delicatula	B	C	0	0	2	0	0	0	1	0	0	0	0	0	0	0
Anomoeoneis sculpta	B	B1	0	0	0	0	1	0	0	0	0	0	0	0	0	0
Caloneis westii	B	B1	8	11	16	13	9	14	8	29	35	24	55	135	75	74
Campylodiscus echeneis	B	B1	1	0	0	0	0	0	0	1	0	0	0	0	0	0
Diploneis didyma	B	B1	8	13	6	3	3	5	1	10	16	5	9	10	14	0
Diploneis interrupta	B	B1	19	14	18	20	7	7	4	4	6	6	3	7	3	30
Frustulia creuzbergensis	B	B1	0	0	0	0	0	1	0	0	0	0	0	0	0	0
Gyrosigma hippocampus	B	U	0	0	0	0	2	0	0	0	0	0	0	0	0	0
Gyrosigma spenceri	B	B1	0	0	0	0	0	0	1	0	0	0	0	0	0	0
Navicula digitoradiata	B	B1	7	6	2	14	29	23	6	7	13	8	7	0	0	0
Navicula peregrina	B	B1	16	32	12	21	18	25	13	15	12	10	90	41	63	53
Nitzschia obtusa	B	B1	0	0	0	0	0	0	1	0	0	0	0	0	0	0
Nitzschia scalaris	B	B1	0	0	1	0	0	0	1	1	0	0	0	0	0	8

Species																
Nitzschia sigma	B	B1	0	1	8	1	5	3	4	5	3	1	1	0	0	0
Petroneis marina	B	U	7	3	0	0	0	0	1	1	4	1	10	1	0	0
Rhaphoneis amphiceros	B	U	16	7	5	7	3	15	8	9	13	2	1	0	2	0
Scolioneis tumida	B	B1	11	19	31	43	36	24	30	32	14	32	26	2	0	0
Surirella striatula	B	B1	0	0	0	0	1	0	0	0	0	0	0	0	0	0
Synedra fasciculata	B	C	0	1	0	0	0	0	0	0	0	0	0	0	0	0
Synedra tabulata	B	C	0	0	0	0	0	0	0	1	0	0	0	0	0	0
Tryblionella acuminata	B	U	0	4	9	4	7	4	10	5	1	2	1	0	1	0
Tryblionella apiculata	B	U	0	0	1	0	0	0	0	0	0	0	0	0	0	0
Tryblionella coarctata	B	U	0	0	0	0	0	0	0	1	0	0	0	0	0	0
Tryblionella navicularis	B	B1	10	5	3	3	1	1	6	16	46	9	13	11	4	2
Tryblionella punctata	B	U	29	10	8	7	7	8	12	4	5	8	4	0	2	0
Amphora veneta	C	B1	0	0	0	1	0	0	0	0	0	0	0	0	0	0
Anomoeoneis sphaeophora	C	B1	0	0	0	0	0	1	0	0	1	0	1	0	0	0
Cocconeis pediculus	C	C	1	0	0	0	2	0	0	0	1	0	0	0	0	0
Cyclostephanos dubius	C	U	0	0	0	0	0	1	1	0	0	0	0	0	0	0
Navicula cincta	C	D	0	1	0	3	4	3	0	6	0	0	1	0	0	1
Nitzschia frustulum	C	B1	0	0	0	0	1	0	0	1	0	0	0	0	0	0
Tryblionella hungarica	C	U	0	0	0	1	0	0	0	0	0	0	0	0	0	0
Amphora copulata	D	U	0	0	0	1	0	0	0	0	0	0	0	0	0	0
Caloneis bacillaris	D	B1	0	0	0	0	1	0	0	0	0	0	0	0	0	0
Caloneis bacillum	D	D	0	0	0	5	1	2	2	2	0	3	0	0	0	0
Cocconeis disculus	D	C	0	0	0	0	0	3	2	1	1	0	0	0	0	0

220

Species																
Cocconeis placentula	D	C	0	1	0	0	0	4	0	2	2	2	0	0	0	0
Cyclotella ocellata	D	A	0	0	0	0	0	0	1	0	0	0	0	0	0	0
Cymbella microcephala	D	C	0	0	0	0	0	0	1	0	0	0	0	0	0	0
Diploneis elliptica	D	D	10	20	19	12	2	10	9	16	15	6	0	0	0	0
Diploneis ovalis	D	D	0	3	1	2	2	2	6	0	5	7	3	26	67	60
Epithemia adnata	D	U	0	0	0	0	0	0	1	0	0	0	0	1	0	0
Epithemia sorex	D	C	3	1	0	1	1	5	0	0	0	3	1	0	0	0
Fragilaria construens var binodis	D	U	1	0	0	0	1	2	2	0	0	0	0	0	0	0
Staurosirella pinnata	D	C	0	0	7	7	0	0	0	0	0	0	0	0	0	0
Gomphonema olivaceum	D	C	0	0	0	0	4	0	0	0	0	0	0	0	0	0
Gyrosigma acuminatum	D	B1	0	0	0	0	0	1	0	0	0	0	0	0	0	0
Mastogloia smithii	D	B1	0	0	0	0	1	1	6	1	0	0	0	0	0	0
Navicula costulata	D	B1	0	0	0	0	0	0	0	2	0	0	0	0	0	0
Navicula placentula	D	B1	0	0	1	0	0	0	0	0	0	0	0	0	0	0
Cosmioneis pusilla	D	B1	0	0	0	0	0	0	1	0	0	0	0	0	0	0
Nitzschia palea	D	D	0	0	0	0	0	1	0	0	0	0	0	0	0	0
Nitzschia recta	D	B1	0	0	0	0	0	0	2	0	0	0	0	0	0	0
Nitzschia supralittorea	D	U	0	0	0	0	0	1	0	0	0	0	0	0	0	0
Pinnularia borealis	D	D	0	0	0	0	0	0	1	0	0	0	0	0	0	0
Pinnularia major	D	U	0	0	0	0	0	0	1	0	0	0	0	0	0	0
Pinnularia viridis	D	D	0	0	0	0	0	1	0	0	0	0	2	7	1	7
Stauroneis phoenicenteron	D	B1	0	1	0	1	0	0	0	0	0	0	0	0	0	0
Pseudostaurosira elliptica	D	A	0	0	0	0	14	19	0	0	0	13	0	0	0	0

Staurosirella lapponica	D	C	0	0	0	0	0	1	0	0	0	0	0	0	0	0
Pseudostaurosira brevistriata	D	A	0	0	0	0	0	0	0	1	0	0	0	0	0	0
Tabellaria flocculosa	E	C	4	0	0	0	0	0	0	0	0	0	0	0	0	0
Cocconeis guttata	U	U	0	0	0	4	0	0	0	0	0	0	0	0	0	0
Cymatosira lorenziana	U	U	0	0	1	0	0	0	0	0	0	0	0	0	0	0
Caloneis borealis	U	U	0	0	1	0	0	0	0	0	0	0	0	0	0	0
Cosmioneis pusilla	U	U	0	0	0	1	0	1	0	3	0	0	0	0	0	0
Staurophora amphioxys	U	U	0	0	0	1	0	1	0	0	0	0	0	0	0	0
Tabularia tabulata	U	U	0	0	0	0	1	0	0	0	0	0	0	0	0	0
Staurosirella pinnata	U	U	0	0	0	0	6	1	0	1	0	1	0	0	0	0
Rhopalodia gibberula	U	U	0	0	0	0	1	0	1	1	0	0	0	0	0	0
Stauroneis alpina	U	U	0	0	0	0	0	0	0	0	0	1	0	0	0	0
Tabularia investiens	U	U	0	0	0	0	0	0	0	0	0	2	0	0	0	0
Pinnunavis elegans	U	U	2	3	0	0	0	0	2	1	2	0	0	0	0	0
Cavinula variostriata	U	U	0	0	1	0	0	0	0	0	0	0	0	0	0	0
Tabularia fasciculata	U	U	0	1	1	0	0	0	0	1	1	0	0	0	0	0
Tabularia fasciculata imposter	U	U	0	0	0	2	7	0	0	0	0	0	0	0	0	0
Rhopolodia musculus	U	U	0	0	0	0	0	0	1	0	0	0	0	0	0	0
Achnanthes promunturii	U	U	0	0	0	0	0	0	0	2	0	0	0	0	0	0
Diploneis novaeseelandiae	U	U	1	0	0	0	0	0	0	0	0	0	0	0	0	0
	Total # of species:		260	256	256	252	257	258	251	268	263	252	259	265	262	256

Appendix 13

Raw diatom counts for MN-16-2, Minsmere. See Appendix 9 for salinity and life-form key.

Diatom species	Salinity	Depth (cm): Life-form	184	188	192	196	200	204	240
Actinoptychus senarius	A	A	45	55	29	53	16	21	37
Cocconeis disculoides	A	C	0	0	2	0	0	0	0
Cocconeis scutellum	A	C	0	0	7	0	0	0	0
Diploneis smithii	A	B1	1	0	1	0	0	0	0
Pseudopodosira westii	A	B1	6	6	3	0	1	5	4
Navicula ramosissima	A	C	0	0	0	0	1	0	0
Opephora pacifica	A	C	0	0	0	0	0	0	0
Paralia sulcata	A	B1	61	58	101	70	49	78	74
Pleurosigma normanii	A	B1	0	1	0	0	0	0	0
Podosira stelligera	A	A	4	10	2	4	6	3	3
Psammodictyon panduriforme	A	B1	0	2	2	2	1	1	3
Delphineis surirella	A	C	19	25	17	18	4	4	18
Thalassiosira leptopa	A	U	4	6	4	3	2	3	3
Trachyneis aspera	A	B1	1	2	2	0	0	0	0
Triceratium alternans	A	B1	1	0	0	0	0	0	1
Triceratium favus	A	A	0	0	0	0	1	0	1
Anomoeoneis sculpta	B	B1	1	0	0	0	0	0	0
Anomoeoneis spaerophora var sculpta	B	B1	0	1	0	0	0	0	0
Caloneis westii	B	B1	2	0	1	0	0	0	0
Campylodiscus clypeus var biscostatus	B	B1	1	0	0	0	0	0	0

Species									
Campylodiscus echeneis	B	B1	0	2	1	5	5	5	2
Diploneis didyma	B	B1	2	1	1	0	1	4	3
Diploneis interrupta	B	B1	0	1	1	0	1	1	0
Fallacia pygmaea	B	B3	0	0	5	0	0	0	0
Navicula digitoradiata	B	B1	2	4	2	1	0	1	6
Navicula peregrina	B	B1	2	2	0	1	0	0	0
Nitzschia sigma	B	B1	0	0	3	0	0	0	1
Petroneis marina	B	U	0	0	0	0	0	0	5
Rhaphoneis amphiceros	B	U	19	25	29	32	4	10	36
Scolioneis tumida	B	B1	1	1	1	0	1	0	0
Surirella striatula	B	B1	0	1	0	2	2	0	2
Thalassiosira eccentrica	B	U	0	0	0	0	0	0	1
Tryblionella acuminata	B	U	0	6	1	0	0	0	1
Tryblionella navicularis	B	B1	4	2	2	3	0	6	8
Tryblionella punctata	B	U	49	24	15	18	79	77	18
Navicula cari var cincta	C	D	0	0	0	0	0	0	1
Surirella subsala	C	B1	1	0	0	0	0	0	0
Tryblionella levidensis	C	B1	0	1	1	1	0	0	1
Tryblionella litoralis	C	B1	0	0	1	0	0	0	0
Amphora copulata	D	U	1	3	2	4	3	3	1
Cocconeis disculus	D	C	0	1	0	0	0	1	0
Cocconeis placentula	D	C	0	0	0	1	4	2	1
Cymbella affinis	D	C	0	0	0	1	0	0	0
Cymbella cistula	D	D	0	0	0	5	0	0	0
Cymbella cybiformis	D	C	0	0	0	0	1	0	0
Cymbella helvetica	D	C	0	0	1	0	1	0	0
Cymatopleura elliptica	D	B1	0	0	0	2	1	1	0
Epithemia adnata	D	U	5	3	5	13	40	13	9
Epithemia porcellus	D	U	6	4	3	13	24	22	6
Epithemia hyndmanii	D	C	0	0	0	0	1	0	0

Epithemia sorex	D	C	2	1	2	0	2	1	1
Epithemia sorex var gracilis	D	C	0	0	0	0	1	0	0
Epithemia turgida	D	C	17	0	0	9	1	0	0
Staurosirella lapponica	D	C	0	0	1	0	0	0	0
Staurosirella pinnata	D	C	0	0	3	0	0	0	0
Gomphonema gracile	D	C	0	0	1	0	0	0	0
Gyrosigma acuminatum	D	B1	0	2	0	0	0	0	0
Navicula cari	D	B1	1	0	0	0	0	0	0
Navicula radiosa	D	B1	0	2	0	0	0	0	0
Pinnularia viridis	D	D	0	0	1	0	2	1	0
Placoneis elginensis	D	U	0	0	0	1	0	0	0
Stauroneis phoenicenteron	D	B1	0	0	1	0	0	0	0
Stephanodiscus rotula	D	U	0	0	1	0	0	0	0
Stephanodiscus rotula	D	U	0	0	0	1	0	0	2
Cyclotella antiqua	E	A	0		1	0	0	0	0
Tryblionella gracilis	E	B1	0	0	0	0	1	0	0
Nitzschia amphiplectans	U	U	0	1	0	0	0	0	0
Synedra puchella	U	U	0	0	0	0	0	0	1
Surirella patella	U	U	0	1	0	0	0	0	0
Thalassiosira tenera	U	U	4	4	7	9	2	1	2
Surirella helvetica	U	U	0	0	0	2	0	0	0
Achnanthes gibberula	U	U	0	0	0	1	0	0	0
Caloneis lativscula	U	U	0	0	1	0	0	0	0
	Total # of species:	262	258	264	275	258	264	252

Appendix 14

Raw diatom counts for MN-16-3, Minsmere. See Appendix 9 for salinity and life-form key.

Diatom species	Salinity	Depth (cm): Life-form	136	138
Actinoptychus senarius	A	A	21	16
Cocconeis pinnata	A	C	1	0
Diploneis crabro	A	B1	0	2
Pseudopodosira westii	A	B1	5	1
Opephora pacifica	A	C	1	0
Paralia sulcata	A	B1	112	140
Plagiogramma staurophorum	A	B1	1	0
Podosira stelligera	A	A	1	4
Psammodictyon panduriforme	A	B1	1	2
Delphineis surirella	A	C	21	19
Thalassiosira leptopa	A	U	1	5
Trachyneis aspera	A	B1	1	1
Campylodiscus echeneis	B	B1	1	1
Diploneis didyma	B	B1	1	0
Navicula digitoradiata	B	B1	0	1
Navicula peregrina	B	B1	0	1
Rhaphoneis amphiceros	B	U	14	17
Rhopolodia musculus	B	C	7	0
Scolioneis tumida	B	B1	1	1
Synedra pulchella	B	C	1	0
Tryblionella acuminata	B	U	0	2
Tryblionella navicularis	B	B1	1	1
Tryblionella punctata	B	U	26	12
Rhopalodia brebissonii	C	U	5	0

Tryblionella levidensis	C	B1	1	0
Tryblionella litoralis	C	B1	0	1
Amphora copulata	D	U	0	2
Cocconeis disculus	D	C	1	1
Cocconeis placentula	D	C	2	2
Diploneis elliptica	D	D	1	0
Diploneis ovalis	D	D	0	1
Epithemia adnata	D	U	21	16
Epithemia turgida	D	C	2	0
Epithemia sorex	D	C	5	0
Pinnularia major	D	U	0	1
Pseudostaurosira brevistriata	D	A	1	0
Eneyonema gracile	E	C	1	0
Rhopalodia gibberula	U	U	0	1
Navicula inflexa	U	U	1	0
Thalassiosira tenera	U	U	0	5
	Total # of species:		259	256

Appendix 15

Raw diatom counts for MN-16-5, Minsmere. See Appendix 9 for salinity and life-form key.

Diatom species	Salinity	Depth (cm): Life-form	76	84	92	100	104	108	112	116
Achnanthes longipes	A	C	0	2	0	0	0	0	0	0
Actinoptychus senarius	A	A	0	0	2	2	2	2	4	6
Auliscus sculpta	A	B1	0	0	0	1	0	0	0	0
Diploneis smithii	A	B1	0	0	0	0	0	0	0	3
Pseudopodosira westii	A	B1	2	2	2	0	3	5	3	0
Navicula forcipata	A	B1	0	0	1	0	0	0	0	0
Opephora pacifica	A	C	0	0	3	0	0	0	0	0
Paralia sulcata	A	B1	15	17	45	39	27	21	45	14
Petroneis humerosa	A	B1	0	0	0	0	0	10	6	0
Podosira stelligera	A	A	0	1	1	2	1	0	1	0
Psammodictyon panduriforme	A	B1	0	0	0	0	0	1	0	0
Surirella comis	A	U	0	0	1	0	0	0	0	0
Delphineis surirella	A	C	0	0	0	0	0	2	0	1
Thalassiosira leptopa	A	U	1	1	0	0	0	0	0	1
Triceratium favus	A	A	0	0	1	0	1	0	0	0
Amphora proteus	B	B1	0	0	1	0	0	0	0	0
Anomoeoneis spaerophora var sculpta	B	B1	0	0	2	0	0	0	0	0
Caloneis westii	B	B1	0	25	36	26	10	0	1	13
Campylodiscus echeneis	B	B1	1	11	0	0	0	0	1	0
Diploneis didyma	B	B1	4	38	19	66	77	1	0	15
Diploneis interrupta	B	B1	3	13	15	6	60	27	4	69
Navicula digitoradiata	B	B1	0	1	8	8	0	0	0	9

Navicula peregrina	B	B1	48	7	18	34	11	128	15	4
Nitzschia sigma	B	B1	0	0	1	0	0	0	0	2
Nitzschia vitrea	B	B1	0	0	0	0	0	3	1	0
Petroneis marina	B	U	0	1	3	0	5	6	0	12
Rhaphoneis amphiceros	B	U	0	0	2	2	0	2	1	2
Scolioneis tumida	B	B1	0	1	18	2	7	0	0	48
Tryblionella acuminata	B	U	0	0	0	1	0	0	0	8
Tryblionella navicularis	B	B1	2	31	20	15	31	2	2	24
Tryblionella punctata	B	U	39	113	21	8	16	2	4	10
Anomoeoneis sphaeophora	C	B1	1	0	0	0	1	2	0	0
Navicula cincta	C	D	0	0	0	0	0	0	0	1
Nitzschia brevissima	C	U	0	0	0	0	0	1	0	0
Rhopalodia brebissonii	C	U	0	0	1	1	2	0	0	0
Surirella subsala	C	B1	0	0	1	4	3	1	0	0
Tryblionella litoralis	C	B1	0	0	1	0	0	0	0	0
Amphora copulata	D	U	0	0	7	2	1	0	0	0
Cocconeis disculus	D	C	0	0	0	0	0	4	0	0
Cocconeis placentula	D	C	0	0	0	0	0	0	2	0
Cyclotella bodanica	D	A	0	0	0	0	0	0	1	0
Cyclotella radiosa	D	U	0	0	0	0	0	0	1	0
Cymbella cistula	D	D	6	1	0	0	0	0	0	0
Cymbella microcephala	D	C	0	0	0	0	0	0	4	0
Diatoma hymale	D	C	0	0	0	0	0	0	0	1
Diploneis elliptica	D	D	2	5	14	3	0	2	0	4
Diploneis ovalis	D	D	0	0	0	22	15	0	0	0
Eunotia pectinalis	D	D	0	0	0	0	0	0	3	0
Epithemia adnata	D	U	0	0	4	8	2	5	8	0
Epithemia porcellus	D	U	2	3	1	0	0	0	0	1
Epithemia hyndmanii	D	C	0	0	4	0	0	0	6	0
Epithemia sorex	D	C	0	0	0	3	1	0	2	0

Epithemia turgida	D	C	1	0	0	0	0	0	0	0
Gomphonema acuminatum var brebissonii	D	C	0	0	0	0	0	0	1	0
Gomphonema angustatum	D	C	0	0	0	0	0	1	0	0
Gomphonema insigne	D	U	0	0	0	0	0	0	17	0
Navicula costulata	D	B1	0	0	1	0	0	1	0	0
Cosmioneis pusilla	D	B1	18	0	0	0	0	0	0	0
Navicula radiosa	D	B1	0	0	0	0	0	2	0	0
Nitzschia palea	D	D	3	0	0	0	0	0	1	0
Pinnularia abaujensis	D	B1	5	3	0	0	0	0	4	0
Pinnularia brevicostata	D	B1	0	0	0	0	0	0	2	0
Pinnularia major	D	U	0	0	0	1	0	0	0	0
Pinnularia viridis	D	D	117	5	0	4	1	17	32	2
Stephanodiscus rotula	D	U	0	0	0	0	0	0	10	0
Synedra capitata	D	C	2	0	0	0	0	1	1	0
Pseudostaurosira brevistriata	D	A	0	0	0	0	0	0	2	0
Cyclotella antiqua	E	A	1	0	1	0	0	0	0	0
Pinnularia episcopalis	E	B1	0	0	0	0	0	0	11	3
Pinnularia rupestris	E	D	0	0	0	0	0	1	0	0
Pinnularia sudetica	E	D	0	0	0	0	0	20	45	0
Tabellaria flocculosa	E	C	0	0	0	0	0	0	6	0
Navicula margalithi	U	U	0	0	0	8	1	2	0	0
Cosmioneis pusilla	U	U	0	1	0	0	0	0	0	0
Staurophora amphioxys	U	U	0	0	0	0	0	0	0	0
Rhopalodia gibberula	U	U	0	0	1	0	0	0	0	0
Pinnunavis elegans	U	U	0	0	0	0	0	3	0	0
Martyana martyi	U	U	0	0	1	0	0	0	0	0
Cyclotella sexnota	U	U	0	0	0	0	0	0	1	0
Eunotia naegelithi	U	U	0	0	0	0	0	1	0	0
Pinnularia isostauron	U	U	0	0	0	0	0	0	1	0

Nitzschia lacunarum	U	U	0	0	0	0	0	0	4	0
Gomphonema vibrio var intricatum	U	U	0	0	2	0	0	0	0	0
Surirella islandica	U	U	1	0	0	0	0	0	0	0
	Total # of species:		274	282	259	268	278	276	253	253

Appendix 16

Raw diatom counts for MN-16-19, Minsmere. See Appendix 9 for salinity and life-form key.

Diatom species	Salinity	Life-form	180	216	220	224	228	234	240	360	364	366	392	400	408	412	416	420	428	436	462	654	686	751
Actinoptychus senarius	A	A	6	4	5	2	0	2	0	0	0	0	1	4	7	8	3	1	1	0	1	1	0	0
Campylosira cymbelliformis	A	A	0	0	1	0	0	1	0	0	0	0	0	0	0	0	0	0	0	0	0	0	0	0
Cocconeis costata	A	C	0	0	0	0	0	1	0	0	0	0	0	0	0	0	0	0	0	0	0	0	0	0
Cocconeis scutellum	A	C	0	0	0	1	0	0	0	0	0	0	0	0	0	1	0	0	0	0	0	0	0	0
Cymatosira belgica	A	A	0	0	1	0	3	0	0	0	0	0	0	0	0	0	0	0	0	0	0	0	0	0
Diploneis crabro	A	B1	0	2	0	0	0	0	0	0	0	0	0	0	0	0	2	0	0	0	0	0	0	0
Diploneis incurvata var dubia	A	B1	0	0	1	0	0	0	0	0	0	0	0	0	0	0	0	0	0	0	0	0	0	0
Diploneis smithii	A	B1	0	5	1	35	0	29	5	0	0	0	0	0	0	0	0	0	0	0	0	0	0	0
Pseudopodosira westii	A	B1	0	1	0	0	0	0	0	0	0	0	0	0	2	1	2	0	0	0	0	0	0	0
Navicula forcipata	A	B1	0	0	0	0	0	0	0	0	0	0	0	0	0	0	0	0	0	1	0	0	0	0
Navicula pennata	A	B1	0	0	0	0	0	1	0	0	0	0	0	0	0	0	0	0	0	0	0	0	0	0
Navicula ramosissima	A	C	0	0	0	0	0	0	0	0	0	0	1	0	0	0	0	0	0		0	0	0	0
Nitzschia socialis	A	B1	0	0	0	0	0	0	0	1	0	0	1	0	0	0	0	0	0	0	0	0	0	0
Paralia sulcata	A	B1	14	30	63	6	9	9	1	2	3	22	6	7	32	84	72	19	7	13	5	14	0	2
Podosira stelligera	A	A	3	3	1	0	0	0	0	0	0	1	0	0	1	0	1	0	0	0	0	1	1	0

Species																								
Psammodictyon panduriforme	A	B1	0	0	2	0	0	0	0	0	0	0	0	0	0	1	0	0	0	1	0	0	0	0
Delphineis surirella	A	C	0	6	6	3	4	4	1	0	0	3	0	0	0	1	0	0	0	0	2	2	0	0
Surirella fastuosa	A	B1	0	0	0	0	0	0	0	0	0	0	0	1	1	0	1	0	0	0	0	0	0	0
Thalassiosira leptopa	A	U	0	0	0	1	0	0	0	1	0	0	0	1	0	1	0	0	0	0	0	0	0	0
Trachyneis aspera	A	B1	1	0	1	0	0	0	0	0	0	1	0	0	1	1	0	0	0	0	0	0	0	0
Achnanthes brevipes	B	C	0	0	0	0	0	0	0	0	0	0	0	0	0	0	0	0	0	0	2	0	0	0
Achnanthes delicatula	B	C	0	0	0	0	5	1	0	0	2	1	3	0	0	2	0	0	1	0	2	0	1	0
Amphora holsatica	B	B1	0	0	0	0	1	0	1	0	0	0	0	0	0	0	0	0	0	0	0	0	0	0
Amphora proteus	B	B1	0	0	1	0	0	0	0	0	0	0	0	0	0	0	0	0	0	0	0	0	1	0
Caloneis westii	B	B1	0	14	20	24	0	9	1	0	0	1	0	2	3	0	0	2	2	3	0	2	1	1
Campylodiscus echeneis	B	B1	0	0	0	0	0	0	0	1	0	0	0	0	0	0	0	0	1	1	1	0	0	0
Cyclotella meneghiniana	B	U	0	0	0	0	0	0	0	6	1	0	0	0	0	0	0	0	0	0	0	0	2	0
Diploneis didyma	B	B1	27	2	3	0	0	0	0	1	0	8	0	4	5	16	40	3	5	3	1	8	1	0
Diploneis interrupta	B	B1	1	11	8	20	30	6	3	0	0	0	1	1	1	1	4	0	6	13	2	22	5	1
Fallacia pygmaea	B	B3	0	0	0	0	1	4	0	0	0	1	0	0	0	0	0	0	0	0	0	0	0	0
Gyrosigma hippocampus	B	U	0	0	0	1	1	0	0	0	0	0	0	0	0	0	0	0	0	0	0	0	0	0
Navicula digitoradiata	B	B1	0	23	5	26	1	7	2	1	0	1	1	1	2	5	0	0	1	1	0	0	0	0
Navicula peregrina	B	B1	0	5	0	14	25	23	11	4	2	8	4	0	2	1	0	1	4	1	5	5	9	1
Navicula salinarum	B	B1	0	0	0	0	0	0	0	0	0	0	0	0	0	0	0	0	0	0	0	0	0	1
Nitzschia sigma	B	B1	1	0	2	0	7	0	0	1	0	0	0	1	3	0	0	1	0	0	1	0	2	2
Nitzschia vitrea	B	B1	0	0	0	7	0	1	0	0	0	0	0	0	0	0	0	0	0	0	0	1	0	0
Petroneis marina	B	U	0	0	0	0	0	0	0	0	0	0	0	1	2	2	12	1	0	0	0	0	0	0

Species																								
Rhaphoneis amphiceros	B	U	3	0	10	1	1	0	1	0	0	0	2	3	1	6	1	1	0	1	2	3	0	2
Rhopolodia musculus	B	C	0	1	0	2	11	2	10	0	0	0	0	0	0	0	0	1	2	4	0	0	0	0
Scolioneis tumida	B	B1	130	73	85	12	0	0	1	0	0	5	3	7	33	20	43	8	12	14	6	25	7	3
Surirella striatula	B	B1	0	0	0	0	0	0	0	0	0	0	0	0	0	0	0	1	0	0	0	0	0	0
Synedra pulchella	B	C	0	0	0	0	0	0	0	0	0	0	0	0	1	0	0	0	0	0	0	0	0	0
Tryblionella acuminata	B	U	0	0	0	1	2	5	1	3	1	5	0	0	2	4	0	0	1	2	2	0	0	0
Tryblionella navicularis	B	B1	60	62	3	24	4	12	2	1	3	76	7	194	94	60	55	36	21	11	13	82	7	17
Tryblionella punctata	B	U	11	4	6	0	0	0	0	0	0	15	0	44	55	26	12	6	7	3	5	14	4	3
Amphora veneta	C	B1	0	0	0	0	0	0	0	0	0	0	0	0	2	0	0	0	0	0	0	0	0	0
Anomoeoneis sphaeophora	C	B1	0	0	0	0	0	0	0	0	0	0	0	0	0	0	0	0	0	0	1	1	2	2
Cocconeis pediculus	C	C	1	0	0	0	0	0	0	47	9	7	0	0	0	0	0	0	0	0	0	0	0	4
Cyclostephanos dubius	C	U	0	1	0	0	0	0	0	0	0	0	0	0	0	0	0	0	0	0	0	0	0	0
Navicula avenacea	C	B1	0	0	0	0	0	2	0	0	0	0	0	0	0	0	0	0	0	0	0	0	0	0
Navicula cari var cincta	C	D	0	1	0	19	31	1	0	1	0	0	2	0	0	2	0	0	2	0	0	0	0	0
Navicula cincta	C	D	0	1	2	0	0	7	2	0	0	0	0	0	0	0	0	0	0	1	0	0	0	0
Navicula cryptocephala	C	B1	0	0	0	0	0	0	0	2	0	0	0	0	0	0	0	0	0	0	0	0	0	0
Navicula eidrigiana	C	U	0	0	0	0	0	3	0	0	0	0	0	0	0	0	0	0	0	0	0	0	0	0
Navicula slesvicensis	C	U	0	0	0	0	0	0	0	0	0	0	1	0	0	0	0	0	0	1	0	2	0	0
Nitzschia brevissima	C	U	0	0	0	0	0	0	0	0	0	0	0	1	0	0	0	0	0	1	0	0	0	0
Rhopalodia brebissonii	C	U	0	0	0	0	0	0	0	0	0	0	0	0	3	0	0	0	0	0	0	0	0	0

Species																								
Stauroneis producta	C	B1	0	0	0	0	0	0	1	0	0	0	0	0	0	0	0	0	0	0	0	0	0
Surirella brebissonii	C	U	0	0	0	0	0	0	0	0	2	0	0	0	0	0	0	0	0	0	0	0	0
Surirella brebissonii var kuetzingii	C	U	0	0	0	0	0	0	0	0	0	0	0	0	0	0	0	0	0	0	0	0	1
Surirella subsala	C	B1	0	1	0	0	0	0	0	0	0	0	0	0	0	0	0	0	0	0	0	0	0
Tryblionella levidensis	C	B1	0	0	0	0	0	0	0	1	0	1	0	0	4	0	0	0	0	2	0	0	0	0
Tryblionella litoralis	C	B1	0	0	0	0	0	1	0	0	1	4	1	1	2	1	0	0	0	0	0	0	1	0
Amphora copulata	D	U	0	0	2	0	12	0	11	3	3	0	6	2	8	0	0	3	3	6	2	8	11	10
Amphora ovalis	D	B1	0	0	0	0	0	0	0	1	0	0	0	0	0	0	0	0	0	0	0	1	0	0
Caloneis bacillum	D	D	0	0	0	0	7	5	7	0	0	0	0	0	0	0	0	2	0	0	0	1	0
Caloneis silicula	D	D	0	0	0	0	0	0	1	0	0	0	0	0	0	0	0	0	0	0	0	0	0
Cocconeis disculus	D	C	0	0	0	0	0	1	0	0	1	0	2	0	0	0	0	0	0	0	0	0	0	0
Cocconeis placentula	D	C	0	1	0	0	1	0	0	91	48	28	3	0	1	1	0	4	2	1	2	9	12	6
Cymbella affinis	D	C	0	0	0	0	0	0	0	0	0	0	0	0	0	0	1	0	1	0	0	0	0
Cymbella cesati	D	C	0	0	0	0	0	0	0	0	0	1	0	0	0	0	0	0	0	0	0	0	0	0
Cymbella cistula	D	D	0	0	0	0	0	0	0	0	4	2	0	0	0	0	0	0	0	0	0	4	1	4
Cymbella cistula var maculata	D	U	0	0	0	0	0	0	0	0	5	0	0	0	0	0	0	0	0	0	0	0	0	1
Cymbella cymbiformis	D	C	0	0	0	0	0	0	0	0	0	0	2	0	0	0	0	0	2	0	0	0	0	0
Cymbella microcephala	D	C	0	0	0	0	0	1	0	0	0	0	0	0	0	0	0	0	0	0	0	0	0	0
Cymbella naviculiformis	D	C	0	0	0	0	0	0	0	0	0	0	0	0	0	0	0	1	0	0	0	0	0	0
Cymbella subaequalis	D		0	0	0	0	0	0	0	2	0	0	0	0	0	0	0	0	0	0	0	0	0	0

Taxon																								
Cymbella tumida	D	C	0	0	0	0	0	0	0	1	0	0	0	0	0	0	0	0	0	0	0	0	0	0
Denticula subtilis	D	D	0	0	0	0	0	1	0	0	0	0	0	0	0	0	0	0	0	0	0	0	0	0
Diploneis elliptica	D	D	0	7	2	31	29	10	4	0	0	0	1	5	1	1	2	1	4	2	4	8	5	1
Diploneis ovalis	D	D	0	0	0	6	28	3	5	0	0	0	0	0	0	2	1	0	5	0	1	0	0	0
Eunotia bilunaris	D	U	0	0	0	0	0	0	0	0	2	0	0	0	0	0	0	0	0	0	0	0	0	0
Epithemia adnata	D	U	0	1	0	0	2	0	0	12	0	4	5	3	2	1	0	5	11	5	0	0	0	0
Epithemia porcellus	D	U	0	0	1	0	0	0	0	12	94	16	0	0	0	0	0	0	0	0	10	22	2	12
Epithemia frickei	D	U	0	0	0	0	0	0	0	0	1	0	0	0	0	0	0	0	0	0	0	0	0	0
Epithemia sorex	D	C	0	0	0	0	0	0	0	9	9	21	4	0	0	2	2	3	2	3	0	3	0	4
Epithemia turgida	D	C	0	0	0	0	0	0	0	6	2	0	0	0	0	0	0	0	0	0	0	0	0	0
Fragilaria capucina var rumpens	D	C	0	0	0	0	0	0	0	0	1	0	0	0	0	0	0	0	0	0	0	0	0	0
Staurosira construens	D	A	0	0	0	0	3	35	61	6	2	2	32	0	0	0	0	0	0	1	2	1	0	1
Staurosirella lapponica	D	C	0	0	0	2	9	6	90	4	1	0	47	0	0	0	0	0	0	0	7	1	3	0
Staurosirella pinnata	D	C	0	0	2	1	22	19	12	0	2	1	29	0	0	1	0	0	0	1	0	0	0	0
Fragilaria vaucheriae	D	B1	0	0	0	0	0	0	0	8	0	0	14	0	0	0	0	0	0	1	0	2	3	8
Gomphonema acuminatum	D	U	0	0	0	0	0	0	0	2	5	0	0	0	0	0	0	0	0	0	0	0	0	1
Gomphonema acuminatum var turris	D	U	0	0	0	0	0	0	0	0	1	0	0	0	0	0	0	0	0	0	0	0	0	0
Gomphonema acuminatum var brebissonii	D	C	0	0	0	0	0	0	0	0	0	0	1	0	0	0	0	0	0	0	0	0	0	2	0
Gomphonema angustatum	D	C	0	0	1	0	0	0	0	4	7	5	0	0	0	0	0	0	0	0	0	0	0	0

Taxon																								
Gomphonema olivaceum	D	C	0	1	0	1	0	0	0	2	0	0	0	0	0	0	0	2		1	0	0	0	0
Gomphonema truncatum	D	B	0	0	0	0	0	0	0	0	0	0	1	0	0	0	0	2	1	0	1	0	0	1
Gomphonema truncatum var capitatum	D	U	0	0	0	0	0	0	0	0	1	0	0	0	0	0	0	0	0	0	0	0	0	0
Gyrosigma acuminatum	D	B1	0	0	1	0	0	0	0	1	1	0	0	0	0	0	0	0	0	0	0	0	1	0
Navicula costulata	D	B1	0	0	0	0	0	0	0	0	0	0	1	0	0	0	0	0	0	0	0	0	0	0
Navicula pupula	D	B1	0	0	0	0	0	0	0	0	0	0	1	0	0	0	0	0	0	0	0	0	0	0
Navicula radiosa	D	B1	0	0	0	0	0	0	0	0	1	0	0	0	0	0	0	0	0	0	0	0	0	0
Navicula rhynchocephala	D	D	0	0	0	0	1	0	0	1	0	0	2	0	0	0	0	0	0	0	1	0	7	0
Nitzschia amphibia	D	D	0	0	0	0	0	0	0	8	3	0	1	0	0	0	0	0	0	0	0	0	0	0
Nitzschia fonticola	D	B1	0	0	0	0	0	0	0	2	4	2	0	0	0	0	0	0	0	0	0	0	0	0
Nitzschia palea	D	D	0	0	0	0	0	0	0	0	0	0	4	0	0	0	0	0	1	0	0	0	0	0
Pinnularia abaujensis	D	B1	0	0	0	0	1	0	0	0	0	0	0	0	0	0	0	0	0	0	0	0	1	0
Pinnularia borealis var breviscostata	D	U	0	0	0	0	1	0	0	0	0	0	0	0	0	0	0	0	0	0	0	0	0	0
Pinnularia major	D	U	0	0	0	0	1	0	0	0	0	0	0	0	0	0	0	0	0	0	0	0	0	0
Pinnularia microstauron	D	D	0	0	0	0	0	0	0	0	0	0	0	0	0	0	0	0	1	0	0	0	0	0
Placoneis elginensis	D	U	0	0	0	0	0	0	0	0	0	0	2	0	0	0	0	0	0	0	1	0	0	0
Rhopolodia gibba	D	C	0	0	0	0	0	0	0	1	5	5	0	0	5	0	0	0	1	1	1	1	4	5
Rhopolodia gibba var ventricosa	D	U	0	0	0	0	0	0	0	2	0	0	0	0	0	0	0	0	0	0	0	0	0	0
Sellaphora laevissima	D	U	0	0	0	0	0	0	0	0	0	0	0	0	0	0	0	0	1	0	0	0	0	0

Species			1	2	3	4	5	6	7	8	9	10	11	12	13	14	15	16	17	18	19	20	21	22
Stauroneis phoenicenteron	D	B1	0	3	0	0	0	0	0	1	0	0	0	0	0	0	0	0	0	0	0	0	1	0
Pseudostaurosira elliptica	D	A	0	0	0	1	1	12	2	1	1	1	18	0	0	0	0	0	0	0	0	0	0	0
Surirella brightwelli	D	B1	0	0	0	0	0	0	0	0	0	0	0	0	0	0	0	0	0	0	0	0	1	0
Synedra capitata	D	C	0	0	1	0	0	0	0	1	0	0	0	0	1	0	0	0	0	0	1	0	0	0
Synedra ulna	D	U	0	0	0	0	0	0	0	1	6	0	0	0	0	0	0	0	0	0	0	0	0	0
Synedra ulna var biceps	D	D	0	0	0	0	0	0	0	0	1	0	0	0	0	0	0	0	0	0	0	0	0	0
Cyclotella antiqua	E	A	0	0	0	1	1	0	0	0	0	0	1	0	0	0	0	0	0	0	0	0	0	0
Pinnularia hemiptera	E	U	0	0	0	0	0	0	0	0	0	0	0	0	0	0	0	0	1	0	0	0	0	0
Amphora normanii	E	D	0	0	0	0	0	1	0	0	0	0	0	0	0	0	0	0	0	0	0	0	0	0
Cymbella tumidula	E	C	0	0	0	0	0	0	0	0	1	0	0	0	0	0	0	0	0	0	0	0	0	0
Denticula tenuis	E	B1	0	0	0	0	0	1	0	0	0	0	0	0	0	0	0	0	0	0	0	0	0	0
Encyonema gracile	E	C	0	0	0	0	0	0	0	0	1	0	0	0	0	0	0	0	0	0	0	0	0	0
Fragilaria leptostauron	E	D	0	0	0	0	0	0	0	0	0	0	1	0	0	0	0	0	0	0	1	0	0	0
Frustulia rhomboides	E	U	0	0	0	0	0	0	0	0	0	1	0	0	0	0	0	0	0	0	0	0	0	0
Pinnularia appendiculata	E	D	0	0	0	0	0	0	0	0	0	0	1	0	0	0	0	0	0	0	0	0	0	0
Tabellaria flocculosa	E	C	0	0	0	0	0	0	0	0	0	0	1	0	0	0	0	0	0	0	0	0	0	0
Cocconeis guttata	U	U	0	0	0	0	0	2	0	0	0	0	0	0	0	0	0	0	0	0	0	0	0	0
Navicula margalithi	U	U	0	0	13	0	0	0	0	0	0	0	0	0	0	2	0	0	0	0	0	0	0	0
Caloneis borealis	U	U	0	0	0	0	0	0	0	1	0	0	0	0	0	0	0	0	0	0	0	0	0	0
Cosmioneis pusilla	U	U	0	0	0	0	1	0	0	0	0	0	0	0	0	0	0	0	0	0	0	0	0	0
Staurosirella pinnata	U	U	0	0	0	0	0	0	0	5	0	0	0	0	0	0	0	0	0	0	0	0	0	0
Rhopalodia gibberula	U	U	0	0	0	5	0	0	0	0	0	0	0	0	0	0	0	1	0	0	3	0	4	0

Stauroneis alpina	U	U	0	1	0	0	0	0	0	0	0	0	0	0	0	0	0	0	0	0	1	0	0
Synedra nana	U	U	0	0	0	0	0	0	0	0	0	0	2	0	0	0	0	0	0	0	0	0	0
Tabularia investiens	U	U	0	0	0	0	0	0	0	0	2	0	0	0	0	0	0	0	0	0	0	0	1
Martyana martyi	U	U	0	0	0	0	0	0	0	0	0	0	3	0	0	0	0	1	0	0	0	0	0
Synedra pulchella	U	U	0	0	0	0	0	0	0	0	0	0	0	0	0	0	0	1	0	0	0	0	0
Tabularia fasisculata	U	U	0	0	0	0	0	0	0	0	1	0	0	0	0	0	0	0	0	0	0	0	0
Caloneis subsalina	U	U	0	0	0	0	0	0	0	0	0	1	0	0	0	0	0	0	0	0	1	0	0
Pseudostaurosia brevistriata	U	U	0	0	0	1	2	1	14	0	0	0	38	0	0	0	0	0	2	1	0	0	0	0
Rhopalodia rupestris	U	U	0	0	0	0	0	35	0	0	0	0	0	1	0	0	0	0	0	0	0	0	0
Surirella patella	U	U	0	1	0	0	0	0	0	0	0	0	0	0	0	0	0	0	0	0	0	0	0
Unknown (Elong. N.p)	U	U	0	0	8	3	0	0	0	0	0	0	0	0	0	0	0	0	0	0	0	0	0
Pinnularia cuneata	U	U	0	0	0	0	0	0	2	0	0	0	0	0	0	0	0	1	0	0	0	0	0
Denticula kuetzingii	U	U	0	0	0	0	0	0	0	0	0	0	0	0	0	0	0	0	0	1	0	0	0
Placoneis pseudanglica	U	U	0	0	0	0	0	0	0	0	0	0	2	0	0	0	0	0	0	0	0	0	0
Gomphonema amoenumn	U	U	0	0	0	0	0	0	0	1	0	0	1	0	0	0	0	0	0	0	0	0	0
Cosmioneis lundstroemii	U	U	0	0	0	0	0	0	0	0	0	0	1	0	0	0	0	0	0	0	0	0	0
Synedra puchella	U	U	0	0	0	0	0	0	0	3	8	4	0	0	0	0	0	0	0	0	0	2	0	3
Eunotia minor	U	U	0	0	0	0	0	0	0	0	1	0	0	0	0	0	0	0	0	0	0	0	0
Encyonema silesiacum	U	U	0	0	0	0	0	0	0	4	2	0	0	0	0	0	0	0	0	0	0	0	0
Encyonema elginense	U	U	0	0	0	0	0	0	0	0	0	1	0	0	0	0	0	0	0	0	0	0	2

Species																								
Amphiphora sulcata	U	U	0	0	1	0	0	0	0	0	0	0	0	0	0	0	0	0	0	0	0	0	0
Gomphonema angustum	U	U	0	0	0	0	0	0	0	1	0	0	0	0	0	0	0	0	0	0	0	0	0
Thalassiosira tenera	U	U	0	0	0	0	0	0	0	1	0	0	0	0	0	0	0	0	0	0	0	0	0
Eunotia valida	U	U	0	0	0	0	0	0	0	1	0	0	0	0	0	0	0	0	0	0	0	0	0
Gyrosigma attenuatum	U	U	0	0	0	0	0	0	0	0	0	2	0	0	0	0	0	0	0	0	0	0	0
Pinnularia aestuanii	U	U	0	0	0	0	0	0	0	0	0	2	0	0	0	0	0	0	0	0	0	0	0
Eunotia pectinalis	U	U	0	0	0	0	0	0	0	0	2	0	0	0	0	0	0	0	0	0	1	0	0	1
Eunotia tenella	U	U	0	0	0	0	0	0	0	0	1	0	0	0	0	0	0	0	0	0	0	0	0	0
Synedra Vauchariae	U	U	0	0	0	0	0	0	0	0	0	0	0	0	0	0	0	0	0	0	14	0	0	0
Navicula tripunctata	U	U	0	0	0	0	0	0	0	0	0	0	0	0	0	0	0	0	0	0	1	0	0	0
Cymbella heteropleura	U	U	0	0	0	0	0	0	0	0	0	0	0	0	0	0	0	0	0	0	0	1	0	0
Lyrella hennedyi	U	U	0	0	0	0	0	0	0	0	0	0	0	0	0	0	0	0	0	0	0	1	0	0
Fragilaria crotenensis	U	U	0	0	0	0	0	0	0	0	0	0	0	0	0	0	0	0	0	0	0	0	1	0
Cyclotella sexnota	U	U	0	0	0	0	0	0	0	0	0	0	0	0	0	0	0	0	0	0	0	0	1	0
Encyonema hebridicum	U	U	0	0	0	0	0	0	0	0	0	0	0	0	0	0	0	0	0	0	0	0	1	0
Stauroneis smithii var sagitta	U	U	0	0	0	0	0	0	0	0	0	0	0	0	0	0	0	0	0	0	0	0	0	2
Cyclotella kuetzingiana var planetophora	U	U	0	0	0	0	0	0	0	0	0	0	0	0	0	0	0	0	0	0	0	0	0	2
Gomphonema gracile	U	U	0	0	0	0	0	0	0	0	0	0	0	0	0	0	0	0	0	0	0	0	0	1
Amphora pediculus	U	U	0	0	0	0	0	0	0	0	0	0	0	0	0	0	0	0	0	0	0	0	1	0

Auliscus sculptus	U	U	1	0	0	0	0	0	0	0	0	0	0	0	0	0	0	0	0	0	0	0
Total # of species:	259	265	259	251	258	264	252	273	253	259	261	284	277	254	253	107	112	102	101	252	103	110

Appendix 17

Foraminifera counts for Sizewell.

Depth (cm): Foraminifera species	65.5	85.5	125.5	165.5	170.5	174.5	177.5	180.5	185.5	191.5	231.5	271.5
Jadammina macrescens	18	27	0	114	113	57	58	77	67	19	0	3
Miliammina fusca	1	0	0	2	10	59	16	20	4	29	0	0
Trochammina inflata	4	1	0	1	1	0	15	12	10	1	0	0
Tiphotrocha comprimata	0	0	0	0	0	0	2	0	2	0	0	0
Haplophragmoides sp.	0	0	0	23	2	21	4	4	1	2	0	0
Total # of species:	23	28	0	140	126	137	95	113	84	51	0	3

Appendix 18

Published (Coles and Funnel 1981; Devoy 1982; Alderton 1983; Brew et al., 1992; Horton et al., 2004), unpublished (Lloyd et al., 2008) and new (Hamilton 2019) sea-level index points and freshwater limiting data for the East Anglia region. Freshwater limiting data produced as part of this thesis for WM-15-6, MN-16-1 and MN-16-19 is omitted, see section 7.2.3 for more information.

Sample ID	Reference	Location		Age			Tendency	Elevation
		Latitude	Longtitude	Radiocarbon age ± 1σ (^{14}C BP)	Calibrated radiocarbon age (cal BP)			Indicative meaning
GDH-16-2 -2.09 m OD	Hamilton 2019	52.3	1.642778	2440 ± 35	2701	2357	+	MHWST-20 cm
GDH-16-2 -2.29 m OD	Hamilton 2019	52.3	1.642778	2775 ± 37	2956	2783	B	MHWST+20 cm
OTM-16-13 -2.03 m OD	Hamilton 2019	52.306333	1.645417	965 ± 39	952	789	+	MHWST-20 cm
OTM-16-13 -5.64 m OD	Hamilton 2019	52.306333	1.645417	5209 ± 35	6170	5906	B	(MTL+HAT)/2
OTM-16-13 -2.45 m OD	Hamilton 2019	52.306333	1.645417	970 ± 30	933	796	-	(MHWST+HAT)/2
WM-15-6 -1.77 m OD	Hamilton 2019	52.300436	1.616072	836 ± 35	894	683	+	MHWST-20 cm
MN-16-3 -3.71 m OD	Hamilton 2019	52.237222	1.623333	2014 ± 38	2101	1880	+	MHWST-20 cm
MN-16-5 -3.05 m OD	Hamilton 2019	52.237222	1.623333	1231 ± 38	1265	1065	+	MHWST-20 cm
MN-16-19 -3.63 m OD	Hamilton 2019	52.237222	1.623333	909 ± 37	917	743	+	MHWST-20 cm
MN-16-19 -4.98 m OD	Hamilton 2019	52.237222	1.623333	1613 ± 35	1592	1408	-	MHWST+60 cm
MN-16-19 -5.54 m OD	Hamilton 2019	52.237222	1.623333	1920 ± 38	1966	1738	+	MHWST-20 cm
SW-17-1 -2.99 m OD	Hamilton 2019	52.217778	1.609444	5263 ± 38	6179	5931	B	(MTL+HAT)/2
SW-17-13 -2.77 m OD	Hamilton 2019	52.217778	1.609444	1431 ± 37	1386	1290	-	((MHWS+HAT)/2)-20 cm
SW-17-13 -3.13 m OD	Hamilton 2019	52.217778	1.609444	1444 ± 37	1395	1294	+	MHWST-20 cm
SW-17-13 -6.92 m OD	Hamilton 2019	52.217778	1.609444	6339 ± 35	7412	7170	B	(MTL+HAT)/2
SW-17-3 -4.07 m OD	Hamilton 2019	52.217778	1.609444	5570 ± 30	6405	6301	B	(MTL+HAT)/2
Q2183	Alderton 1983	52.479722	1.5941666	1755 ± 40	1808	1562	-	((HAT+MHWS)/2) - 0.2 m
Q2038	Alderton 1983	52.538611	1.6438888	4970 ± 55	5891	5596	-	((HAT+MHWS)/2) - 0.2 m
Q2037	Alderton 1983	52.53861111	1.643888889	4295 ± 58	5041	4649	-	((HAT+MHWS)/2) - 0.2 m

Q2036	Alderton 1983	52.53861111	1.643888889	4905 ± 56	5844	5484	+	MHWS
AA25600	Horton et al 2004 PGA	52.73208333	1.642333333	2760 ± 45	2954	2767	+	MHWS - 0.2 m
Q2195	Alderton 1983	52.55861111	1.642222222	2440 ± 50	2706	2355	+	MHWS - 0.1 m
SRR3480	Brew et al 1992	52.3225	1.668333333	6385 ± 20	7415	7265	+	MHWS - 0.1 m
Q2087	Alderton 1983	52.47388889	1.665555556	2330 ± 55	2682	2156	+	MHWS - 0.1 m
SRR3484	Brew et al 1992	52.31888889	1.670277778	6510 ± 120	7605	7175	+	MHWS - 0.1 m
HAR2535	Coles & Funnel 1981	52.61083333	1.715	7580 ± 90	8546	8194	+	MHWS - 0.1 m
SRR3483	Brew et al 1992	52.31888889	1.670277778	4575 ± 65	5467	4989	-	((HAT+MHWS)/2) - 0.1 m
Q2089	Alderton 1983	52.47388889	1.665555556	4120 ± 65	4831	4444	+	MHWS
AA25599	Horton et al 2004 PGA	52.73863889	1.665388889	2490 ± 45	2738	2380	+	MHWS - 0.2 m
Q2196	Alderton 1983	52.55861111	1.642222222	2705 ± 45	2917	2748	+	MHWS
SRR3479	Brew et al 1992	52.3225	1.668333333	4400 ± 70	5285	4847	-	((HAT+MHWS)/2) - 0.2 m
Q2090	Alderton 1983	52.47388889	1.665555556	4700 ± 55	5582	5317	-	((HAT+MHWS)/2) - 0.2 m
Q2034	Alderton 1983	52.53861111	1.643888889	540 ± 55	652	504	-	((HAT+MHWS)/2) - 0.2 m
Q2091	Alderton 1983	52.47388889	1.665555556	6305 ± 55	7414	7028	+	MHWS - 0.1 m
Q2182	Alderton 1983	52.53861111	1.643888889	3380 ± 40	3719	3484	+	MHWS
Q2035	Alderton 1983	52.53861111	1.643888889	2640 ± 50	2866	2547	+	MHWS
Q2039	Alderton 1983	52.53861111	1.643888889	5655 ± 55	6599	6306	+	MHWS - 0.1 m
Q2088	Alderton 1983	52.47388889	1.665555556	3560 ± 60	4068	3650	+	MHWS
Q2200	Alderton 1983	52.55861111	1.642222222	7470 ± 50	8377	8189	+	MHWS - 0.1 m
Q2086	Alderton 1983	52.47388889	1.665555556	2170 ± 55	2324	2007	+	MHWS - 0.1 m
Q2197	Alderton 1983	52.55861111	1.642222222	3145 ± 45	3453	3242	+	MHWS
SRR575	Coles & Funnel 1981	52.61722222	1.436944444	1609 ± 50	1611	1388	-	((HAT+MHWS)/2) - 0.2 m
SRR573	Coles & Funnel 1981	52.58666667	1.475	1973 ± 50	2051	1819	+	MHWS - 0.1 m
Q2184	Alderton 1983	52.47972222	1.594166667	1985 ± 40	2039	1828	+	MHWS - 0.1 m
SRR3482	Brew et al 1992	52.31888889	1.670277778	4300 ± 65	5211	4628	+	MHWS - 0.1 m

SRR3481	Brew et al 1992	52.3225	1.668333333	6755 ± 70	7722	7483	+	MHWS
Q2198	Alderton 1983	52.55861111	1.642222222	3686 ± 45	4148	3897	+	MHWS
Q2199	Alderton 1983	52.55861111	1.642222222	4920 ± 55	5861	5490	-	((HAT+MHWS)/2) - 0.2 m
SRR3478	Brew et al 1992	52.3225	1.668333333	4260 ± 80	5039	4538	+	MHWS - 0.1 m
I3230	Devoy PGA 1982	52.10083333	1.591388889	7010 ± 130	8150	7588	B	(HAT+MTL)/2
Q2202	Alderton 1983	52.47972222	1.594166667	3910 ± 50	4513	4158	B	(HAT+MTL)/2
I3430	Devoy PGA 1982	52.10083333	1.591388889	7010 ± 130	8150	7588	B	(HAT+MTL)/2
Q2201	Alderton 1983	52.55861111	1.642222222	8540 ± 45	9554	9471	B	(HAT+MTL)/2
Q2092	Alderton 1983	52.47388889	1.665555556	7750 ± 55	8626	8417	B	(HAT+MTL)/2
Q2040	Alderton 1983	52.53861111	1.643888889	6460 ± 110	7566	7172	B	(HAT+MTL)/2
MM02-56	Lloyd et al 2008	52.250528	1.584389	1330 ± 40	1307	1181	-	MHWST
MM02-141	Lloyd et al 2008	52.250528	1.584389	1440 ± 40	1398	1291	+	MHWST
SM30-2.5-48	Lloyd et al 2008	52.243528	1.595167	330 ± 40	484	305	-	MHWST
SM30-2.5-252	Lloyd et al 2008	52.243528	1.595167	3160 ± 40	3459	3253	+	MHWST
GH04-148	Lloyd et al 2008	52.223139	1.613111	1780 ± 40	1819	1574	-	MHWST
GH04-181	Lloyd et al 2008	52.223139	1.613111	2360 ± 40	2678	2318	+	MHWST
NH01-242	Lloyd et al 2008	52.248444	1.625472	2510± 40	2745	2458	+	MHWST

References

Aaby, B., 1986. Palaeoecological studies of mires. In: Berglund, B.E. (Ed.), Handbook of Holocene Palaeoecology and Palaeohydrology. John Wiley & Sons, Ltd, Chichester, pp. 145–164.

Aaby, B., Berglund, B.E., 1986. Characterisation of peat and lake sediments. In: Berglund, B.E. (Ed.), Handbook of Holocene Palaeoecology and Palaeohydrology. John Wiley & Sons, Ltd, Chichester, pp. 231–246.

Admiralty Tide Tables, 2016. Volume 1: United Kingdom and Ireland including European Channel Ports. United Kingdom Hydrographic Office.

Agas, R., 1587. A plan exhibiting the remains of the ancient city of Dunwich.

Albay, M., Aykulu, G., 2002. Invertebrate Grazer - Epiphytic Algae Interactions on Submerged Macrophytes in a Mesotrophic Turkish Lake. Journal of Fisheries & Aquatic Sciences 19, 247–258.

Alderton, A.M., 1983. Flandrian vegetational history and sea-level change of the Waveney Valley. PhD Thesis, University of Cambridge.

Alison Farmer Associates, 2012. Touching the Tide- Landscape Character Assessment. Cambridge.

Allen, J., Potter, V., Poulter, M., 2002. The building of Orford Castle: A translation from the Pipe Rolls 1163-78. Orford Museum, Orford.

Allen, J.R.L., 1993. Muddy alluvial coasts of Britain: field criteria for shoreline position and movement in the recent past. Proceedings of the Geologists' Association 104, 241–262. doi:10.1016/S0016-7878(08)80044-2

Allen, J.R.L., 1995. Salt-marsh growth and fluctuating sea level: implications of a simulation model for Flandrian coastal stratigraphy and peat-based sea-level curves. Sedimentary Geology 100, 21–45. doi:10.1016/0037-0738(95)00101-8

Allen, J.R.L., 2000. Morphodynamics of Holocene salt marshes : a review sketch from the Atlantic and Southern North Sea coasts of Europe. Quaternary Science Reviews 19, 1155–1231.

Allen, J.R.L., Thornley, D.M.M., 2004. Laser granulometry of Holocene estuarine silts: effects of hydrogen peroxide treatment. The Holocene 14, 290–295. doi:10.1191/0959683604hl681rr

Andrews, D., Brooks, H., 1989. An Essex Dunwich: the lost church at Little Holland Hall. Essex Archaeology and History 20, 74–83.

Andrews, J., Boomer, I., Bailiff, I., Balson, P., Bristow, C., Chroston, N., Funnell, B.M., Harwood, G., Jones, R., Maher, B., Shimmield, G., 2000. Sedimentary evolution of the north Norfolk barrier coastline in the context of Holocene sea-level change. In: Shennan, I., Andrews, J. (Eds.), Holocene Land-Ocean Interaction and Environmental Change around the North Sea. Geological Society, Special Publication 166(1), London, pp. 219–251.

Arnott, W.G., 1973. Alde Estuary. Boydell Press, Ipswich.

Ascough, P.L., Cook, G.T., Hastie, H., Dunbar, E., Church, M.J., Einarsson, A., McGovern, T.H., Dugmore, A.J., 2011. An Icelandic freshwater radiocarbon reservoir effect: Implications for lacustrine 14C chronologies. The Holocene 21, 1073–1080. doi:10.1177/0959683611400466

Asselen, S. van, 2011. The contribution of peat compaction to total basin subsidence: Implications for the provision of accommodation space in organic-rich deltas. Basin Research 23, 239–255. doi:10.1111/j.1365-2117.2010.00482.x

Austin, R.M., 1991. Modelling Holocene tides on the NW European Continental shelf. Terra Nova 3, 276–288.

Axel, H., Hosking, E., 1977. Minsmere: Portrait of a Bird Reserve. Hutchinson, London.

Baeteman, C., 1999. The Holocene depositional history of the Ijzer palaeovalley (western Belgian coastal plain) with reference to the factors controlling the formation of intercalated peat beds. Geologica Belgica 2/3, 39–72.

Baeteman, C., Declercq, P.-Y., 2002. A synthesis of early and middle Holocene coastal changes in the western Belgian lowlands. Belgeo 2, 77–107. doi:10.4000/belgeo.15994

Baeteman, C., Scott, D.B., Strydonck, M. van, 2002. Changes in coastal zone processes at a high sea-level stand: A late Holocene example from Belgium. Journal of Quaternary Science 17, 547–559. doi:10.1002/jqs.707

Baeteman, C., Waller, M., Kiden, P., 2011. Reconstructing middle to late Holocene sea-level change: A methodological review with particular reference to "A new Holocene sea-level curve for the southern North Sea" presented by K.-E. Behre. Boreas 40, 557–572. doi:10.1111/j.1502-3885.2011.00207.x

Bailey, M., 1990. Coastal fishing off south east Suffolk in the century after the Black Death. Proceedings of the Suffolk Institute of Archaeology and History 37, 102–114.

Balesdent, J., 1987. The turnover of soil organic fractions estimated by radiocarbon dating. The Science of the Total Environment 62, 405–408.

Ball, D., 1964. Loss-on-ignition as an estimate of organic matter and organic carbon in non-calcareous soils. Journal of Soil Science 15, 84–92.

Ballantyne, C.K., 2010. Extent and deglacial chronology of the last British-Irish Ice Sheet: implications of exposure dating using cosmogenic isotopes. Journal of Quaternary Science 25, 515–534. doi:10.1002/jqs.1310

Ballantyne, C.K., Hall, A., 2008. The altitude of the last ice sheet in Caithness and east Sutherland , northern Scotland. Scottish Journal of Geology 44, 169–181.

Bao, R., Freitas, M.D.C., Andrade, C., 1999. Separating eustatic from local environmental effects: A late-Holocene record of coastal change in Albufeira Lagoon, Portugal. The Holocene 9, 341–352. doi:10.1191/095968399675815073

Bao, R., Alonso, A., Delgado, C., Pagés, J.L., 2007. Identification of the main driving mechanisms in the evolution of a small coastal wetland (Traba, Galicia, NW Spain) since its origin 5700 cal yr BP. Palaeogeography, Palaeoclimatology, Palaeoecology 247, 296–312. doi:10.1016/j.palaeo.2006.10.019

Barker, P., Fontes, J.C., Gasse, F., Druart, J.C., 1994. Experimental dissolution of diatom silica in concentrated salt solutions and implications for palaeoenvironmental reconstruction. Limnology and Oceanography 39, 99–110. doi:10.4319/lo.1994.39.1.0099

Barlow, N.L.M., Long, A.J., Saher, M.H., Gehrels, W.R., Garnett, M.H., Scaife, R.G., 2014. Salt-marsh reconstructions of relative sea-level change in the North Atlantic during the last 2000 years. Quaternary Science Reviews 99, 1–16. doi:10.1016/j.quascirev.2014.06.008

Barlow, N.L.M., Bentley, M.J., Spada, G., Evans, D.J.A., Hansom, J.D., Brader, M.D., White, D.A., Zander, A., Berg, S., 2016. Testing models of ice cap extent, South Georgia, sub-Antarctic. Quaternary Science Reviews 154, 157–168. doi:10.1016/J.QUASCIREV.2016.11.007

Bassett, S., Milne, G., Mitrovica, J., Clark, P., 2005. Ice Sheet and Solid Earth Influences on Far-Field Sea-level Histories. Science 309, 925–928. doi:10.1029/2002GL016722

Battarbee, R., 1986. Diatom Analysis. In: Berglund, B.E. (Ed.), Handbook of Holocene Palaeoecology and Palaeohydrology. John Wiley & Sons, Ltd, Chichester, pp. 527–570.

Beets, D.J., Spek, A.J.F. van der, 2000. The Holocene evolution of the barrier and the back-barrier basins of Belgium and the Netherlands as a function of late Weichselian morphology, relative sea-level rise and sediment supply. Geologie en Mijnbouw 79, 3–16. doi:10.1017/S0016774600021533

Beets, D.J., Valk, L. van der, Stive, M.J.F., 1992. Holocene evolution of the coast of Holland. Marine Geology 103, 423–443. doi:10.1016/0025-3227(92)90030-L

Beets, D.J., Spek, A.J.F. van der, L., van der V., 1994. Holocene ontwikkeling van de Nederlandse kust. Rijksgeologische Dienst, The Netherlands, rapport 40.016, Project Kustgenese, 53.

Beltrones, S., Hernández, U.A., 2014. Particular Structure of an epiphytic diatom assemblage living on Ploclamium cartilagineum (lamoroux) dixon (rhodophyceae : gigartinales). CICIMAR Oceànides 29, 11–24.

Berglund, B.E., 1971. Littorina transgression in Blekinge, South Sweden, a preliminary survey. Geologiska Foreningen Stockholm Forhandlinger 93, 626–652.

Bernhardt, C.E., Willard, D.A., 2015. Pollen and spores of terrestrial plants. In: Shennan, I., Long, A.J., Horton, B.P. (Eds.), Handbook of Sea-Level Research. John Wiley & Sons, Ltd, Chichester, pp. 218–232.

Best, L., 2016. Late Holocene Relative Sea-Level Change and the Implications for the Groundwater Resource, Humber Estuary, UK. PhD thesis, University of York.

Beyens, L., Denys, L., 1982. Problems in diatom analysis of deposits: allochthonous valves and fragmentation. Geologie en Mijnbouw 61, 159–162.

Blott, S.J., Pye, K., 2001. GRADISTAT : A grain size distribution and statistics package for the analysis of unconsolidated sediments. Earth Surface Processes and Landforms 26, 1237–1248.

Boer, G. de, Carr, A.P., 1969. Early Maps as Historical Evidence for Coastal Change. The Geographical Journal 135, 17–39.

Boomer, I., Godwin, M., 1993. Palaeoenvironmental Reconstruction in the Breydon Formation, Holocene of East Anglia. Journal of Micropalaeontology 12, 35–45. doi:10.1144/jm.12.1.35

Boomer, I., Horton, B.P., 2006. Holocene relative sea-level movements along the North Norfolk Coast, UK. Palaeogeography, Palaeoclimatology, Palaeoecology 230, 32–51. doi:10.1016/j.palaeo.2005.07.004

Boyle, J.F., 2001. Inorganic Geochemical Methods in Palaeolimnology. In: Last, W., Smol, J. (Eds.), Tracking Environmental Change Using Lake Sediments. Volume 2: Physical and Geochemical Methods. Kluwer Academic Publishers, Dordrecht, Netherlands, pp. 83–141. doi:10.1007/0-306-47670-3_5

Boyle, J.F., 2004. A comparison of two methods for estimating the organic matter content of sediments. Journal of Paleolimnology 31, 125–127.

Brader, M.D., Lloyd, J.M., Barlow, N.L.M., Norðdahl, H., Bentley, M.J., Newton, A.J., 2017. Postglacial relative sea-level changes in northwest Iceland: Evidence from isolation basins, coastal lowlands and raised shorelines. Quaternary Science Reviews 169, 114–130. doi:10.1016/j.quascirev.2017.05.022

Bradley, S.L., Milne, G., Zong, Y., Horton, B.P., 2008. Modelling sea-level data from China and Malay–Thai Peninsula to infer Holocene eustatic sea- level change. In: American Geophysical Union, Fall Meeting 2008, Abstract #GC33A-0763.

Bradley, S.L., Milne, G.A., Shennan, I., Edwards, R., 2011. An improved glacial isostatic adjustment model for the British Isles. Journal of Quaternary Science 26, 541–552. doi:10.1002/jqs.1481

Bradwell, T., Stoker, M.S., 2015. Submarine sediment and landform record of a palaeo-ice stream within the British-Irish ice sheet. Boreas 44, 255–276.

Brain, M.J., 2006. Autocompaction of mineralogenic intertidal sediments. PhD Thesis, Durham University.

Brain, M.J., 2015. Compaction. In: Shennan, I., Long, A.J., Horton, B.P. (Eds.), Handbook of Sea-Level Research. John Wiley & Sons, Ltd, Chichester, pp. 452–469.

Brain, M.J., Long, A.J., Petley, D.N., Horton, B.P., Allison, R.J., 2011. Compression behaviour of minerogenic low energy intertidal sediments. Sedimentary Geology 233, 28–41. doi:10.1016/j.sedgeo.2010.10.005

Brain, M.J., Long, A.J., Woodroffe, S.A., Petley, D.N., Milledge, D.G., Parnell, A.C., 2012. Modelling the effects of sediment compaction on salt marsh reconstructions of recent sea-level rise. Earth and Planetary Science Letters 345–348, 180–193.

Brew, D.S., 1990. Sedimentary environments and Holocene evolution of the Suffolk estuaries. PhD Thesis, University of East Anglia.

Brew, D.S., Funnell, B.M., Kreiser, A., 1992. Sedimentary environments and Holocene evolution of the lower Blyth estuary, Suffolk (England), and a comparison with other East Anglian coastal sequences. Proceedings of the Geologists' Association 103, 57–74.

Brew, D.S., Mitlehner, A.G., Funnell, B.M., 1996. Holocene Vegetation and Salinity Changes in the Upper Blyth Estuary, Suffolk. Bulletin of the Geological Society of Norfolk No. 43.

Brew, D.S., Holt, T., Pye, K., Newsham, R., 2000. Holocene sedimentary evolution and palaeocoastlines of the Fenland embayment, eastern England. Geological Society, London, Special Publications 166, 253–273. doi:10.1144/GSL.SP.2000.166.01.13

Briggs, D., Smithson, P., 1987. Fundamentals of Physical Geography, 3rd ed. Hutchinson, London.

Brockmann, C., 1940. Diatomeen als Leitfossilien in Küstenablagerungen. Westkuste 150–181.

Brooks, A., Edwards, R., 2006. The development of a sea-level database for Ireland. Irish Journal of Earth Sciences 24, 13–27. doi:10.3318/IJES.2006.24.1.13

Brooks, A., Bradley, S.L., Edwards, R., Milne, G., Horton, B.P., Shennan, I., 2008. Postglacial relative sea-level observations from Ireland and their role in glacial rebound modelling. Journal of Quaternary Science 23, 175–192. doi:10.1002/jqs

Brooks, S.M., Spencer, T., 2010. Temporal and spatial variations in recession rates and sediment release from soft rock cliffs, Suffolk coast, UK. Geomorphology 124, 26–41. doi:10.1016/j.geomorph.2010.08.005

Brooks, S.M., Spencer, T., 2012. Shoreline retreat and sediment release in response to accelerating sea level rise: Measuring and modelling cliffline dynamics on the Suffolk Coast, UK. Global and Planetary Change 80–81, 165–179. doi:10.1016/j.gloplacha.2011.10.008

Burningham, H., French, J.R., 2014. Travelling forelands : complexities in drift and migration patterns. Journal of Coastal Research 102–108. doi:10.2112/SI70-018.1

Burningham, H., French, J.R., 2017. Understanding coastal change using shoreline trend analysis supported by cluster-based segmentation. Geomorphology 282, 131–149. doi:10.1016/j.geomorph.2016.12.029

Cambers, G., 1973. The retreat of unconsolidated Quaternary cliffs. PhD Thesis, University of East Anglia.

Cambers, G., 1975. Sediment transport and coastal change. East Anglian Coastal Research Programme Report No. 3. Norwich, UK.

Carr, A.P., 1970. The evolution of Orfordness, Suffolk before 1600 AD: Geomorphological evidence. Zeitschrift fur Geomorphologie 14, 289–300.

Carr, A.P., 1971. Orford, Suffolk: Further Data on the Quaternary Evolution of the area. Geological Magazine 108, 311–316. doi:10.1017/S0016756800051372

Carr, A.P., 1979. Sizewell-Dunwich Banks Field Study Topic Report 2: Long-term changes in the coastline and offshore banks., Institute of Oceanographic Science Reports.

Carr, A.P., 1981. Evidence for the sediment circulation along the coast of East Anglia. Marine Geology 40, 9–22. doi:10.1016/0025-3227(81)90134-1

Carr, A.P., Baker, R.E., 1968. Orford, Suffolk: Evidence for the Evolution of the Area during the Quaternary. Transactions of the Institute of British Geographers 45, 107–123.

Carter, R.W.G., 1988. Coastal Environments- An introduction to the physical, ecological and cultural systems of coastlines. Academic Press, London.

Carter, R.W.G., Woodroffe, C.D., 1994. Coastal Evolution- Late Quaternary shoreline morphodynamics. Cambridge University Press, Cambridge.

Carter, R.W.G., Forbes, D.L., Jennings, S.C., Orford, J.D., Shaw, J., Taylor, R.B., 1989. Barrier and lagoon coast evolution under differing relative sea-level regimes: examples from Ireland and Nova Scotia. Marine Geology 88, 221–242. doi:10.1016/0025-3227(89)90099-6

Carter, R.W.G., Orford, J.D., Forbes, D.L., Taylor, R.B., 1990. Morphosedimentary development of drumlin-flank barriers with rapidly rising sea level, Story Head, Nova Scotia. Sedimentary Geology 69, 117–138. doi:10.1016/0037-0738(90)90104-2

Cazenave, A., Palanisamy, H., Ablain, M., 2018. Contemporary sea level changes from satellite altimetry : What have we learned ? What are the new challenges ? Advances in Space Research 62, 1639–1653. doi:10.1016/j.asr.2018.07.017

Chant, K., 1974. The History of Dunwich. Dunwich Museum, Dunwich, UK.

Church, J.A., Clark, P.U., Cazenave, A., Gregory, J.M., Jevrejeva, S., Levermann, A., Merrifield, M.A., Milne, G.A., Nerem, R.S., Nunn, P.D., Payne, A.J., Pfeffer, W.T., Stammer, D., Unnikrishnan, A.S., 2013. Sea-Level Change. In: Stocker, T.F., Qin, D., Plattner, G.-K., Tignor, M., Allen, S.K., Boschung, J., Nauels, A., Xia, Y., Bex, V., Midgley, P.M. (Eds.), Climate Change 2013: The Physical Science Basis. Contribution of Working

Group I to the Fifth Assessment Report of the Intergovernmental Panel on Climate Change. Cambridge University Press, Cambridge, United Kingdom.

Clark, C.D., Hughes, A.L.C., Greenwood, S.L., Jordan, C., Sejrup, H.P., 2012. Pattern and timing of retreat of the last British-Irish Ice Sheet. Quaternary Science Reviews 44, 112–146. doi:10.1016/j.quascirev.2010.07.019

Clark, C.D., Ely, J.C., Greenwood, S.L., Hughes, A.L.C., Meehan, R., Barr, I.D., Bateman, M.D., Bradwell, T., Doole, J., Evans, D.J.A., Jordan, C.J., Monteys, X., Pellicer, X.M., Sheehy, M., 2018. BRITICE Glacial Map, version 2: a map and GIS database of glacial landforms of the last British–Irish Ice Sheet. Boreas 47, 11–27. doi:10.1111/bor.12273

Clarke, D.W., Boyle, J.F., Chiverrell, R.C., Lario, J., Plater, A.J., 2014. A sediment record of barrier estuary behaviour at the mesoscale: Interpreting high-resolution particle size analysis. Geomorphology 221, 51–68. doi:10.1016/j.geomorph.2014.05.029

Cleve-Euler, A., 1923. Forsok til analys av Nordens senkvartara nivaforandringar jamte nagra konsekvenser. Geol.Foren.Stockholm Forh. 45, 19–107.

Cleve-Euler, A., 1944. Die Diatomeen als quartargeologische Indikatoren. Geol.Foren.Stockholm Forh. 66, 383–410.

Coles, B.P., 1977. The Holocene foraminifera and palaeogeography of Central Boadland (vol. 1). PhD Thesis, University of East Anglia.

Coles, B.P., Funnell, B.M., 1981. Holocene palaeoenvironments of Broadland, England. Special Publication of the International Association of Sedimentologists 5, 123–131.

Comfort, N., 1994. The Lost City of Dunwich. Terence Dalton Ltd, Lavenham, Suffolk.

Cooper, J.A.G., Green, A.N., Loureiro, C., 2018. Geological constraints on mesoscale coastal barrier behaviour. Global and Planetary Change 168, 15–34. doi:10.1016/j.gloplacha.2018.06.006

Croudace, I.W., Rindby, A., Rothwell, R.G., 2006. ITRAX: description and evaluation of a new multi-function X-ray core scanner. In: Rothwell, R.G. (Ed.), New Techniques in Sediment Core Analysis. Geological Society, London, Special Publications, pp. 51–63. doi:10.1144/GSL.SP.2006.267.01.04

Darby, H.C., 1935. The Domesday Geography of Norfolk and Suffolk. The Geographical Journal 85, 432–447.

Dean, W., 1974. Determination of carbonate and organic matter in calcareous sediments and sedimentary rocks by loss on ignition: comparison with other methods. Journal of Sedimentary Petrology 44, 242–248.

Defra, 2006. Flood and Coastal Defence Appraisal Guidance. FCDPAG3 Economic Appraisal. Supplementary Note to Operating Authorities — Climate Change Impacts. London.

Dellwig, O., Watermann, F., Brumsack, H.J., Gerdes, G., 1999. High-resolution reconstruction of a Holocene coastal sequence (NW Germany) using inorganic geochemical data and diatom inventories. Estuarine, Coastal and Shelf Science 48, 617–633. doi:10.1006/ecss.1998.0462

Denys, L., 1984. Diatom analysis of coastal deposits: methodological aspects. Bulletin de la Société belge de Géologie 93, 291–295.

Denys, L., 1993. Paleoecologisch diatomeeënonderzoek van de Holocene afzetting in de westelijke Belgische kustvlakte. PhD Thesis, University of Antwerpen.

Denys, L., Baeteman, C., 1995. Holocene evolution of relative sea level and local mean high water spring tides in Belgium- a first assessment. Marine Geology 124, 1–19. doi:10.1016/0025-3227(95)00029-X

Denys, L., Wolf, H. De, 1999. Diatoms as indicators of coastal paleoenvironments and relative sea-level change. In: Stoermer, E., Smol, J. (Eds.), The Diatoms: Applications for the Environmental and Earth Sciences. Cambridge University Press, Cambridge.

Devoy, R.J., 1982. Analysis of the geological evidence for Holocene sea-level movements in southeast England. Proceedings of the Geologists' Association 93, 65–90. doi:10.1016/S0016-7878(82)80033-3

Dezileau, L., Sabatier, P., Blanchemanche, P., Joly, B., Swingedouw, D., Cassou, C., Castaings, J., Martinez, P., Grafenstein, U. Von, 2011. Intense storm activity during the Little Ice Age on the French Mediterranean coast. Palaeogeography, Palaeoclimatology, Palaeoecology 299, 289–297. doi:10.1016/j.palaeo.2010.11.009

Dietze, E., Hartmann, K., Diekmann, B., Ijmker, J., Lehmkuhl, F., Opitz, S., Stauch, G., Wünnemann, B., Borchers, A., 2012. An end-member algorithm for deciphering modern detrital processes from lake sediments of Lake Donggi Cona, NE Tibetan Plateau, China. Sedimentary Geology 243–244, 169–180. doi:10.1016/j.sedgeo.2011.09.014

Dietze, E., Maussion, F., Ahlborn, M., Diekmann, B., Hartmann, K., Henkel, K., Kasper, T., Lockot, G., Opitz, S., Haberzettl, T., 2014. Sediment transport processes across the

Tibetan Plateau inferred from robust grain-size end members in lake sediments. Climate of the Past 10, 91–106. doi:10.5194/cp-10-91-2014

Dinelli, E., Ghosh, A., Rossi, V., Vaiani, S.C., 2012. Multiproxy reconstruction of late Pleistocene-Holocene environmental changes in coastal successions: Microfossil and geochemical evidences from the Po Plain (Northern Italy). Stratigraphy 9, 153–167.

Doody, J.P., 1996. Management and use of dynamic estuarine shorelines. In: Nordstrom, K.F., Roman, C.T. (Eds.), Estuarine Shores: Evolution, Environments and Human Alterations. Wiley, Chichester, pp. 421–434.

Duffy, W., Belknap, D.F., Kelley, J.T., 1989. Morphology and stratigraphy of small barrier-lagoon systems in Maine. Marine Geology 88, 243–262. doi:10.1016/0025-3227(89)90100-X

Dura, T., Hemphill-Haley, E., Sawai, Y., Horton, B.P., 2016. The application of diatoms to reconstruct the history of subduction zone earthquakes and tsunamis. Earth-Science Reviews 152, 181–197. doi:10.1016/J.EARSCIREV.2015.11.017

Dymond, D.P., Martin, E.A., 1999. An Historical Atlas of Suffolk. Archaeological Service, Suffolk City Council.

Edwards, R., Wright, A., 2015. Foraminifera. In: Shennan, I., Long, A.J., Horton, B.P. (Eds.), Handbook of Sea-Level Research. Wiley, Chichester, pp. 191–217.

Eglinton, T.I., Benitez-Nelson, B.C., Pearson, A., McNichol, A.P., Bauer, J.E., Druffel, E.R.M., 1997. Variability in radiocarbon ages of individual organic compounds from marine sediments. Science 277, 796–799. doi:10.1126/science.277.5327.796

Environment Agency, 2009. Minsmere Flood Risk Management Study. Peterborough.

Fabel, D., Ballantyne, C.K., Xu, S., 2012. Trimlines, blockfields, mountain-top erratics and the vertical dimensions of the last British–Irish Ice Sheet in NW Scotland. Quaternary Science Reviews 55, 91–102. doi:10.1016/j.quascirev.2012.09.002

Farrell, W.E., Clark, J.A., 1976. On Postglacial Sea Level. Geophysical Journal of the Royal Astronomical Society 46, 647–667. doi:10.1111/j.1365-246X.1976.tb01252.x

Fawn, A.J., Davies, G.M.R., Evans, K.A., McMaster, I., 1990. The Red Hills of Essex: Salt Making in Antiquity. Colchester Archaeology Group, Colchester.

Fitzgerald, D.M., Buynevich, I.V., Davis Jr, R.A., Fenster, M.S., 2002. New England tidal inlets with special reference to riverine-associated inlet systems. Geomorphology 48, 179–208.

Fitzgerald, D.M., Fenster, M.S., Argow, B.A., Buynevich, I. V., 2008. Coastal Impacts Due to Sea-Level Rise. Annual Review of Earth and Planetary Sciences 36, 601–647. doi:10.1146/annurev.earth.35.031306.140139

Flemming, B.W., 2007. The influence of grain-size analysis methods and sediment mixing on curve shapes and textural parameters: Implications for sediment trend analysis. Sedimentary Geology 202, 425–435. doi:10.1016/j.sedgeo.2007.03.018

Flemming, N.C., 1982. Multiple regression analysis of earth movements and eustatic sea-level change in the United Kingdom in the past 9000 years. Proceedings of the Geologists' Association 93, 113–125. doi:10.1016/S0016-7878(82)80035-7

Flower, R.J., 1993. Diatom preservation: experiments and observations on dissolution and breakage in modern and fossil material. Hydrobiologia 269–270, 473–484. doi:10.1007/BF00028045

Folk, R.L., Ward, W.C., 1957. Brazos River Bar: A study in the significance of grain size parameters. Journal of Sedimentary Petrology 21, 3-26. doi:10.1306/74D70646-2B21-11D7-8648000102C1865D

Forbes, D.L., Orford, J.D., Carter, R.W.G., Shaw, J., Jennings, S.C., 1995. Morphodynamic evolution, self-organisation, and instability of coarse-clastic barriers on paraglacial coasts. Marine Geology 126, 63–85. doi:10.1016/0025-3227(95)00066-8

Freitas, M.C., Andrade, C., Cruces, A., 2002. The geological record of environmental changes in southwestern Portuguese coastal lagoons since the Lateglacial. Quaternary International 93–94, 161–170. doi:10.1016/S1040-6182(02)00014-9

Friedman, G., Sanders, E., 1978. Principles of sedimentology. John Wiley, New York.

Funnell, B.M., 1979. History and prognosis of subsidence and sea-level change in the lower Yare Valley. Bulletin of the Geological Society of Norfolk 31, 35–44.

Funnell, B.M., Pearson, I., 1989. Holocene sedimentation on the North Norfolk barrier coast in relation to relative sea-level change. Journal of Quaternary Science 4, 25–36. doi:10.1002/jqs.3390040104

Gale, S.J., Hoare, P.G., 1991. Quaternary sediments: petrographic methods for the study of unlithified rocks. Wiley, New York.

García-Rodríguez, F., Sprechmann, P., Metzeltin, D., Scafati, L., Melendi, D.L., Volkheimer, W., Mazzeo, N., Hiller, A., Tümpling, W. von, Scasso, F., 2004. Holocene

trophic state changes in relation to sea level variation in Lake Blanca, SE Uruguay. Journal of Paleolimnology 31, 99–115. doi:10.1023/b:jopl.0000013281.31891.8e

Gardner, T., 1754. An historical account of Dunwich,... Blithburgh,... Southwold,... with remarks on some places contiguous thereto. Gardner, London.

Gehrels, W.R., 1999. Middle and Late Holocene Sea-Level Changes in Eastern Maine Reconstructed from Foraminiferal Saltmarsh Stratigraphy and AMS 14C Dates on Basal Peat. Quaternary Research 52, 350–359. doi:10.1006/qres.1999.2076

Gehrels, W.R., 2002. Intertidal foraminifera as palaeoenvironmental indicators. In: Haslett, S.K. (Ed.), Quaternary Environmental Micropalaeontology. Arnold, London, pp. 91–114.

Gehrels, W.R., Belknap, D.F., Pearce, B.R., Gong, B., 1995. Modelling the contribution of M2 tidal amplification to the Holocene rise of mean high water in the Gulf of Maine and the Bay of Fundy. Marine Geology 124, 71–85. doi:10.1016/0025-3227(95)00033-U

Gehrels, W.R., Roe, H.M., Charman, D.J., 2001. Foraminifera, testate amoebae and diatoms as sea-level indicators in UK saltmarshes: a quantitative multiproxy approach. Journal of Quaternary Science 16, 201–220. doi:10.1002/jqs.588

Gerrard, A.J., Adlam, B.H., Morris, L., 1984. Holocene coastal changes-methodological problems. Quaternary Newsletter 44, 7–14.

Gessner, F., 1959. Hydrobotanik vol. 2. Veb Deutscher Verlag der Wissenschaften, Berlin.

Geyh, M.A., Krumbein, W.E., Kudraus, H.R., 1974. Unreliable 14C dating of long stored deep-sea sediments due to bacterial activity. Marine Geology 17, 45–50.

Glew, J., Smol, J., Last, W., 2001. Sediment Core Collection & Extrusion. In: Last, W., Smol, J. (Eds.), Tracking Environmental Change Using Lake Sediments Volume 1: Basin Analysis, Coring and Chronological Techniques. Springer, Netherlands, pp. 73–105.

Godwin, H., 1940. Pollen analysis and forest history of England and Wales. New Phytologist 39, 370–400.

Godwin, H., 1978. Fenland: Its Ancient Past and Uncertain Future. Cambridge University Press, Cambridge.

Good, C., Plouviez, J., 2007. Archaeological Service Report: The Archaeology of the Suffolk Coast, Suffolk County Council Archaeological Service. Suffolk.

Greensmith, J.T., Tucker, E.V., 1971. The effects of late Pleistocene and Holocene sea-level changes in the vicinity of the River Crouch, East Essex. Proceedings of the Geologists' Association 82, 301–321. doi:10.1016/S0016-7878(71)80011-1

Griffiths, S.D., Hill, D.F., 2015. Tidal modeling. In: Shennan, I., Long, A.J., Horton, B.P. (Eds.), Handbook of Sea-Level Research. John Wiley & Sons, Ltd, pp. 438–451.

Grimm, E., 1987. CONISS: a FORTRAN 77 program for stratigraphically constrained cluster analysis by the method of incremental sum of squares. Computers and Geosciences 13, 13–35.

Groot, T.A.M. de, Gans, W. de, 1996. Facies variations and sea-level response in the lowermost Rhine/Meuse area during the last 15000 years (the Netherlands). Mededelingen Rijks Geologische Dienst 57, 229–250.

Guiry, M.D., Guiry, M.D., 2019. AlgaeBase, World-wide electronic publication, National University of Ireland, Galway.

Hamblin, R.J.O., Moorlock, B.S.P., Booth, S.J., Jeffery, D.H., Morigi, A.N., 1997. The Red Crag and Norwich Crag formations in Eastern Suffolk. Proceedings of the Geologists' Association 108, 11–23. doi:10.1016/S0016-7878(97)80002-8

Hamilton, C.A., 2017. Auger Survey Report- Chapel Hill field, Minsmere Part of DigVentures Leiston Abbey Project. Liverpool.

Hamilton, C.A., Kirby, J.R., Lane, T.P., Plater, A.J., Waller, M.P., 2019. Sediment supply and barrier dynamics as driving mechanisms of Holocene coastal change for the southern North Sea basin. Quaternary International In Press, 1–12. doi:10.1016/j.quaint.2019.02.028

Hamilton, S., Shennan, I., 2005. Late Holocene great earthquakes and relative sea-level change at Kenai, southern Alaska. Journal of Quaternary Science 20, 95–111. doi:10.1002/jqs.903

Hartley, B., Barber, H.G., Carter, J.R., 1996. An Atlas of British Diatoms. Biopress Limited, Bristol.

Haskoning, 2009. Suffolk SMP2 Sub-cell 3c: Policy Development Zone 3 – Easton Broad to Dunwich Cliffs.

Haslett, S.K., Davies, P., Curr, R.H.F., Davies, C.F.C., Kennington, K., King, C.P., Margetts, A.J., 1998. Evaluating the late-Holocene relative sea-level change in the Somerset Levels, southwest Britain. The Holocene 8, 197–207.

Heiri, O., Lotter, A., Lemcke, G., 2001. Loss on ignition as a method for estimating organic and carbon content in sediments: reproducibility and comparability of results. Journal of Paleolimnology 25, 101–110.

Hemphill-Haley, E., 1993. Taxonomy of recent and fossil (Holocene) diatoms (Bacillariophyta) from northern Willapa Bay, Washington. US Geological Survey 93–289, 1–151.

Hendey, N.I., 1974. A revised check-list of British marine diatoms. Journal of the Marine Biological Association of the United Kingdom 54, 277–300. doi:10.1017/S0025315400058549

Hijma, M.P., Engelhart, S.E., Törnqvist, T.E., Horton, B.P., Hu, P., Hill, D.F., 2015. A protocol for a geological sea-level database. In: Shennan, I., Long, A.J., Horton, B.P. (Eds.), Handbook of Sea-Level Research. John Wiley & Sons, Ltd, Chichester, pp. 536–556.

Hodskinson, J., 1783. The County of Suffolk. William Faden, London.

Hoeksema, R.J., 2007. Three stages in the history of land reclamation in the Netherlands. Irrigation and Drainage 56, S113–S126. doi:10.1002/ird

Horton, B.P., 1997. Quantification of the indicative meaning of a range of Holocene sea-level index points drom the western North Sea. PhD Thesis, Durham University.

Horton, B.P., Edwards, R.J., 2005. The application of local and regional transfer functions to the reconstruction of Holocene sea levels, north Norfolk, England. The Holocene 15, 216–228. doi:10.1191/0959683605hl787rp

Horton, B.P., Shennan, I., 2009. Compaction of Holocene strata and the implications for relative sea-level change on the east coast of England. Geology 37, 1083–1086. doi:10.1130/G30042A.1

Horton, B.P., Edwards, R.J., Lloyd, J.M., 1999. A foraminiferal-based transfer function: Implications for sea-level studies. Journal of Foraminiferal Research 29, 117–129.

Horton, B.P., Edwards, R.J., Lloyd, J.M., 2000. Implications of a microfossil-based transfer function in Holocene sea-level studies. In: Shennan, I., Andrews, J.E. (Eds.), Holocene Land-Ocean Interaction and Environmental Change around the North Sea. Geological Society, Special Publication 166 (1), London, pp. 41–54.

Horton, B.P., Innes, J.B., Shennan, I., Lloyd, J.M., McArthur, J.J., 2004. Holocene coastal change in East Norfolk, UK: palaeoenvironmental data from Somerton and Winterton Holmes, near Horsey. Proceedings of the Geologists' Association 115, 209–220. doi:10.1016/S0016-7878(04)80002-6

Horton, B.P., Corbett, R., Culver, S.J., Edwards, R.J., Hillier, C., 2006. Modern saltmarsh diatom distributions of the Outer Banks, North Carolina, and the development of a transfer function for high resolution reconstructions of sea level. Estuarine, Coastal and Shelf Science 69, 381–394. doi:10.1016/j.ecss.2006.05.007

Horton, B.P., Engelhart, S.E., Hill, D.F., Kemp, A.C., Nikitina, D., Miller, K.G., Peltier, W.R., 2013. Influence of tidal-range change and sediment compaction on Holocene relative sea-level change in New Jersey, USA. Journal of Quaternary Science 28, 403–411. doi:10.1002/jqs.2634

Hu, P., 2010. Developing a quality-controlled postglacial sea-level database for coastal Louisiana to assess conflicting hypotheses of Gulf Coast sea-level change. MSc thesis, Tulane University.

Hubbard, A., Bradwell, T., Golledge, N., Hall, A., Patton, H., Sugden, D., Cooper, R., Stoker, M., 2009. Dynamic cycles, ice streams and their impact on the extent, chronology and deglaciation of the British–Irish ice sheet. Quaternary Science Reviews 28, 758–776. doi:10.1016/j.quascirev.2008.12.026

Hustedt, F., 1953. Die Systematik der Diatomeen in ihren Beziehungen zur Geologie und Okologie nebst einer Revision des Halobien-systems. Svensk Botanisk Tidskrift 47, 509–519.

Imbrie, J., 1963. Factor and vector analysis programs for analyzing geologic data. Technical Report 6, ONR Task No. 389-135. Office of Naval Research, Geography Branch.

Inman, D.L., 1952. Measures for describing the size distribution of sediments. Journal of Sedimentary Petrology 22, 125–145.

Innes, A.G., 1912. Tidal action of the Bure and its tributaries. Transactions of the Norwich and Norfolk Natural History Society 9, 244–262.

Jelgersma, S., 1961. Holocene sea-level changes in the Netherlands. Mededelingen Geologische Stichtig Series C 1, 1–100.

Jennings, J.N., 1955. Further pollen data from the Norfolk Broads: Data for the Study of Post-Glacial History XIV. New Phytologist 54, 199–207. doi:10.1111/j.1469-8137.1955.tb06172.x

Jennings, S.C., Carter, R.W.G., Orford, J.D., 1995. Implications for sea-level research of salt marsh and mudflat accretionary processes along paraglacial barrier coasts. Marine Geology 124, 129–136. doi:10.1016/0025-3227(95)00036-X

Jennings, S.C., Orford, J.D., Canti, M., Devoy, R.J.N., Straker, V., 1998. The role of relative sea-level rise and changing sediment supply on Holocene gravel barier development: the example of Porlock, Somerset, UK. The Holocene 8, 165–181. doi:10.1191/095968398667901806

Johnson, T.C., 1974. The dissolution of siliceous microfossils in surface sediments of the eastern tropical Pacific. Deep Sea Research and Oceanographic Abstracts 21, 851–864. doi:10.1016/0011-7471(74)90004-7

Joliffe, I.P., 1963. A Study of Sand Movements on the Lowestoft Sandbank Using Fluorescent Tracers. The Geographical Journal 129, 480–493.

Jorgensen, E.G., 1955. Solubility of silica in Diatoms. Physiologia Plantarum 8, 846–851.

Juggins, S., 2003. C2 User guide. Software for ecological and palaeoecological data analysis and visualisation. University of Newcastle, Newcastle Upon Tyne.

Kaye, C.A., Baghoorn, E.S., 1964. Quaternary sea-level change and crustal rise at Boston, Massachussetts, with notes on the autocompaction of peat. Geological Society of American Bulletin 75, 63–80.

Keeling, P., 1962. Some experiments on the low-temperature removal of carbonaceous material from clays. Clay Minerals Bulletin 28, 155–158.

Kemp, A.C., Horton, B.P., Corbett, D.R., Culver, S.J., Edwards, R.J., Plassche, O. van de, 2009. The relative utility of foraminifera and diatoms for reconstructing late Holocene sea-level change in North Carolina, USA. Quaternary Research 71, 9–21. doi:10.1016/j.yqres.2008.08.007

Kemp, A.C., Vane, C.H., Horton, B.P., Culver, S.J., 2010. Stable carbon isotopes as potential sea-level indicators in salt marshes, North Carolina, USA. Holocene 20, 623–636. doi:10.1177/0959683609354302

Kemp, A.C., Vane, C.H., Khan, N.S., Ellison, J.C., Engelhart, S.E., Horton, B.P., Nikitina, D., Smith, S.R., Rodrigues, L.J., Moyer, R.P., 2019. Testing the Utility of Geochemical Proxies to Reconstruct Holocene Coastal Environments and Relative Sea Level: A Case Study from Hungry Bay, Bermuda. Open Quaternary 5, 1–17. doi:10.5334/oq.49

Khan, N.S., Vane, C.H., Horton, B.P., 2015a. Stable carbon isotope and C/N geochemistry of coastal wetland sediments as a sea-level indicator. In: Shennan, I., Long, A.J., Horton, B.P. (Eds.), Handbook of Sea-Level Research. John Wiley & Sons, Ltd, Chichester, pp. 295–311.

Khan, N.S., Vane, C.H., Horton, B.P., Hillier, C., Riding, J.B., Kendrick, C.P., 2015b. The application of δ13C, TOC and C/N geochemistry to reconstruct Holocene relative sea levels and paleoenvironments in the Thames Estuary, UK. Journal of Quaternary Science 30, 417–433. doi:10.1002/jqs.2784

Kidson, C., Carr, A.P., 1959. The Movement of Shingle Over the Sea Bed Close Inshore. The Geographical Journal 125, 308–389.

Kidson, C., Heyworth, A., 1978. Holocene eustatic sea level change. Nature 273, 748–750.

Kidson, C., Carr, A.P., Smith, D.B., 1958. Further Experiments Using Radioactive Methods to Detect the Movement of Shingle over the Sea Bed and Alongshore. The Geographical Journal 124, 210–218.

Kirby, J., 1737. An Actual Survey of the County of Suffolk. Issac Basire, London.

Kolbe, R., 1927. Zur Okologie, Morphologie und Systematik der Brackwasser-Diatomeen. Pflanzenforschung 7, 1–146.

Kopp, R.E., Kemp, A.C., Bittermann, K., Horton, B.P., Donnelly, J.P., Gehrels, W.R., Hay, C.C., Mitrovica, J.X., Morrow, E.D., Rahmstorf, S., 2016. Temperature-driven global sea-level variability in the Common Era. Proceedings of the National Academy of Sciences of the United States of America 113, E1434-41. doi:10.1073/pnas.1517056113

Krammer, K., Lange-Bertalot, H., 1991. Bacillariophyceae. 3: Teil: Centrales, Fragilariaceae, Eunotiaceae. In: Ettl, H., Gartner, G., Gerloff, J., Heynig, H., Mollenhauer, D. (Eds.), Susswasserflora von Mitteleuropa, Band 2/3. Gustav Fischer Verlag, Stuttgart, p. 576.

Kraus, N.C., 2004. Analytical Model of Incipient Breaching of Coastal Barriers. Coastal Engineering Journal 45, 511–531. doi:10.1142/s057856340300097x

Krumbein, W.C., 1934. Size frequency distributions of sediments. Journal of Sedimentary Petrology 4, 65–77.

Kuchar, J., Milne, G., Hubbard, A., Patton, H., Bradley, S.L., Shennan, I., Edwards, R.J., 2012. Evaluation of a numerical model of the British-Irish ice sheet using relative sea-level data: implications for the interpretation of trimline observations. Journal of Quaternary Science 27, 597–605. doi:10.1002/jqs.2552

Kunze, G., Dixon, J., 1987. Pretreatment for mineralogical analysis. In: Klute, A. (Ed.), Methods of Soil Analysis Part 1: Physical and Mineralogical Methods 1. American Society of Agronomy, Madison, Wisconsin, pp. 91–100.

Kylander, M.E., Ampel, L., Wohlfarth, B., Veres, D., 2011. High-resolution X-ray fluorescence core scanning analysis of Les Echets (France) sedimentary sequence: New insights from chemical proxies. Journal of Quaternary Science 26, 109–117. doi:10.1002/jqs.1438

Lamb, A.L., Wilson, G.P., Leng, M.J., 2006. A review of coastal palaeoclimate and relative sea-level reconstructions using δ13C and C/N ratios in organic material. Earth-Science Reviews 75, 29–57. doi:10.1016/j.earscirev.2005.10.003

Lambeck, K., 1993a. Glacial rebound of the British Isles-1. Preliminary model results. Geophysical Journal International 115, 941–959.

Lambeck, K., 1993b. Glacial rebound of the British Isles-II. A high-resolution, high-precision model. Geophysical Journal International 115, 960–990.

Lambeck, K., 1995. Late Devensian and Holocene shorelines of the British Isles and North Sea from models of glacio-hydro-isostatic rebound. Journal of the Geological Society 152, 437–448. doi:10.1144/gsjgs.152.3.0437

Lange, C.B., Tiffany, M.A., 2002. The diatom flora of the Salton Sea, California. Hydrobiologia 473, 179–201. doi:10.1023/A:1016550205461

Lario, J., Spencer, C., Plater, A.J., Zazo, C., 2002. Particle size characterisation of Holocene back-barrier sequences from North Atlantic coasts (SW Spain and SE England). Geomorphology 42, 25–42.

Leenheer, L. De, Hove, J. Van, Ruymbeke, M. Van, 1957. Determination quantitative de la matiere organique du sol. Pedologie 7, 324–347.

Lees, B.J., 1983. Observations of Tidal and Residual Currents in the Sizewell-Dunwich area, East Anglia, UK. Deutsche Hydrographische Zeitschrift 36, 1–24.

Lewin, J.C., 1961. The dissolution of silica from diatom walls. Geochimica et Cosmochimica Acta 21, 182–198. doi:10.1016/S0016-7037(61)80054-9

Lloyd, J.M., Evans, J.R., 2002. Contemporary and fossil foraminifera from isolation basins in northwest Scotland. Journal of Quaternary Science 17, 431–443. doi:10.1002/jqs.719

Lloyd, J.M., Zong, Y., Woods, A., 2008. Preliminary investigation of the relative sea-level and inundation history of the Sizewell and Minsmere coastline, Suffolk, British Energy Estuarine and Marine Studies. Technical Report 07/08 no. 015.

Long, A.J., 1992. Coastal responses to changes in sea-level in the East Kent Fens and southeast England, UK over the last 7500 years. Proceedings of the Geologists' Association 103, 187–199. doi:10.1016/S0016-7878(08)80229-5

Long, A.J., Innes, J.B., 1993. Holocene sea-level changes and coastal sedimentation in Romney Marsh, southeast England, UK. Proceedings of the Geologists' Association 104, 223–237. doi:10.1016/S0016-7878(08)80040-5

Long, A.J., Innes, J.B., 1995. The back-barrier and barrier depositional history of Romney Marsh, Walland Marsh and Dungeness, Kent, England. Journal of Quaternary Science 10, 267–283. doi:10.1002/jqs.3390100306

Long, A.J., Scaife, R.G., Edwards, R.J., 1999. Pine pollen in intertidal sediments from Poole Harbour, UK; implications for late-Holocene sediment accretion rates and sea-level rise. Quaternary International 55, 3–16. doi:10.1016/S1040-6182(98)00017-2

Long, A.J., Plater, A.J., Waller, M.P., Innes, J.B., 1996. Holocene coastal sedimentation in the Eastern English Channel: New data from the Romney Marsh region, United Kingdom. Marine Geology 136, 97–120.

Long, A.J., Scaife, R.G., Edwards, R.J., 2000. Stratigraphic architecture, relative sea-level, and models of estuary development in southern England: new data from Southampton Water. Geological Society, London, Special Publications 175, 253–279. doi:10.1144/GSL.SP.2000.175.01.19

Long, A.J., Hipkin, S., Clarke, H., 2002. Romney Marsh: Coastal and Landscape Change Through the Ages. Oxbow, Oxford.

Long, A.J., Waller, M.P., Plater, A.J., 2006a. Coastal resilience and late Holocene tidal inlet history: The evolution of Dungeness Foreland and the Romney Marsh depositional complex (U.K.). Geomorphology 82, 309–330. doi:10.1016/j.geomorph.2006.05.010

Long, A.J., Waller, M.P., Stupples, P., 2006b. Driving mechanisms of coastal change: Peat compaction and the destruction of late Holocene coastal wetlands. Marine Geology 225, 63–84. doi:10.1016/j.margeo.2005.09.004

Long, A.J., Barlow, N.L.M., Gehrels, W.R., Saher, M.H., Woodworth, P.L., Scaife, R.G., Brain, M.J., Cahill, N., 2014. Contrasting records of sea-level change in the eastern and

western North Atlantic during the last 300 years. Earth and Planetary Science Letters 388, 110–122. doi:10.1016/j.epsl.2013.11.012

Lowe, J., Walker, M., 1997. Reconstructing Quaternary Environments, 2nd ed. Longman, Essex, England.

Ludwig, G., Müller, H., Streif, H., 1981. New dates on Holocene sea-level changes in the German Bight. International Association of Sedimentologists Special Publication 5, 211–219.

Lysakova, M., Kitner, M., Poulickova, A., 2007. The epipelic algae of fishponds of Central and Northern Moravia (The Czech Republic). Journal of the Czech Phycological Society 7, 69–75. doi:10.5507/fot.2007.006

Mann, D.G., Poulickova, A., 2010. Mating system, auxosporulation, species taxonomy and evidence for homoploid evolution in Amphora (Bacillariophyta). Phycologia 49, 183–201. doi:10.2216/09-08.1

Massey, A.C., Gehrels, W.R., Charman, D.J., White, S.V., 2006. An intertidal foraminifera-based transfer function for reconstructing Holocene sea-level change in southwest England. The Journal of Foraminiferal Research 36, 215–232. doi:10.2113/gsjfr.36.3.215

Mauquoy, D., Geel, B. Van, 2007. Plant macrofossil methods and studies: Mire and Peat Macros. In: Elias, S.A. (Ed.), Encyclopedia of Quaternary Science. Elsevier Science, Amsterdam, Netherlands, pp. 2315–2336.

McCave, I.N., 1978. Grain-size trends and transport along beaches: Example from eastern England. Marine Geology 28, 43–51. doi:10.1016/0025-3227(78)90092-0

McCave, I.N., 1987. Fine sediment sources and sinks around the East Anglian Coast (UK). Journal of the Geological Society 144, 149–152. doi:10.1144/gsjgs.144.1.0149

McCloskey, T.A., Liu, Kam-biu, 2012. A 7000 year record of paleohurricane activity from a coastal wetland in Belize. Holocene 23, 278–291. doi:10.1177/0959683612460782

McQuoid, M.R., Nordberg, K., 2003. The diatom *Paralia sulcata* as an environmental indicator species in coastal sediments. Estuarine, Coastal and Shelf Science 56, 339–354. doi:10.1016/S0272-7714(02)00187-7

Medlycott, M., 1994. The Othona Community Site, Bradwell-on-Sea, Essex: the extra mural settlement. Essex Archaeology and History 25, 60–71.

Mellett, C.L., Hodgson, D.M., Lang, A., Mauz, B., Selby, I., Plater, A.J., 2012. Preservation of a drowned gravel barrier complex: A landscape evolution study from the north-eastern English Channel. Marine Geology 315–318, 115–131. doi:10.1016/j.margeo.2012.04.008

Meyers, P., Teranes, J., 2001. Sediment Organic Matter. In: Last, W., Smol, J. (Eds.), Tracking Environmental Change Using Lake Sediments Volume 2: Physical and Geochemical Methods. Springer, Netherlands, pp. 239–269.

Moore, P., Webb, J., Collinson, M., 1991. Pollen Analysis, 2nd ed. Blackwell Scientific Publications, Oxford.

Morton, R.A., White, W.A., 1997. Characteristics of and corrections for core shortening in unconsolidated sediments. Journal of Coastal Research 13, 761–769.

Mrani-Alaoui, M., Anthony, E.J., 2011. New data and a morphodynamic perspective on mid- to late-Holocene palaeoenvironmental changes in the French Flanders coastal plain, Southern North Sea. The Holocene 21, 445–453. doi:10.1177/0959683610385724

Murray, J.W., 1979. British nearshore foraminiferids. Academic Press, London.

Natural England, 2013. National Character Area Profile- Suffolk Coast and Heaths.

Neill, S.P., Scourse, J.D., Uehara, K., 2010. Evolution of bed shear stress distribution over the northwest European shelf seas during the last 12,000 years. Ocean Dynamics 60, 1139–1156. doi:10.1007/s10236-010-0313-3

Nelson, A., Kashima, K., 1993. Diatom zonation in southern Oregon tidal marshes relative to vascular plants, foraminifera, and sea level. Journal of Coastal Research 9, 673–697.

Nenquin, J., 1961. Salt: a study in economic prehistory. Brugge, Belgium.

Neuman, B.S., 1977. Thermal techniques. In: Zussman, J. (Ed.), Physical Methods in Determinative Mineralogy. Academic Press, London, pp. 605–662.

Nicholls, R.J., Branson, J., 1998. Coastal Resilience and Planning for an Uncertain Future : An Introduction. The Geographical Journal 164, 255–258.

Nicholls, R.J., Wong, P.P., Burkett, V.R., Codignotto, J.O., Hay, J.E., McLean, R.F., Ragoonaden, S., Woodroffe, C.D., 2007. Coastal Systems and Low-Lying Areas. In: Parry, M.L., Canziani, O.F., Palutikof, J.P., Linden, P.J. van der, Hanson, C.E. (Eds.), Climate Change 2007: Impacts, Adaptation and Vulnerability. Contribution of Working Group II to the Fourth Assessment Report of the Intergovernmental Panel on Climate Change. Cambridge University Press, Cambridge.

Ohkouchi, N., Eglinton, T.I., 2008. Compound-specific radiocarbon dating of Ross Sea sediments: A prospect for constructing chronologies in high-latitude oceanic sediments. Quaternary Geochronology 3, 235–243. doi:10.1016/j.quageo.2007.11.001

Olsson, I.U., 1991. Accuracy and precision in sediment chronology. Hydrobiologia 214, 25–34.

Onyett, D., Simmonds, A., 1983. Beach transport and longshore transport. East Anglian Coastal Research Programme Report No. 8 University of East Anglia, Norwich, UK.

Orford, J.D., Carter, R.W.G., Jennings, S.C., 1991. Coarse clastic barrier environments: Evolution and implications for Quaternary sea level interpretation. Quaternary International 9, 87–104. doi:10.1016/1040-6182(91)90068-Y

Palmer, A., Abbott, W., 1986. Diatoms as indicators of sea-level change. In: Plassche, O. van de (Ed.), Sea-Level Research: A Manual for the Collection and Evaluation of Data. Geo books, Norwich, pp. 457–488.

Parker, R., 1978. Men of Dunwich. Collins, London.

Paterson, G.A., Heslop, D., 2015. New methods for unmixing sediment grain size data. Geochemistry, Geophysics, Geosystems 16, 4494–4506. doi:10.1002/2015GC006070

Patton, H., Andreassen, K., Bjarnadottir, L.R., Dowdeswell, J.A., Winsborrow, M.C.M., Noormets, R., Polyak, L., Auriac, A., Hubbard, A., 2015. Geophysical constraints on the dynamics and retreat of the Barents Sea ice sheet as a paleobenchmark for models of marine ice sheet deglaciation. Reviews of Geophysics 53, 1051–1098.

Paul, M.A., Barras, B.F., 1998. A geotechnical correction for post-depositional sediment compression: examples from the Forth Valley, Scotland. Journal of Quaternary Science 13, 171–176.

Peltier, W.R., 1998. Postglacial variations in the level of the sea: Implications for climate dynamics and solid-earth geophysics. Reviews of Geophysics 36, 603–689.

Peltier, W.R., 2002. On eustatic sea level history: Last Glacial Maximum to Holocene. Quaternary Science Reviews 21, 377–396.

Peltier, W.R., Shennan, I., Drummond, R., Horton, B.P., 2002. On the postglacial isostatic adjustment of the British Isles and the shallow viscoelastic structure of the Earth. Geophysical Journal International 148, 443–475. doi:10.1046/j.1365-246x.2002.01586.x

Pierik, H.J., Cohen, K.M., Vos, P.C., Spek, A.J.F. van der, Stouthamer, E., 2017. Late Holocene coastal-plain evolution of the Netherlands: the role of natural preconditions in

human-induced sea ingressions. Proceedings of the Geologists' Association 128, 180–197. doi:10.1016/j.pgeola.2016.12.002

Plassche, O. van de, 1980. Holocene water-level changes in the Rhine-Meuse delta as a function of changes in relative sea level, local tidal range, and river gradient. Geologie en Mijnbouw 59, 343–351.

Plassche, O. van de, 1982. Sea-level change and water-level movements in The Netherlands during the Holocene. Mededelingen Rijks Geologische Dienst 36, 3–93.

Plassche, O. van de, 1986. Sea-level Research: a manual for the collection and evaluation of data. Geobooks, Norwich.

Plater, A.J., Kirby, J.R., 2011. Sea-Level Change and Coastal Geomorphic Response. Treatise on Estuarine and Coastal Science 39–72. doi:10.1016/B978-0-12-374711-2.00304-1

Plater, A.J., Long, A.J., Spencer, C.D., Delacour, R.A.P., 1999. The stratigraphic record of sea-level change and storms during the last 2000 years: Romney Marsh, southeast England. Quaternary International 55, 17–27. doi:10.1016/S1040-6182(98)00020-2

Plater, A.J., Stupples, P., Roberts, H.M., 2009. Evidence of episodic coastal change during the Late Holocene: The Dungeness barrier complex, SE England. Geomorphology 104, 47–58. doi:10.1016/j.geomorph.2008.05.014

Plater, A.J., Kirby, J.R., Boyle, J.F., Shaw, T., Mills, H., 2015. Loss on ignition and organic content. In: Shennan, I., Long, A.J., Horton, B.P. (Eds.), Handbook of Sea-Level Research. John Wiley & Sons, Ltd, Chichester, pp. 312–330.

Preuss, H., 1979. Progress in computer evaluation of sea-level data within the IGCP project no. 61. In: Flexor, I. (Ed.), International Symposium on Coastal Evolution in the Quaternary. Sao-Paulo, Brazil, pp. 104–134.

Priju, C.P., Narayana, A.C., 2007. Particle size characterization and late Holcoene depositional processes in Vembanad Lagoon, Kerala: inferences from suite statistics. Journal of the Geological Society of India 69, 311–318.

Pye, K., Blott, S.J., 2004. Particle size analysis of sediments, soils and related particulate materials for forensic purposes using laser granulometry. Forensic Science International 144, 19–27. doi:10.1016/j.forsciint.2004.02.028

Pye, K., Blott, S.J., 2006. Coastal Processes and Morphological Change in the Dunwich-Sizewell Area, Suffolk, UK. Journal of Coastal Research 223, 453–473. doi:10.2112/05-0603.1

Pye, K., Blott, S.J., 2009. Progressive Breakdown of a Gravel-Dominated Coastal Barrier, Dunwich-Walberswick, Suffolk, UK: Processes and implications. Journal of Coastal Research 25, 589–602.

Pye, K., Saye, S., Blott, S.J., 2007. Joint Defra/EA Flood and Coastal Erosion Risk Management R & D Programme. Sand dune processes and management for flood and coastal defence. Part 3: The geomorphological and management status of coastal dunes in England and Wales. R & D Technical Report FD1302/TR.

Rea Price, J., Robb, D., 2015. The Draining of the Minsmere Levels- The saga of a project and a community. Leiston Press Ltd, Leiston, Suffolk.

Reid, W.J., 1958. Coastal experiments with radioactive tracers: Recent work on the coast of Norfolk. The Dock and Harbour Authority 39, 84–88.

Rippon, S., 2000. The transformation of coastal wetlands; Exploitation and management of marshland landscapes in North West Europe during the Roman and Medieval periods. Oxford University Press, Oxford.

Rippon, S., 2002. Romney Marsh: Evolution of the Historic Landscape and its Wider Setting. In: Long, A.J., Hipkin, S., Clarke, H. (Eds.), Romney Marsh: Coastal and Landscape Changes through the Ages. Oxbow, Oxford, pp. 84–100.

Rippon, S., 2009. "Uncommonly rich and fertile" or "not very salubrious"? The Perception and Value of Wetland Landscapes. Landscapes 10, 36–60.

Robinson, A.H.W., 1966. Residual currents in relation to shoreline evolution of the East Anglian coast. Marine Geology 4, 57–84. doi:10.1016/0025-3227(66)90037-5

Robinson, A.H.W., 1980. Erosion and accretion along part of the Suffolk coast of East Anglia, England. Marine Geology 37, 133–146. doi:10.1016/0025-3227(80)90014-6

Robinson, M., 1982. Diatom Analysis of Early Flandrian Lagoon Sediments from East Lothian, Scotland. Journal of Biogeography 9, 207–221.

Roelofs, A.K., 1984. Distributional patterns and variation of valve diameter of *Paralia sulcata* in surface sediments of Southern British Columbia Inlets. Estuarine, Coastal and Shelf Science 18, 165–176. doi:10.1016/0272-7714(84)90104-5

Rosati, J.D., 2005. Concepts in sediment budgets. Journal of Coastal Research 21, 307–322.

Round, F.E., 1964. The diatom sequence in lake deposits: some problems of interpretation. Verinigung fr Theoretische und Angewandte Limnologie 15, 1012–1020.

Roy, P.S., 1984. New South Wales estuaries: their origin and evolution. In: Thom, B.G. (Ed.), Coastal Geomorphology in Australia. Academic Press, Australia, pp. 99–121.

Roy, P.S., Cowell, P.J., Ferland, M.A., Thom, B.G., 1994. Wave-dominated coasts. In: Carter, R.W.G., Woodroffe, C.D. (Eds.), Coastal Evolution- Late Quaternary Shoreline Morphodynamics. Cambridge University Press, Cambridge, pp 121-186.

Ryves, D.B., Juggins, S., Fritz, S.C., Battarbee, R.W., 2001. Experimental diatom dissolution and the quantification of microfossil preservation in sediments. Palaeogeography, Palaeoclimatology, Palaeoecology 172, 99–113. doi:10.1016/S0031-0182(01)00273-5

Ryves, D.B., Battarbee, R.W., Fritz, S.C., 2009. The dilemma of disappearing diatoms: Incorporating diatom dissolution data into palaeoenvironmental modelling and reconstruction. Quaternary Science Reviews 28, 120–136. doi:10.1016/j.quascirev.2008.08.021

Saar, A. Du, 1967. Results and problems in diatom investigation at the geological survey in Haarlem. Geologie en Mijnbouw 46, 105–108.

Sáez, A., Carballeira, R., Pueyo, J.J., Vázquez-Loureiro, D., Leira, M., Hernández, A., Valero-Garcés, B.L., Bao, R., 2018. Formation and evolution of back-barrier perched lakes in rocky coasts: An example of a Holocene system in north-west Spain. Sedimentology 65, 1891–1917. doi:10.1111/sed.12451

Saxton, C., 1575. Suffolk. Christopher Saxton, scale ca. 1:240,000, 1 sheet. British Museum map C.7.c.1, reprinted by Taylowe Ltd., London, 1969.

Scott, D.B., Medioli, F.S., 1978. Vertical zonations of marsh foraminifera as accurate indicators of former sea-levels. Nature 272, 528–531. doi:10.1038/272528a0

Scott, D.B., Medioli, F.S., 1980. Quantitative studies of marsh foraminiferal distributions in Nova Scotia: Implications for sea level studies. Cushman Foundation for Foraminiferal Research Special Publication 17, 1–58.

Sear, D.A., Bacon, S., Murdock, A., Doneghan, G., LeBas, T.P., 2008. Dunwich 2008 Project Report. GeoData Research Report No. UC1064.

Sear, D.A., Bacon, S.R., Murdock, A., Doneghan, G., Baggaley, P., Serra, C., LeBas, T.P., 2011. Cartographic, Geophysical and Diver Surveys of the Medieval Town Site at Dunwich, Suffolk, England. International Journal of Nautical Archaeology 40, 113–132. doi:10.1111/j.1095-9270.2010.00275.x

Sear, D.A., Murdock, A., LeBas, T.P., Baggaley, P., Gubbins, G., 2013. Dunwich, Suffolk: Mapping and assessing the inundated medieval town. Historic England. doi:10.1017/CBO9781107415324.004

Sear, D.A., Scaife, R., Langdon, C., 2015. Touching The Tide Dunwich Land based Archaeological Survey : 2014-15. Technical Report, University of Southampton.

Shennan, I., 1980. Flandrian sea-level changes in the Fenland. PhD Thesis, Durham University.

Shennan, I., 1982. Interpretation of Flandrian sea-level data from the Fenland, England. Proceedings of the Geologists' Association 93, 53–63. doi:10.1016/S0016-7878(82)80032-1

Shennan, I., 1986. Flandrian sea-level changes in the Fenland . II : Tendencies of sea-level movement , altitudinal changes , and local and regional factors. Journal of Quaternary Science 1, 155–179. doi:10.1002/jqs.3390010205

Shennan, I., 1989. Holocene crustal movements and sea-level changes in Great Britain. Journal of Quaternary Science 4, 77–89.

Shennan, I., 2007. Sea-level studies; Overview. In: Elias, S. (Ed.), Encyclopedia of Quaternary Science. Elsevier, pp. 2967–2974.

Shennan, I., 2015. Handbook of sea-level research: framing research questions. In: Shennan, I., Long, A.J., Horton, B.P. (Eds.), Handbook of Sea-Level Research. John Wiley & Sons, Ltd, Chichester, pp. 3–25.

Shennan, I., Horton, B.P., 2002. Holocene land- and sea-level changes in Great Britain. Journal of Quaternary Science 17, 511–526. doi:10.1002/jqs.710

Shennan, I., Hamilton, S., 2006. Coseismic and pre-seismic subsidence associated with great earthquakes in Alaska. Quaternary Science Reviews 25, 1–8. doi:10.1016/J.QUASCIREV.2005.09.002

Shennan, I., Tooley, M.J., Davis, M.J., Haggart, B.A., 1983. Analysis and interpretation of Holocene sea-level data. Nature. doi:10.1038/302404a0

Shennan, I., Innes, J.B., Long, A.J., Zong, Y., 1994. Late Devensian and Holocene relative sea-level changes at Loch nan Eala, near Arisaig, northwest Scotland. Journal of Quaternary Science 9, 261–283.

Shennan, I., Innes, J.B., Long, A.J., Zong, Y., 1995. Holocene relative sea-level changes and coastal vegetation history at Kentra Moss, Argyll, northwest Scotland. Marine Geology 124, 43–59.

Shennan, I., Green, F., Innes, J.B., Lloyd, J.M., Rutherford, M., Walker, K., 1996. Evaluation of Rapid Relative Sea-Level Changes in North-West Scotland During the Last Glacial- Interglacial Transition: Evidence from Ardtoe and Other Isolation Basins. Journal of Coastal Research 12, 862–874.

Shennan, I., Scott, D.B., Rutherford, M., Zong, Y., 1999. Microfossil analysis of sediments representing the 1964 earthquake, exposed at Girdwood Flats, Alaska, USA. Quaternary International 60, 55–73. doi:10.1016/S1040-6182(99)00007-5

Shennan, I., Lambeck, K., Horton, B.P., Innes, J.B., Lloyd, J.M., McArthur, J., Rutherford, M.M., 2000a. Holocene isostacy and relative sea-level changes on the east coast of England. Holocene land-ocean interaction and environmental change around the North Sea 275–298.

Shennan, I., Lambeck, K., Flather, R., Horton, B.P., McArthur, J., Innes, J., Lloyd, J., Rutherford, M., Wingfield, R., 2000b. Modelling western North Sea palaeogeographies and tidal changes during the Holocene. Geological Society, London, Special Publications 166, 299–319. doi:10.1144/GSL.SP.2000.166.01.15

Shennan, I., Peltier, W., Drummond, R., Horton, B.P., 2002. Global to local scale parameters determining relative sea-level changes and the post-glacial isostatic adjustment of Great Britain. Quaternary Science Reviews 21, 397–408. doi:10.1016/S0277-3791(01)00091-9

Shennan, I., Coulthard, T., Flather, R., Horton, B.P., Macklin, M., Rees, J., Wright, M., 2003. Integration of shelf evolution and river basin models to simulate Holocene sediment dynamics of the Humber Estuary during periods of sea-level change and variations in catchment sediment supply. The Science of the Total Environment 314–316, 737–754. doi:10.1016/S0048-9697(03)00081-0

Shennan, I., Hamilton, S., Hillier, C., Woodroffe, S., 2005. A 16000-year record of near-field relative sea-level changes, North-west Scotland, United Kingdom. Quaternary International 133–134, 95–106. doi:10.1016/j.quaint.2004.10.015

Shennan, I., Bradley, S.L., Milne, G., Brooks, A., Bassett, S., Hamilton, S., 2006. Relative sea-level changes, glacial isostatic modelling and ice-sheet reconstructions from the British Isles since the Last Glacial Maximum. Journal of Quaternary Science 21, 585–599. doi:10.1002/jqs

Shennan, I., Barlow, N.L.M., Combellick, R., 2008. Palaeoseismological records of multiple great earthquakes in south-central Alaska – a 4000 year record at Girdwood. In: Freymueller, J., Haeussler, P., Wessen, R., Ekstrom, G. (Eds.), Active Tectonics and Seismic Potential of Alaska. Geophysical Monograph Series, Vol. 179. American Geophysical Union Washington, pp. 185–199.

Shennan, I., Milne, G., Bradley, S.L., 2012. Late Holocene vertical land motion and relative sea-level changes: lessons from the British Isles. Journal of Quaternary Science 27, 64–70. doi:10.1002/jqs.1532

Shennan, I., Bradley, S.L., Edwards, R.J., 2018. Relative sea-level changes and crustal movements in Britain and Ireland since the Last Glacial Maximum. Quaternary Science Reviews 188, 143–159. doi:10.1016/j.quascirev.2018.03.031

Simonsen, R., 1969. Diatoms as indicators in esturaine environments. Veroffentlichungen des Instituts fur Meeresforschung 11, 287–291.

Simper, R., 1994. Rivers Alde, Ore and Blyth. Creekside Publishing, Lavenham.

Sparrenbom, C.J., Bennike, O., Fredh, D., Randsalu-Wendrup, L., Zwartz, D., Ljung, K., Björck, S., Lambeck, K., 2013. Holocene relative sea-level changes in the inner Bredefjord area, southern Greenland. Quaternary Science Reviews 69, 107–124. doi:10.1016/j.quascirev.2013.02.020

Spencer, C.D., Plater, A.J., Long, A.J., 1998. Rapid coastal change during the mid- to late Holocene: the record of barrier estuary sedimentation in the Romney Marsh region, southeast England. The Holocene 8, 143–163. doi:10.1191/095968398673197622

Steers, J.A., 1926. Orfordness: A study in coastal physiography. Proceedings of the Geologists' Association 37, 306–325. doi:10.1016/S0016-7878(26)80023-9

Steers, J.A., 1927. The East Anglian Coast. The Geographical Journal 69, 24–43.

Steers, J.A., 1951. Notes on Erosion Along the Coast of Suffolk. Geological Magazine 88, 435–439. doi:10.1017/S001675680007000X

Steers, J.A., 1953. The East Coast Floods. The Geographical Journal 119, 280–295.

Stokes, G.G., 1851. On the effect of the internal friction of fluids on the motion of pendulums. Transactions of the Cambridge Philosophical Society 9.

Stuiver, M., Reimer, P.J., Reimer, R.W., 2018. CALIB 7.1, World-wide electronic publication. http://calib.org

Sturt, F., Garrow, D., Bradley, S.L., 2013. New models of North West European Holocene palaeogeography and inundation. Journal of Archaeological Science 40, 3963–3976. doi:10.1016/j.jas.2013.05.023

Suffolk Coastal District Council, 2010. Suffolk SMP2 Sub-cell 3c. Policy Development Zone 4- Dunwich Cliffs to Thorpeness. http://www.suffolksmp2.org.uk.

Suffolk Coastal District Council, 2013. Walberswick: Conservation Area Appraisal-Supplementary Planning Document. Suffolk.

Sun, D., Bloemendal, J., Rea, D.K., Vandenberghe, J., Jiang, F., An, Z., Su, R., 2002. Grain-size distribution function of polymodal sediments in hydraulic and aeolian environments, and numerical partitioning of the sedimentary components. Sedimentary Geology 152, 263–277. doi:10.1016/S0037-0738(02)00082-9

Sutherland, R.A., Lee, C.-T., 1994. Discrimination between coastal subenvironments using textural characteristics. Sedimentology 41, 1133–1145. doi:10.1111/j.1365-3091.1994.tb01445.x

Switzer, A.D., 2013. Measuring and analyzing particle size in a geomorphic context. In: Shroder, J.F. (Ed.), Treatise on Geomorphology. Academic Press, San Diego, pp. 224–242.

Switzer, A.D., Jones, B.G., 2008. Large-scale washover sedimentation in a freshwater lagoon from the southeast Australian coast: Sea-level change, tsunami or exceptionally large storm? The Holocene 18, 787–803. doi:10.1177/0959683608089214

Switzer, A.D., Pile, J., 2015. Grain size analysis. In: Shennan, I., Long, A.J., Horton, B.P. (Eds.), Handbook of Sea-Level Research. Wiley, Chichester, pp. 331–348.

Tanner, W.F., 1991a. Application of suite statistics to stratigraphy and sea-level changes. In: Syvitski, J. (Ed.), Principles, Methods and Applications of Particle Size Analysis. Cambridge University Press, Cambridge, United Kingdom, pp. 283–292. doi:10.1017/CBO9780511626142.026

Tanner, W.F., 1991b. Suite statistics: the hydrodynamic evolution of the sediment pool. In: Syvitski, J. (Ed.), Principles, Methods and Applications of Particle Size Analysis. Cambridge University Press, Cambridge, United Kingdom, pp. 225–236.

Tanner, B.R., Uhle, M.E., Mora, C.I., Kelley, J.T., Schuneman, P.J., Lane, C.S., Allen, E.S., 2010. Comparison of bulk and compound-specific $\delta 13C$ analyses and determination of carbon sources to salt marsh sediments using n-alkane distributions (Maine, USA). Estuarine, Coastal and Shelf Science 86, 283–291. doi:10.1016/j.ecss.2009.11.023

Tooley, M.J., 1979. Sea-level changes during the Flandrian Stage and the implications for coastal development. In: Proceedings of the "1978 International Symposium on Coastal Evolution in the Quaternary." Sao-Paulo, Brazil, pp. 552–572.

Tooley, M.J., 1982. Sea-level changes in northern England. Proceedings of the Geologists' Association 93, 43–51. doi:10.1016/S0016-7878(82)80031-X

Törnqvist, T.E., Ree, M.H.M. van, van't Veer, R., Geel, B. van, 1998. Improving methodology for high-resolution reconstruction of sea-level rise and neotectonics by paleoecological analysis and AMS 14C dating of basal peats. Quaternary Research 49, 72–85. doi:10.1006/qres.1997.1938

Törnqvist, T.E., González, J.L., Newsom, L.A., Borg, K. van der, Jong, A.F.M. de, Kurnik, C.W., 2004. Deciphering Holocene sea-level history on the U.S. Gulf Coast: A high-resolution record from the Mississippi Delta. Geological Society of America Bulletin 116, 1026–1039. doi:10.1130/B2525478.1

Törnqvist, T.E., Rosenheim, B.E., Hu, P., Fernandez, A.B., 2015. Radiocarbon dating and calibration. In: Shennan, I., Long, A.J., Horton, B.P. (Eds.), Handbook of Sea-Level Research. Wiley, Chichester, pp. 349–360.

Troels-Smith, J., 1955. Characterisation of Unconsolidated Sediments. Danmarks Geologiske Undersogelse Series IV, 38–73.

Uehara, K., Scourse, J.D., Horsburgh, K.J., Lambeck, K., Purcell, A.P., 2006. Tidal evolution of the northwest European shelf seas from the Last Glacial Maximum to the present. Journal of Geophysical Research 111, 1–15. doi:10.1029/2006JC003531

Vincent, C.E., 1979. Longshore sand transport rates- a simple model for the East Anglian coastline. Coastal Engineering 3, 113–136.

Vos, P.C., Heeringen, R.M. van, 1997. Holocene geology and occupation history of the Province of Zeeland, Holocene evolution of Zeeland (SW Netherlands). Mededelingen Nederlands Instituut voor Toegepaste Geowetenschappen TNO.

Vos, P.C., Wolf, H. De, 1988. Methodological aspects of paleo-ecological diatom research in coastal areas of the Netherlands. Geologie en Mijnbouw 67, 31–40.

Vos, P.C., Wolf, H. De, 1993. Diatoms as a tool for reconstructing sedimentary environments in coastal wetlands ; methodological aspects. Hydrobiologia 269/270, 285–296.

Walker, M., Head, M.J., Berkelhammer, M., Bjorck, S., Cheng, H., Cwynar, L.C., Fisher, D., Long, A.J., Lowe, J., Newnham, R., Rasmussen, S.O., Weiss, H., 2018. Formal ratification of the subdivision of the Holocene Series/ Epoch (Quaternary System/Period): two new Global Boundary Stratotype Sections and Points (GSSPs) and three new stages/ subseries. Episodes 41, 213–223. doi:10.18814/epiiugs/2018/018016

Waller, M.P., 1993. Flandrian vegetational history of south-eastern England. Stratigraphy of the Brede Valley and pollen data from Brede Bridge. New Phytologist 124, 345–369.

Waller, M.P., 1994. The Fenland Project Number 9: Flandrian Environmental Change in Fenland, East Anglia. Archaeology Report Number 70, Fenland Project Committee. Cambridge County Council, Cambridge.

Waller, M.P., Kirby, J., 2002. Late Pleistocene/Early Holocene environmental change in the Romney Marsh region: new evidence from Tilling Green, Rye. In: Long, A.J., Hipkin, S., Clarke, H. (Eds.), Romney Marsh: Coastal and Landscape Changes through the Ages. Oxbow, Oxford, pp. 22–39.

Ward, S.L., Neill, S.P., Scourse, J.D., Bradley, S.L., Uehara, K., 2016. Sensitivity of palaeotidal models of the northwest European shelf seas to glacial isostatic adjustment since the Last Glacial Maximum. Quaternary Science Reviews 151, 198–211. doi:10.1016/j.quascirev.2016.08.034

Warner, P., 2000. Bloody Marsh: a seventeenth-century village in crisis. Windgather Press Ltd, Macclesfield.

Watcham, E.P., Shennan, I., Barlow, N.L.M., 2013. Scale considerations in using diatoms as indicators of sea-level change: lessons from Alaska. Journal of Quaternary Science 28, 165–179. doi:10.1002/jqs.2592

Watson, E.B., Pasternack, G.B., Gray, A.B., Goñi, M., Woolfolk, A.M., 2013. Particle size characterization of historic sediment deposition from a closed estuarine lagoon, Central California. Estuarine, Coastal and Shelf Science 126, 23–33. doi:10.1016/j.ecss.2013.04.006

Wells, C.E., Wheeler, B.D., 1999. Evidence for possible climatic forcing of late-Holocene vegetation changes in Norfolk Broadland floodplain mires, UK. The Holocene 9, 595–608. doi:10.1191/095968399675019770

Weltje, G.J., 1997. End-member modeling of compositional data: Numerical-statistical algorithms for solving the explicit mixing problem. Mathematical Geology 29, 503–549. doi:10.1007/BF02775085

Weltje, G.J., Prins, M.A., 2007. Genetically meaningful decomposition of grain-size distributions. Sedimentary Geology 202, 409–424. doi:10.1016/j.sedgeo.2007.03.007

Wentworth, C., 1922. A scale of grade and class terms for clastic sediments. The Journal of Geology 5, 377–392.

Werff, H. van der, Huls, H., 1957-1974. Diatomeenflora van Nederland (8 parts). Published privately, De Hoef, The Netherlands.

Wilkinson, T.J., Murphy, P.L., 1995. The archaeology of the Essex coast, volume 1: The Hullbridge Survey. Chelmsford.

Wilkinson, T.J., Murphy, P.L., Juggins, S., Manson, K., 1988. Wetland development and human acivity in Essex Estuaries during the Holocene transgression. In: Murphy, P.L., French, C. (Eds.), The Exploitation of Coastal Wetlands. Symposia of the Association for Environmental Archaeology, 7. BAR British Series 186.

Williamson, T., 2005. Sandlands: The Suffolk Coast and Heaths. Windgather Press Ltd, Cheshire.

Wilson, G.P., 2017. On the application of contemporary bulk sediment organic carbon isotope and geochemical datasets for Holocene sea-level reconstruction in NW Europe. Geochimica et Cosmochimica Acta 214, 191–208. doi:10.1016/j.gca.2017.07.038

Wolf, H. De, 1982. Method of coding of ecologial data from diatoms for computer utilisation. Mededelingen Rijks Geologische Dienst 36, 95–98.

Woodroffe, S.A., 2006. Holocene relative sea-level changes in Cleveland Bay, North Queensland, Australia. PhD thesis, Durham University.

Woodroffe, S.A., Long, A.J., 2010. Reconstructing recent relative sea-level changes in West Greenland: Local diatom-based transfer functions are superior to regional models. Quaternary International 221, 91–103. doi:10.1016/j.quaint.2009.06.005

Woodworth, P.L., Teferle, F.N., Bingley, R.M., Shennan, I., Williams, S.D.P., 2009. Trends in UK mean sea level revisited. Geophysical Journal International 176, 19–30. doi:10.1111/j.1365-246X.2008.03942.x

WoRMS Editorial Board, 2019. World Register of Marine Species. World-wide electronic publication, VLIZ. http://www.marinespecies.org

Yamane, M., Yokoyama, Y., Miyairi, Y., Suga, H., Matsuzaki, H., Dunbar, R.B., Ohkouchi, N., 2014. Compound-Specific 14C Dating of IODP Expedition 318 Core U1357A Obtained Off the Wilkes Land Coast, Antarctica. Radiocarbon 56, 1009–1017. doi:10.2458/56.17773

Zong, Y., 1993. Flandrian sea-level changes and impacts of projected sea-level rise on the coastal lowlands of Morecambe Bay and the Thames Estuary, UK. PhD thesis, Durham University.

Zong, Y., 1997. Implications of *Paralia Sulcata* Abundance in Scottish Isolation Basins. Diatom Research 12, 125–150. doi:10.1080/0269249X.1997.9705407

Zong, Y., Tooley, M.J., 1996. Holocene sea-level changes and crustal movements in Morecambe Bay, northwest England. Journal of Quaternary Science 11, 43–58.

Zong, Y., Horton, B.P., 1998. Diatom zones across intertidal flats and coastal saltmarshes in Britain. Diatom Research 13, 375–394.

Zong, Y., Horton, B.P., 1999. Diatom-based tidal-level transfer functions as an aid in reconstructing Quaternary history of sea-level movements in the UK. Journal of Quaternary Science 14, 153–167. doi:10.1002/(SICI)1099-1417(199903)14:2<153::AID-JQS425>3.0.CO;2-6

Zong, Y., Tooley, M.J., 1999. Evidence of mid-Holocene storm-surge deposits from Morecambe Bay, northwest England: A biostratigraphical approach. Quaternary International 55, 43–50. doi:10.1016/S1040-6182(98)00022-6

Zong, Y., Sawai, Y., 2015. Diatoms. In: Shennan, I., Long, A.J., Horton, B.P. (Eds.), Handbook of Sea-Level Research. Wiley, Chichester, pp. 233–248.